# The functional assembly of the mammalian minichromosome maintenance complex

Emma Louise Hesketh

PhD

University of York

Biology

November 2014

# Abstract

The minichromosome maintenance complex (MCM2-7) is the putative DNA helicase in eukaryotes, and is essential for DNA replication. Mis-regulation of its assembly and function can lead to genomic instability, replication stress and genome re-replication, which are powerful drivers toward the acquisition of mutations and the formation of cancer.

I have produced and purified recombinant human MCM2-7 (hMCM) in *Escherichia coli* (*E. coli*). Recombinant hMCM has ATP hydrolysis and helicase activity, when assayed in the absence of post-translational modifications or accessory proteins. Using electron microscopy asymmetric single particle reconstruction, I have produced 23 Å resolution structures. The structures reveal that recombinant hMCM forms an asymmetric complex that changes conformation in the presence of a forked DNA substrate.

By applying serial extractions to mammalian cells synchronised by release from quiescence, I have revealed dynamic changes in the sub-nuclear compartmentalisation of MCM2 as cells pass through late G1 and early S phase, identifying a brief window when MCM2 becomes transiently attached to the nuclear matrix. This suggests that functional MCM2-7 loading takes place at the nuclear matrix. Using this information I have developed a system to study the regulated assembly of recombinant hMCM, to support molecular dissection of the loading process. Using cellular extracts, I show regulated binding of recombinant hMCM, which translates into initiation of DNA replication and is stimulated by cyclin E/CDK2. Furthermore, I have demonstrated that both cyclin A/CDK2 and Dbf4/Drf1-dependant kinase (DDK) are required for inducing a conformational change in hMCM that is associated with S phase of the cell cycle.

Understanding of the assembly of hMCM will serve as a foundation for analysis of corruption of the process, its effect on genome instability and gene expression, and how these events lead to the 'birth' of cancer cells. Very early events in the development of cancer cells are most likely to yield new and effective opportunities for detection and treatment of a broad range of cancers.

# Table of Contents

**Abstract** ..... **2**
**Table of Contents** ..... **3**
**List of Figures** ..... **9**
**List of Tables** ..... **12**
**Acknowledgements** ..... **13**
**Declaration** ..... **14**
**1 Introduction** ..... **16**
**1.1 Cell cycle** ..... **16**
1.1.1 Quiescence ..... 18
**1.2 Cell cycle control** ..... **18**
1.2.1 Cyclin dependent kinase (CDK) ..... 19
1.2.2 Cyclin A/CDK2 ..... 20
1.2.3 Cyclin E/CDK2 ..... 20
1.2.4 DDK ..... 21
**1.3 DNA replication** ..... **22**
**1.4 Minichromosome maintenance (MCM2-7) complex** ..... **22**
1.4.1 Localisation of MCM proteins ..... 25
1.4.2 MCM complexes hydrolyse ATP ..... 26
1.4.3 MCM as a helicase ..... 27
**1.5 MCM2-7 loading** ..... **28**
1.5.1 Origins ..... 31
1.5.2 ORC ..... 31
1.5.3 Cdc6 ..... 32
1.5.4 Cdt1 ..... 33
1.5.5 MCM2-7 ..... 34
1.5.6 Metazoan specific proteins involved in MCM2-7 loading ..... 36
**1.6 MCM2-7 activation** ..... **37**
1.6.1 Pre-IC ..... 38
1.6.2 Pre-LC ..... 38
1.6.3 Cdc45 ..... 41
1.6.4 GINS ..... 41
1.6.5 MCM10 ..... 42

1.6.6 Ctf4 ... 42
1.6.7 Metazoan specific initiation proteins ... 42
1.6.8 CMG activation ... 43
**1.7 Phosphorylation of MCM proteins ... 44**
1.7.1 Phosphorylation by DDK ... 44
1.7.2 MCM4 phosphorylation ... 45
1.7.3 MCM2 phosphorylation ... 46
1.7.4 Order of CDK and DDK kinase activity ... 47
**1.8 Structure of MCM2-7 complexes ... 48**
**1.9 Nuclear matrix ... 49**
**1.10 Aims ... 52**
**2 Material and methods ... 55**
**2.1 *E. coli* cell culture ... 55**
2.1.1 Growth media ... 55
2.1.2 Antibiotics ... 55
2.1.3 Preparation of heat shock competent *E. coli* cells with rubidium chloride ... 55
2.1.4 *E. coli* transformation ... 56
**2.2 Mammalian cell culture ... 56**
2.2.1 Growth media and conditions ... 56
2.2.2 Cell synchrony ... 57
2.2.2.1 G1 phase synchrony ... 57
2.2.2.2 S phase synchrony ... 57
**2.3 Protein analysis ... 58**
2.3.1 SDS PAGE ... 58
2.3.1.1 Preparation and running of gels ... 58
2.3.1.2 Sample preparation ... 59
2.3.2 Native PAGE ... 59
2.3.2.1 Preparation and running of gels ... 59
2.3.2.2 Sample preparation ... 59
2.3.3 Coomassie blue staining ... 59
2.3.4 Western blotting ... 60
2.3.4.1 Transfer ... 60
2.3.4.2 Antibody detection ... 60
2.3.5 Immunofluorescence (IF) ... 61

2.3.5.1 Mounting coverslips ..... 61
2.3.5.2 Image analysis ..... 62
2.3.6 Determining protein concentration ..... 64
**2.4 hMCM production and purification ..... 64**
2.4.1 Expression of hMCM ..... 64
2.4.2 hMCM purification ..... 65
**2.5 ATP hydrolysis assay ..... 66**
**2.6 DNA helicase assay ..... 67**
2.6.1 Substrate preparation ..... 67
2.6.1.1 Oligonucleotide labelling ..... 67
2.6.1.2 Oligonucleotide annealing ..... 67
2.6.1.3 Substrate purification ..... 68
2.6.1.4 Substrate quantification ..... 68
2.6.2 Assay conditions ..... 69
**2.7 Electron microscopy (EM) ..... 69**
2.7.1 Binding of duplex DNA to hMCM for EM ..... 69
2.7.2 Negative stain EM ..... 70
2.7.3 Image processing ..... 70
2.7.4 Domain fitting ..... 71
**2.8 Mammalian cell analysis ..... 72**
2.8.1 Assay for DNA synthesis ..... 72
2.8.2 Protein extraction for western blot ..... 72
2.8.3 Protein extraction for immunofluorescence ..... 75
2.8.3.1 Cross-linking ..... 77
**2.9 Cell free system ..... 77**
2.9.1 Harvesting of nuclei and cytoplasmic extracts ..... 77
2.9.2 DNA initiation assays ..... 78
2.9.2.1 Two-step assays ..... 78
2.9.2.2 Analysis by fluorescence ..... 79
2.9.2.3 Analysis by western blotting ..... 79
2.9.3 *in vitro* phosphorylation assays ..... 80
2.9.3.1 Phosphatase assays ..... 80
2.9.3.2 Inhibitors ..... 80
**2.10 Statistical analysis ..... 80**
**3 Production and purification of recombinant hMCM ..... 83**

**3.1 Introduction** ..... **83**
**3.2 Aims** ..... **84**
**3.3 Experimental design** ..... **84**
**3.4 Results and discussion** ..... **84**
3.4.1 Production and Purification of Recombinant hMCM ..... 84
3.4.2 Production and purification of mutant hMCM ..... 93
3.4.3 ATP hydrolysis activity of hMCM ..... 93
3.4.4 ATP-dependent DNA unwinding by hMCM ..... 100
3.4.5 Structural analysis ..... 102
**3.5 Conclusion** ..... **109**

**4 Expression and localisation of endogenous mammalian MCM proteins ..111**
**4.1 Introduction** ..... **111**
**4.2 Aims** ..... **112**
**4.3 Experimental design** ..... **112**
**4.4 Results** ..... **112**
4.4.1 Cells released from quiescence enter G1 in a highly regulated manner ..... 112
4.4.2 MCM protein expression peaks at the initiation of DNA replication .... 113
4.4.3 Sub-cellular localisation of MCM2 ..... 116
4.4.4 MCM2 is transiently bound to the nuclear matrix ..... 116
4.4.5 MCM2 is tightly associated with chromatin after initiation ..... 120
**4.5 Discussion** ..... **122**
**4.6 Conclusions** ..... **123**

**5 Functional assembly of recombinant hMCM ..... 127**
**5.1 Introduction** ..... **127**
**5.2 Aims** ..... **128**
**5.3 Experimental design** ..... **128**
**5.4 Results and discussion** ..... **128**
5.4.1 Cell free characterisation ..... 128
5.4.2 Regulated binding of hMCM in isolated nuclei ..... 130
5.4.3 Recombinant cyclin A/CDK2 and cyclin E/CDK2 improve hMCM loading in isolated nuclei ..... 133
5.4.4 hMCM is functionally loaded onto chromatin *in vitro* ..... 133
5.4.5 Effect of DDK on hMCM loading ..... 136

5.4.6 MCM2 mobility shift is dependent on both DDK and cyclin A/CDK2 ... 136
5.4.7 Mobility shift of MCM proteins is a reversible phosphorylation ... 140
5.4.8 Cyclin A/CDK2 is required before DDK to induce increased mobility of MCM2 ... 140
**5.5 Conclusions ... 147**
**6 Discussion and future work ... 149**
**6.1 Recombinant hMCM is active ... 149**
6.1.1 hMCM stoichiometry ... 150
6.1.2 Essential residues in hMCM ... 151
**6.2 Recombinant hMCM undergoes a conformational change when bound to DNA ... 151**
6.2.1 Subunit arrangement and orientation ... 152
6.2.2 Which MCM2-7 subunit preferentially binds DNA? ... 152
6.2.3 X-ray crystal structure of hMCM ... 152
**6.3 MCM2 is transiently associated with the nuclear matrix at initiation ... 153**
6.3.1 Effect of kinase inhibitors on transient nuclear matrix binding of MCM2 ... 153
6.3.2 Additional proteins bound to nuclear matrix ... 154
6.3.3 Identification of novel proteins involved in DNA replication initiation ... 155
**6.4 Regulated hMCM loading ... 155**
6.4.1 What component of late-G1 phase extract inhibits hMCM loading? ... 156
6.4.2 Ability of ATPase deficient mutant hMCM to functionally load onto chromatin ... 156
6.4.3 Does hMCM bind to the nuclear matrix? ... 157
6.4.4 Effect of DDK on *in vitro* DNA replication initiation ... 157
**6.5 MCM2 undergoes a structural change by the sequential action of cyclin A/CDK2 followed by DDK ... 157**
6.5.1 Effect of phosphorylation on hMCM hexamer ... 158
6.5.2 Role of phosphorylated MCM2 in DNA replication ... 158
6.5.3 Analysis of phosphorylation sites on hMCM ... 159
6.5.4 Is the mobility shift of MCM2 due to a conformational change? ... 160
**6.6 How does MCM2-7 unwind DNA? ... 160**

**6.7 Conclusions ..... 161**

**Appendix A ..... 163**

**Appendix B ..... 177**

**Appendix C ..... 180**

**Appendix D ..... 194**

**Abbreviations ..... 218**

**References ..... 222**

## List of Figures

**Figure 1.1.** Schematic showing phases of the cell cycle……...…… 17

**Figure 1.2.** Semi-conservative DNA replication…… 23

**Figure 1.3.** MCM2-7 subunit configuration…… 24

**Figure 1.4.** Pre-replication complex (pre-RC) assembly……. 30

**Figure 1.5.** Assembly of Cdc45-MCM2-7-GINS (CMG) complex in *S. cerevisiae*……39

**Figure 1.6.** Electron microscopy of *Mt*MCM in different conformational states…….. 50

**Figure 2.1.** Flow diagram to show nuclear matrix protein extraction for analysis by SDS PAGE and western blot…… 73

**Figure 2.2.** Flow diagram to show nuclear matrix protein extraction for analysis by immunofluorescence…… 76

**Figure 3.1.** hMCM plasmid maps and schematic of conformation…… 85

**Figure 3.2.** Summary of hMCM production from a typical 50 L bioreactor run…… 87

**Figure 3.3.** Summary of immobilised metal affinity chromatography (IMAC) purification of hMCM. …….. 88

**Figure 3.4.** Summary of gel filtration purification of hMCM……..... 89

**Figure 3.5.** Summary of anion exchange purification of hMCM...…….. 90

**Figure 3.6.** Summary of hMCM purification.……..… 92

**Figure 3.7.** Summary of immobilised metal affinity chromatography (IMAC) purification for mutant hMCM……. 94

**Figure 3.8.** Summary of gel filtration and anion exchange purification of mutant hMCM. ……...… 95

**Figure 3.9.** Screening of assay conditions for ATPase activity of hMCM…….. 96

**Figure 3.10.** Effect of salt and DNA on ATPase activity of hMCM……...98

**Figure 3.11.** Effect of hMCM and ATP concentration on ATPase activity of hMCM and mutant hMCM…..…….. 99

**Figure 3.12.** hMCM shows strand displacement activity ……..… 101

**Figure 3.13.** Negative stain electron microscopy of hMCM …...……...105

**Figure 3.14.** hMCM undergoes a conformational change when bound to forked DNA..……... 106

**Figure 3.15.** hMCM EM reconstructions fit crystal structures……. 107

**Figure 3.16.** Additional views of hMCM reconstructions…….. 108

**Figure 4.1.** Cell cycle re-entry from quiescence.…… 114

**Figure 4.2.** MCM protein levels peak at initiation.…… 115

**Figure 4.3.** Nuclear matrix binding revealed by DNase I digestion……... 118

**Figure 4.4.** Nuclear matrix binding revealed by DNase I digestion in G1 phase and early S. ……..... 119

**Figure 4.5** Using DTSP MCM2 is shown to be associated with chromatin after initiation…...……...… 121

**Figure 4.6.** Schematic showing three states of MCM2-7 complex binding in late G1 phase……...…… 125

**Figure 5.1.** Schematic representation of cell free components prepared from cells synchronised by re-entry to the cell cycle from quiescence.… 129

**Figure 5.2.** Regulated binding of hMCM within late-G1 phase nuclei *in vitro*..131

**Figure 5.3.** Regulated binding of hMCM within mid-G1 phase nuclei *in vitro*. 132

**Figure 5.4.** Effect of recombinant cyclin E/CDK2 and cyclin A/CDK2 on hMCM loading……...……..… 134

**Figure 5.5.** Effect of recombinant cyclin E/CDK2 on initiation of DNA replication…….....……..... 135

**Figure 5.6.** Effect of recombinant DDK on hMCM loading…….....……..... 137

**Figure 5.7.** Increased mobility of MCM2 requires both cyclin A/CDK2 and DDK…….…… 139

**Figure 5.8.** MCM2 and MCM4 mobility shift is reversed by dephosphorylation by λ phosphatase…… 141

**Figure 5.9.** Effect of the CDK2 inhibitor roscovitine on MCM2 and MCM4 mobility…… 143

**Figure 5.10.** Effect of the DDK inhibitor PHA-767491 on MCM2 and MCM4 mobility…… 144

**Figure 5.11.** Order of additions experiment, which shows that cyclin A/CDK2 must act before DDK in order to induce the MCM2 mobility shift. ……. 146

**Figure 6.1.** Model for MCM2-7 unwinding…..…… 162

## List of Tables

**Table 1.1.** MCM amino acid insertions comparison of *S. cerevisiae (Sc)* and Human *(Hs)* MCM……..……..……..……..…..29

**Table 2.1.** Components of SDS PAGE resolving and stacking gel……...……. 58

**Table 2.2.** Primary antibody details……..……. 62

**Table 2.3.** Secondary antibody details……..……. 63

**Table 2.4.** Oligonucleotide sequences……..…….…..67

**Table 3.1.** The fold purification and concentration of recombinant hMCM from a typical 50 L fermenter run……....…..……..……91

**Table 3.2.** MCM amino acid insertions comparison of Human (*Hs*) and *Sulfolobus solfactaricus* (*Sso*) MCM…….....……. 104

## Acknowledgements

Firstly, I would like to thank Yorkshire Cancer Research for funding this PhD. I would also like to thank my supervisors James Chong and Dawn Coverley. Together they came up with a fantastic project that I have thoroughly enjoyed. I am also extremely grateful to all past and present members of both Chong and Coverley labs particularly Gill, Rose, Henry and Dorian who have provided me with continued help over the years and made the lab an enjoyable place to be.

I am thankful to the members of my training advisory panel, Christoph Baumann and Paul Genever who have given me lots of advice that has helped with the completion of my thesis. I am grateful to members of the technology facility at York particularly Jared Cartwright and Mick Miller who helped with the production and purification of hMCM. I am also thankful to Elena Orlova at the University of Birkbeck who hosted me for a month to complete the electron microscopy work on hMCM. I am particularly grateful to Richard Parker-Manuel for the research carried out on hMCM before I started my PhD.

And finally I would like to thank my friends and family. My friends Heather, Jessica, Kaylei, Lindsay and Saski who have given me infinite distractions from my PhD with weddings, Hen Do's, cocktail party's and a huge list of other exciting activities as well as encouragement to work hard. My Mum, Dad and sister Rachael who have always made me believe I can do anything I put my mind to. And of course Ryan who has been a great support and has listened to endless performances of every talk I have ever done!

## Declaration

All the research in this thesis is my own with the following exceptions:

- The constructs in Chapter 3 used to produce hMCM and ATPase deficient mutant hMCM were designed and created by Dr Richard Parker-Manuel.
- The hMCM used for electron microscopy in Chapter 3 was produced by Dr Richard Parker-Manuel.
- The negative stain electron microscopy pictures used in Chapter 3 were taken by Dr Yuriy Chaban.
- The recombinant Dbf4-dependant kinase used in Chapter 5 was produced and purified by Dr Richard Parker-Manuel.
- The recombinant cyclin E/cyclin dependent kinase 2 used in Chapter 5 was produced and purified by Dr Dawn Coverley.
- The recombinant cyclin A/cyclin dependent kinase 2 used in Chapter 5 was produced and purified by Dr Nikki Copeland.

*Chapter 1*

# Introduction

# 1 Introduction

Genome duplication is essential for the growth of all living organisms. Over the past 30 years there has been much investigation of the precise mechanism of DNA replication and transmission to daughter cells. Although our knowledge has improved, the exact mechanism underlying eukaryotic genome duplication is not fully understood.

DNA replication occurs in a highly orchestrated and coordinated fashion that is spatially and temporally regulated (reviewed in Bell and Dutta, 2002). Errors in DNA replication are linked with a variety of diseases including cancer (reviewed in Blow and Gillespie, 2008). The primary regulation of DNA replication is at initiation; when the mammalian minichromosome maintenance (MCM2-7) complex, the putative DNA helicase in eukaryotes, is loaded onto chromatin. Altered levels of MCM subunits have been associated with numerous cancer types (reviewed in Semple and Duncker, 2004, Gonzalez et al., 2005).

This research focuses on the loading and activation of the human MCM2-7 complex in mammalian cells, and provides new information into how this fundamental process is controlled.

## 1.1 Cell cycle

As cells grow and divide they pass through a series of carefully coordinated events that make up the cell cycle. Proliferating cultured mammalian cells pass through the mitotic cell cycle roughly every 24 hours (Fig. 1.1A). During growth phase 1 (G1) of the cell cycle, the cell prepares for DNA replication by synthesising nucleotides and proteins involved in duplicating the genome. Once the cell is ready for DNA replication, it can pass the restriction point (R, Pardee, 1974) and is committed to the cell cycle. Following R the cell is under the control of cyclin dependent kinases (CDKs, reviewed in Murray, 2004). The cell then moves into the synthesis (S) phase of the cell cycle when the entire genome is faithfully replicated, generating one complete genome per daughter cell (reviewed in Sclafani and Holzen, 2007).

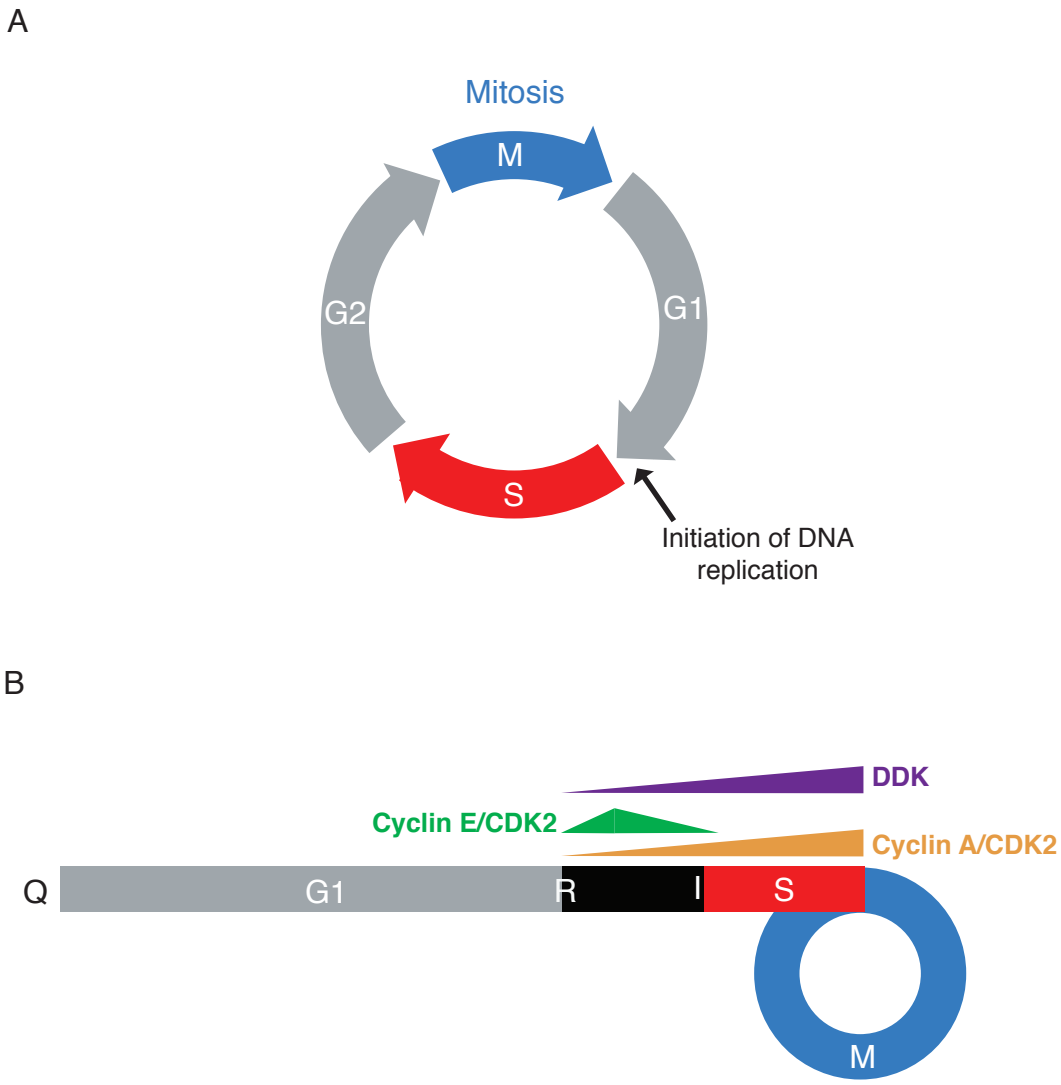


**Figure 1.1** Schematic showing phases of the cell cycle. A. The mitotic cell cycle. Showing mitosis (M), Growth 1 (G1), Synthesis (S) and Growth 2 (G2) phases. Initiation of DNA replication is highlighted between G1 and S phase. B. The cell cycle following release from quiescence (Q). The cells pass through a prolonged G1 and the restriction point (R) before the initiation of DNA replication (I). The levels of DDK, cyclin E/CDK2 and cyclin A/CDK2 are indicated.

The cell then enters growth 2 phase (G2) where cells prepare for division by production of proteins required for mitosis (M). During M phase the cell divides into two identical daughter cells, which both then continue into G1 phase and the cycle begins again (Norbury and Nurse, 1992).

### 1.1.1 Quiescence

In the absence of growth factors or when cells are at a high density and in contact, they can enter quiescence or G0 (Martin and Stein, 1976, Smith and Martin, 1973, reviewed in Spencer et al., 2013). Quiescence is a non-proliferating state where proteins required for cell growth, such as DNA replication and mitotic spindle formation, are down regulated (reviewed in Coller, 2007). Originally, cells in quiescence were thought to be withdrawn from the cell cycle and in a passive state. However, several lines of evidence show that quiescence is actually a maintained state (Zetterberg and Larsson, 1985, reviewed in Fox et al., 2005) as quiescent cells have also been shown to up regulate many genes (Coller et al., 2006, Coppock et al., 1993, Polyak et al., 1994). In our laboratory, cells are driven into quiescence by a combination of contact inhibition and serum depletion under a precise regime. When cells are stimulated to re-enter the cell cycle from quiescence, they pass through a prolonged G1 phase where a series of coordinated events that control the assembly of the pre-replication complex (pre-RC) takes place with precise timing (Fig. 1.1B, Coverley et al., 2002). In adult tissues the majority of cells are quiescent. Failure to maintain quiescence leading to unscheduled re-entry to the cell cycle is thought to underlie the formation of some cancers.

## 1.2 Cell cycle control

The cell cycle is controlled by its regulated passage through checkpoints. The cell can only pass through a checkpoint if the prior stage of the cell cycle has been successfully completed. The restriction point (Fig. 1.1B) occurs in late-G1 phase (Pardee, 1974). At this point the cell must decide if conditions are favourable and to continue with the cell cycle or, if the extracellular environment is not ideal, the cell will enter quiescence (Zetterberg and Larsson, 1985). Once the cell passes through the restriction point it is committed to the cell cycle even if the

extracellular environment changes (Pardee, 1974). The cell can only pass through the restriction point and into S phase if it is fully prepared for DNA replication (Blagosklonny and Pardee, 2002). Cyclins are regulatory proteins which integrate information from outside the cell and subsequently bind and activate cyclin dependent kinases (CDK, Sherr and Roberts, 2004). Cyclin D transfers extracellular information to the cells nucleus during G1 phase prior to the restriction point (Sherr and Roberts, 1999, Sewing et al., 1993). Cyclin D binds and activates CDK4 and CDK6, and phosphorylates retinoblastoma protein (pRb) which in turn releases the transcription factor E2F (reviewed in Sherr, 1994). This allows expression of a number of target genes including cyclin E (Nevins, 1998, Dyson, 1998), cyclin A and components of the pre-RC (Harbour et al., 1999, reviewed in Sherr, 1994). Cyclin E/CDK2 phosphorylates multiple proteins driving the cell through the restriction point (Dahmann et al., 1995).

Following the restriction point the cell's activities, including initiation of DNA replication, are controlled by cyclins and their associated CDK (Aguda, 2001). Here I will focus on kinases that are thought to target and control the activity of pre-RC components, in particular the MCM2-7 complex.

### 1.2.1 Cyclin dependent kinase (CDK)

CDK's phosphorylate substrate proteins at serine or threonine residues to control their activity (reviewed in Malumbres and Barbacid, 2005). In *Saccharomyces cerevisiae* (*S. cerevisiae*) and *Schizosaccharomyces pombe* (*S. pombe*) there is one type of cyclin active around G1/S, commonly known as S-CDK (Nguyen et al., 2001). S-CDK is expressed in S phase of the cell cycle and has been shown to control a number of DNA replication initiation proteins by phosphorylation (reviewed in Blow and Dutta, 2005).

In mammals there are more than ten identified CDKs, controlled differentially by cyclins (reviewed in Malumbres and Barbacid, 2005). CDK2 has numerous targets including components of the pre-RC, and so its activity was thought to be essential for replication. However, mice can develop normally and survive in the absence of CDK2 (Ortega et al., 2003, Berthet et al., 2003). The activity of CDK2 is controlled by both cyclin A and cyclin E, which have separate, sequential and

concentration-dependent functions in the initiation of mammalian DNA replication (Coverley et al., 2002). The expression levels of cyclin A and E varies throughout the cell cycle (Morgan, 1997) and therefore so does the activity of CDK2.

### 1.2.2 Cyclin A/CDK2

Cyclin A expression increases throughout G1 phase and peaks in S phase (Sherr, 1996). Its initial involvement in DNA replication was hypothesised from its expression in relation to the cell cycle (Erlandsson et al., 2000) and its localisation at sites of DNA replication (Cardoso et al., 1993). Mammalian cells encode both cyclin A1 and A2 (Nieduszynski et al., 2002). Cyclin A1 is germ cell specific (Ravnik and Wolgemuth, 1999) whereas cyclin A2 is expressed in all proliferating cells (Pines and Hunter, 1990). Ablation of cyclin A1 and A2 in embryonic cells inhibits cell cycle progression. However in fibroblasts, cyclin A is redundant (Kalaszczynska et al., 2009). It appears cyclin E can replace cyclin A under these conditions to ensure cell cycle progression (Kalaszczynska et al., 2009).

### 1.2.3 Cyclin E/CDK2

There are two E type cyclins, E1 and E2, both of which bind and activate CDK2 (Morgan, 1997). Cyclin E1 and cyclin E2 are expressed in proliferating cells (Geng et al., 2001). Expression of cyclin E begins just after the restriction point, peaks before S phase and is down regulated shortly after passing into S phase (Ekholm et al., 2001, Dulic et al., 1992). Embryonic development of mice is normal when cyclin E1 and E2 is ablated, as was the phosphorylation of pRB, a known target of cyclin E (Geng et al., 2003). These data suggest that, cyclin A is able to substitute for cyclin E, however under these conditions the association of MCM proteins with chromatin during exit from quiescence was decreased (Geng et al., 2003). Consistent with this, over expression of cyclin E in cultured mammalian cells speeds up G1 phase (Ohtsubo and Roberts, 1993) possibly by increasing MCM2-7 loading.

### 1.2.4 DDK

The gene encoding Cell division cycle 7 (Cdc7) was first identified in *S. cerevisiae* (Hartwell et al., 1974), and was shown to be conserved in humans (Sato et al., 1997, Jiang and Hunter, 1997, Hess et al., 1998). Cdc7 is a serine/threonine (S/T) kinase that targets S/T residues followed by either an aspartic acid (D), a glutamic acid (E) or a S/T that has been phosphorylated by another kinase (Montagnoli et al., 2006, Cho et al., 2006, Charych et al., 2008). The activity of Cdc7 is controlled by regulatory subunits Dbf4 (Dumbbell-forming 4, Jiang et al., 1999, Jackson et al., 1993, Kumagai et al., 1999, Masai et al., 2000) or Drf1 (Dbf4 related factor 1, Montagnoli et al., 2002). Drf1 is specific to metazoans and it is hypothesised that Drf1 and Dbf1 have different roles in controlling Cdc7 activity, similar to the control of CDK2 by both cyclin A and cyclin E (Montagnoli et al., 2002). However, the reciprocal role of Drf1 and Dbf1 are yet to be defined. Collectively, Cdc7 bound to either Dbf1 or Drf1 are commonly referred to as Dbf4/Drf1 dependent kinase (DDK). The levels of Cdc7 within *S. cerevisiae* remain constant throughout the cell cycle (Weinreich and Stillman, 1999). However, Cdc7 appears to be degraded in quiescent mammalian cells and resynthesised following release as the cell passes into S phase, similar to the profile of cyclin A (Montagnoli et al., 2006). DDK binds to chromatin in G1 phase after loading of the MCM2-7 complex and stays bound throughout S phase (Weinreich and Stillman, 1999). It appears that DDK acts locally at each replication origin as Dbf4 can be isolated using origin DNA as bait (Dowell et al., 1994). DDK activity is thought to be restricted to S phase (Bousset and Diffley, 1998, Donaldson et al., 1998, Patel et al., 2008).

Cdc7 is essential for G1/S phase transition (Kumagai et al., 1999) and plays a crucial role in activation of the pre-RC at each origin (Donaldson et al., 1998, Bousset and Diffley, 1998). Its importance is demonstrated by specific inhibition, which leads to cell cycle arrest in S phase (Kim et al., 2002). Cdc7 is often found to be over expressed in tumour cell lines (Hess et al., 1998). As a result, Cdc7 inhibitors are being developed as cancer therapeutics and such drugs have been shown to preferentially kill cancer cells (Swords et al., 2010, Montagnoli et al., 2008, Poh et al., 2014).

## 1.3 DNA replication

The initiation of DNA replication is critical for correct and timely genome duplication, it is highly controlled to ensure duplication occurs once and only once per cell cycle. All living organisms replicate their DNA with the same underlying mechanism. Initiation begins at origins of replication where a set of specialised activities results in the formation of a 'protein machine' to unwind DNA and provides a template strand for semi conservative DNA replication (Fig. 1.2, Meselson and Stahl, 1958). The more evolutionarily advanced an organism, the more complex initiation of DNA replication. With this in mind, from the study of prokaryotes, archaea and lower eukaryotes we have learnt a huge amount regarding DNA replication initiation. Eukaryotic DNA replication is increasingly well understood in unicellular eukaryotic systems such as yeast, where many of the steps of the initiation process can be reconstituted *in vitro*, and the regulation of the putative replicative helicase, MCM2-7, has been studied in detail (reviewed in Labib, 2010, Li and Araki, 2013, Sclafani and Holzen, 2007). It is, however, becoming apparent that there are a number of differences between the domains of life and also between lower eukaryotes and metazoans (reviewed in Shen and Prasanth, 2012). This leads to the need to study more advanced mammalian systems.

## 1.4 Minichromosome maintenance (MCM2-7) complex

MCM proteins were first discovered via a number of temperature sensitive mutants in *S. cerevisiae* (Maine et al., 1984). The mammalian orthologue of *S. cerevisiae* MCM3 was initially identified in cultured human cells and shown to localised within the nucleus (Thömmes et al., 1992). MCM proteins are conserved from archaea to eukaryotes (Maiorano et al., 2006). Most archaea contain a single MCM protein (with the exception of three species to date), which form homohexameric complexes *in vivo* (Chong et al., 2000, Wasserfallen et al., 2000, Kelman et al., 1999, Shechter et al., 2000, Poplawski et al., 2001, Carpentieri et al., 2002). Eukaryotes are unique in possessing six highly related MCM subunits that form a heterohexameric complex (MCM2-7, Chong et al., 1996). Each MCM subunit is evolutionarily related to the other but each subunit is unique and

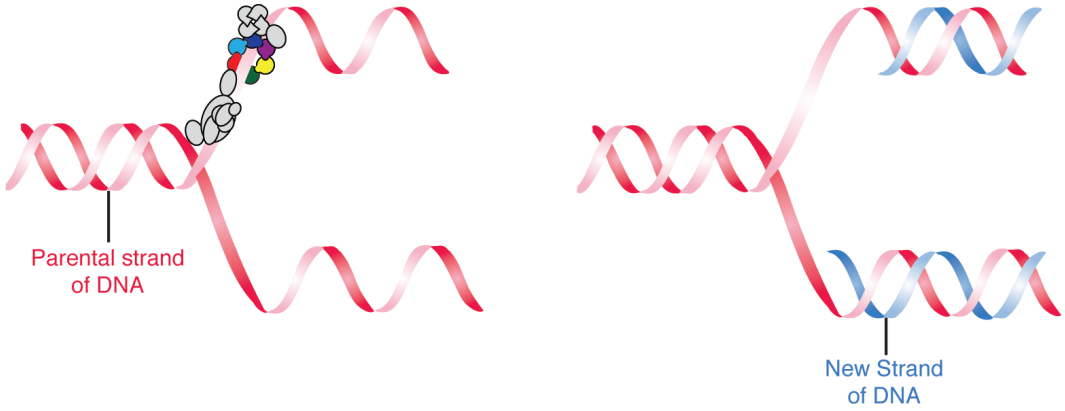


**Figure 1.2.** Semi-conservative DNA replication. Duplex DNA is unwound to provide template strands for DNA polymerase to copy.

conserved throughout eukaryotes (reviewed in Bell and Dutta, 2002). In *Xenopus laevis* (*Xenopus*) all six MCM subunits have been shown to associate with chromatin before the onset of DNA replication suggesting that all six MCMs are required for DNA replication initiation (Thömmes et al., 1997). Consistent with these findings, deletion of any MCM subunit in *S. cerevisiae* or *S. pombe* causes lethality (reviewed in Dutta and Bell, 1997, Kelly and Brown, 2000) indicating each subunit has its own independent function. In addition, MCM2-7 complex assembly has been demonstrated to be essential in *S. cerevisiae* as mutants that disrupt complex formation are not viable (Dalton and Hopwood, 1997, Lei et al., 2002).

The requirement for MCM proteins called for a detailed functional analysis. In *S. cerevisiae* studies utilising degron-tagged proteins, where immediately after production tagged proteins are directed for degradation, demonstrated that all six MCM genes are required for DNA replication initiation and elongation (Labib et al., 2000). Consistent with this, immunodepletion in *Xenopus* egg extracts showed that MCM proteins are required for replication initiation (Chong et al., 1995) and MCM7 was shown to be essential for replication elongation (Pacek and Walter, 2004). In *S. pombe*, little MCM2-7 is required for initiation but significant amounts are required for completion of DNA replication (Liang et al., 1999), suggesting that MCM2-7 is involved in events after replication initiation. This is

consistent with the idea that the MCM2-7 complex is a genomic DNA helicase (reviewed in Tye, 1999).

The six distinct classes of MCM proteins assemble in a ring conformation and examination of subunit pairs has led to the suggestion that the order of the MCM subunits in the ring is 5-3-7-4-6-2 (Fig. 1.3A, Davey et al., 2003). Later studies confirmed this subunit arrangement, using subunit dimer association experiments (Bochman et al., 2008) and negative stain electron microscopy (EM, Costa et al., 2011). The interaction between subunits MCM2 and MCM5 is weak (Davey et al., 2003, Bochman et al., 2008, Crevel et al., 2001) and the MCM2-7 ring appears to break open between these two subunits (Fig. 1.3B, Costa et al., 2011, Lyubimov et al., 2012, Samel et al., 2014). The opening between MCM subunits 2 and 5 is now commonly referred to as the '2/5 gate'. To date ring opening has not been seen in archaeal MCMs.

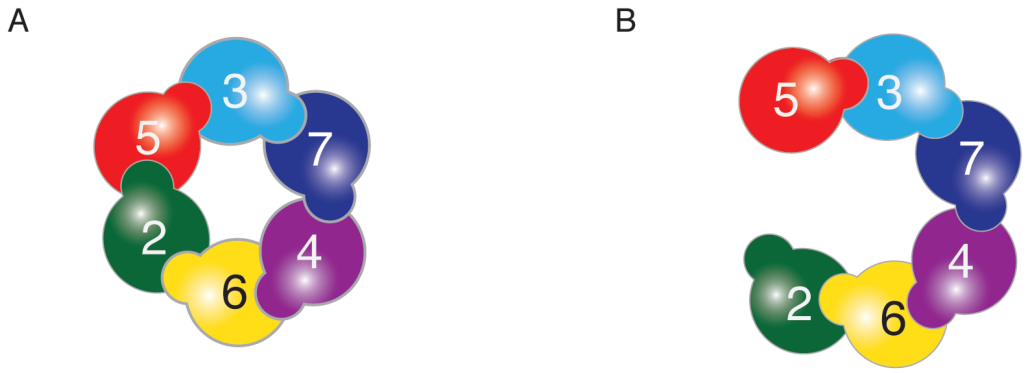


**Figure 1.3.** MCM2-7 subunit configuration. A. Schematic representation of the MCM2-7 heterohexamer. B. MCM2-7 heterohexamer opens at the '2/5 gate'.

MCM proteins are able to form sub-complexes. Purified *S. cerevisiae* MCM subunits form hexameric complexes containing just MCM4, 6 and 7 or just MCM4 and 7 *in vitro* (Bochman and Schwacha, 2008, Kanter et al., 2008, Biswas-Fiss et al., 2005). Sub-complexes of hexameric MCM have also been found *in vivo*. A dimer of trimers of MCM4, 6 and 7 has been purified from HeLa cells (Ishimi, 1997). However, this may be an unregulated form of MCM that only appears in cancer cells, as to date there is no evidence of this complex in 'normal cells'. It

appears that the dominant form of the MCM complex within cells is heterohexameric as when replication complexes are purified from *Drosophila melanogaster (Drosophila)* and *S. cerevisiae,* all six MCM subunits are present – as well as accessory proteins (Gambus et al., 2006, Moyer et al., 2006). In addition, only heterohexameric MCM2-7 is capable of inducing DNA replication in *Xenopus* egg extracts (Prokhorova and Blow, 2000).

As the eukaryotic replicative helicase, the MCM2-7 complex has been studied in great detail in a range of organisms. In addition to playing a key role in DNA replication, the eukaryotic MCM2-7 complex has been implicated in transcription (Fitch et al., 2003, Snyder et al., 2005), chromatin remodelling (Groth et al., 2007, Tan et al., 2006, Burke et al., 2001, Iizuka and Stillman, 1999) and genome stability including a role in DNA damage responses and checkpoint signaling (Honeycutt et al., 2006, Shima et al., 2007).

### 1.4.1 Localisation of MCM proteins

MCM2 and MCM3 have nuclear localisation sequences (NLS) in *S. cerevisiae* and mammals (Ishimi et al., 2001, Pasion and Forsburg, 1999, Takei and Tsujimoto, 1998, Young et al., 1997). However the NLS of MCM2 is not sufficient for transportation into the nucleus suggesting MCM2 must be complexed with other MCM subunits for transport (Pasion and Forsburg, 1999). MCM3 also contains a nuclear export sequence (NES, Liku et al., 2005). In cycling mammalian cells, MCM proteins are mainly nuclear (Kimura et al., 1994, Todorov et al., 1995, Fujita et al., 1996, Krude et al., 1996) and a large number of studies have shown MCM proteins to be stably bound to chromatin in G1 phase in a range of eukaryotes (Donovan et al., 1997, Chong et al., 1995, Symeonidou et al., 2013, Krude et al., 1996, Ohta et al., 2003, Kuipers et al., 2011, Mendez and Stillman, 2000). In *S. cerevisiae*, MCM proteins enter the nucleus at mitosis where they remain until the initiation of DNA synthesis, after which MCM proteins are exported to the cytoplasm (Dalton and Whitbread, 1995), presumably to prevent re-initiation by promiscuous MCM2-7-chromatin binding. In *S. pombe* and metazoans, MCM proteins remain in the nucleus throughout S phase (Lei and Tye, 2001) indicating that there are other mechanisms for regulating MCM2-7-chromatin binding.

Mammalian MCM proteins do not co-localise with newly synthesised DNA at the replication fork in isolated nuclei (Krude et al., 1996, Dimitrova et al., 1999). More recently consistent results were obtained using fluorescently tagged MCM proteins in living mammalian cells (Kuipers et al., 2011). Furthermore, the abundance of MCM proteins is far higher than other components of the pre-RC (Lei et al., 1996, Donovan et al., 1997) and excess MCM2-7 is loaded at each replication origin (reviewed in Laskey and Madine, 2003). These two observations raise questions regarding the function of MCM2-7 and together are commonly known as the 'MCM paradox'. There are a number of hypotheses to explain the MCM paradox. One hypothesis is at DNA replication initiation, the majority of MCM proteins are evicted from the replication foci and the remaining MCM proteins are undetectable (Dimitrova and Gilbert, 1999). Analysis of HeLa cells demonstrated that MCM proteins co-localise with newly synthesised DNA from the previous cell cycle, agreeing with this hypothesis (Aparicio et al., 2012). In both *Xenopus* and human cells, excess chromatin bound MCM proteins can be activated along with dormant origins when the cell experiences replication stress (Woodward et al., 2006, Ibarra et al., 2008, Ge et al., 2007) and checkpoint activation (Cortez et al., 2004). The MCM paradox has also lead to a hypothesis regarding the mechanism of MCM2-7 unwinding, suggesting that MCM2-7 complexes are located away from replication fork and pump ssDNA towards replication foci, i.e. where DNA is synthesised (reviewed in Laskey and Madine, 2003).

### 1.4.2 MCM complexes hydrolyse ATP

Each MCM subunit has an ATPase domain (Koonin, 1993) and is a member of the AAA+ superfamily of ATPases (Iyer et al., 2004, Erzberger and Berger, 2006). Crystal structures of the archaeal *Sulfolobus solfataricus* (*Sso*) MCM showed functional ATPase sites are formed between two MCM subunits (Brewster et al., 2008). One subunit contains both Walker A and Walker B motifs responsible for ATP binding and hydrolysis respectively (Neuwald et al., 1999, Walker et al., 1982) and the adjoining subunit contributes an essential arginine finger (Davey et al., 2003). No MCM subunit alone is capable of hydrolysing ATP, as it requires an arginine finger and P-loop motif in the neighbouring subunit (Davey et al., 2003).

The first *in vitro* analysis of the MCM complex able to hydrolyse ATP was from a sub-complex containing MCM4, 6 and 7 purified from HeLa cells (Ishimi, 1997). Subsequently ATP hydrolysis activity was demonstrated for homohexameric archaeal MCM complexes (Jenkinson and Chong, 2006, Kelman et al., 1999, Chong et al., 2000, Shechter et al., 2000, McGeoch et al., 2005, Kasiviswanathan et al., 2004). The Walker A motif contains a conserved lysine residue (K). When the conserved K is mutated to a glutamic acid (E), ATP hydrolysis by *Methanothermobacter thermautotrophicus* (*Mt*) MCM is significantly reduced (Chong et al., 2000). This essential residue is conserved from archaea to eukaryotes and subsequent work on *S. cerevisiae* confirmed the essentiality of the conserved K residue, as when mutated to an alanine (A) in one of the MCM subunits, ATP hydrolysis by MCM2-7 is notably reduced (Schwacha and Bell, 2001). Taken together this suggests each individual MCM subunit contributes to ATPase activity. Recently ATPase sites of different MCM subunits have been demonstrated to be essential in different stages of its loading and activation in *S. cerevisiae* (Kang et al., 2014, Coster et al., 2014). In *S. cerevisiae*, the ATP hydrolysis activity of MCM2-7 does not appear to be affected by the presence of DNA (Schwacha and Bell, 2001, Davey et al., 2003, Bochman and Schwacha, 2008). This contrasts with archaeal MCM complexes and eukaryotic MCM hexamers containing only MCM4, 6, 7 which have been shown to be stimulated by exogenous DNA (Ishimi et al., 1998, Lee and Hurwitz, 2000, Lee and Hurwitz, 2001, You et al., 2003, Liew and Bell, 2011, McGeoch et al., 2005, Kasiviswanathan et al., 2004).

### 1.4.3 MCM as a helicase

MCM proteins are members of the Superfamily 6 (SF6) helicases (reviewed in Singleton et al., 2007, Lyubimov et al., 2011). Robust helicase activity by MCM proteins was first demonstrated in archaea (Kelman et al., 1999, Chong et al., 2000, Shechter et al., 2000). Analysis of the K to E mutation, which inhibits ATP hydrolysis, also inhibits helicase activity, consistent with a role for ATP hydrolysis in DNA unwinding (Chong et al., 2000, You et al., 1999). However, mutation of the Walker A motif does not affect *in vivo* helicase activity in *S. pombe* (Gomez et al., 2002).

Early analysis showed that a sub-complex of eukaryotic MCM, presumably existing as a dimer of trimers containing only MCM4, 6, 7, possesses ATP-dependent DNA helicase activity (Lee and Hurwitz, 2001, You et al., 2003, Ishimi, 1997, Lee and Hurwitz, 2000). Moreover, addition of MCM2 or MCM2/5 to the MCM4, 6, 7 complex inhibited helicase activity suggesting a regulatory role for MCM2 and MCM5 (Lee and Hurwitz, 2000, Ishimi et al., 1998, Lee and Hurwitz, 2001) and, despite intense experimentation, helicase activity of heterohexameric MCM2-7 could not be detected. However, salt-sensitive DNA helicase activity of *S. cerevisiae* heterohexameric MCM2-7 purified after *Baculovirus* expression has been achieved (Bochman and Schwacha, 2008). To date, DNA unwinding activity of higher eukaryotic heterohexameric MCM2-7 alone has not been reported. However, a complex purified from *S. cerevisiae, Drosophila* and *Xenopus* containing all six MCM subunits as well as accessory proteins has been shown to have helicase activity (Gambus et al., 2006, Moyer et al., 2006, Pacek et al., 2006).

Analysis of archaeal MCM has yielded information regarding functional MCM residues as well as insight into the mechanism by which MCM unwinds DNA. *Mt*MCM forms a double hexamer, which is dependent on the N-terminus (Chong et al., 2000). Subsequently, formation of double hexamers has also been shown for complexes containing MCM4, 6, 7 from *S. pombe* (Lee and Hurwitz, 2001), heterohexameric *S. cerevisiae* MCM2-7 when loaded on to DNA (Remus et al., 2009, Evrin et al., 2009) and *Xenopus* heterohexameric MCM2-7 (Gambus et al., 2011). From the study of *Mt*MCM and a hexamer of MCM4, 6, 7 a preference for unwinding DNA in the 3′ – 5′ direction was identified (Chong et al., 2000, Ishimi, 1997). Also from the analysis of *Mt*MCM, a conserved domain known as the helix 2 insert (h2i) was identified and mutation of the h2i domain inhibits helicase activity but not ATP hydrolysis (Jenkinson and Chong, 2006).

## 1.5 MCM2-7 loading

In cycling cells the nucleus is 'licensed' for DNA replication in G1 phase when MCM2-7 is loaded onto chromatin (Chong et al., 1995). Loading of MCM2-7 is dependent on a number of accessory proteins that form a large protein machine known as the pre-RC. To ensure nuclear DNA is only replicated 'once per cell

cycle', pre-RCs can only form when CDK levels are low (in G1 phase, reviewed in Sclafani and Holzen, 2007).

*S. cerevisiae* have a closed mitosis, requiring proteins that would not normally do so, to cross the nuclear envelope (Byers and Goetsch, 1975). MCM subunits are good examples of such proteins and the *S. cerevisiae* MCM subunits possess significant insertions to cater to this requirement (Table 1.1). Moreover, in recent years a number of metazoan specific proteins have been discovered that are essential for MCM2-7 loading (reviewed in Shen and Prasanth, 2012). It is therefore not surprising that as well as a number of unifying similarities among all eukaryotes with regards to DNA replication, there are also a number of significant differences in the details regarding these systems. The pathway for MCM2-7 loading in metazoans is shown in fig. 1.4 and described below.

**Table 1.1. MCM amino acid insertions comparison of *S. cerevisiae* and Human (*Hs*) MCM.** The number of amino acids present in *S. cerevisiae* and human MCM2-7 are compared. In all MCM subunits other than MCM2 an increase in the number of amino acids in *S. cerevisiae* is observed. These extra amino acids are observed in the N-terminus of *S. cerevisiae* MCM subunits.

| MCM | *S. cerevisiae* (aa*) | *Human* (aa) | aa difference (*Sc-Hs*) | insertion locations |
|---|---|---|---|---|
| **2** | 868 | 904 | -36 (-4%) | C |
| **3** | 971 | 808 | 163 (20%) | N, C |
| **4** | 933 | 863 | 70 (8%) | N |
| **5** | 775 | 734 | 41 (6%) | N |
| **6** | 1017 | 821 | 196 (24%) | N, (C) |
| **7** | 845 | 719 | 126 (18%) | N |

* amino acids

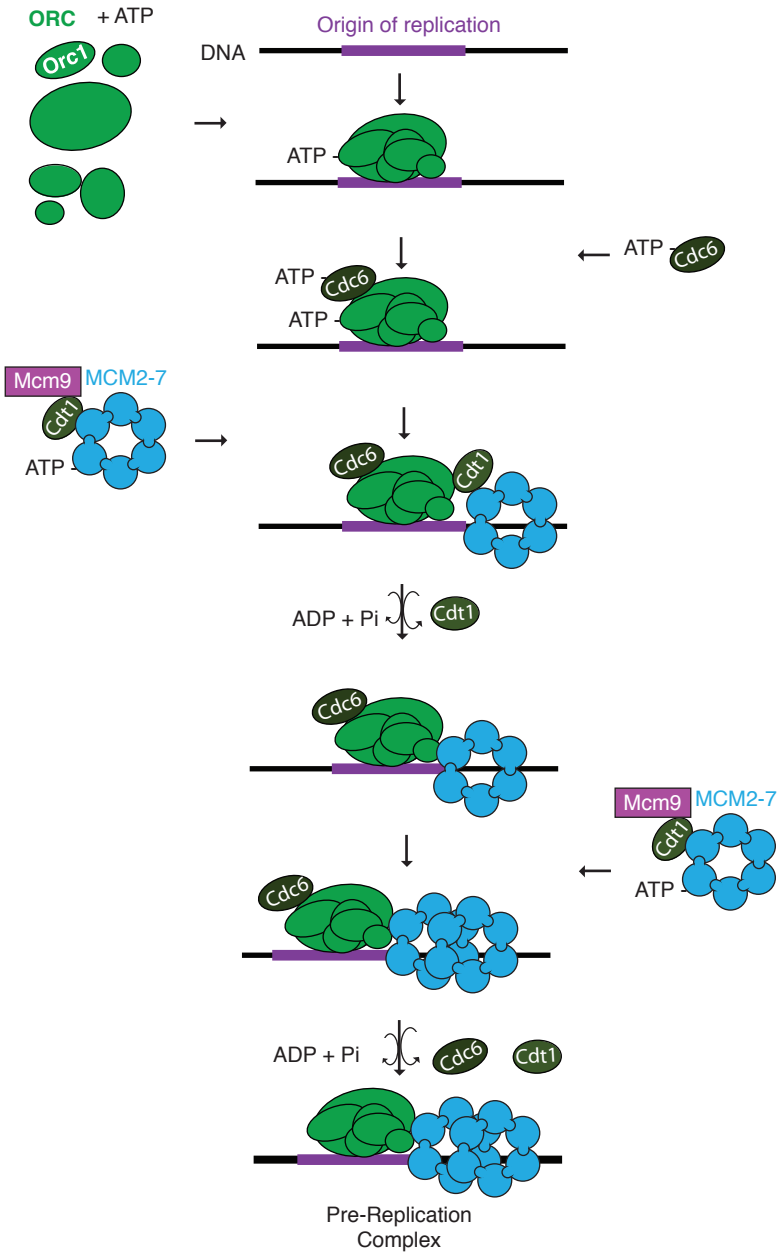


**Figure 1.4.** Pre-Replication Complex (pre-RC) assembly. ATP binding is required for the assembly of ORC subunits. ORC bound to ATP binds origin DNA and subsequently recruits Cdc6 (bound to ATP). Mcm9 assists Cdt1 in MCM2-7 binding with at least one MCM subunit bound to DNA. Cdt1 is released and MCM2-7 hydrolyses ATP before the second MCM2-7 is loaded making a double hexamer. Both Cdc6 and Cdt1 are released in addition to ATP hydrolysis by MCM2-7. For simplicity Geminin, HBO1, MCM8, and Hox-D13 are omitted. Adapted from Coster et al., 2014.

### 1.5.1 Origins

Replication origins specify where pre-RC components bind to chromatin and so where DNA replication begins. Due to the large size of eukaryotes genomes, replication originates at multiple chromosomal origins. In mammalian cells it is predicted there are tens of thousands of origins (reviewed in Edenberg and Huberman, 1975). This allows the full genome to be replicated in a relatively short period of time. In *S. cerevisiae*, origins are defined by an autonomous replication sequence (ARS, Stinchcomb et al., 1979) that contains the ARS consensus sequence (ACS, Deshpande and Newlon, 1992) and in *S. pombe*, origins contain an adenosine and thymidine rich segment (Chuang and Kelly, 1999, Lee et al., 2001). However in higher eukaryotes, origins are not simply defined by nucleotide sequence but appear to be defined by chromosomal environment and structure (reviewed in Mechali, 2010). Extensive evidence places origins at the nuclear matrix, a ribo-proteinaceous structure found in the nuclei of metazoans (reviewed in Wilson and Coverley, 2013, see section 1.9). Pre-RC assembly occurs in a stepwise manner (reviewed in Bell and Dutta, 2002) and begins by the binding of the Origin Recognition Complex (ORC) to origins.

### 1.5.2 ORC

ORC is essential for the initiation of DNA replication and for MCM2-7 binding to chromatin in higher eukaryotes (Carpenter et al., 1996, Rowles et al., 1996, Aparicio et al., 1997). ORC is a complex of six proteins (Orc1-6). Subunits 1 - 5 contain AAA+ ATPase domains (Iyer et al., 2004, Clarey et al., 2006). However in *S. cerevisiae* only Orc1 is capable of ATP hydrolysis (Speck et al., 2005, Randell et al., 2006). Orc6 is essential for MCM2-7 loading onto DNA in *S. cerevisiae* (Chen et al., 2007) but is not essential for ORC-origin binding (Lee and Bell, 1997). *S. cerevisiae* and *S. pombe* ORC have extremely high affinity for DNA and bind sequence specific origins and usually one ORC binds per origin (Rowley et al., 1995). ORC-origin binding is dependent on Orc1 binding ATP but not hydrolysis (Bell and Stillman, 1992, Lee and Bell, 1997, Klemm and Bell, 2001, Rowley et al., 1995). Using purified proteins from *S. cerevisiae*, ATP hydrolysis by ORC has been shown as non-essential for functional loading of MCM2-7 (Coster et al., 2014, Bowers et al., 2004, Evrin et al., 2013). Mammalian ORC requires ATP to

promote the ordered assembly of its subunits and stimulate DNA binding (Ranjan and Gossen, 2006, Vashee et al., 2001). However mammalian ORC does not appear to have specificity for a sequence and other unknown factors must affect its origin binding. This may be due to additional metazoan specific proteins such as HMGA1, which preferentially binds the minor groove of regions of DNA rich in adenosine and thymidine (Thomae et al., 2008).

The expression of Orc1 peaks in G1 phase, its activity is inhibited at the G1/S phase transition and it is degraded in S phase. The cell cycle dependent expression and activity of ORC is known as the 'ORC cycle' (reviewed in DePamphilis, 2003) and is an important mechanism used to ensure ORC only binds to origins in G1 phase once per cell cycle. In *S. cerevisiae*, phosphorylation of ORC by CDK causes inactivation (Nguyen et al., 2001, Wilmes et al., 2004, Chen and Bell, 2011).

### 1.5.3 Cdc6

The next step in MCM2-7 loading is the binding of Cell division cycle 6 (Cdc6) to ORC. In *S. cerevisiae, S. pombe* and metazoans, Cdc6 is essential for initiation of DNA replication and binding of MCM proteins to chromatin (Coleman et al., 1996, Cocker et al., 1996, Tanaka et al., 1997, Hateboer et al., 1998, Kelly et al., 1993, Lau et al., 2006, Santocanale and Diffley, 1996).

Cdc6 is an AAA+ ATPase (reviewed in Lee and Bell, 2000) and ATP hydrolysis by Cdc6 in *S. cerevisiae*, is essential for MCM2-7 loading (Randell et al., 2006, Seki and Diffley, 2000). In *S. cerevisiae* the initial function of Cdc6 is to ensure ORC is bound to origin DNA. Cdc6 preferentially binds to ATP bound Orc1 and so origin bound ORC (Klemm and Bell, 2001). In addition, when Cdc6 binds ORC bound to non-origin DNA, Cdc6 hydrolyses ATP and dissociates (Speck and Stillman, 2007) and so Cdc6 binding increases the origin sequence specificity of ORC (Mizushima et al., 2000, Speck et al., 2005). A stable interaction between Cdc6 and origin bound ORC requires ATP binding by Cdc6 (Evrin et al., 2013, Coster et al., 2014, Frolova et al., 2002), but not ATP hydrolysis (Kang et al., 2014). Structural studies of *S. cerevisiae* proteins indicate together ORC and Cdc6 make a

ring shaped structure, which is similar to the surface of MCM2-7 (Speck et al., 2005). This is predicted to act as a MCM2-7 loading machine.

In *S. cerevisiae*, Cdc6 is phosphorylated by CDK when cells pass into S phase causing release from origins, ubiquination and degradation (Drury et al., 1997, Weinreich et al., 2001). Over expression of Cdc6 in *S. cerevisiae* causes re-initiation (Nishitani et al., 2000). In addition to Cdc6 degradation, in mammalian cells the localisation of Cdc6 is also controlled by CDK phosphorylation (Pelizon et al., 2000, Delmolino et al., 2001). Free Cdc6 not bound to origins is destroyed by proteolysis triggered specifically by cyclin A/CDK2 in S phase (Coverley et al., 2000). However analysis of cancer cell lines, show Cdc6 is protected from degradation by cyclin E/CDK2 dependent phosphorylation (Mailand and Diffley, 2005).

### 1.5.4 Cdt1

The next step in MCM2-7 loading involves Cdc10-dependent transcription factor (Cdt1). Cdt1 was first identified as an essential component of the replication licensing factor in *Xenopus* egg extracts (Chong et al., 1995) and is required after Cdc6 and ORC for DNA replication initiation (Chong et al., 1995, Tada et al., 1999). Subsequently Cdt1 homologues were discovered in *S. pombe* (Nishitani et al., 2000), *S. cerevisiae* (Tanaka and Diffley, 2002), *Drosophila* (Whittaker et al., 2000) and mammals (Cook et al., 2004).

In *S. cerevisiae*, Orc6 contains two binding sites for Cdt1 (Chen et al., 2007, Takara and Bell, 2011). Cdt1 is also capable of binding MCM2-7 prior to loading (Tanaka and Diffley, 2002, Remus et al., 2009), leading to the suggestion that the main role of Cdt1 is as a chaperone for guiding MCM2-7 to ORC-Cdc6 (Chen and Bell, 2011). A more recent study suggests MCM2-7-Cdt1 initially binds chromatin via an interaction between the C-terminal of MCM3 and ORC-Cdc6 (Frigola et al., 2013), suggesting Cdt1 is not required for initial MCM2-7 recruitment. In addition Cdt1 binding to MCM2-7 is not sufficient for MCM2-7 origin binding (Evrin et al., 2013). Following MCM2-7 loading Cdt1 is released from chromatin by the hydrolysis of ATP by Cdc6 (Randell et al., 2006). Metazoan Cdt1 has also been shown to interact with MCM2-7 (Cook et al., 2004), specifically MCM6

(Yanagi et al., 2002, Teer and Dutta, 2008, Ferenbach et al., 2005) and this interaction facilitates MCM2-7 loading onto chromatin by inducing a conformational change in MCM6 (Zhang et al., 2010).

Cdt1 accumulates in G1 and is destabilised after initiation or exported from the nucleus in *S. cerevisiae* and *S. pombe* (Nishitani et al., 2001, Tanaka and Diffley, 2002). In these lower eukaryotes, cellular location appears to be the main mechanism for controlling Cdt1 (reviewed in Blow and Dutta, 2005). However in metazoans, if excess Cdt1 is present in S phase or G2 it causes illegitimate re-replication (Arias and Walter, 2005, Li and Blow, 2005, Maiorano et al., 2005, Yoshida et al., 2005, Lutzmann et al., 2006). Cdt1 is the only member of the pre-RC that is capable of this in metazoans and so cells have evolved numerous mechanisms for Cdt1 regulation. In both *Xenopus* and human cells, Cdt1 is negatively regulated by ubiquitination-mediated proteolysis when cells enter S phase (Arias and Walter, 2005, Nishitani et al., 2006, Arias and Walter, 2006, Senga et al., 2006). In human cells, Cdt1 is also degraded in G2, mediated by FBXO31 which ubiquitinates Cdt1 (Johansson et al., 2014).

The action of Cdt1 is also controlled by Geminin, a metazoan specific protein expressed in S and G2 phase (Wohlschlegel et al., 2000, Tada et al., 2001). Geminin binds Cdt1 in a 2:1 complex (Lee et al., 2004), which dimerises to mask Cdt1 regions required for initiation (De Marco et al., 2009).

### 1.5.5 MCM2-7

Together Cdt1 and MCM2-7 are bound to chromatin. In *S. cerevisiae* ATP hydrolysis by Cdc6 promotes a stable association of MCM2-7 with DNA (Bowers et al., 2004, Randell et al., 2006), presumably mediating the transition from chromatin bound MCM2-7 to loaded MCM2-7 (Fernandez-Cid et al., 2013). ATP hydrolysis by ORC is required for MCM2-7 loading (Bowers et al., 2004, Evrin et al., 2013). A recent study of *S. cerevisiae* MCM2-7 analysed the individual MCM ATP binding and hydrolysis sites between each MCM subunit ATPase motif. As two MCM subunits contribute to ATP hydrolysis activity, analysis of the effect of MCM ATP binding and hydrolysis was assessed between subunit pairs. Only mutants between subunits MCM3/7 did not effect MCM loading and so ATPase

activity in all four other subunit interfaces are required (Kang et al., 2014). This work demonstrates ATPase sites of different MCM subunits are implicated and essential in different stages of its loading and activation (Kang et al., 2014). Conversely, in a *Xenopus* cell free system MCM2-7 ATPase activity is not required for pre-RC formation (Ying and Gautier, 2005). Following MCM2-7 loading, Cdc6 and Cdt1 are released from chromatin when washed with high salt but MCM2-7 remains bound demonstrating a strong chromatin association (Remus et al., 2009, Evrin et al., 2009, Kawasaki et al., 2006, Bowers et al., 2004, Donovan et al., 1997), that could reflect encircling of DNA.

In *S. cerevisiae* and *Xenopus* egg extracts MCM2-7 complexes have been shown to load as a double hexamer encircling double stranded (ds) DNA (Evrin et al., 2009, Remus et al., 2009, Gambus et al., 2011). Once MCM2-7 is loaded it can slide along the dsDNA but not unwind it in an ATP independent manner (Remus et al., 2009, Evrin et al., 2009) suggesting another catalytic event is required to separate the double hexamer and stimulate DNA helicase activity. The current hypothesis is the MCM2-7 complex must open at the 2/5 gate in order to encircle chromatin. A recent study of *S. cerevisiae* MCM2-7, which biochemically links subunits MCM2 and MCM5, demonstrates opening of the MCM2-7 ring between 2/5 is essential for pre-RC loading (Samel et al., 2014). In *S. cerevisiae*, opening and closing the MCM2/5 gate has been shown to be dependent on ATP (Bochman and Schwacha, 2010, Bochman et al., 2008) but ATP binding does not open the gate in *Drosophila* or *Encephalitozoon cuniculi* (*E. cuniculi,* Costa et al., 2011, Lyubimov et al., 2012).

Following MCM2-7 loading in *S. cerevisiae,* ORC, Cdc6 and Cdt1 dissociate from DNA and this is dependent on ATP hydrolysis (Tsakraklides and Bell, 2010). *S. cerevisiae* MCM2-7 loading is not ATP dependent suggesting MCM2-7 loading and double hexamer formation are separate events (Samel et al., 2014). Binding and hydrolysis of ATP by MCM2-7 purified from *S. cerevisiae* has been shown to be required for Cdt1 release and infers a conformational change and double hexamer formation (Coster et al., 2014, Evrin et al., 2014). In addition, ATP hydrolysis by Orc1 is required for Cdt1 release and the binding of the second MCM2-7 (i.e. double hexamer formation, Fernandez-Cid et al., 2013). If MCM2-7-

Cdt1 is not loaded correctly on chromatin ATP hydrolysis by Cdc6 releases the incorrectly loaded MCM2-7 (Kang et al., 2014). MCM ATP hydrolysis, particularly by MCM5, is required for Cdt1 release and successful MCM2-7 loading (Kang et al., 2014), suggesting an interaction between MCM5 and Cdt1. Moreover, using EM a complex of MCM2-7, Cdt1, Cdc6 and ORC show Cdt1 is in close proximity to MCM5 (Sun et al., 2013). The formation of MCM2-7 double hexamer appears to be the limiting step in pre-RC assembly (Evrin et al., 2014). This recent work suggests loading of the first MCM2-7 is not dependant on ATP hydrolysis but is dependant on ORC, Cdc6 and Cdt; however, whether loading of the second MCM2-7 complex requires Cdc6 and Orc is not known (reviewed in Riera et al., 2014, Yardimci and Walter, 2014).

Initial studies implied ORC was able to remodel DNA prior to MCM2-7 loading and so provided initial DNA duplex opening (Lee and Bell, 1997, Rowley et al., 1995). However, MCM2-7 loads as a double hexamer and recent results demonstrate ORC can be eluted from DNA after MCM2-7 loading, and before unwinding, suggesting ORCs essential job is in pre-RC assembly (Gros et al., 2014). Indicating that initial unwinding is dependent on MCM2-7.

### 1.5.6 Metazoan specific proteins involved in MCM2-7 loading

There are a number of newly identified proteins, specific to metazoans that are involved in controlling MCM2-7 loading (reviewed in Shen and Prasanth, 2012). Many of these proteins, like Geminin (Wohlschlegel et al., 2000), appear to specifically modulate Cdt1. For example MCM9, a metazoan specific MCM2-7 homologue, was shown to be required for MCM2-7 loading in *Xenopus* egg extract (Lutzmann and Mechali, 2008). MCM9 is an activating binding partner for Cdt1 appearing to have an opposing role to Geminin (Lutzmann and Mechali, 2008). However, a second study in *Xenopus* egg extract demonstrates MCM9 is not essential for DNA replication initiation and an interaction with Cdt1 could not be found (Gambus and Blow, 2013). Consistent with this, MCM9 is dispensable for DNA replication initiation in mouse cells (Hartford et al., 2011).

Histone acetylase binding to Orc1 protein (HBO1) interacts with Orc1 (Iizuka and Stillman 1999). Knockdown of HBO1 in mammalian cells has no effect on ORC

and Cdc6 chromatin binding but affects MCM2-7 loading (Iizuka et al., 2008). HBO1 associates with origins in G1 phase and interacts with Cdt1 (Miotto and Struhl, 2008), suggesting the role of HBO1 is to assist Cdt1 in MCM2-7 loading (Miotto and Struhl, 2008, Wu and Liu, 2008, Iizuka et al., 2008).

In addition MCM8, another MCM2-7 homologue, is believed to facilitate Cdc6 loading and interacts with Cdc6, Orc2 and MCM4, 6, 7 (Kinoshita et al., 2008, Volkening and Hoffmann, 2005). However a recent study in *Xenopus* egg extracts demonstrates MCM8 is not essential for DNA replication initiation (Gambus and Blow, 2013). Homobox protein Hox-D13 (HOXD13) is also believed to facilitate Cdc6 loading (Salsi et al., 2009).

## 1.6 MCM2-7 activation

Once loaded onto chromatin, MCM2-7 remains inactive until the initiation of DNA replication at the G1/S boundary (reviewed in Boos et al., 2012, Li and Araki, 2013, Labib, 2010). The temporal separation of MCM2-7 loading and activation stops cells from re-loading MCM2-7 once the cell passes into S phase ensuring once per cell cycle DNA replication (Bell and Stillman, 1992, Diffley et al., 1994). It has been suggested this gap is also used to ensure enough MCM2-7 is loaded to replicate the whole genome before passing into S phase (Ge and Blow, 2009, Liu et al., 2009).

As discussed above, MCM2-7 complexes are loaded as a double hexamer presumably to provide a mechanism for bi-directional replication. However, some evidence suggests otherwise. In *S. cerevisiae* and human cells, live cell imaging suggests sister replication forks stay close together during replication (Kitamura et al., 2006, Ligasova et al., 2009). In addition, coupling of sister chromatids is not required for replication as replication was equally efficient whether one or both ends of the DNA are immobilised (Yardimci et al., 2010).

DDK in *S. cerevisiae* is referred to as the 'activating' kinase. However DDK activity alone is not sufficient for separating MCM2-7 double hexamers, although it does stimulate a small conformational change (On et al., 2014). Together, the

cellular kinases DDK and CDK appear to control the formation of the Cdc45-MCM2-7-GINS (CMG) complex via the pre-Loading Complex (pre-LC, Muramatsu et al., 2010) and the pre-Initiation Complex (pre-IC, Zou and Stillman, 1998). Much less is known about the formation of the pre-LC, pre-IC and CMG complex, particularly in metazoans. What is known about CMG assembly in *S. cerevisiae* is detailed below and shown in fig 1.5.

### 1.6.1 Pre-IC

In *S. cerevisiae*, the pre-IC is a large protein machine that requires DDK to assemble (Zou and Stillman, 2000). *S. cerevisiae* pre-IC consists of Cell division cycle 45 (Cdc45), Synthetically lethal with Dpb11 (Sld)3, Sld7 and MCM2-7 (Kamimura et al., 2001, Kanemaki et al., 2003, Zou and Stillman, 2000, Tanaka et al., 2011). Sld3 and Cdc45 are able to bind to MCM2-7 in late G1 phase when the levels of CDK are low (Aparicio et al., 1999, Kamimura et al., 2001, Kanemaki and Labib, 2006, Heller et al., 2011, Tanaka and Araki, 2011) and this binding is promoted by DDK activity (Gros et al., 2014, Heller et al., 2011). Consistent with this, *S. pombe* Sld3 requires DDK phosphorylation but not CDK phosphorylation for chromatin binding and DNA replication initiation (Nakajima and Masukata, 2002). However chromatin association of the Sld3 metazoan homologue, Treslin/Ticrr (Kumagai et al., 2010, Kumagai et al., 2011, Sanchez-Pulido et al., 2010, Boos et al., 2011), is dependent on phosphorylation by CDK (Kumagai et al., 2010). In a similar way to *S. cerevisiae*, Treslin/Ticrr binds Cdc45 and is required for association of Cdc45 with chromatin (Kumagai et al., 2010, Sanchez-Pulido et al., 2010). MTBP is a metazoan specific protein that has been suggested as a candidate for the homologue of Sld7 due to its association with Treslin/TICRR (Boos et al., 2013).

### 1.6.2 Pre-LC

The pre-LC assembles away from chromatin. In *S. cerevisiae*, the pre-LC consists of Sld2, DNA polymerase B possible subunit 11 (Dpb11), polymerase (pol) ε and Go-Ichi-Ni-San (GINS) and its assembly is dependent on CDK and DDK (Muramatsu et al., 2010). Origin binding of Sld2 and Dbp11 is dependent on both DDK and CDK activities (Gros et al., 2014, Zegerman and Diffley, 2007, Tanaka et

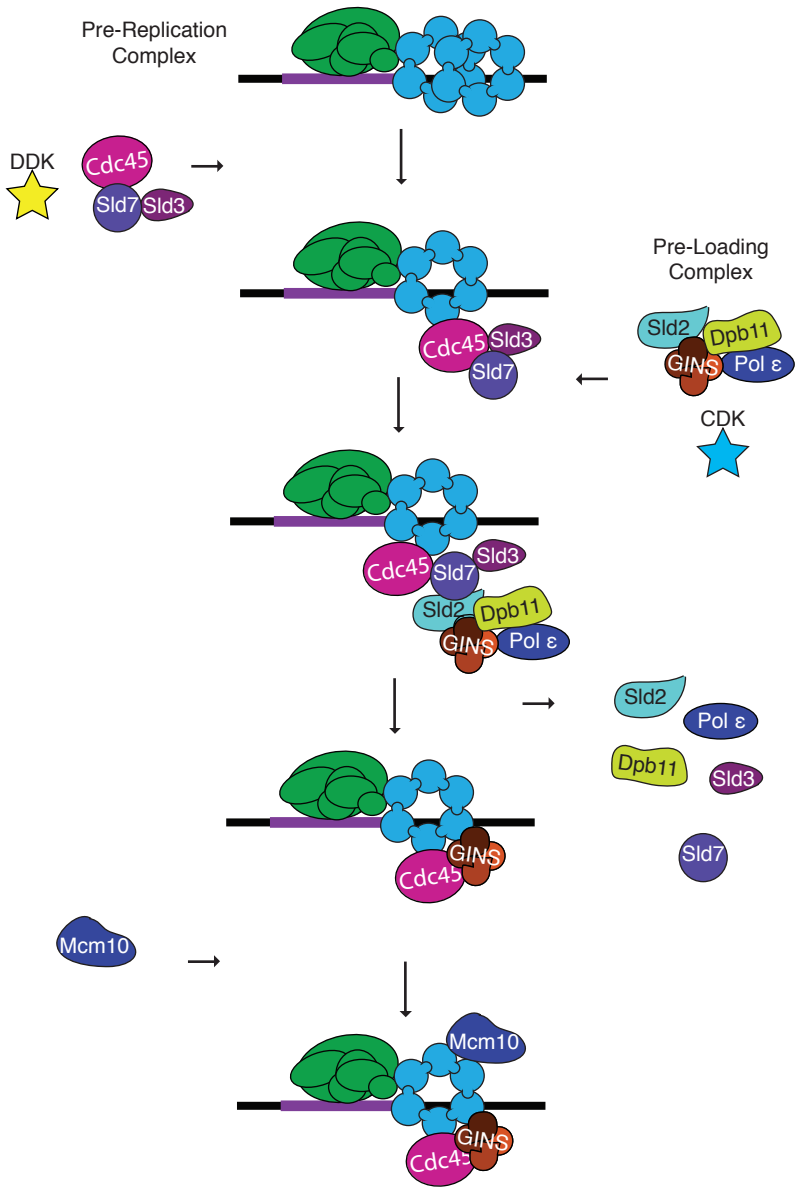


**Figure 1.5**. Assembly of Cdc45-MCM2-7-GINS (CMG) complex based on analysis in *S. cerevisiae*. MCM2-7 is loaded as an inactive double hexamer. Activation involves the binding of Sld3-Sld7-Cdc45 complex to each MCM2-7 hexamer (for simplicity only one is shown). This is dependent on DDK activity. The pre-Loading Complex (pre-LC) composed of Sld2, Dpb11, GINS and polymerase DNA Pol ε form the pre-Initiation Complex (pre-IC) on chromatin in a CDK-dependent manner. Components of the pre-IC are released leaving the CMG complex. Mcm10 binds to chromatin following CMG formation. Adapted from Li and Araki 2013.

al., 2007). This agrees with cell cycle studies showing that Sld2 and Dbp11 bind to chromatin during initiation when both CDK and DDK are present (Tanaka et al., 2007, Zegerman and Diffley, 2007, Muramatsu et al., 2010).

In metazoans RecQ4 is the homologue of Sld2. RecQ4s interaction with chromatin is dependent on TopBP1 (metazoan Dpb11 homologue) and independent of CDK activity (Matsuno et al., 2006, Sangrithi et al., 2005), in contrast to the function of Sld2 in *S. cerevisiae*, which is dependent on CDK activity. RecQ4 has also been shown to associate with chromatin after GINS and Cdc45 loading and depletion of RecQ4 in *Xenopus* egg extracts did not affect Cdc45 and GINS loading (Sangrithi et al., 2005). However in human cells, depletion of RecQ4 significantly reduced Cdc45 and GINS chromatin loading (Im et al., 2009). Agreeing with *S. cerevisiae* data, RecQ4 has been shown to be essential for DNA replication initiation in *Drosophila* and *Xenopus* (Wu et al., 2008, Sangrithi et al., 2005).

In human cells TopBP1 is essential for activation of cyclin E/CDK2 and the loading of replication components onto chromatin (Jeon et al., 2007) suggesting TopBP1 behaves similarly to Dpb11. In addition TopBP1 knockout mice exhibited early embryonic lethality (Jeon et al., 2011). However the essentiality of TopBP1 in human cells has been controversial. In two different osteosarcoma cell lines (Saos-2 and U2OS cells) depletion of TopBP1 using siRNA demonstrated cell cycle arrest at the G1/S phase transition showing TopBP1 is essential for DNA replication initiation (Jeon et al., 2007, Kumagai et al., 2010). Conversely another study analysing aggressive cervical carcinoma cells (HeLa), again using siRNA to deplete TopBP1, demonstrated TopBP1 had no effect on CMG formation (Im et al., 2009) suggesting, in this cell line, TopBP1 is not essential for DNA replication initiation.

In *S. cerevisiae*, the pre-LC is recruited to origins via an interaction between Dpb11 and origin bound Sld3 (Tanaka et al., 2007, Zegerman and Diffley, 2007, Tanaka and Araki, 2010). This is dependent on Sld3 phosphorylation by DDK (Heller et al., 2011). Consistent with this, binding of Treslin/Ticrr (Sld3) to chromatin in metazoans is independent of TopBP1 (Dbp11) chromatin binding

(Kumagai et al., 2010). In addition TopBP1 and Treslin/Ticrr associate in *Xenopus* egg extracts (Kumagai et al., 2010). It appears the main function of the pre-IC and pre-LC is to form the CMG complex as all proteins other than Cdc45, MCM2-7 and GINS disassociate from chromatin soon after binding (Kanemaki and Labib, 2006, reviewed in Labib, 2010).

### 1.6.3 Cdc45

*S. cerevisiae* and *Xenopus* Cdc45 have been shown to be required for initiation and replication fork progression (Aparicio et al., 1997, Labib et al., 2000, Pacek and Walter, 2004). Moreover, in human cells Cdc45 is a limiting factor for DNA replication initiation (Wong et al., 2011). Cdc45 is unique in replication proteins as it can be re loaded at replication origins where previously lost (Tercero et al., 2000). *S. cerevisiae*, *Xenopus* and human Cdc45 is recruited to chromatin in G1 phase and at initiation tightly associates with origin DNA dependent on DDK and CDK activities (Jares and Blow, 2000, Masuda et al., 2003, Owens et al., 1997, Aparicio et al., 1999, Zou and Stillman, 2000, Sheu and Stillman, 2006, Walter and Newport, 2000, Im et al., 2009). Recently Cdc45 has been shown to contain a conserved RecJ exonuclease domain that is catalytically inactive but is capable of binding ssDNA (Sanchez-Pulido and Ponting, 2011, Krastanova et al., 2012, Szambowska et al., 2014).

Knockout of Cdc45 in mice is embryonically lethal (Yoshida et al., 2001). Cdc45 is degraded in quiescent human cells and once the cell passes the restriction point, expression of Cdc45 increases until S phase (Pollok et al., 2007). In mammalian cells Cdc45 is also controlled by ubiquitin mediated degradation (Pollok and Giosse, 2007).

### 1.6.4 GINS

GINS is a tetramer comprising Partner of Sld five (Psf)1, Psf2, Psf3 and Sld5 subunits (Kanemaki et al., 2003, Kubota et al., 2003, Takayama et al., 2003, Labib and Gambus, 2007). GINS is highly conserved from *S. cerevisiae* to humans (Kubota et al., 2003, Takayama et al., 2003). The structure of human GINS has been solved by x-ray crystallography demonstrating a stable complex (Kamada

et al., 2007). In the absence of DNA, *S. cerevisiae* GINS has a high ATP independent affinity for MCM2-7 (Bruck and Kaplan, 2011). GINS is required for recruiting pol ε to origins (Kanemaki and Labib, 2006). In human cells, GINS is expressed in cycling cells and depleted in quiescent cells (Aparicio et al., 2009). Down regulation of GINS in human cells impairs entry to S phase and S phase progression (Aparicio et al., 2009), suggesting a role in both initiation and elongation of DNA replication.

### 1.6.5 MCM10

The involvement of MCM10 in origin activation is unclear. Some studies in *S. cerevisiae* suggest MCM10 binds to pre-RCs in G1 phase (van Deursen et al., 2012, Ricke and Bielinsky, 2004). Moreover in human cells MCM10 has been shown to promote Cdc45 and RecQ4 (Sld2) chromatin binding (Xu et al., 2009). However other studies in *S. cerevisiae* and *S. pombe* suggest the role of MCM10 comes much later following CMG formation and is dependent on both CDK and DDK (Watase et al., 2012, Heller et al., 2011, Gros et al., 2014, Kanke et al., 2012). In *S. cerevisiae*, MCM10 has also been shown to regulate the association of Pol α with chromatin (Eisenberg et al., 2009).

### 1.6.6 Ctf4

Ctf4 is conserved in eukaryotes. In *S. cerevisiae* it is not essential for viability (Gambus et al., 2009). In mammalian cells, Ctf4 is required for both CMG assembly and Pol α chromatin recruitment (Im et al., 2009). After initiation Ctf4 moves with the replication fork and is believed to be involved in linking Pol α to MCM2-7 in *S. cerevisiae* (Gambus et al., 2009, Tanaka et al., 2009). Using both EM and X-ray crystallography, a recent study shows *S. cerevisiae* Ctf4 naturally forms a trimer and provides a link between CMG and two Pol α molecules (Simon et al., 2014).

### 1.6.7 Metazoan specific initiation proteins

A geminin related protein, geminin coiled coil containing protein (GEMC1), is required for initiation in *Xenopus* egg extracts and mouse cells in culture (Balestrini et al., 2010). GEMC1 is phosphorylated by CDK *in vitro* and co-

immunopreticipates with cyclin E/CDK2 from *Xenopus* egg extract (Balestrini et al., 2010). TopBP1 promotes GEMC1 chromatin binding stimulating DNA replication initiation (Balestrini et al., 2010, Piergiovanni and Costanzo, 2010).

DUE-B (DNA unwinding element binding protein) is required for the association of Cdc45 and TopBP1 with chromatin in *Xenopus* eggs (Chowdhury et al., 2010). Levels of DUE-B in human cancer cells remained constant throughout the cell cycle with preferential phosphorylation of DUE-B in cells arrested in S phase (Casper et al., 2005). Inhibition of DUE-B in human cancer cells slowed G1 - S phase progression and induced cells to die in S phase (Casper et al., 2005).

### 1.6.8 CMG activation

*In vivo*, the ability of MCM2-7 to processively unwind DNA is hypothesised to only be possible when associated with both Cdc45 and GINS in the CMG complex. Comparison of the helicase activity of MCM2-7 alone and CMG complex purified from *Xenopus* egg extract demonstrates significantly higher DNA unwinding activity when MCM2-7 is in a complex with Cdc45 and GINS (Ilves et al., 2010). Also, following initiation Cdc45, GINS and MCM2-7 move with the replication fork (Gambus et al., 2006, Kanemaki et al., 2003, Labib et al., 2000, Takayama et al., 2003).

S. *cerevisiae*, *Drosophila* and *Xenopus* replication complexes have been shown to contain a single MCM2-7 hexamer within the CMG complex (Gambus et al., 2006, Moyer et al., 2006, Pacek et al., 2006). Using *Xenopus* egg extracts CMG has been shown to translocate along template DNA in 3′ to 5′ direction (Fu et al., 2011). 'Roadblocks' on the leading strand, but not the lagging strand, inhibited CMG mediated unwinding (Fu et al., 2011), if the CMG translocated along dsDNA a roadblock on either strand would inhibit unwinding. Purified human CMG complex has also been shown to have a preference for unwinding DNA on the leading strand opposed to the lagging strand (Kang et al., 2012). Moreover, EM reconstructions of *Drosophila* and *E. cuniculi* MCM2-7 found in an open ring conformation, which is closed in EM reconstructions of CMG (Costa et al., 2011, Lyubimov et al., 2012). Suggesting Cdc45 and GINS close the open ring of MCM2-7 to induce a conformational change and a side channel, which is

hypothesised to partition the lagging strand for DNA unwinding (Costa et al., 2011). A recent EM study identified *Drosophila* CMG complexes in both dimer and single CMG when analysed in the presence on a non-hydrolysable ATP analogue (Costa et al., 2014), suggesting formation of the CMG is not sufficient for splitting the double hexamer.

## 1.7 Phosphorylation of MCM proteins

Exactly how MCM2-7 double hexamers separate and are activated to unwind DNA is not understood. Many lines of evidence suggest the precise phosphorylation of MCM2-7 proteins directly affect the activity of MCM2-7 in terms of, i) MCM2-7 ring opening and loading, ii) MCM2-7 ring closing around single stranded and double stranded DNA and iii) MCM2-7 activation for duplex unwinding.

Protein kinases CDK and DDK control MCM2-7 loading and activation in all eukaryotes. A number of studies have analysed the effects of CDK and DDK on MCM proteins (reviewed in Labib, 2010, Araki, 2010). This work has been controversial and it would seem the concentration as well as order of kinase addition has an effect on phosphorylation (reviewed in Sclafani and Holzen, 2007).

### 1.7.1 Phosphorylation by DDK

MCM2-7 is a crucial target of Cdc7 and many subunits are phosphorylated during DNA replication initiation (reviewed in Forsburg, 2004, Labib, 2010). Initially, biochemical studies indicated MCM proteins were important targets for Cdc7 (Sato et al., 1997, Brown and Kelly, 1998, Takeda et al., 1999) and phosphorylation of MCM2 by Cdc7 is thought to be physiologically important (Lei et al., 1997, Hardy et al., 1997, Masai and Arai, 2002). In *S. cerevisiae*, DDK has been shown to interact with MCM2 and phosphorylate MCM2 *in vivo* and *in vitro* (Brown and Kelly, 1998, Lei et al., 1997). Subsequently *in vitro* phosphorylation of *S. cerevisiae* MCM3, MCM4, MCM6 and MCM7 was demonstrated (Weinreich and Stillman, 1999, Young and Tye, 1997). MCM5 has not been shown to be phosphorylated by DDK in any species. In *Xenopus* egg

extract and mammalian cells Cdc7 has been shown to phosphorylate MCM2, 4 and 6 complex proteins (Masai et al., 2000, Montagnoli et al., 2006, Takahashi and Walter, 2005, Takeda et al., 1999, Walter, 2000, Ishimi and Komamura-Kohno, 2001, Randell et al., 2010, Cho et al., 2006).

Dbf4 interacts with MCM2-7 complex via conserved motifs (Varrin et al., 2005, Jones et al., 2010). Dbf4 and Cdc7 have been shown to have differential binding partners within the *S. cerevisiae* MCM2-7 hexamer. Dbf4 interacts most strongly with MCM2 (Bruck and Kaplan, 2009, Ramer et al., 2013). Whereas MCM4 and MCM5 interact most strongly with Cdc7 (Ramer et al., 2013), suggesting a mechanism to recruit both Cdc7 and Dbf4 to the pre-RC. In addition mutation of Cdc7 and Dbf4 binding sites in MCM proteins strongly inhibits cell growth in *S. cerevisiae* (Ramer et al., 2013). This indicates spatial regulation of DDK is an important feature of its regulation. Studies suggest that the phosphorylation of MCM proteins differs depending on the context. For example, when MCM2-7 is origin bound, MCM4 and MCM6 are preferentially phosphorylated (Francis et al., 2009). Whereas when MCM2-7 is free from chromatin MCM2 phosphorylation is preferential (Francis et al., 2009).

In *S. cerevisiae* a requirement for Cdc7 is partially bypassed by introducing mutant MCM5 containing a substitution of Proline 83 to a Lysine, this mutant is known as the MCM5-bob1 mutant (Hardy et al., 1997, Hoang et al., 2007). As MCM5 itself is not phosphorylated by DDK, it is hypothesised the MCM5-bob1 mutant bypasses the requirement for DDK by causing a conformational change in the MCM2-7 complex (Hardy et al., 1997, Hoang et al., 2007). Crystal structures of *Mt*MCM further support the idea that MCM5-bob1 mutation may induce a conformational change (Fletcher et al., 2003, Chen et al., 2005). Furthermore, mutation of a DDK phosphorylation site in MCM2 at Ser170 causes lethality in *S. cerevisiae* (Bruck and Kaplan, 2009). This lethality is bypassed by the addition of the MCM5-bob1 mutant (Bruck and Kaplan, 2009).

### 1.7.2 MCM4 phosphorylation

A number of studies suggest that in *S. cerevisiae* and *S. pombe* MCM4 is the primary target for DDK during DNA replication initiation (Francis et al., 2009,

Masai et al., 2000, Masai et al., 2006, Sheu and Stillman, 2006, Lee et al., 2003). MCM4 has also been shown to be phosphorylated by DDK in *Xenopus* extracts (Pereverzeva et al., 2000). The N-terminal of MCM4 is not conserved but is rich in serine and threonine (24% of hMCM4's first 148 amino acids) and contains multiple Cdc7 phosphorylation motifs (reviewed in Labib, 2010). The N-terminal of MCM4 also contains sites where CDK could prime MCM4 for phosphorylation by Cdc7 (Masai et al., 2000, Devault et al., 2008).

The initial biochemical effects of phosphorylation were noted by phosphorylation at CDK dependent sites on MCM4 which lead to loss of helicase activity of mouse MCM4, 6, 7 (Ishimi and Komamura-Kohno, 2001). Subsequent experiments demonstrated that in *S. cerevisiae*, the association of MCM2-7 with Cdc45 and Sld3 is stimulated by DDK activity (Sheu and Stillman, 2006, Heller et al., 2011). DDK binds to MCM4 via a kinase-docking domain, preferentially when MCM2-7 is origin bound (Sheu and Stillman, 2006, Masai et al., 2006). This allows significant phosphorylation by DDK in the N-terminal domain of MCM4 (Sheu and Stillman, 2006). The N-terminal domain of MCM4 has been shown to be inhibitory in MCM2-7-Cdc45 binding and DDK dependent phosphorylation of N-terminal MCM4 alleviates this inhibition (Sheu and Stillman, 2010).

### 1.7.3 MCM2 phosphorylation

MCM2 phosphorylation is noted by its unusual increased mobility shift in SDS PAGE (Coverley et al., 2002 and others). This form of MCM2 is detected in S phase through to mitosis (Masai et al., 2006). Analysis of mouse MCM2 demonstrated that the N-terminal portion of the protein contains major phosphorylation sites (Ishimi et al., 2001). This work led to a number of studies that have investigated DDK phosphorylation sites on human MCM2. One study, analysing the bacterially expressed, recombinant N-terminal of human MCM2 (containing amino acids 10-294), identified three DDK sites (Ser40, Ser53 and Ser108, Montagnoli et al., 2006). In addition the authors also identified CDK sites (Ser13, Ser27, Ser41). Another study, analysing N-terminal and full length human MCM2 expressed in bacterial cells revealed two dominant DDK sites (Ser5 and Ser53) and three minor DDK sites (Ser4, Ser7 and Thr59, Cho et al., 2006). A third

study analysed human MCM proteins produced in insect cells and identified three major (Ser27, Ser41 and Ser139) and two minor (Ser53 and Ser108) phosphorylation sites (Tsuji et al., 2006). These serine residues are conserved from *Drosophila* through to humans. The discrepancies within these results maybe due to the different methods of MCM production or may be in fact due to the concentration of DDK used, as previous studies suggest different outcomes depending on concentration gradients of kinases (Coverley et al., 2002). Interestingly, phosphorylation of MCM2 at Ser53 was found in all three studies.

Arresting cells using hydroxyurea prevents DNA replication (Aparicio et al., 1997, Rialland et al., 2002), induces MCM hyperphosphorylation at sites specific to Cdc7 and prevents release of MCM2 from chromatin (Montagnoli et al., 2006). Depletion of Cdc7 using siRNA impairs MCM2 phosphorylation at Ser40 and Ser53 (Tenca et al., 2007). Moreover, using antibodies specific to MCM2 phosphorylation sites in synchronised HeLa cells showed the presence of MCM2 phosphorylation at Ser40/41, Ser53 and Ser108 in S phase (Montagnoli et al., 2006). Also, inhibition of DDK using a small molecule inhibitor PHA-767491 impairs MCM2 phosphorylation at Ser40 and Ser53 (Montagnoli et al., 2008). Taken together these results show that MCM2 phosphorylation at Ser40 and Ser53 is dependent on Cdc7.

In HeLa cells, MCM2-7 phosphorylation by DDK was shown to be essential for DNA replication initiation and phosphorylation of MCM2 by DDK was demonstrated to be critical for MCM2-7 ATPase activity *in vitro* (Tsuji et al., 2006). A couple of studies have analysed the effect of DDK phosphorylation on MCM2-7 loading, with conflicting results. In *Xenopus* egg extract, loading of MCM2-7 was not affected by DDK phosphorylation (Tsuji et al., 2006). On the other hand, analysis of human cells released from quiescence, showed phosphorylation of MCM2 at Ser5 by DDK promotes chromatin loading of MCM2 (Chuang et al., 2009).

### 1.7.4 Order of CDK and DDK kinase activity

Studies in *S. cerevisiae* have shown DDK and CDK are required throughout S phase for firing of both early and late origins (Bousset and Diffley, 1998,

Donaldson et al., 1998). In mammalian cells CDK is also required throughout S phase (Thomson et al., 2010). The order cells require CDK and DDK kinase activity is unclear due to conflicting results in different eukaryotic systems. In *Xenopus* egg extracts Cdc7 can complete its role in the absence of CDK but CDK cannot complete its role without Cdc7 (Jares et al., 2000, Walter, 2000). However in *S. cerevisiae*, Cdc7 cannot complete its activity in the absence of CDK activity (Nougarede et al., 2000). *In vitro*, phosphorylation of human MCM2 by CDK facilitates phosphorylation by DDK (Masai et al., 2000), suggesting phosphorylation of MCM2 by CDK induces a conformational change allowing DDK to access different sites. Dependence on prior CDK phosphorylation was only apparent when MCM2 was complexed in a tetramer of subunits MCM2, 4, 6 and 7 (Masai et al., 2000) and not when tested on MCM2 monomer.

Despite the precise mapping of MCM subunit phosphorylation sites, the significance of these phosphorylation sites within a hexamer and how the kinases render the complex functional is still not understood. The prevailing generalised hypothesis is that phosphorylation of MCM subunits causes a structural change within the MCM2-7 hexamer, regulating events in MCM2-7 loading and causes activation to occur.

## 1.8 Structure of MCM2-7 complexes

The first EM images of MCM2-7 were generated from purified *S. pombe* (Adachi et al., 1997). These images illustrated the hexameric shape of MCM2-7 with a deep cavity down the centre of the protein. More recently EM was used to produce a three dimensional (3D) reconstruction of archaeal *Mt*MCM (Yu et al., 2002, Pape et al., 2003) and analysis of a number of mutant *Mt*MCM complexes depict conformational changes in the MCM double hexamer (Jenkinson et al., 2009). The reconstruction showed similar features to that shown in the original EM images - a two tiered protein with a central channel. Hexameric (Pape et al., 2003) and heptameric (Yu et al., 2002) complexes have been identified as well as helical filaments, although it is not expected to form filaments *in vivo* (Chen et al., 2005). When bound to dsDNA *Mt*MCM forms a double hexamer (Costa et al., 2006). Analysis of *Mt*MCM in the presence of a large segment of dsDNA using

cryo-EM demonstrates a single hexameric ring with DNA bent around the outside of the ring (Costa et al., 2008), possibly showing an intermediate step in MCM DNA loading (Fig 1.6).

To date there are no crystal structures of eukaryotic MCM2-7 complexes. Inherently MCM2-7 complexes are difficult to crystalise and so homohexameric MCM complexes from archaea have been useful models for crystal structure analysis. The crystal structure of the N-terminal domain from *Mt*MCM was shown to form a double hexamer through the interdigitation of zinc finger motifs and hydrogen bonding (Fletcher et al., 2003, Liu et al., 2008). More recently a near-full length structure of the *Sso*MCM and a high-resolution structure of a recombinant, redundant and functionally inactive *in vitro* MCM from *Methanopyrus kandleri* have provided additional structural information that can be related to the eukaryotic heterohexameric complex (Bae et al., 2009, Brewster et al., 2008).

A recent crystal structure of N-terminal *Pyrococcus furious* (*Pf*) MCM bound to ssDNA revealed a MCM single-stranded binding motif (MSSB) which is suggested to be important in helicase activation (Froelich et al., 2014). Subsequently the same group produced a chimera of N-terminal *Sso*MCM and the ATPase domain of *Pf*MCM (Miller et al., 2014). This chimeric MCM is active and the crystal structure has led to a hypothesis for MCM DNA unwinding activity. They suggest the h2i clamps down on the leading strand of DNA in order to facilitate strand retention and regulate ATP hydrolysis (Miller et al., 2014).

## 1.9 Nuclear matrix

The term nuclear matrix was first used in 1974 by Berezney and Coffey (1974) to refer to the insoluble RNA and protein fraction of the nucleus which remained after salt extraction. The nuclear matrix consists of a network of 10 nm filaments that can be visualised by EM, which persist when chromatin, soluble proteins and lipids are removed (Capco et al., 1982, Wan et al., 1999). This nuclear structure has been sub-categorised and is known as the nuclear scaffold, nuclear

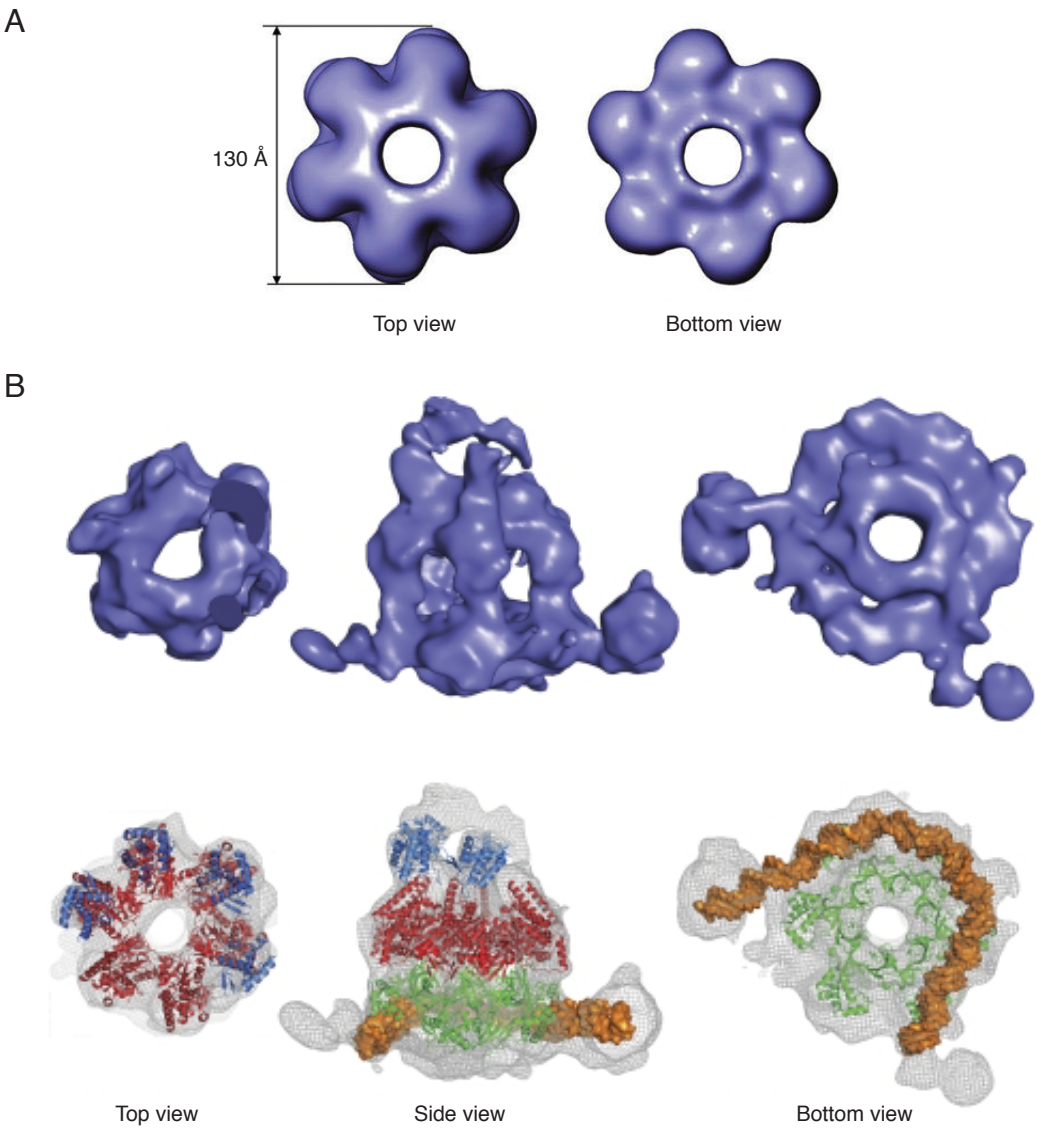


**Figure 1.6.** Electron microscopy of MtMCM in different conformational states. A. Reproduced from Pape et al., 2003. Electron density of MtMCM without DNA. B. Reproduced from Costa et al., 2008. MtMCM bound to long dsDNA. Top shows electron density. Bottom shows placement of DNA by fitting in crystallographic structures. Blue – Cdc6, Red – AAA+ domain of MtMCM, Green – N-terminal of MtMCM, Orange - roughly 80 base pairs of dsDNA.

skeleton or the nuclear matrix dependent on the method used to extract it. Although the term the nuclear matrix has become the most widely adopted name for the proteins which resist aggressive methods of extraction, it referred originally to those proteins resistant to extraction with 2.0 M NaCl (Berezney and Coffey, 1974). This method has been criticised because of its potential to cause aggregation of proteins and so a new method was developed by Capco et al. (1982), which used more physiological buffers with lower salt (0.5 M NaCl) and included nucleases (DNase I) to digest chromatin. This was termed the 'in situ nuclear matrix' as the cytoskeleton is also maintained (for more information see appendix A). A role of the nuclear matrix as the site for; transcription (Jackson and Cook 1985), DNA repair (Qiao et al., 2001), splicing (Zeitlin et al., 1987), chromatin remodelling (Reyes et al., 1997) and DNA replication (Jackson and Cook, 1986, Cook, 1999) has been demonstrated.

Here I will focus on the role of the nuclear matrix in initiation of DNA replication (reviewed in Wilson and Coverley, 2013). Chromatin is periodically attached to the nuclear matrix, specifying its characteristic loop organisation in interphase nuclei. DNA sequences that are associated with the nuclear matrix are known as matrix attached regions (MARs) and the size of intervening loops correlates with the length of replicons (Buongiorno-Nardelli et al., 1982, Lemaitre et al., 2005). Extensive evidence places replication origins, components of the pre-RC and machinery that supports cell-cycle regulated initiation (Radichev et al., 2005, Buckler-White et al., 1980, Dijkwel et al., 1979, Dijkwel et al., 1991, Razin et al., 1986, van der Velden et al., 1984, Lagarkova et al., 1998, Berezney and Coffey, 1975) in proximity to the nuclear matrix within what are referred to as DNA replication factories; aggregates of replication proteins and multiple co-regulated origins (reviewed in Wilson and Coverley, 2013).

Experiments show that a number of replication proteins remain in extracted nuclei when chromatin is depleted using nucleases (reviewed in Cook, 1991), although the relationship of MCM proteins with the nuclear matrix is not understood. A number of studies have looked into the association of MCM proteins in different cell lines. In human cancer cells (Raji cells), MCM3 was solubilised by nuclease and so not nuclear matrix bound (Mendez and Stillman,

2000), which is in agreement with work in another human cancer cell line (HeLa cells) showing MCM3, MCM2 and MCM7 to be solubilised by nuclease (Fujita et al., 1997, Todorov et al., 1995). Studies in asynchronous fibroblast cells (REF-52 and NIH3T3 cells) showed MCM2, MCM3, MCM5 and MCM7 were solubilised by nuclease (Cook et al., 2002, Cook et al., 2004, Stoeber et al., 1998). However other studies of HeLa cells showed MCM7 and MCM3 to be resistant to nuclease digestion and so nuclear matrix bound (Fujita et al., 2002, Burkhart et al., 1995). Proteomic screens of human and *Drosophila* cell lines identified MCM2, 3, 4 and 7 in nuclear matrix preparations (Mitulovic et al., 2004). In addition, MCM2 has been shown to interact with the nuclear matrix anchoring protein AKAP95 in HeLa cells (Eide et al., 2003). This lack of consensus may be in part because interaction is transient, and in asynchronous cells masked by the bulk fraction of MCM protein. Evidence also suggests that tumours, transformed cells in culture, and stem-like cells appear to have a compromised or immature nuclear matrix (Gerner et al., 2002, Varma and Mishra, 2011) raising questions about its role in DNA replication.

## 1.10 Aims

The aims of this thesis are to integrate two related strands of research into the structure and function of mammalian MCM2-7 complexes, using a combination of biochemistry and cell based biology. Specifically I aimed to:

- Produce and purify recombinant human MCM (hMCM) in *E. coli*.
- Characterise recombinant hMCM function.
- Analyse the configuration and structure of recombinant hMCM
- Investigate the location and time of expression of endogenous MCM proteins in relation to initiation of DNA replication in mammalian cells.
- Examine the relationship of MCM2-7 complex proteins with the nuclear matrix.
- Use the information and materials acquired to reconstitute mammalian MCM2-7 complex assembly and the requirement for properly regulated function.

- Unpick the requirements for MCM2-7 phosphorylation by cellular kinases.

This research will expand on our current understanding of the initiation of DNA replication and will give insight into how this fundamental process is controlled in a mammalian context. The identification of differences between cancer cells and 'normal' cells has potential to generate information that can be used to design novel cancer therapies.

*Chapter 2*

# Materials and methods

# 2 Material and methods

## 2.1 *E. coli* cell culture

### 2.1.1 Growth media

*E. coli* cells were cultured in Luria – Bertani (LB) growth media (10 g/L tryptone, 5 g/L yeast extract and 171 mM sodium chloride (NaCl, Bertani, 1951) unless stated otherwise. For growth on agar plates LB-agar was used (LB plus 15 g/L agar). LB and LB-agar were autoclaved immediately after preparation.

### 2.1.2 Antibiotics

Antibiotics were made as 1,000x stocks, filter sterilised and stored at -20°C for up to one year. The final concentration of the antibiotics used were: carbenicillin 50 µg/ml, chloramphenicol 34 µg/ml, kanamycin 30 µg/ml and spectinomycin 50 µg/ml.

### 2.1.3 Preparation of heat shock competent *E. coli* cells with rubidium chloride

*E. coli* cells were streaked onto an agar plate (with the appropriate antibiotic if required) and grown overnight at 37°C. A single colony was picked into two 3 ml Super Optimal Broth (SOB, 171 mM NaCl, 5 g/L yeast extract, 20 g/L tryptone, 10 mM magnesium chloride ($MgCl_2$) and 10 mM magnesium sulphate ($MgSO_4$)) and incubated at 37°C at 225 revolutions per minute (rpm) for five hours. The cultures were used to inoculate 100 ml of SOB and incubated at 37°C at 225 rpm overnight.

Cultures were cooled on ice for five minutes and spun at 4,000 x *g* at 4°C for five minutes. The supernatant was discarded and the cells were re-suspended in ice-cold TFB1 buffer (100 mM rubidium chloride (RbCl), 50 mM manganese chloride ($MnCl_2$), 30 mM potassium acetate (KAc), 10 mM calcium chloride ($CaCl_2$), 15% v/v glycerol. The pH was adjusted to 5.8 with 1 M acetic acid). Cells were incubated on ice for 90 minutes before spinning at 4,000 x *g* at 4°C for five minutes. The supernatant was discarded and the cells were re-suspended in ice-

cold TFB2 buffer (10 mM MOPS, 10 mM RbCl, 75 mM $CaCl_2$, 15% v/v glycerol. The pH was adjusted to 6.8 with 1 M potassium hydroxide (KOH)). Cells were aliquoted and snap frozen in liquid nitrogen.

### 2.1.4 *E. coli* transformation

For protein production Rosetta 2 *E. coli* competent cells (Novagen) were used. These contain a chloramphenicol resistant plasmid allowing the expression of tRNAs normally rare in *E. coli* cells.

The competent cells were thawed on ice and 50 ng of plasmid DNA was added to 50 µl of competent cells. The cells were incubated on ice for 30 minutes, incubated at 42°C for 30 seconds and immediately returned to ice for two minutes. 250 µl of 37°C SOB was added to the cells and incubated for one hour at 37°C at 225 rpm to allow the antibiotic resistance to develop. 125 µl of the culture was spread onto an agar plate containing the suitable antibiotic and incubated overnight at 37°C.

## 2.2 Mammalian cell culture

### 2.2.1 Growth media and conditions

Mammalian cells were grown in Dulbecco's modified eagle medium (DMEM), low glucose (1 g/L), supplemented with GlutaMAX and pyruvate (Gibco). The GlutaMAX supplement reduces ammonia build up that can be toxic to cells. It also improves cell viability and growth. DMEM was supplemented with 10% v/v fetal bovine serum (Biosera) and penicillin/streptomycin/glutamine (10 units/ml, 10 µg/ml, 2.92 mg/ml, respectively, Gibco). Henceforth this is referred to as 3T3 media.

All cells were grown on Nunclon polystyrene tissue culture dishes (Nunc) at 37°C in a humidified (with the relative humidity approximately 80%) incubator with 5% v/v $CO_2$. S3 HeLa cells were cultured in 2 L roller bottles (Corning) at 37°C and gassed every 24 hours with 5% v/v $CO_2$ in air through a Maximum recovery filtered pipette tip (Axygen).

Cells were passaged by washing once in Dulbecco's phosphate buffered saline without calcium, magnesium or phenol red (dPBS, Gibco), followed by incubation with 0.1% w/v trypsin-Ethylenediaminetetraacetic acid (EDTA, Gibco) for approximately five minutes in a humidified chamber in 5% v/v $CO_2$ at 37°C or until the cells had detached from the plate. The trypsin was quenched with an equal volume of media.

All three cell lines used are morphologically distinct, and exhibit different and specific responses to synchrony agents that were previously characterised and reported (Coverley et al., 2002, Marheineke et al., 2005). Any non-experimental deviations from the expected kinetics for passage through the cell cycle triggered reversion to a fresh liquid nitrogen stock as a precaution against accumulation of genetic drift.

### 2.2.2 Cell synchrony

#### *2.2.2.1 G1 phase synchrony*

Mouse 3T3 cells were grown until confluent. This usually took three to four days. Care was made to ensure no cycling cells were present. The media was changed and the cells were left for a further four days to make sure cells were in deep quiescence. Cells were released into fresh media by passaging as described in section 2.2.1 with a split by ¼ (i.e. if the total volume of cells in solution was 4 ml, 1 ml of culture was used to inoculate a new plate of the same dimensions). When releasing cells special attention was made to ascertain each cell was individual and not in contact with any others to optimise release from quiescence (Stoeber et al., 1998, Coverley et al., 2002).

#### *2.2.2.2 S phase synchrony*

S3 and flat HeLa cells were synchronised at the G1/S phase boundary by culturing in the presence of 2.5 mM thymidine for 24 hours (Krude et al., 1997). Cells were washed extensively in warm dPBS, fresh media was added and the cells incubated in a humidified chamber (with the relative humidity approximately 80%) in 5% v/v $CO_2$ at 37°C for one hour to release into early S phase.

## 2.3 Protein analysis

### 2.3.1 SDS PAGE

#### *2.3.1.1 Preparation and running of gels*

Sodium dodecyl sulphate polyacrylamide gel electrophoresis (SDS PAGE) gels were run on either; the Mini-PROTEAN gel system (Bio-Rad), minigel system (CBS Scientific) or slab size electrophoresis system (Atto). The resolving gel was poured and left to polymerise, unpolymerised acrylamide was washed away with $dH_20$ (PURELAB Ultra, 18.2 MΩ-cm conductivity, Elga), the stacking gel was poured on top of the resolving gel and a comb inserted. The components of the resolving and stacking gels are listed in Table 2.1. Gels were run in 1 x SDS running buffer (25 mM Tris, 0.19 M glycine and 3.5 mM SDS) at 80 mA for one to six hours. Occasionally SDS PAGE Precast gels (Expedeon) were used according to the manufacturers guidelines. Protein standard were run on each gel so that the molecular weight of each band could be estimated. For gels that were to be Coomassie blue stained (see 2.3.3); 10 µl of Precision Plus Protein Unstained standards (Bio-Rad) were loaded onto the gel. For gels that were to be western blotted (see 2.3.4), 10 µl of either; PageRuler Plus Prestained Protein Ladder (Thermo scientific) or Precision Plus Protein standards (Bio-Rad) were used.

**Table 2.1 Components of SDS PAGE resolving and stacking gel**

| Components | 8% w/v resolving gel | 10% w/v resolving gel | 5% w/v stacking gel |
|---|---|---|---|
| **Acrylamide (Proteogel mix 37.5:1)** | 26.6% v/v | 33% v/v | 17% v/v |
| **Tris pH 8.8** | 37.5% v/v | 37.5% v/v | - |
| **Tris pH 6.8** | -- | - | 12.5% v/v |
| **Water** | 34% v/v | 27.8% v/v | 67% v/v |
| **10% w/v APS*** | 0.8% v/v | 0.4% v/v | 1% v/v |
| **TEMED**** | 0.13% v/v | 0.2% v/v | 0.2% v/v |

| | | | |
|---|---|---|---|
| **10% w/v SDS*** ** | 1% v/v | 1% v/v | 2% v/v |

*APS – ammonium persulphate (prepared daily)

**TEMED – N,N,N′,N′-Tetramethylethylenediamine

***SDS - Sodium dodecyl sulphate

#### *2.3.1.2 Sample preparation*

4x SDS PAGE loading buffer (240 mM Tris pH 6.8, 8% w/v SDS, 40% v/v glycerol, 0.1% w/v bromophenol blue and 6.8% v/v β mecaptoethanol) was added to protein samples. Samples were mixed and heated to 100°C for five minutes and vortexed before loading on to the gel.

### 2.3.2 Native PAGE

#### *2.3.2.1 Preparation and running of gels*

Mini protean TGX precast gels (Bio-rad) were run in 1x Tris/glycine running buffer for Native PAGE (Bio-Rad). Wells were washed thoroughly prior to loading with running buffer. NativeMark™ (Life Technologies) protein standard were run on each gel so that the molecular weight of each band could be estimated. Native gels were soaked in denaturing buffer (2% w/v SDS, 1x Tris glycine buffer (Bio-Rad) for 30 minutes prior to transfer to nitrocellulose as described in 2.3.4).

#### *2.3.2.2 Sample preparation*

Native PAGE loading buffer (Bio-Rad) was added to samples at a 1:1 ratio. Samples were stored on ice prior to gel loading.

### 2.3.3 Coomassie blue staining

Protein gels were stained to visualise proteins in one of two ways. Firstly by staining with Coomassie blue R250 stain (40% v/v methanol, 10% v/v acetic acid and 0.1% w/v Coomassie blue R250 (Fisher)) for 10 minutes and destained for one to 12 hours using destain (40% v/v methanol, 10% v/v acetic acid). Or secondly, using SimplyBlue Safe Stain (Life Technologies) according to the manufacturers guidelines.

### 2.3.4 Western blotting

#### *2.3.4.1 Transfer*

SDS PAGE gels were transferred to nitrocellulose membrane using an iBlot (Life Technologies) using proprietary kits (SDS PAGE gels were transferred using program P0 for seven minutes, native PAGE gels was transferred using P8 for 13 minutes) or to PROTRAN nitrocellulose transfer membrane (Whatman) using a semi dry blotter (Sigma Aldrich) by the following method. The gel was soaked for 15 minutes in semi dry blotting buffer (297 mM Tris, 10 mM CAPS, 10% v/v methanol and 0.02% w/v SDS) and laid on top of four pieces of 3MM chromatography paper (Whatman) wetted in semi dry blotting buffer. Another four pieces of wet 3MM were laid on top of the gel and all air bubbles were removed. The semi dry blotter was run at 0.8 mA per $cm^2$ for two hours. Gels were transferred to a PVDF membrane (GE Healthcare) using a Transblot-SD semi dry transfer cell (Bio-Rad). The transfer stack was assembled with two pieces of 3MM chromatography paper soaked in anode I buffer (0.3 M Tris pH 10.4 and 10% v/v methanol), one piece of chromatography paper soaked in anode II buffer (25 mM Tris pH 10.4, and 10% v/v methanol) followed by the PVDF membrane prepared by soaking in 100% v/v methanol for 15 seconds, $ddH_20$ water for two minutes and anode II buffer for a minimum of five minutes. The gel was added to the stack pre-soaked in cathode buffer (25 mM Tris pH 9.4, 40 mM glycine and 10% v/v methanol) for at least 15 minutes and three pieces of chromatography paper soaked in cathode buffer (any air bubbles were removed). The semi dry blotter was run at 1.2 mA per $cm^2$ for one hour.

#### *2.3.4.2 Antibody detection*

Nitrocellulose membranes were stored at -20°C and processed by putting straight into blocking buffer. PVDF membranes were stored at room temperature 21 ± 2˚C. (RT) and re-wetted by soaking in 100% v/v methanol for two minutes, $dH_20$ water for five minutes and then blocked. Membranes were blocked for 30 minutes to one hour in blocking buffer (Tris buffered saline and tween 20 (TBST); 50 mM Tris pH 7.6, 150 mM NaCl and 0.05% v/v tween and 5% w/v dried milk (Marvel, 0% fat)). Membranes were incubated with the primary antibody for two hours at RT or overnight at 4°C. See Table 2.2 for primary antibody details and

dilutions. Membranes were washed for 30 minutes in TBST with four to six buffer changes (blocking buffer). The membrane was incubated with the appropriated secondary antibody (see Table 2.3) in blocking buffer for one hour at RT. Membranes were washed for 30 minutes in TBST with four to six buffer changes. Proteins were detected using EZ-ECL (Biological Industries) or SuperSignal West Pico Chemiluminescent Substrate (Thermo Scientific) western blotting reagents and exposed to Hyperfilm ECL (GE Healthcare). Film was developed using an XO graph compact X9 analyser (Packard) and quantified using ImageJ software (1.47v, National Institutes of Health, USA). Relative protein concentrations were quantified, corrected for background and normalised by dividing by a loading control.

### 2.3.5 Immunofluorescence (IF)

Cells on glass coverslips (MIC3306, 13 mm diameter, No. 1 (0.13 – 0.155mm), henceforth referred to as 'coverslips') were washed in 0.5% v/v Triton X-100 in dPBS. Cells were fixed by incubation in 4% w/v neutral pH paraformaldehyde (PFA) for ten minutes, and then washed for five minutes in 0.5% v/v Triton X-100 in dPBS thrice. The coverslips were blocked for 30 minutes in antibody buffer (10 mg/ml nuclease and protease free bovine serum albumin (BSA, Jackson, Cat: 001-000-162), 0.02% w/v SDS, 0.1% v/v Triton X-100 in PBS). Coverslips were incubated at 37°C for two hours with primary antibody diluted in antibody buffer (see Table 2.2). Coverslips were then washed for five minutes in antibody buffer thrice. The appropriate secondary antibody (see Table 2.3) and Hoechst 33258 at 1/100,000 in dPBS was incubated with the cells for one hour at 37°C in the dark. Coverslips were washed for a final three times in antibody buffer for five minutes at RT.

#### *2.3.5.1 Mounting coverslips*

The coverslips were dipped in water and mounted onto Vectashield (Vector). Once dry coverslips were analysed using fluorescent microscope (Axiovert 200M, Zeiss).

*2.3.5.2 Image analysis*

All microscopy images were captured using a Zeiss Axiovert 200M inverted light microscope fitted with an AxioCam HRm digital camera and Openlab software (Perkin Elmer) using a 63x or 40x oil immersion objective. Microscope was illuminated using a halogen lamp. Zeiss filter sets 2, 10 and 15 were used for analysis. Filter set 2 excites at wavelengths 365 - 395 nm, filter set 10 excites at wavelengths 450 – 490 nm and filter set 15 excites at 580 – 590 nm.

All images in a dataset were collected with constant exposure parameters (between 100 – 300 ms for Alexa 488 and Alexa 568 and 5 – 20 ms for Hoechst 33258). To measure intensity the perimeter of the nuclei were measured using the polygon tool in ImageJ software (National Institutes of Health, USA). For each dataset over 98 images were randomly selected for quantification and corrected for background. All quantification was carried out before any manipulation. Example images shown were adjusted using Adobe Photoshop CS4 to increase image intensity for reproduction. In all cases, control and test samples were treated identically.

**Table 2.2 Primary antibody details**

| **Antibody (clone)** | **Host/Isotype** | **Dilution for WB and buffer** | **Dilution for IF** | **Supplier (Order No.)** |
|---|---|---|---|---|
| hMCM2 | Rabbit/ Polyclonal | 1/10,000 5% milk*, TBST | N/A | (Ekholm-Reed et al., 2004) |
| hMCM3 (3A2) | Mouse/ Monoclonal | 1/1,000 5% BSA**, TBST | N/A | MBL*** (M038-3) |
| hMCM4 (C-10) | Mouse/ Monoclonal | 1/400 5% BSA**, TBST | N/A | SC Biotech**** (sc48407) |
| hMCM5 (33) | Mouse/ Monoclonal | 1/2,000 5% BSA**, TBST | N/A | BD Biosciences (611750) |
| hMCM6 (1/MCM6) | Mouse/ Monoclonal | 1/2,000 5% BSA**, TBST | N/A | BD Biosciences (611622) |

| | | | | |
|---|---|---|---|---|
| hMCM7 (141.2) | Mouse/ Monoclonal | 1/5,000 5% milk*, TBST | N/A | SC Biotech**** (sc9966) |
| MCM7 (EP1974Y) | Rabbit/ Monoclonal | 1/5,000 5% milk*, TBST | N/A | Abcam (ab52489) |
| MCM2/BM28 (46) | Mouse/ Monoclonal | 1/1,000 5% milk*, TBST | 1/50 | BD Biosciences (610700) |
| MCM3 [EPR7081] | Rabbit/ Monoclonal | 1/1,000 5% milk*, TBST | N/A | Abcam (ab126723) |
| Cyclin A (CY-A1) | Mouse/ Monoclonal | 1/1,000 5% milk*, TBST | N/A | Sigma Aldrich (C4710) |
| Actin (AC40) | Mouse/ Monoclonal | 1/1,000 5% milk*, TBST | N/A | Sigma Aldrich (A4700) |
| Lamin B2 (EPR9700(B)) | Rabbit/ Monoclonal | 1/1,000 5% milk*, TBST | 1/100 | Abcam (ab138516) |
| Histone H3 | Rabbit/ Polyclonal | 1/10,000 5% milk*, TBST | N/A | Abcam (ab1791) |

* 5% w/v dried milk (Marvel, 0% fat)

** 5% w/v Bovine Serum Albumin

*** Medical and Biological Laboratories

**** Santa Cruz Biotechnology Inc.

**Table 2.3 Secondary antibody details**

| **Antibody** | **Host** | **Dilution for WB** | **Dilution for IF** | **Supplier (Order No.)** |
|---|---|---|---|---|
| Anti-mouse HRP (ZyMAX) | Rabbit | 1/20,000 | N/A | Life Technologies (81-672) |
| Anti-mouse HRP | Rabbit | 1/10,000 | N/A | Abcam (ab6789) |
| Anti-rabbit HRP | Goat | 1/10,000 | N/A | Abcam (ab6721) |

| | | | | |
|---|---|---|---|---|
| Anti-mouse, Alexa, 488 | Goat | N/A | 1/2,000 | Life Technologies (A1101) |
| Anti-rabbit, Alexa, 568 | Goat | N/A | 1/2,000 | Life Technologies (A11011) |

### 2.3.6 Determining protein concentration

To determine protein concentration a Bio-Rad Protein Assay Dye Reagent Concentrate kit was used according to manufactures guidelines (Cat: 500-0006).

## 2.4 hMCM production and purification

WT hMCM was encoded by three plasmids, each encoding two of the hMCM subunits. ATPase deficient mutant hMCM constructs were produced using site-directed mutagenesis on each of the hMCM subunits in the above constructs. Each hMCM was mutated by modifying the conserved lysine in the Walker A motif to a glutamic acid. All constructs were made previously by Richard P. Parker-Manuel. WT and mutant hMCM were expressed and purified in the same way.

### 2.4.1 Expression of hMCM

The three hMCM constructs were transformed into *E. coli* Rosetta 2 (DE3, Novagen) and grown in LB broth containing carbenicillin, chloramphenicol, kanamycin and spectinomycin at 37°C and rotating at 225 rpm. The starter culture (5 ml) was grown for eight hours and 750 µl of the starter culture was used to inoculate a medium culture (750 ml) and grown overnight. The medium culture was used to inoculate a 50 L fermenter. Once the optical density ($OD_{600}$) of the cultures reached 0.4, minus a media only control, the temperature was shifted to 18°C in anticipation the $OD_{600}$ would be 0.6 once the temperature reached 18°C. The production of hMCM was induced by the addition of 1 mM

Isopropyl β-D-1-thiogalactopyranoside (IPTG) and incubated at 18°C for a further 21 hours until the OD reached approximately 6.0 at 600 nm.

Cell pellets were harvested by centrifugation at 7,500 x *g*, for ten minutes at 3˚C and re-suspended in buffer 1 (25 mM Tris, 300 mM NaCl, pH 8.0) containing protease inhibitors (Pepstatin A 1 µg/µl, Aprotinin 2 µg/µl, Leupeptin 2 µg/µl, Bestatin 5 µ M, 4-(2-Aminoethyl) benzenesulfonyl fluoride hydrochloride (AEBSF) 0.1 M and 2 mM β mecaptoethanol). Re-suspended pellets were stored at -80˚C.

### 2.4.2 hMCM purification

Re-suspended cell pellets were thawed and 5 mM $MgCl_2$ and 5 mg/ml DNase I was added. Cells were lysed using an automated cell disrupter (Constant cell disruption systems, UK) at 21 Kilopound per square inch (Kpsi). Cells were clarified by centrifugation at 10,000 x *g* for 40 minutes. His-Select Cobalt Affinity gel (Sigma) was prepared by washing thrice in 25 ml per 1 ml bead bed of buffer 1. Washing was carried out by re-suspending and centrifugation at 3220 x *g* for five minutes. The clarified lysate was mixed with 1 ml of beads per 25 ml lysate. 10 ml of buffer 1 was added and the beads were mixed gently at 4°C for 30 minutes. The beads were collected by centrifugation at 3220 x *g* for 10 minutes (supernatant = flow through). The beads were packed into a XK16/20 column, washed with five column volumes (CV) of buffer 2 (as buffer 1 plus 1 mM imidazole) at 2 ml/min. The column was washed with 5 CV of buffer 3 (as buffer 1 plus 7.5 mM imidazole and 5% v/v glycerol) at 1 ml/min. To elute the proteins bound to the cobalt beads buffer 4 (buffer 1 plus 250 mM imidazole and 5% v/v glycerol) was added and 1 ml elution fractions were collected. The peak elution fractions were pooled and applied to a HiLoad 26/600 Superdex 200 gel filtration column (GE Healthcare Life Sciences). The column was initially equilibrated with buffer 5 (25 mM Tris-HCl, 150 mM NaCl, 5% v/v glycerol, pH 8.0, 1 mM dithiothreitol (DTT) and 0.1 mM AEBSF). The proteins were collected in 4 ml fractions. Eluted fractions of the expected hMCM molecular weight were pooled and loaded onto a 1 ml MonoQ anion exchange column (GE Healthcare Life Sciences). The column was initially equilibrated in buffer 5 and 0.5 ml fractions

were eluted over a 10 CV linear gradient (buffer 5 with 1 M NaCl). Fractions containing hMCM were pooled, dialysed against buffer 6 (25 mM HEPES, pH 8.0, 200 mM sodium glutamate, 1 mM DTT and 0.1 mM AEBSF), flash frozen using liquid nitrogen in small aliquots and stored at -80°C.

## 2.5 ATP hydrolysis assay

Reaction mixes contained PDB buffer (30 mM $K_2HPO_4/KH_2PO_4$ buffer, pH 8.5, 1 mM DTT, 100 µg/ml BSA (New England Biolabs (NEB)), 2% v/v glycerol, 10 mM magnesium acetate (MgAc), 1.5 nmol cold adenosine triphosphate (ATP, GE Healthcare), 3.08 pmol of [α-$^{32}$P] ATP (800 Ci/mmol, (ICN)), DNA (double stranded circular (pUC119, 3,162 base pair (bp)), single stranded circular (M13, 6,407 bases) or duplex (Appendix B, Fig. B1) as stated in text and 176 nM of protein (unless stated otherwise) were assembled on ice. Reactions were incubated at 37°C for 45 minutes and were stopped by the addition of EDTA to 20 mM. ATP hydrolysis was visualised by using thin-layer chromatography (TLC). Reactions were spotted onto TLC polyethylenimine (PEI) Cellulose F plates (Merck). Plates were developed in 1 M formic acid and 0.5 M lithium chloride (LiCl), dried, and exposed to a phosphor imaging plate. Signals were detected using a personal molecular imager (PMI, Bio-Rad) and quantified by using Quantity One software (Bio-Rad). To determine ATP concentration, data were calibrated by using a dilution series of the ATP stock performed in parallel with the experiment. The standard concentration of cold ATP in the reaction was 75 pmol/µl and the concentration of hot ATP was determined using the following equation (specific activity of [α-$^{32}$P] ATP = 30 KBq/pmol).

$$N = N_0 e^{-(0.693t/14.3)}$$

$N_0$ = initial activity (KBq/µl), t = decay time in days, N = final activity (KBq/µl), 14.3 days is $^{32}$P half-life.

## 2.6 DNA helicase assay

### 2.6.1 Substrate preparation

#### *2.6.1.1 Oligonucleotide labelling*

Oligonucleotide (oligo) HS2 (Table 2.4) was radiolabelled using γ[$^{32}$P]ATP 3,000 Ci/mmol (Perkin Elmer). Labeling reaction (5 μM HS2 oligo, 1 unit T4 polynucleotide kinase (PNK, Promega), 1x PNK buffer (Promega) and 3.6 μl γ[$^{32}$P]ATP) was incubated at 37°C for one hour. The PNK was denatured by heating to 90°C for ten minutes. The labelled substrate was stored at 4°C. 0.5 μl of the annealed substrate was mixed with 24.5 μl of T0.1E buffer (10 mM Tris pH 8.0, 25 mM NaCl and 0.1 mM EDTA) and used as a 100 nM control sample for quantification.

#### *2.6.1.2 Oligonucleotide annealing*

Radiolabelled labelled HS2 was annealed to oligo HS1 (Table 2.4) to produce a forked DNA substrate with a 26 bp double-stranded region. The 40 μl annealing reaction (5 μM HS2, 5 μM HS1, 200 mM HEPES pH7.5, 250 mM NaCl and 5 mM EDTA) was heated to 95°C and cooled at 0.02°C per second to 20°C. Annealed oligos were stored at -20˚C.

**Table 2.4 Oligonucleotide sequences**

| Oligo name | Oligo sequence (5′ – 3′) |
|---|---|
| **HS1** | GGGACGCGTCGGCCTGGCACGTCGGCCGCTGCGGCCAGG CACCCGATGGCGTTTGTTTGTTTGTTTGTTTGTTT |
| **HS2** | TTTGTTTGTTTGTTTGTTTGTTTGTTTGTTTGCCGACGTGCCA GGCCGACGCGTCCC |
| **HF150** | CCTGGCGTTACCCAACTTAATCGCCTTGCAGCACATCCCCC TTTCTTTTTTTTTTTTTTTTTTTTTTTTTTTTTTTTTTTTTTTT TTTTTTTTTTTTTTTT |
| **HR80** | TTTTTTTTTTTTTTTTTTTTTTTTTTTTTTTTTTTGAAAGGGGG ATGTGCTGCAAGGCGATTAAGTTGGGTAACGCCAGG |

#### 2.6.1.3 *Substrate purification*

6x loading dye (50% v/v glycerol, 0.1% w/v xylene cyanol FF and 0.1% w/v bromophenol blue) was added to the substrate. The substrate was run on a 12% w/v acrylamide gel (1x Tris/borate/EDTA (TBE, 0.09 M Tris, 0.09 M boric acid and 0.08 M EDTA), 12% v/v acrylamide:bis-acrylamide from a 19:1 20% w/v stock, 0.07% w/v APS, 0.1% v/v TEMED) for one hour at 80 V in 1x TBE. The gel was exposed to Hyperfilm ECL (GE Healthcare) for five minutes and developed using an XO graph compact X9 analyser (Packard). The band containing the annealed substrate was excised and placed in a clean, pre-weighed micro centrifuge tube. The substrate was eluted from the gel by adding 3 µl of PAGE elution buffer (0.5 M sodium acetate (NaAc), 10 mM MgAc, 1 mM EDTA and 0.1% w/v SDS) per 1 µg of gel slice.

The slice was incubated in PAGE elution buffer for two hours at 4°C. The supernatant was removed and the same volume of PAGE elution buffer was added to the gel slice which was incubated overnight at 4°C rotating. The gel and buffer was spun at 16,000 x *g* for two minutes and the supernatant was removed and added to that previously collected. Glycogen (20 µg) was added to the eluted substrate. The DNA was ethanol precipitated by; adding 3x sample volume of 100% v/v ethanol and mixing. The sample was centrifuged at 16,000 x *g* for 20 minutes at RT. The supernatant was removed and discarded. 750 µl of 80% v/v ethanol was added and centrifuged at 16,000 x *g* for five minutes. The supernatant was discarded, 500 µl of 100% v/v ethanol was added and centrifuged at 16,000 x *g* for five minutes. The supernatant was discarded and the pellet was dried in a DNA Speed Vac (Savant) for 20 minutes. The DNA pellet was re-suspended in 50 µl of buffer (10 mM Tris pH 8.0, 10 mM NaCl, 0.1 mM EDTA).

#### 2.6.1.4 *Substrate quantification*

The labelled substrate was quantified by spotting onto DE81 paper (Whatman) using the 100 nM control substrate (see 2.6.1.1) as a control. The DE81 paper was washed for five minutes in 0.5 M $K_2HPO_4/KH_2PO_4$ buffer pH 7.0 thrice. The paper was subsequently washed for ten minutes each in 70% v/v ethanol and

100% v/v ethanol. The paper was air dried and exposed to a phosphor imaging plate. The plate was developed using a PMI system (Bio-Rad) and quantified using Quantity One software (Bio-Rad). The concentration of the substrate was determined using the following equation.

$$\frac{\text{average signal substrate}}{\text{average signal 100 nM sample}} \times 100 \text{ nM} = [\text{substrate}] \text{ nM}$$

### 2.6.2 Assay conditions

Helicase reactions (4 nM forked substrate, hMCM as indicated, 30 mM $K_2HPO_4/KH_2PO_4$ buffer, pH 8.5, 300 mM potassium glutamate (KGlut), 1 mM DTT, 100 μg/ml BSA (NEB), 2% v/v glycerol, 10 mM MgAc, 4 mM ATP) were incubated (one hour, 37°C) and stopped by the addition of ¼ volume of 5x stop buffer (80 mM EDTA, 0.8% w/v SDS, 40% v/v glycerol, 0.04% w/v xylene cyanol, 0.04% w/v bromophenol blue). Reaction products were separated on 11% w/v polyacrylamide TBE gel (two hours, at a constant voltage of 80 V). Gels were fixed in 7% v/v acetic acid for five minutes and dried for 20 minutes at 80°C using a gel dryer (Bio-Rad). The dried gel was exposed to a phosphor screen overnight. The phosphor screen was imaged and quantified using a PMI system and Quantity One software (Bio-Rad).

## 2.7 Electron microscopy (EM)

### 2.7.1 Binding of duplex DNA to hMCM for EM

hMCM was bound to duplex DNA. 5x No salt annealing buffer (200 mM HEPES pH 8.0, 5 mM EDTA) was added to 1 μM HF150 oligo (150 bp) and 1 μM HR80 oligo (80 bp, see Table 2.4). The DNA was annealed using a Biometra (T-personal) by placing it under the following heat cycle; 95°C for three minutes, cool at 0.02°C per second until reached 23°C. 8 μg of hMCM was incubated with 60 nM duplex DNA in annealing buffer (50 mM HEPES pH 7.5, 2 mM DTT, 50 μg/ml BSA (NEB), 10 mM MgAc and 4 mM ATP) for one hour at 37°C to bind the hMCM and duplex DNA. The samples were snap frozen in liquid nitrogen.

### 2.7.2 Negative stain EM

Electron microscopy of hMCM was carried out by Yuriy Chaban at Birkbeck Collage London with the following method. hMCM samples were applied to continuous carbon grids and stained with freshly made methylamine tungstate, pH 7. Data were collected on a FEI T12 microscope at magnification 67,000 and accelerating voltage 120 kV. Data were recorded on to Kodak SO-163 films and digitised using a Zeiss Photoscan densitometer (14 μm scanning step, corresponding to 2.5 Å/pixel) before analysis.

### 2.7.3 Image processing

Particle picking was carried out automatically using the program 'Boxer' (EMAN suite, Tang et al., 2007). Analysis of the CTF and correction was completed using the program 'CTFIT' (EMAN suite, Tang et al., 2007). The following image analysis was performed using IMAGIC-5 (van Heel et al., 1996): Images were normalised to the same standard deviation and band-pass filtered; the low-resolution cut-off was ~100 Å to remove uneven background in particle images and the high-resolution cut-off was ~7 Å. Then images were subjected to an alignment procedure followed by statistical analysis. Alignment and classification of images was performed as previously described (van Heel et al., 1996) and yielded classes representing characteristic views of the molecule. Primary structural analysis for hMCM and hMCM plus DNA complexes were performed using an *ab initio* approach where the orientations of the best 10-15 image classes were determined by angular reconstitution using C1 start up. 3D maps were calculated using the exact-filter back projection algorithm (van Heel et al., 1996). Structural analysis was performed using several starting models with several different sets of image classes for *ab initio* reconstructions. The first reconstructions were used for the following rounds of alignment and classification of images. The structures of the complexes were refined by an iterative procedure with the number of classes gradually increased. The final reconstruction for hMCM alone was calculated from the best 100 classes containing ~11 images each. For hMCM plus DNA, the final reconstruction was calculated from the best 155 classes containing ~10 images each. Resolution of the

map was assessed using the 0.5 threshold of Fourier Shell Correlation (van Heel et al., 2000), which corresponds to 23 Å.

### 2.7.4 Domain fitting

Domain fitting into the 3D map of hMCM and hMCM plus DNA complexes was performed manually with Chimera (Goddard et al., 2007). Illustrations were generated using Chimera. Surface representations (unless stated otherwise) are displayed at a threshold level of 1σ (standard deviation of densities within EM maps) that corresponds to ~100% of the expected mass at the specific protein density of 0.84 kDa/Å$^3$.

## 2.8 Mammalian cell analysis

### 2.8.1 Assay for DNA synthesis

The percentage of cells in S phase was determined using (5-ethynyl-2-deoxyuridine) Edu. Edu is a nucleoside analogue and is incorporated into DNA during DNA synthesis. The Click-iT Edu Cell Proliferation Assay kit (Life Technologies, Cat: C10337) was used. Cycling cells grown on glass coverslips were incubated with 0.01 mM Edu in media (see 2.2.1) at 37°C, 5% v/v $CO_2$ for 30 minutes. Coverslips were fixed in 4% w/v PFA for 15 minutes, then stored at -20°C for future processing or processed immediately. Coverslips were washed twice in 3% w/v BSA (Jackson, Cat: 001-000-162) in dPBS. The cells were made permeable by incubating the coverslips in 0.5% v/v Triton X-100 in dPBS and then washed twice in 3% w/v BSA in dPBS. Edu is detected by covering the coverslip in 20 µl of Click iT cocktail (1x Click-iT reaction buffer, 4 mM aqueous copper sulphate ($CuSO_4$), 0.24% v/v Alexa Flour 488 azide, 1x Click-iT reaction buffer additive) for 30 minutes in the dark at RT. Coverslips were subsequently washed in 3% w/v BSA in dPBS and once in dPBS. The DNA was detected by a 30 minute incubation in Hoechst 33258 (1/10,000 in dPBS) at 37°C in the dark. Coverslips were washed twice in dPBS before mounting (as described in 2.3.5.1).

### 2.8.2 Protein extraction for western blot

Cells were grown as described in 2.2. Samples were processed to reveal i.) total protein, ii.) detergent resistant pellet (insoluble proteins and those attached to insoluble structures), iii.) detergent soluble proteins, iv.) 0.5 M NaCl soluble proteins, v.) DNase I resistant proteins (bound to the nuclear matrix), vi.) DNase I sensitive proteins (chromatin bound proteins), vii.) high salt resistant proteins (Mock sample which contains protein tightly bound to chromatin or the nuclear matrix) and viii.) control sample to show proteins released during 37°C incubation period. This method is summarised in figure 2.1. A protocol for this method was accepted for publication during the course of this PhD (Wilson et al., 2014, Appendix A).

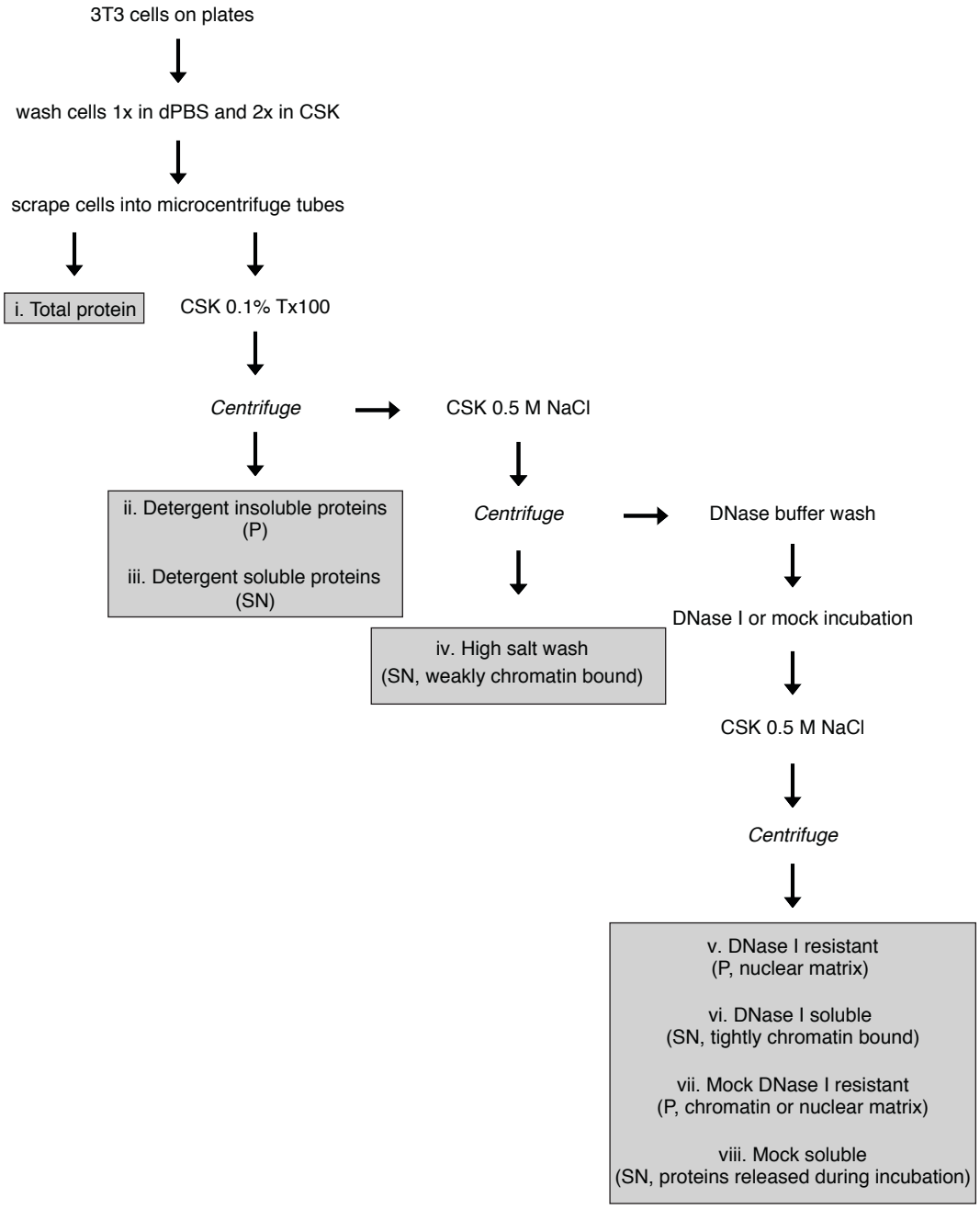


**Figure 2.1.** Flow diagram to show nuclear matrix protein extraction for analysis by SDS-PAGE and western blot. dPBS (Dulbecco's phosphate buffered saline without calcium, magnesium or phenol red), CSK (cytoskeletal buffer ), Tx100 (triton x-100, P (pellet), SN (supernatant).

Tissue culture plates were washed once in dPBS and twice in cytoskeletal buffer (CSK, 10 mM Pipes pH 6.8, 300 mM sucrose, 100 mM NaCl, 1 mM $MgCl_2$, 1 mM ethylene glycol tetraacetic acid (EGTA), 1 mM DTT and protease inhibitors (cOmplete®, EDTA-free; Roche)). The plates were tilted on a 45° angle for two minutes and excess buffer was removed before harvesting the cells by scraping. The volume of cells was measured and put into a clean micro centrifuge tube. Final concentrations of 2 mM phenylmethanesulfonylfluoride (PMSF) and 0.1% v/v Triton X-100 were added to the cells.

The volume of cells was split between four micro centrifuge tubes (1x vol) and one tube (i.) was prepared for SDS PAGE as described in section 2.3.1.2. The remaining three tubes were incubated on ice for two minutes and spun at 6,800 x *g* for two minutes at 4°C. The supernatant from ii. was transferred to a clean micro centrifuge tube labelled iii. (detergent soluble proteins) and the pellet ii. (insoluble fraction) was re-suspended in 1x volume CSK buffer plus 0.1% v/v Triton X-100. ii. and iii were prepared for SDS PAGE as described in section 2.3.1.2. The supernatant from the remaining two tubes was discarded and the pellet washed (by re-suspending and centrifugation at 6,800 x *g* for three minutes at 4°C) in 1x volume CSK plus 0.1% v/v Triton X-100 and 0.5 M NaCl. The supernatant from one tube was transferred to a clean micro centrifuge tube iv. (high salt wash) and prepared for SDS PAGE as described in section 2.3.1.2. The supernatant from the remaining tube was discarded and both pellets re-suspended in 100 µl DNase I incubation buffer (400 mM Tris-HCl, 100 mM NaCl, 60 mM $MgCl_2$, 10 mM $CaCl_2$ at pH 7.9). Samples were centrifuged at 9,500 x *g* for three minutes at 4°C and the supernatant was discarded. Pellets were re-suspended in 1x volume DNase I incubation buffer. $1/30^{th}$ of volume DNase I, RNase free (Roche) was added to v. Both samples were incubated at 37°C for one hour flicking every ten minutes. $1/10^{th}$ of volume 5 M NaCl was added to the samples and incubated at 37°C for a further five minutes. Samples were centrifuged at 9,500 x *g* for five minutes. The supernatant was transferred to clean micro centrifuge tubes. Pellets were re-suspended in 1x volume DNase I incubation buffer. Remaining samples were prepared for SDS PAGE as described in section 2.3.1.2. Samples plus DNase I give v. DNase pellet (nuclear matrix bound proteins) and vi. DNase supernatant (chromatin bound proteins). Samples

minus DNase I give vii. Mock pellet (chromatin and nuclear matrix bound proteins) and viii. Mock supernatant (proteins released during incubation period).

Samples were analysed by SDS PAGE and western blotting as described in 2.3.1 and 2.3.4.

### 2.8.3 Protein extraction for immunofluorescence

Throughout the procedure coverslips are processed with the cells on the top surface. Coverslips were processed to reveal i. total protein, ii. detergent resistant proteins, iii. high salt and DNase I resistant proteins (nuclear matrix bound proteins) and iv. high salt resistant proteins (chromatin or nuclear matrix bound proteins). This method is summarised in figure 2.2. A protocol for this method was accepted for publication during the course of this PhD (Wilson et al. (in press), Appendix A).

Cells grown on coverslips were removed from media and washed in dPBS in a 24 well plate. i. was moved to 4% w/v PFA to fix the cells for ten minutes at RT then dPBS at 4°C. Remaining coverslips were moved into CSK plus 0.1% v/v Triton X-100 for one minute at RT. ii. was moved to dPBS and processed as i. above. The remaining coverslips were moved to CSK plus 0.1% v/v Triton X-100 and 0.5 M NaCl for one minute at RT. Coverslips were washed twice in DNase I incubation buffer by incubation for one minute at RT. Coverslips were incubated at 37°C for one hour, iii. in 20 µl of DNase I incubation buffer plus 1/10$^{th}$ volume DNase I, RNase free (Roche), iv. in 20 µl of DNase I incubation buffer. Coverslips were washed in CSK plus 0.1% v/v Triton X-100 and 0.5 M NaCl for one minute at RT, then moved to dPBS and processed as i. above.

Following extraction coverslips were analysed straightaway by IF as described in 2.3.5.

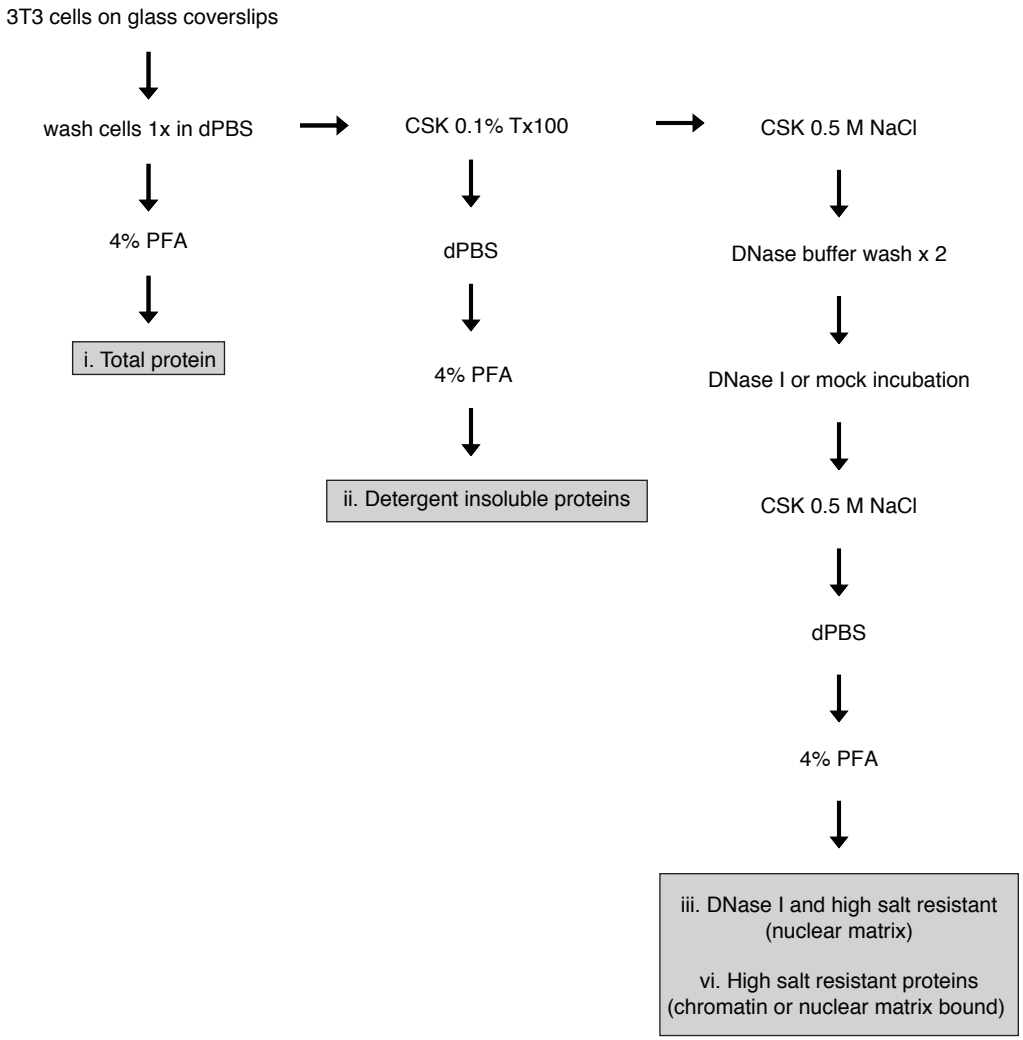


**Figure 2.2.** Flow diagram to show nuclear matrix protein extraction for analysis by immunofluorescence. dPBS (Dulbecco's phosphate buffered saline without calcium, magnesium or phenol red), PFA (paraformaldehyde), CSK (cytoskeletal buffer ), Tx100 (triton x-100, P (pellet), SN (supernatant).

#### *2.8.3.1 Cross-linking*

Where stated cells were treated prior to extraction with a cell-permeable reducing cross-linker dithiobis succinimidyl propionate (DTSP) which binds proteins to proteins (Baumert and Fasold, 1989). DTSP is a reversible cross linker that reacts specifically with amine functional groups via N-hydroxysuccinimide (NHS) esters in DTSP. Cells growing on 15 cm dishes were washed three times with dPBS at RT then incubated 15 ml cross-link buffer (dPBS, 1 mM $MgCl_2$, 0.01% v/v Triton X-100) with DTSP (Sigma) at 200 µg/ml, on a rotary shaker for 10 minutes at RT (Ainscough et al., 2007). Reactions were quenched with 15 ml 10 mM Tris-HCl pH 7.6, 1 mM EDTA.

## 2.9 Cell free system

### 2.9.1 Harvesting of nuclei and cytoplasmic extracts

Cells were synchronised as described in 2.2.2. Nuclei and cell extracts were prepared at precise time points after release from quiescence in order to harvest cells in a particular phase of the cell cycle. For 3T3 cells, mid-G1 phase nuclei and cytoplasmic extracts were prepared 15 hours after release and late-G1 phase nuclei and cytoplasmic extracts were prepared 17 hours after release. HeLa cells were harvested one hour following synchrony at the G1/S phase boundary (see 2.2.2.2).

Tissue culture dishes were washed once in ice-cold dPBS and twice in ice-cold hypotonic buffer (20 mM K–HEPES pH 7.8, 5 mM KAc, 0.5 mM $MgCl_2$, 1 mM DTT). At 4°C dishes were incubated in hypotonic buffer plus protease inhibitors (cOmplete®, EDTA-free; Roche) at half the recommended concentration for ten minutes. The hypotonic buffer was removed and the plates were tilted at a 45° angle for ten minutes at 4°C. Excess buffer was discarded before scraping the cells from the plates into a 1 ml Dounce homogeniser (Wheaton). The cells were gently homogenised to release the nuclei but keep the nuclear membrane intact. Sufficient homogenisation was verified by viewing a small sample microscopically. Approximately ten strokes for 3T3 cells or 20 strokes for HeLa cells were required for adequate homogenisation. The cell mixture was centrifuged at 980 x *g* at 4°C for two minutes. The pellet (nuclei) was re-

suspended in an equal volume of hypertonic buffer plus protease inhibitors (as above) and frozen as 10 µl beads in liquid nitrogen. The nuclei concentration was approximately 2.5 x $10^4$ per µl. The supernatant was removed and re-centrifuged for 20 minutes at 16,000 x *g*. This high-speed centrifugation separated the fraction into three parts: the top lipid layer, the middle cytoplasmic extract and the pellet. The middle layer was isolated and frozen as 20 µl beads in liquid nitrogen (Coverley et al., 2000, Krude et al., 1997).

### 2.9.2 DNA initiation assays

DNA initiation assays were adapted from the following: Coverley et al. (2005), Krude et al. (1997), Copeland et al. (2010), Coverley et al. (2002). Typically reactions contained 10 µl of cytosolic extract supplemented with the following in the proceeding order; 1:10 PreMix (400 mM HEPES-KCl pH 7.8, 70 mM $MgCl_2$, 30 mM ATP (Sigma), 1 mM each of GTP, CTP, UTP (all Sigma), 1 mM each of dATP, dGTP, and dCTP (all Sigma), 0.5 mM DTT and 400 mM phosphocreatine; PreMix was made in bulk and stored in small aliquots at -80°C), 1:75 0.1 M $MgCl_2$ and 1:50 creatine phosphate kinase (CPK; Calbiochem, stored in aliquots at -20°C and made fresh before use by diluting 0.1 g/ml in CPK buffer; 50% v/v glycerol, 100 mM HEPES-KCl pH 7.8, 1 nM DTT). For experiments to be analysed at the next step by fluorescence microscopy 1:100 1 mM biotin-16-dUTP (Roche) was added. The final concentration of the components in a DNA initiation assay were: 40 mM HEPES-KCl pH 7.8, 7 mM $MgCl_2$, 3 mM ATP, 0.1 mM each of GTP, CTP, UTP, 0.1 mM each of dATP, dGTP, and dCTP, 0.05 mM DTT, 40 mM phosphocreatine, 2 mg/ml creatine phosphokinase and 10 µM biotin-16-dUTP when required. Recombinant proteins were added at this point and mixed thoroughly (please see results for details). 2 µl nuclei were added last and mixed by careful pipetting. The nuclei and supplemented extracts were incubated together for 30 minutes at 36.5°C (Coverley et al., 2005, Stoeber et al., 1998, Krude et al., 1997, Coverley et al., 2000, Coverley et al., 2002).

#### *2.9.2.1 Two-step assays*

To analyse the capability of nuclei to initiate DNA synthesis, DNA initiation assays (see 2.9.2) were centrifuged at 3,300 x *g* for one minute. Between 10 and 12

µl of the supernatant was removed and prepared for SDS PAGE as described in 2.3.1.2. The nuclei were resuspended in 20 µl of S phase extract supplemented with 1:10 PreMix, 1:75 $MgCl_2$, 1:50 CPK and 1:100 biotin-16-dUTP as described in 2.9.2. Reactions were incubated for 30 or 60 minutes at 37°C and prepared for microscopic analysis (2.9.2.2).

### *2.9.2.2 Analysis by fluorescence*

To visualise DNA synthesis, cell free reactions were quenched by addition of 200 µl 0.2% v/v Triton X-100 in dPBS and 200 µl 8% w/v PFA and incubated at RT for 20 minutes. Poly-lysine coated coverslips were prepared by dipping clean, glass coverslips in 2 mg/ml poly-L-lysine hydrobromide (4,000 – 15, 000 Da, Sigma) and leaving to dry overnight. The polylysine-coated coverslips were placed at the bottom of a tube, with a diameter similar to the size of the cover slip, and 0.5 ml 20% w/v sucrose was placed on top of the coverslip. The DNA initiation reaction was loaded on top of the sucrose. The nuclei were bound to polylysine-coated coverslips by centrifugation at 500 x *g* for seven minutes. The sucrose solution was discarded before removing the coverslip from the tube. Coverslips were washed in 0.5% v/v Triton X-100 in dPBS for five minutes twice. Incorporated biotinylated-nucleotides were detected with streptavidin–FITC (Trevigen) diluted 1/400 in dPBS and DNA was stained with Hoechst 33258 (1/100,000) in dPBS. These dyes were incubated with the coverslips in the dark for one hour at 37°C. The amount of light available to the coverslips was minimised. The coverslips were washed for five minutes in 0.5% v/v Triton X-100 in dPBS thrice. Coverslips were mounted and analysied as described in 2.3.5.1.

### *2.9.2.3 Analysis by western blotting*

For analysis of nuclei and soluble fraction by SDS PAGE and western blotting 10 µl of ice cold 0.2% v/v Triton X-100 in dPBS was added to DNA initiation assays (see 2.9.2). Reactions were mixed and spun at 3,300 x *g* for one minute. The supernatant was isolated and prepared for SDS PAGE and western blotting (see 2.3.1 and 2.3.4**)**. The pellet was re suspended in 20 µl of 0.2% v/v Triton X-100 in

dPBS and prepared for SDS PAGE and western blotting as described in 2.3.1 and 2.3.4.

### 2.9.3 *in vitro* phosphorylation assays

To examine the capability of recombinant kinases to phosphorylate recombinant hMCM reactions were carried out in the presence of buffer, an ATP regenerating system and recombinant proteins only. Reactions contained 10 µl hMCM dilution buffer (25 mM HEPES, pH 8.0, 200 mM sodium glutamate) supplemented with 1:10 PreMix (400 mM HEPES-KCl pH 7.8, 70 mM $MgCl_2$, 30 mM ATP (Sigma), 1 mM each of GTP, CTP, UTP (all Sigma), 1 mM each of dATP, dGTP, and dCTP (all Sigma), 5 mM DTT and 400 mM phosphocreatine), 1:75 0.1 M $MgCl_2$, 1:50 CPK (0.1 g/ml in CPK buffer; 50% v/v glycerol, 100 mM HEPES-KCl pH 7.8, 1 nM DTT). Recombinant hMCM (88 nM), cyclin E/CDK2 (6.8 nM), cyclin A/CDK2 (1.72 µM) and/or DDK (71 nM or 35.5 nM) were added as described in the results. Reactions were mixed thoroughly before incubation at 37°C for 30 minutes. Reactions were prepared for SDS PAGE and western blotting as described in 2.3.1 and 2.3.4.

#### *2.9.3.1 Phosphatase assays*

Lambda Protein Phosphatase (P0753S, NEB) was used according to the manufacturers guidelines.

#### *2.9.3.2 Inhibitors*

Stock solutions of 20 mM, PHA-767491 (DDK inhibitor, Sigma) and Roscovitine (CDK inhibitor, Sigma) were aliquoted and stored at -80°C. Inhibitors were added to reactions at concentrations indicated in the text, mixed thoroughly and incubated on ice for two minutes prior to kinase addition.

## 2.10 Statistical analysis

All statistical analyses were performed using students T-test in Microsoft Excel (version 14.3.8). Statistical significance is indicated by stars. Exact values are

shown in the figure legend. Error bars are standard error of the mean (SEM) or standard deviation (SD) as indicated.

*Chapter 3*

# Production, purification and function of recombinant hMCM complex

# 3 Production and purification of recombinant hMCM

The following work has been prepared for publication as is shown in paper format in Appendix C.

## 3.1 Introduction

Historically, isolation of intact, functional MCM2-7 heterohexamers has proved challenging. The first functional MCM2-7 complex was purified from *Xenopus* egg extracts using a "replication licensing factor" (RLF) assay (Chong et al., 1995). The biochemical characterisation of the eukaryotic MCM2-7 complex is less than complete, although recently significant progress has been made in the purification of functional recombinant MCM2-7 complexes from *S. cerevisiae* (Bochman and Schwacha, 2008, Bochman and Schwacha, 2007, Schwacha and Bell, 2001). A *S. cerevisiae* MCM2-7 complex expressed in insect cells has been purified and demonstrated to possess helicase activity *in vitro* (Bochman and Schwacha, 2008). Helicase activity of *S. cerevisiae* MCM2-7 is boosted by the addition of potassium glutamate and is inhibited by the addition of potassium chloride (Bochman and Schwacha, 2008), suggesting for helicase activity MCM2-7 requires specific salt conditions. In metazoan systems, in addition to the *Xenopus* system, a "CMG" (Cdc45-MCM2-7-GINS) complex has been isolated from *Drosophila* egg extracts that displays robust DNA helicase activity (Moyer et al., 2006, Ilves et al., 2010). To date helicase activity involving human MCM proteins has been limited to that described for a sub-complex (probably a dimer of trimers) consisting of human MCM4, 6 and 7 (Ishimi, 1997, You et al., 2003).

This chapter describes the production of recombinant human MCM (hMCM) that displays ATP hydrolysis activity and is capable of unwinding duplex DNA. Using single particle asymmetric electron microscopy reconstruction, we demonstrate that hMCM forms a hexamer that undergoes a conformational change when bound to a forked DNA substrate. Recombinant hMCM provides an important tool for the biochemical reconstitution of the putative human replicative helicase.

## 3.2 Aims

- To produce and purify recombinant hMCM.
- To analyse the activity of hMCM *in vitro.*
- To determine the asymmetric three dimensional (3D) structure of hMCM.

## 3.3 Experimental design

*In vitro*, MCM2-7 is targeted by CDKs and DDKs that phosphorylate MCM subunits to control loading and activation of the MCM2-7 complex (see Chapter 1 for details). If grown in eukaryotic systems there is a high chance hMCM would be phosphorylated by cellular kinases that could potentially inhibit hMCM activity. In order to understand the role of post-translational modifications in the functional loading of hMCM it is important to analyse naïve hMCM (i.e. without any post-translational modifications). Subsequently a method for production of naïve, recombinant hMCM in *E. coli* was devised.

## 3.4 Results and discussion

### 3.4.1 Production and Purification of Recombinant hMCM

Dr Richard P. Parker-Manuel, a previous member of the Chong lab, devised a protocol to produce recombinant hMCM in *E. coli* (Hesketh et al., under review). Three constructs were designed each encoding two hMCM proteins. hMCM5, 6 and 7 have an N-terminal His-tag to allow purification and hMCM7 also has two antibody tags, S tag and Trx tag, to aid future analysis (Fig. 3.1A). A schematic of the expected hMCM conformation is depicted in figure 3.1B. The three constructs encoding hMCM were co-expressed in a single *E. coli* cell to increase solubility of the complex. hMCM was grown from a single colony to a 50 L culture as shown in the flow diagram in figure 3.2A (for details see Chapter 2.4). The 50 L culture was grown in a fermenter to allow the pH, dissolved oxygen and temperature to be monitored. The growth of the *E. coli* culture was monitored by measuring the OD at 600 nm (Fig. 3.2B). The temperature was reduced to 18°C prior to induction to enhance production of soluble protein. Soluble and insoluble samples were isolated from aliquots at numerous time points after induction to

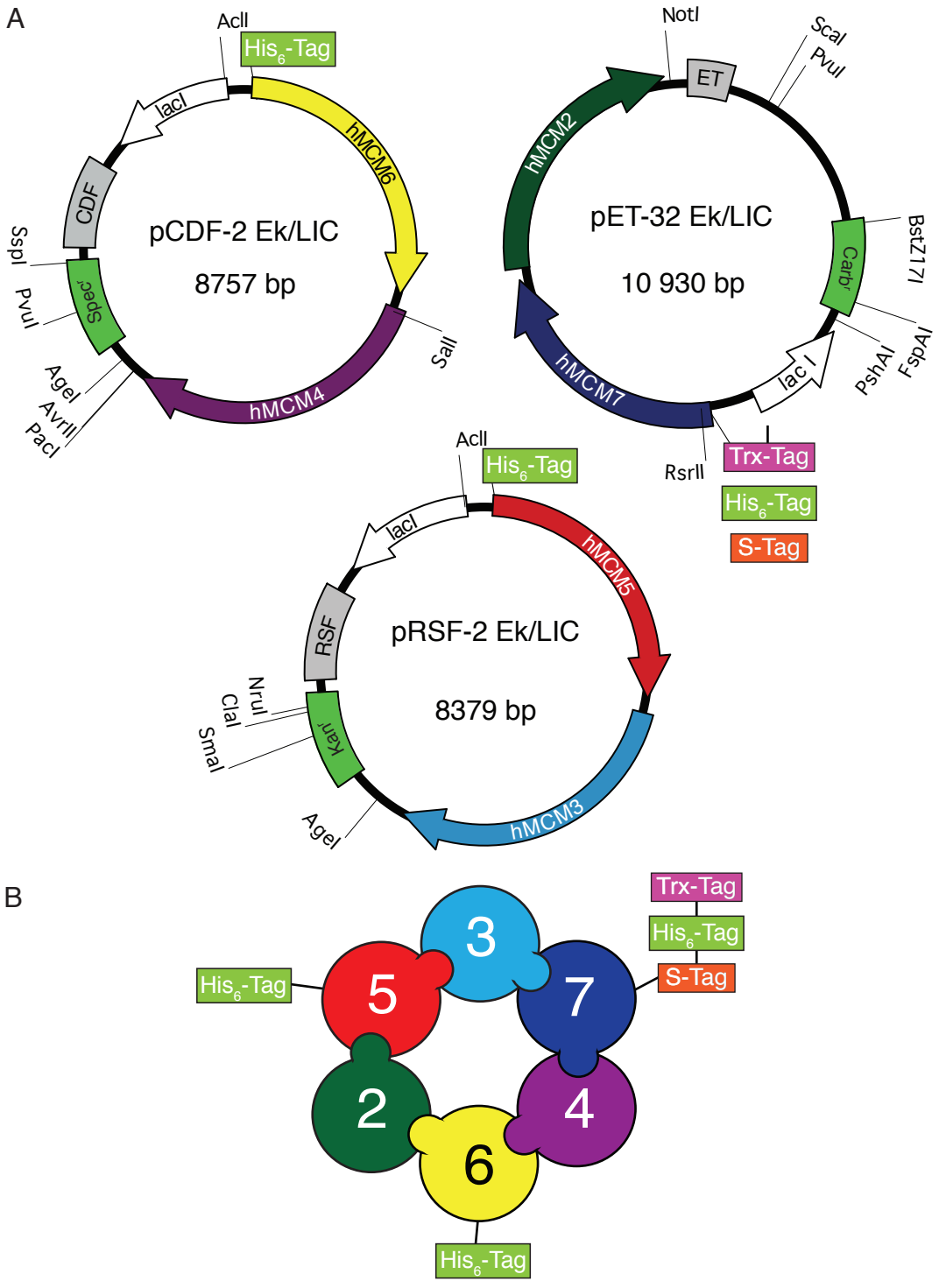


**Figure 3.1.** hMCM plasmid maps and schematic of conformation. A. Plasmid maps of each construct. The lac operon, origin (grey box), resistance marker (spectinomycin (spec), kanamycin (kan), carbenicillin (carb), purification tags ($His_6$-Tag) and antibody tags (S-Tag and Trx-Tag) and each hMCM subunit is shown. The commercial name and full length of each construct is indicated in base pairs (bp). A number of restriction sites are indicated. B. Schematic of the expected conformation of hMCM showing purification tags ($His_6$-Tag) and antibody tags (S-Tag and Trx-Tag). These plasmids were made previously by Dr Richard P. Parker-Manuel.

monitor the expression of each hMCM subunit by western blotting. Each hMCM subunit was expressed in the soluble fraction of harvested culture (Fig 3.2C, D).

The recombinant hMCM was purified according to the scheme outlined in figure 3.3A. Immobilised metal affinity chromatography (IMAC) was used to purify the His-tagged proteins. The elution profile and Coomassie stained SDS PAGE gel of elution fractions (Fig. 3.3B) shows the peak of protein. Elution fractions E10 – E16 were pooled and further purified by gel filtration to separate the proteins by size (Fig. 3.4). The elution fractions corresponding to the predicted molecular weight of hMCM (567 KDa) were pooled for further purification (A5 – A10, Fig. 3.4B, C). The subsequent peaks are thought to be single his-tagged hMCM subunits (such as hMCM5) or smaller hMCM complexes such as dimers or trimers. The pooled elutant was subsequently purified by anion exchange to separate proteins by charge (Fig. 3.5). Elution fractions were analysed by western blotting to determine which peak corresponded to hMCM containing all six hMCM subunits (Fig 3.5D). Human, *Xenopus*, *Drosophila S. pombe* and *S. cerevisiae* MCM proteins have been previously isolated as a sub-complex of MCM hexamer containing only subunits MCM4, 6, and 7 (Ishimi, 1997, Kanter et al., 2008, Schwacha and Bell, 2001). To ensure purification of heterohexameric hMCM, western blots were probed for subunits hMCM2 and 4 and fractions containing both these subunits were pooled (A15 – B11, Fig. 3.5D).

The presence of all six hMCM subunits in the purified complex was demonstrated by western blotting using specific antibodies (Fig 3.6A). Putative degradation products in addition to all six full-length hMCM subunits were detected. To show the extent of purification, samples from each purification step were analysed by SDS PAGE and stained with Coomassie blue (Fig 3.6B). The results depict the concentration of a band running at approximately 100 KDa, which is the approximate size of hMCM4 and hMCM6, and the loss of a lower non-specific 60 KDa band. The extent of purification determined by protein concentration was calculated and is shown in Table 3.1. The clarified *E. coli* lysate was purified nearly 90,000 fold to produce 2.5 mg of hMCM at a concentration of 1 mg/ml. Typically 82.5 μg of hMCM per litre *E. coli* culture is produced. This is the first report of production of a recombinant human MCM2-7 complex, and

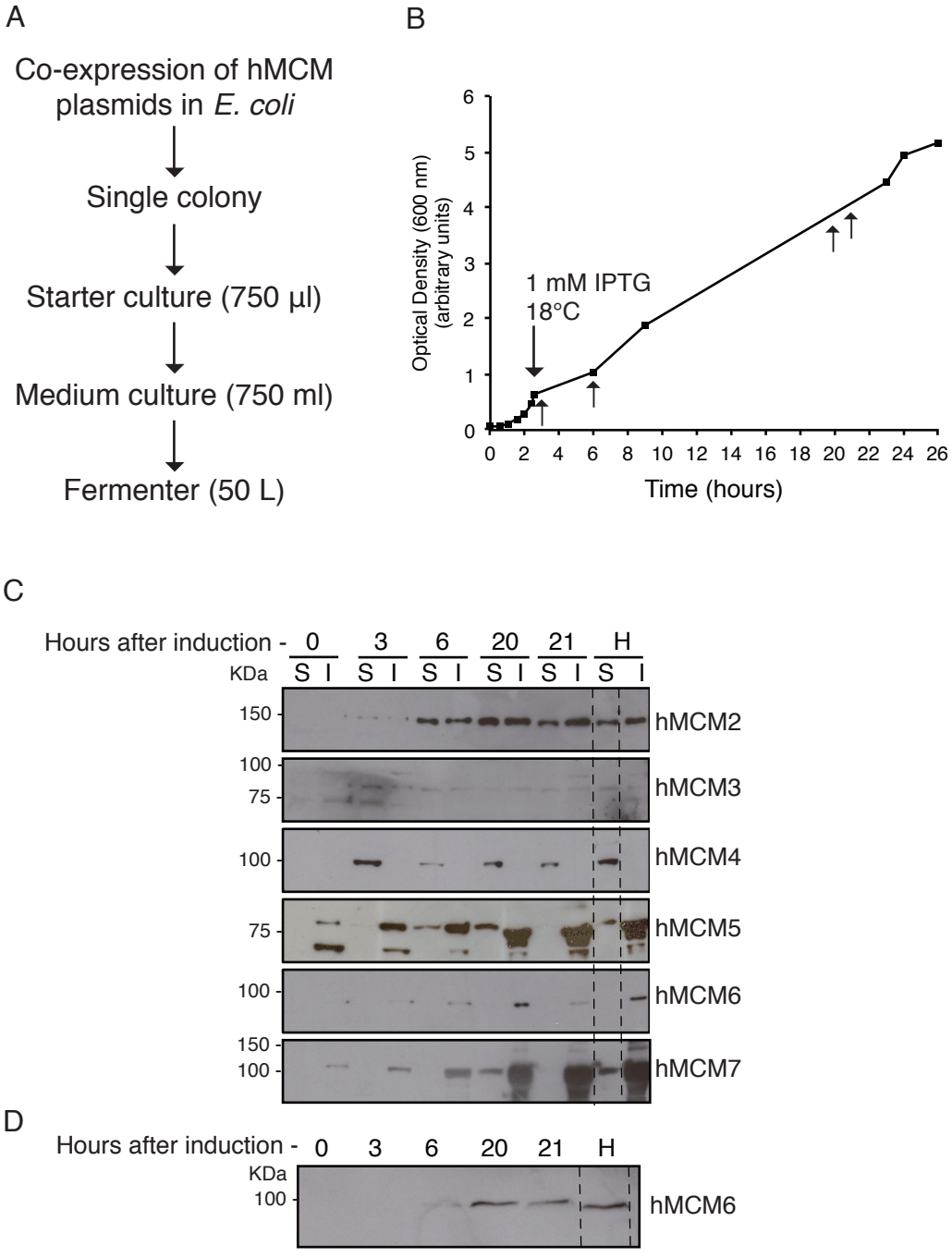


**Figure 3.2.** Summary of hMCM production from a typical 50 L bioreactor run A. Flow diagram of the scheme outlined for hMCM production. B. The growth of *E. coli* in a 50 L bioreactor expressing hMCM monitored by measuring the optical density at 600 nm at numerous time points after inoculation. The addition of IPTG and temperature change to 18°C is indicated with downwards arrow. Arrows pointing up indicate when samples were taken for western blot analysis (C). C. Western blots probed for each hMCM subunit, of soluble (S) and insoluble (I) samples taken from the 50 L fermenter at a number of time points after induction. The highlighted lane in the harvest (H) sample shows the sample purified. D. Western blot probed for hMCM6 showing soluble samples only as in C. Western blot in D is a higher exposure. Marker is Precision Plus Protein standards (Bio-Rad).

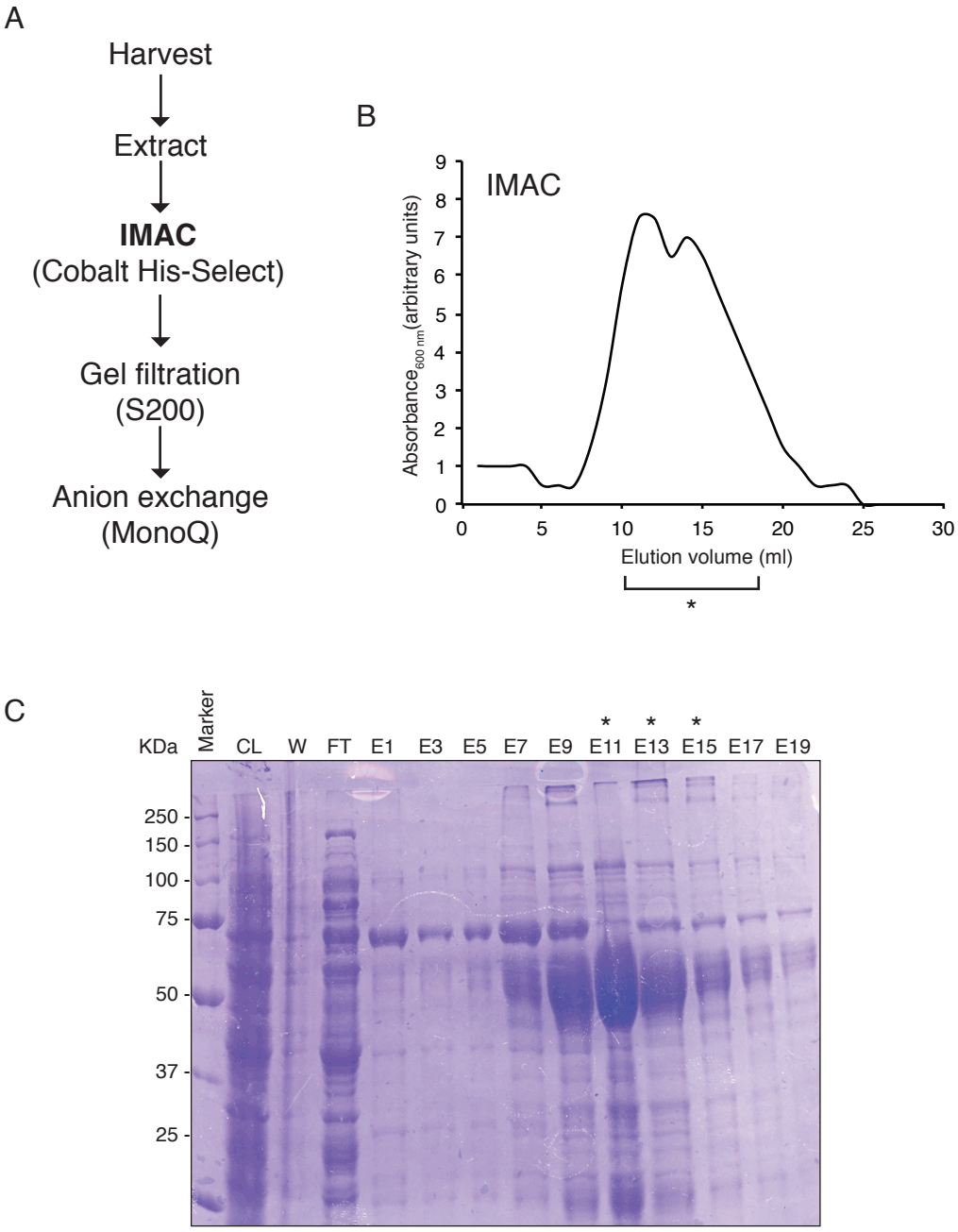


**Figure 3.3.** Summary of immobilised metal affinity chromatography (IMAC) purification of hMCM. A. Schematic of hMCM purification. B. Elution profile for IMAC purification step. hMCM was bound to 24 ml His-Select cobalt beads by batch binding before packing into a XK16/20 column. * indicates elution samples taken to the next purification step. C. Coomassie stained SDS-PAGE gel to show extent of purification. CL - clarified lysate, W - wash, FT - flow through, E1 - E19 - Elution fractions 1-19. Elution fractions E10 - E16 were taken to the next purification step (indicated by *). Marker is Precision Plus Protein standards (Bio-Rad).

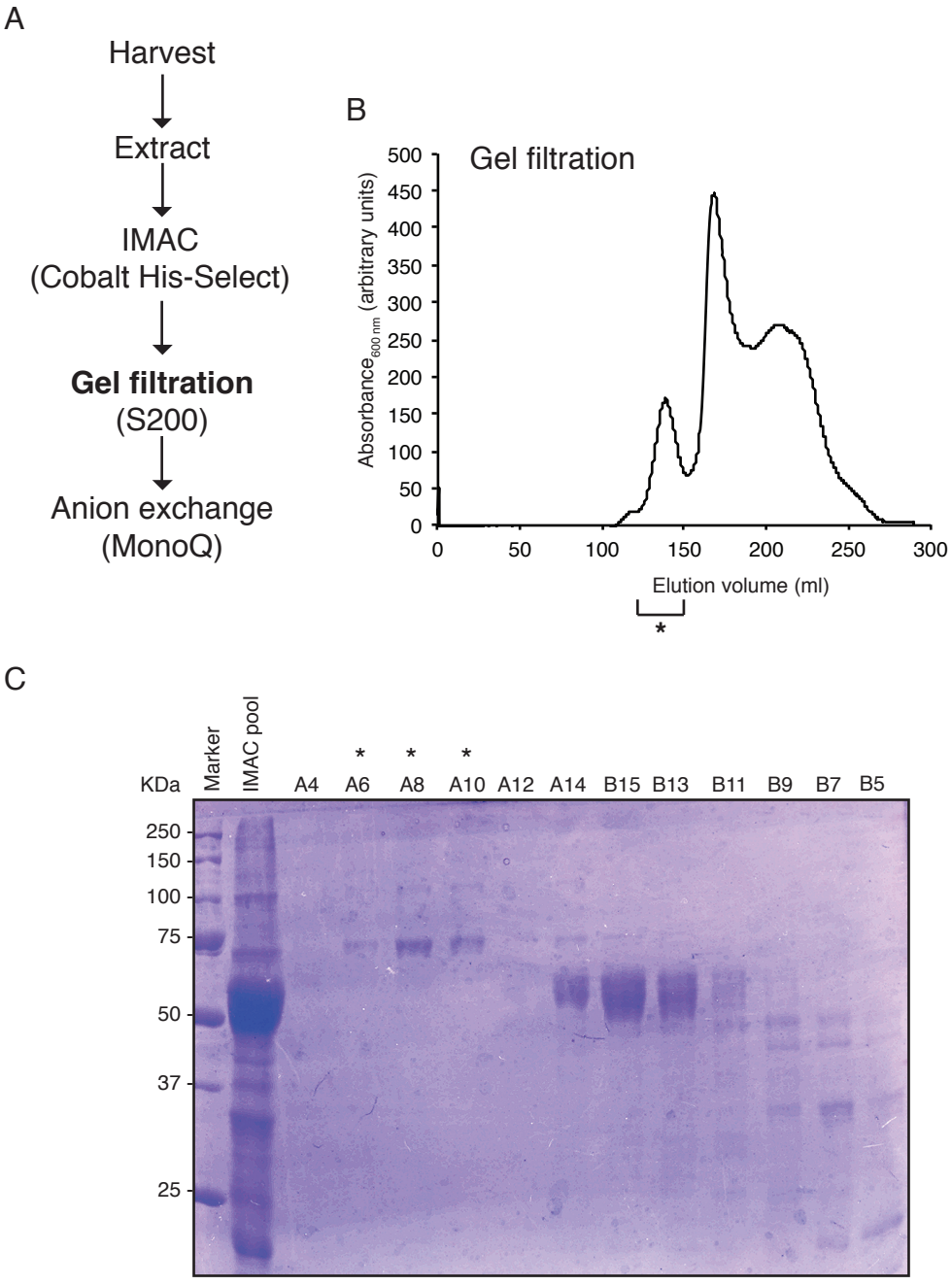


**Figure 3.4.** Summary of gel filtration purification of hMCM. A. Schematic of hMCM purification. B. Elution profile for gel filtration (S200) purification step. Pooled fractions from IMAC were further purified using a 320 ml HiLoad 26/600 Superdex 200 column. * indicates elution samples taken to the next purification step. C. Coomassie stained SDS-PAGE gel to show extent of purification. IMAC pool - pooled samples from previous purification step, A4 - B5 - elution fractions. Elution fractions A5 – A10 were taken to the next purification step (indicated by *). Marker is Precision Plus Protein standards (Bio-Rad).

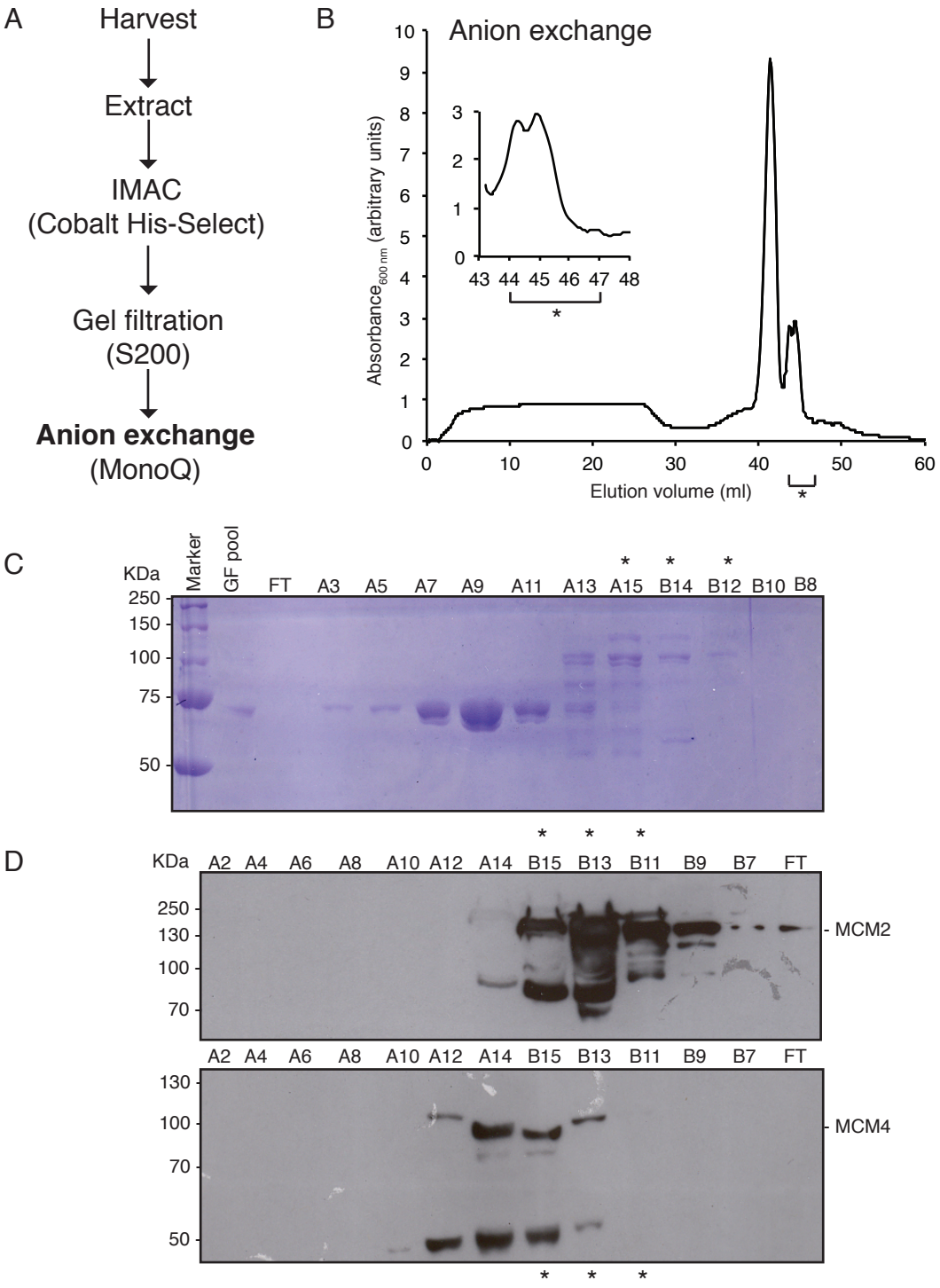


**Figure 3.5.** Summary of anion exchange purification of hMCM. A. Schematic of hMCM purification. B. Elution profile for anion exchange (MonoQ) purification step. Pooled fractions from gel filtration were further purified using a 1 ml MonoQ column. Insert focuses on the pooled fractions. * indicates elution samples taken to the next purification step. C. Coomassie stained SDS-PAGE gel to show extent of purification. GF pool - pooled samples from previous purification step, FT - flow through, A3 - B8 - Elution fractions. Marker is Precision Plus Protein standards (Bio-Rad). D. Western blots of elution fractions A2 - B7 and FT probed for MCM2 and MCM4. Marker is PageRuler Plus Prestained (Thermoscientific). Elution fractions A15 – B11 were pooled (indicated by *).

will enable the first detailed human protein-specific analysis of MCM2-7 function.

**Table 3.1.** The fold purification and concentration of recombinant hMCM from a typical 50 L fermenter run. The protein concentration is determined using a Bio-Rad Protein Assay Dye Reagent (see Chapter 2.3.6 for details).

| Purification Step | [Protein] (mg/ml) | Volume (ml) | Total Protein (mg) | Percentage yield (%) |
|---|---|---|---|---|
| Extract | 34.29 | 600 | 20576.65 | N/A |
| IMAC* (Cobalt His-Select) | 11.448 | 9 | 103.03 | 0.5 |
| Gel filtration (S200) | 0.554 | 24 | 13.31 | 0.06 |
| Anion exchange (MonoQ) | 0.999 | 2.5 | 2.5 | 0.012 |

*IMAC – immobilised metal affinity chromatography

The protocol used to produce hMCM has been demonstrated to be reproducible. A further 14 mg of hMCM has been produced, through three fermentations, during the course of this PhD. The 14 mg of hMCM was sent to collaborators at University of Southern California who are attempting to produce crystal structures.

The western blot of purified hMCM (Fig. 3.6A) shows multiple hMCM bands indicating degradation of the hMCM sample. When producing more hMCM an improved method to reduce proteolysis is required. In addition to the current protease inhibitors used (please see Chapter 2.4), EGTA could be used after IMAC purification to inhibit any metallo-proteases.

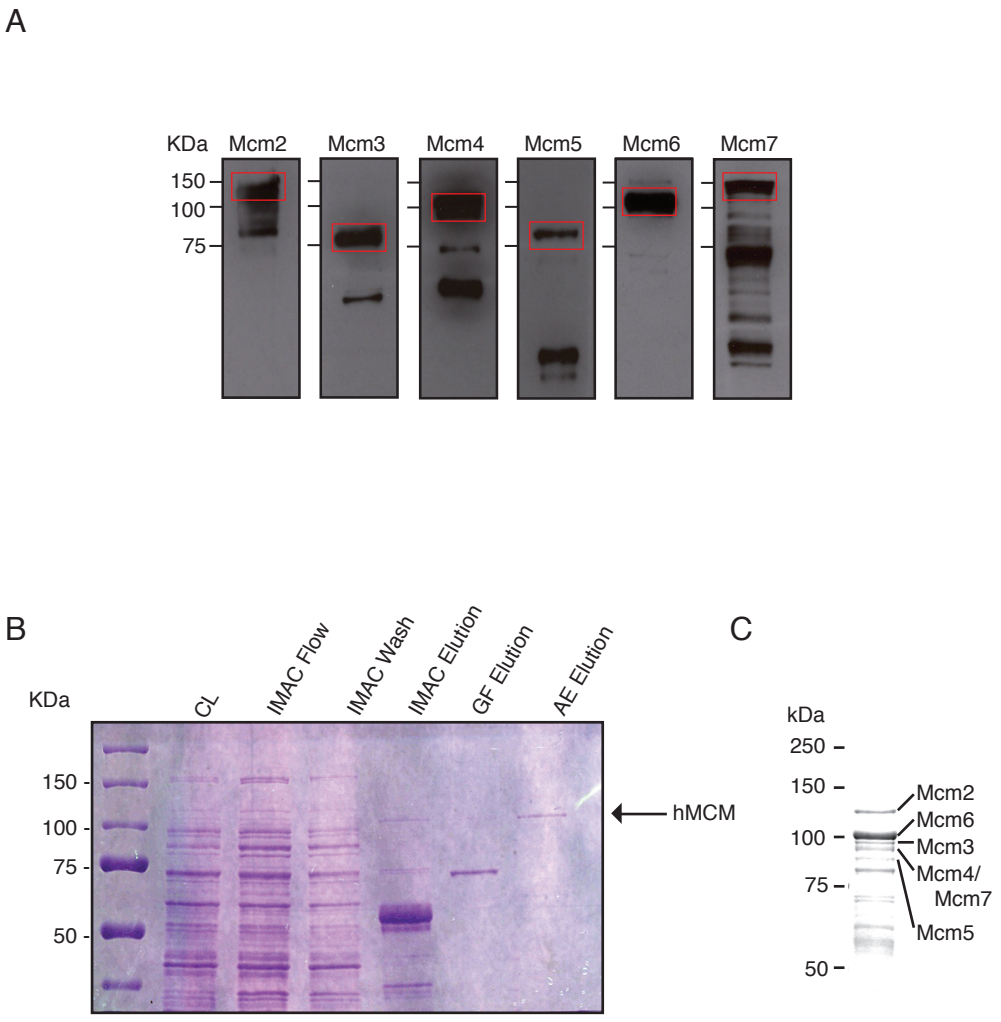


**Figure 3.6.** Summary of hMCM purification A. Western blot of purified hMCM probed with each hMCM subunit. The correct molecular weight substrate is indicated with a red box for each subunit. B. Coomassie stained gel of hMCM from different stages in the purification; clarified lysate (CL), immobilised metal affinity chromatography (IMAC), gel filtration (GF), anion exchange (AE). C. Coomassie stained gel of hMCM at a higher concentration than shown in B. to allow visualisation of all hMCM subunits. Marker is Precision Plus Protein standards (Bio-Rad).

### 3.4.2 Production and purification of mutant hMCM

An ATPase deficient mutant was produced using three constructs, each encoding two of six hMCM subunits harbouring a point mutation to inactivate the Walker A motif for each hMCM subunit (Schwacha and Bell, 2001, Chong et al., 2000). These constructs were produced previously by (Dr Richard P. Parker-Manuel). Point mutations were in MCM2 - K529E, MCM3 - K351E, MCM4 - K516E, MCM5 - K387E, MCM6 - K402E and MCM7 - K387E. These constructs were transformed into *E. coli* Rosetta 2 (DE3, Novagen) and mutant hMCM was purified in the same way as WT hMCM (Fig. 3.7, 3.8). This protein will be used as a negative control in future experiments and is referred to as 'mutant hMCM'.

### 3.4.3 ATP hydrolysis activity of hMCM

Previously, ATP hydrolysis has been demonstrated for MCM complexes derived from archaea (Chong et al., 2000, Jenkinson and Chong, 2006, Kelman et al., 1999) and eukaryotes (Schwacha and Bell, 2001, Tye, 1999, Davey et al., 2003, Ishimi, 1997). In order to identify the optimal conditions for ATP hydrolysis, purified recombinant WT hMCM was tested for its ability to hydrolyse ATP to ADP under a variety of conditions. The percentage of ADP released from ATP over 45 minutes was calculated for initial experiments (Fig 3.9). Control reactions in the presence and absence of 76 nM hMCM and 3.5 nM DNA were used to demonstrate background ADP release, which ranged from 2% to 6.5% as radiolabelled ATP decayed. Nevertheless, ADP release was shown to increase with time (Fig. 3.9A), was optimal in phosphate buffer pH 8.5 (Fig 3.9B) and at a magnesium concentration of 15 mM (Fig 3.9C). As a result future experiments were carried out under these conditions for 45 minutes.

For subsequent experiments the amount of ADP produced was calculated over time using a dilution series of radiolabelled ATP stock in parallel with each experiment. Based on previous reports of specific salt requirements for *S. cerevisiae* MCM2-7 activity *in vitro* (Bochman and Schwacha, 2008), the ability of hMCM to hydrolyse ATP in the presence of sodium chloride, sodium glutamate, potassium chloride and potassium glutamate was examined (Fig. 3.10A). Increased sodium chloride concentrations resulted in a statistically significant

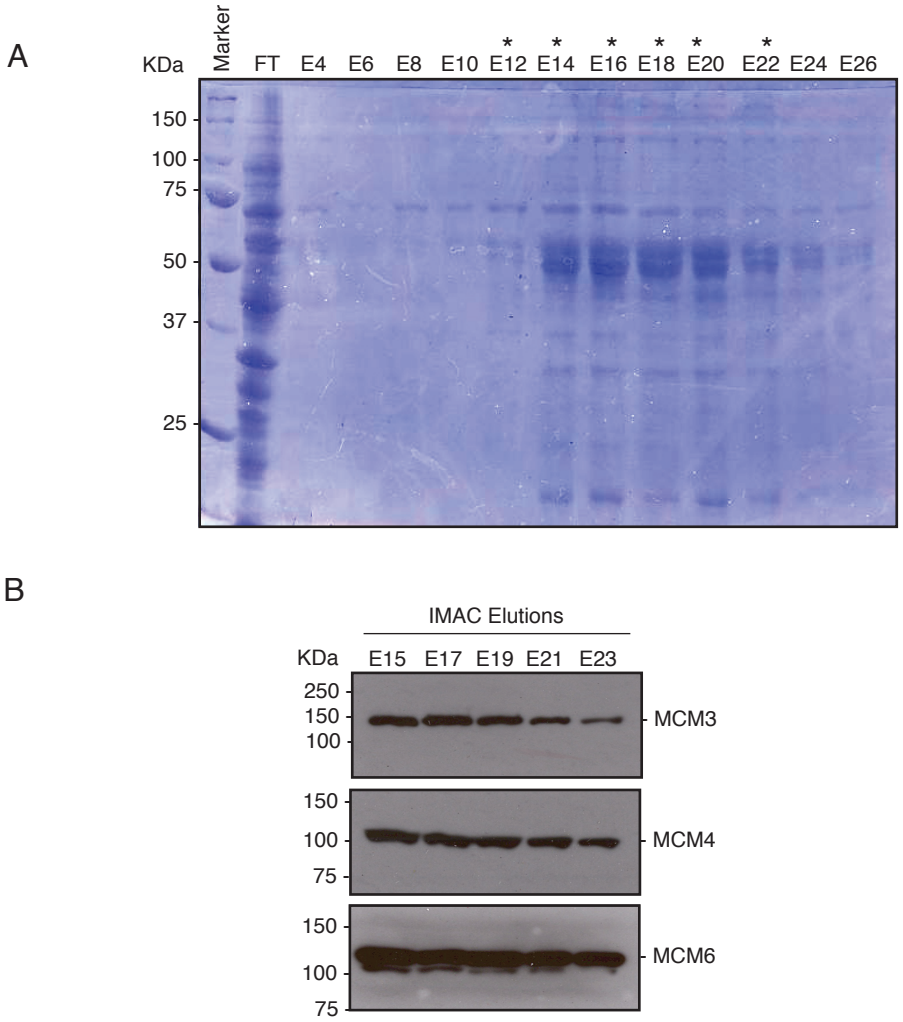


**Figure 3.7.** Summary of immobilised metal affinity chromatography (IMAC) purification for mutant hMCM. A. Coomassie stained SDS-PAGE gel to show extent of purification using IMAC. hMCM was bound to 20 ml His-Select cobalt beads by batch binding before packing into a XK16/20 column. FT - flow through, E4 -E26 - elution fractions. Elution fractions E11 - E23 were taken to the next purification step (indicated by *). B. Western blot of peak IMAC elution fractions probed with MCM3, MCM4 and MCM6. Marker is Precision Plus Protein standards (Bio-Rad).

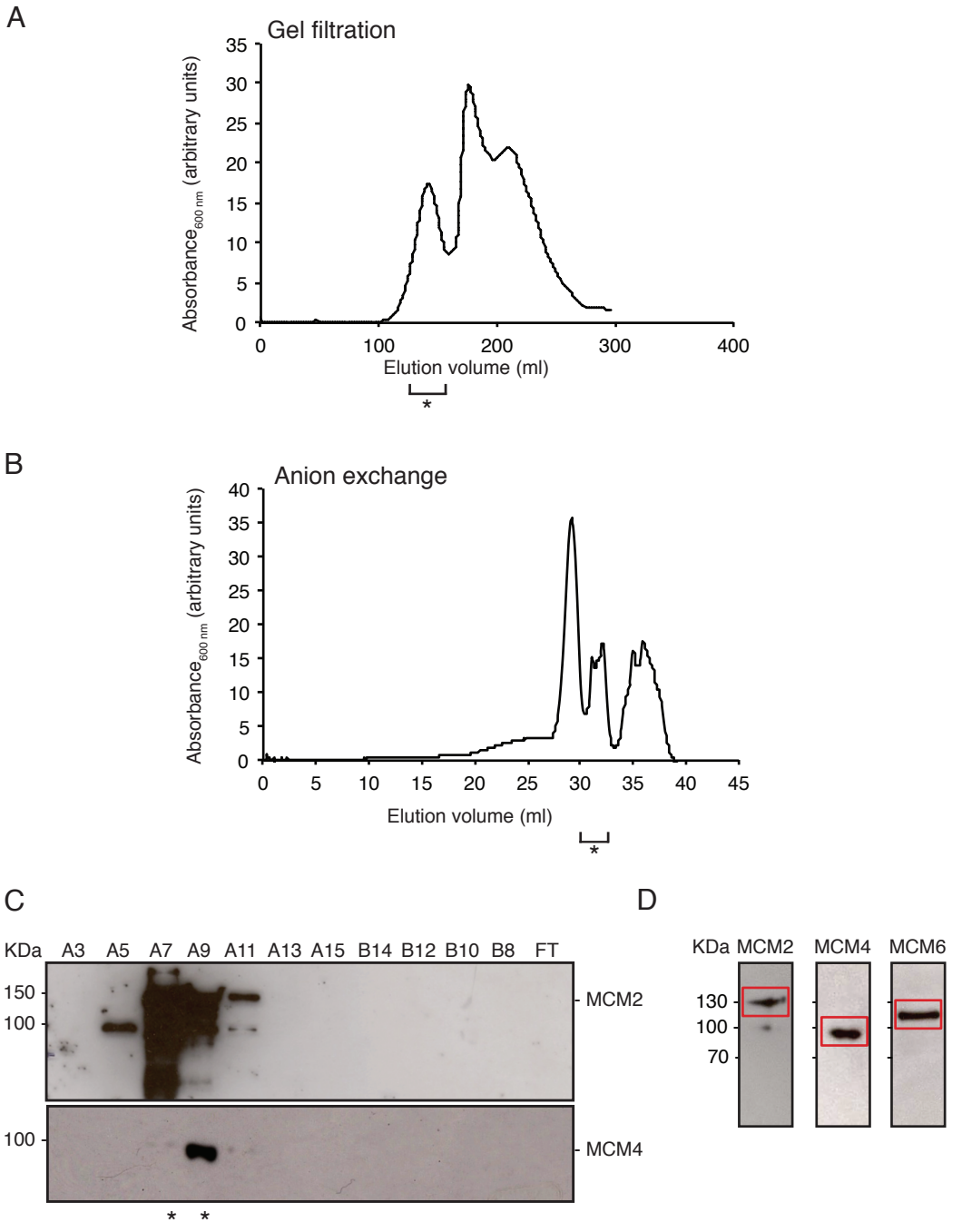


**Figure 3.8.** Summary of gel filtration and anion exchange purification of mutant hMCM. A. Elution profile for gel filtration purification. IMAC pooled fractions were further purified using a 320 ml HiLoad 26/600 Superdex 200 column. Pooled fractions (indicated by *) were A5 - A13. B. Elution profile anion exchange purification. Pooled fractions from gel filtration were further purified using a 1 ml MonoQ column. Pooled fractions (indicated by *) were A6 - A9. C. Western blots of anion exchange elution fractions A3 - B8 and flow through (FT) probed for MCM2 and MCM4. Marker is Precision Plus Protein standards (Bio-Rad). Elution fractions A6 – A9 were pooled (indicated by *). D. Western blots of purified mutant hMCM probed with MCM2, MCM4 and MCM6. The correct molecular weight substrate is indicated with a red box for each subunit. Marker is PageRuler Plus Prestained (Thermoscientific).

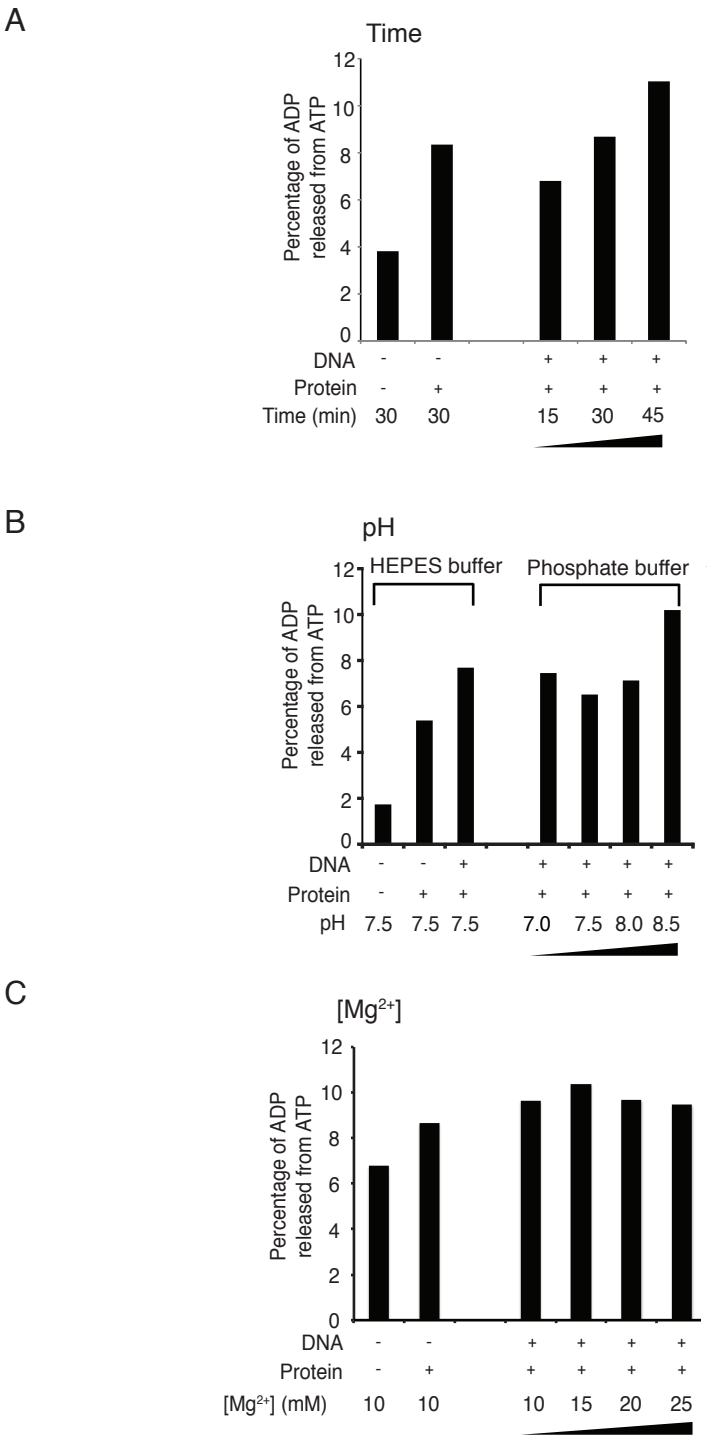


**Figure 3.9.** Optimisation of assay conditions for ATPase activity of hMCM. Determined by thin layer chromatography of radiolabelled ATP hydrolysis. Control reactions in the presence and absence of 176 nM hMCM and 3.5 nM DNA are shown for each reaction. A. ATP hydrolysis increases over time. B. Phosphate buffer at pH 8.5 is the optimal pH for ATP hydrolysis. C. Optimal concentration of Magnesium acetate ($Mg^{2+}$) is 15 mM. Reactions B and C were run over 45 minutes.

decrease in ATP hydrolysis. A similar effect was observed for sodium glutamate. The addition of 50 mM potassium chloride resulted in a pronounced inhibition of ATPase activity consistent with results reported for the *S. cerevisiae* MCM2-7 (Bochman and Schwacha, 2008). Strikingly the presence of 300 mM potassium glutamate, twice the physiological salt concentration, had no effect on ATPase activity (Fig. 3.10A).

ATP hydrolysis activity by *Mt*MCM is stimulated by the presence of DNA (Chong et al., 2000) in contrast to reports of *S. cerevisiae* MCM2-7 ATPase activity where DNA did not stimulate ATP hydrolysis (Bochman et al., 2008, Schwacha and Bell, 2001) and so the ATP hydrolysis activity of recombinant hMCM was tested in the presence and absence of a series of DNA substrates (Fig 3.10B). hMCM exhibited ATP hydrolysis that was not increased by the addition of DNA consistent with reports of heterohexameric MCM2-7 from *S. cerevisiae*. It is worth noting that this is in contrast to the MCM4, 6, 7 sub-complex, which is stimulated by ssDNA (Biswas-Fiss et al., 2005, You et al., 2003). High concentrations of dsDNA (46 nM, with a ratio of hMCM hexamer:DNA of 3.8:1) inhibited ATP hydrolysis by ~50% compared to lower concentrations of dsDNA. This agrees with previous observations from *Mt*MCMs (Chong et al., 2000) and is possibly due to a substrate competition effect preventing the MCMs from forming a productive complex. Or could represent productive loading of hMCM which requires post-translational modifications to unwind the DNA. A similar, but smaller, effect was observed for ssDNA. A forked substrate had negligible effect on hydrolysis activity at the concentrations tested.

As expected, increasing concentrations of hMCM resulted in increased ATP hydrolysis (Fig. 3.11A). Addition of 20 mM EDTA significantly reduced ATP hydrolysis by hMCM, as did replacing the WT protein with the ATPase deficient mutant complex (Fig. 3.11A). This concurs with previous studies in *S. cerevisiae* and *Mt*MCM (Schwacha and Bell, 2001, Chong et al., 2000). Using the optimal assay conditions identified, the rate of ATP hydrolysis for WT and ATPase deficient mutant hMCM was measured (Fig. 3.11B). The specific activity of ATP hydrolysis for WT hMCM was 16.7 pmol ADP released/min/pmol hMCM compared to 3.9 pmol ADP released/min/pmol for the ATPase deficient mutant

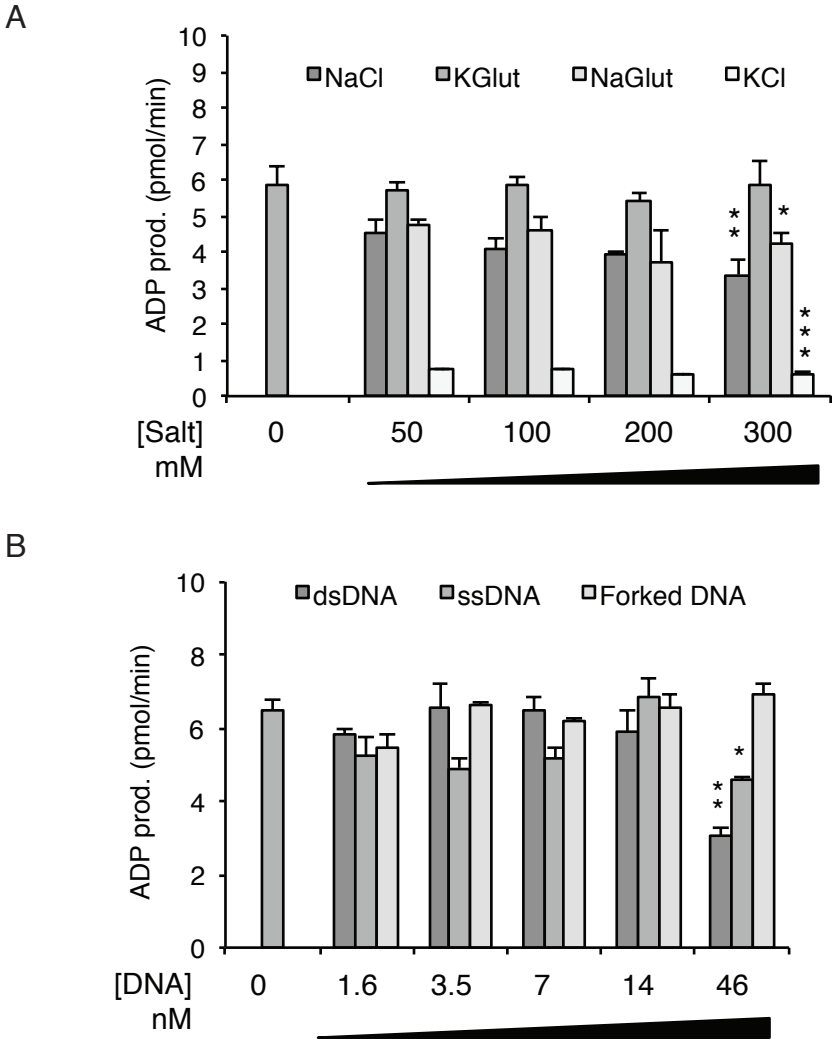


**Figure 3.10.** Effect of salt and DNA on ATPase activity of hMCM. Determined by thin layer chromatography of radiolabelled ATP hydrolysis. The data shown are mean values of three replicates, error bars indicate SEM. Reactions contain 176 nM hMCM and in the presence of 3.5 nM dsDNA unless stated otherwise. A. Potassium glutamate (KGlut) had no effect on ATPase activity, increasing the concentrations of sodium chloride (NaCl) and sodium glutamate (NaGlut) reduced ATP hydrolysis and addition of potassium chloride (KCl) substantially reduced ATP hydrolysis. Statistics compare labelled bar to 0 mM salt. *p=0.018, **p=0.013 and ***p=0.00027. B. DNA has little effect on ATP hydrolysis at low concentrations. At 46 nM (when the molar ratio of [hMCM hexamer]:[DNA] was [3.8:1]) single stranded (ss) DNA (6,407 bases) reduced ATP hydrolysis by one third and double stranded (ds) DNA (3,162 bp) reduced ATP hydrolysis by ~50%. Forked DNA (Fig D1), had little overall effect. Statistics compare labelled bar to 0 nM DNA *p=0.022 and **p=0.0019.

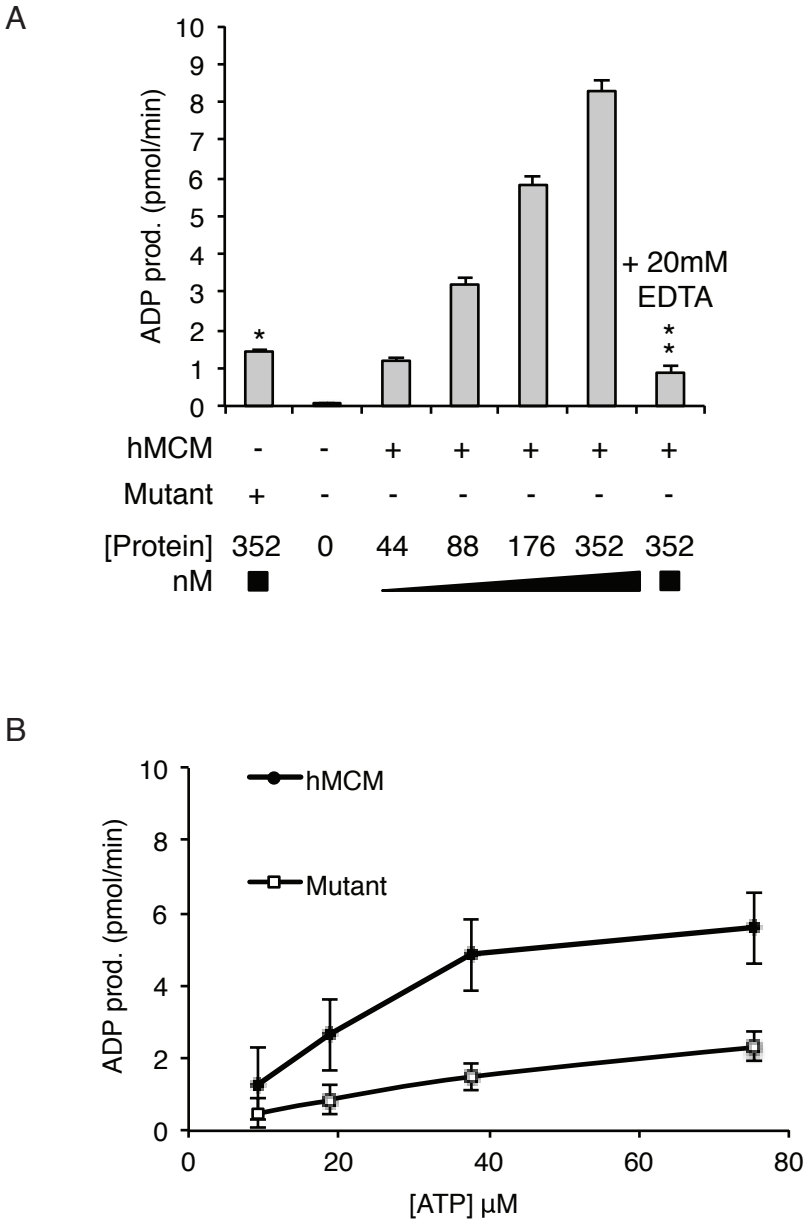


**Figure 3.11.** Effect of hMCM and ATP concentration on ATPase activity of hMCM and mutant hMCM. Determined by thin layer chromatography of radiolabelled ATP hydrolysis. Reactions contain 176 nM hMCM and in the presence of 3.5 nM dsDNA unless stated otherwise A. ATPase activity increases with protein concentration and is inhibited by the addition of 20 mM EDTA to chelate the $Mg^{2+}$. Mutant hMCM shows 6-fold lower ATP hydrolysis activity than wild type (WT) hMCM. The mean value of three replicates is shown, error bars indicate SEM. Statistics compare labelled bar to 352 nM hMCM *p=0.0015 and **p=0.00014. B. The rate of ATP hydrolysis by hMCM and mutant hMCM in pmol of ADP released per minute. The specific activity of ATP hydrolysis for WT hMCM is 16.7 pmol ADP produced/min/pmol hMCM and 3.9 pmol ADP produced/min/pmol mutant hMCM. The mean values of two assays is shown, error bars show the standard deviation.

hMCM. It is possible that ATP hydrolysis is still shown in the hMCM mutant reactions due to contaminants from *E. coli* such as nucleases.

Binding and hydrolysis of ATP by MCM2-7 purified from *S. cerevisiae* has recently been shown to be required for Cdt1 release and double hexamer formation (Coster et al., 2014). The ATPase sites of different MCM subunits have been implicated in different stages of its loading and activation (Kang et al., 2014). The MCM '2-5 gate' is thought to be controlled by ATP hydrolysis (Bochman and Schwacha, 2008) and has obvious implications in MCM2-7 loading and activation. The recombinant hMCM produced here is an important tool to further analyse these findings.

### 3.4.4 ATP-dependent DNA unwinding by hMCM

MCM2-7 complexes from *S. cerevisiae* (Bochman and Schwacha, 2008), and a human MCM4, 6, 7 complex purified from tissue culture cells (Ishimi, 1997) have previously been shown to exhibit ATP-dependent DNA helicase activities. However, DNA unwinding activity of higher eukaryotic MCM2-7 complexes has only been observed with the CMG complex from *Drosophila* (Moyer et al., 2006). In addition, previous studies indicate MCM2-7 complexes require very specific conditions for DNA duplex unwinding and so the optimal conditions derived from ATP hydrolysis experiments were used in the helicase experiments (detailed in Chapter 2.6). The DNA helicase activity of recombinant hMCM was analysed to examine if post-translational modifications or accessory proteins were absolutely required for unwinding. The helicase assays were carried out using 4 nM of a forked DNA substrate incubated with increasing concentrations of recombinant hMCM and were tested for its ability to unwind DNA in the presence or absence of ATP (Fig. 3.12). hMCM exhibited an ATP-dependent DNA unwinding activity (Fig. 3.12). 352 nM WT hMCM is capable of unwinding over 50% of the DNA substrate available in one hour (Fig. 3.12B). The lack of unwinding and ATPase activities in the ATPase deficient mutant hMCM assays suggests that the mutant and WT protein preparations were both free from contaminating *E. coli* helicases/ATPases. Under conditions where ATP could not be hydrolysed – that is, either WT hMCM in the absence of ATP, or mutant hMCM in the presence of ATP – helicase activity was substantially reduced (Fig.

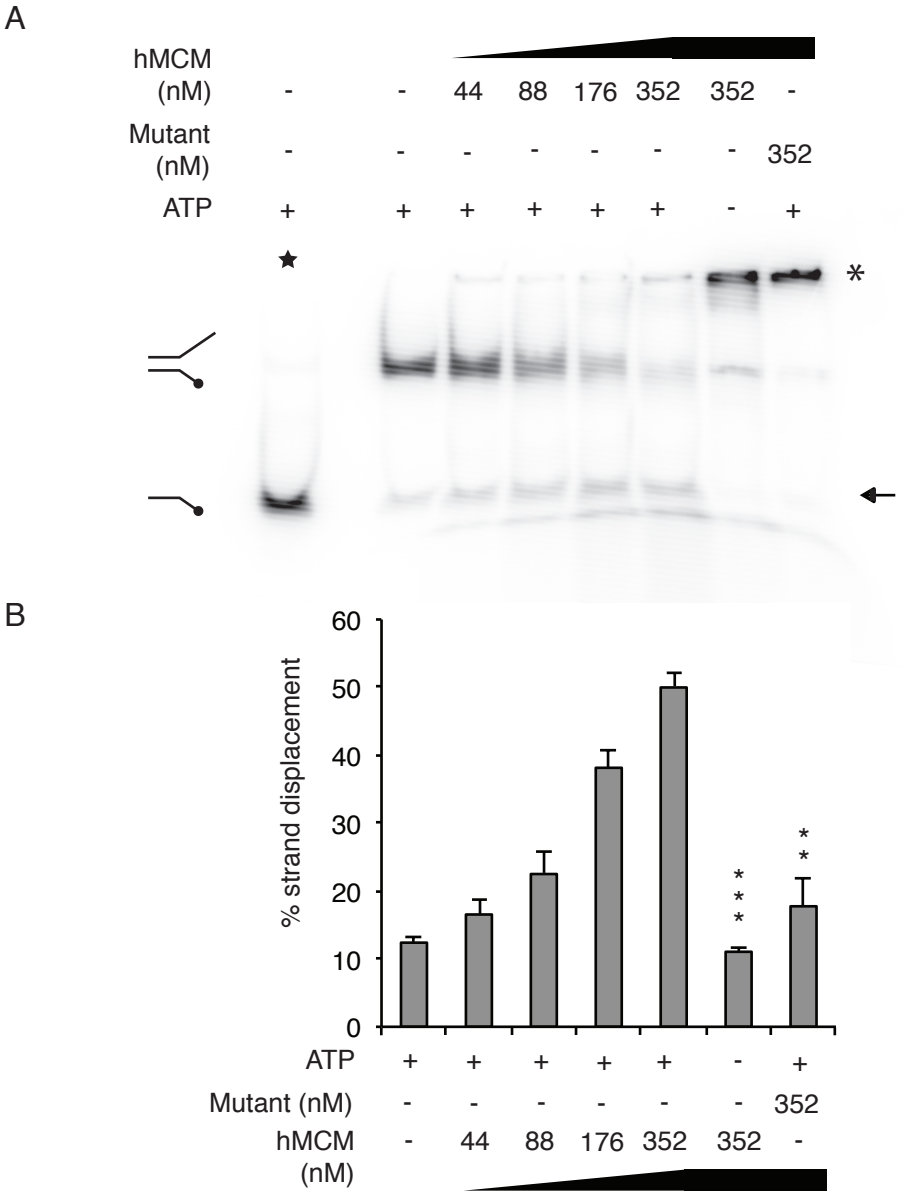


**Figure 3.12.** hMCM shows strand displacement activity. A. Heat denatured boiled substrate (★) and no protein lanes are included as controls. An arrow indicates the position of displaced substrate, an asterisk indicates substrate with unusual mobility, perhaps indicating hMCM that is bound to DNA. B. The amount of single stranded substrate (4 nM total concentration) in each reaction was quantified as a percentage of the boiled substrate control. The data shown are mean values for four independent assays, an example of which is shown in (A). Error bars indicate SEM. Statistics compare labelled lane to 352 nM hMCM plus ATP. ***p=0.00013 and **p=0.0014.

3.12B). This is consistent with ATP hydrolysis being required for helicase activity. Under these conditions a large proportion of the substrate migrated more slowly by native PAGE. Similar mobility shift effects have been previously observed for the *Mt*MCM when samples have been incubated on ice (Jenkinson and Chong, 2006). This suggests that hMCM binds to the DNA substrate in the absence of ATP (or ATP hydrolysis) but cannot unwind it. This is consistent with the idea that ATP hydrolysis is not required for DNA-protein interactions but is required for DNA unwinding (McGeoch et al., 2005). Recent studies suggest ATP hydrolysis is required for loading *S. cerevisiae* MCM2-7 (Kang et al., 2014, Coster et al., 2014). Therefore these results may indicate MCM2-7 DNA binding (DNA binding to the outside of MCM2-7 hexamers) rather than MCM2-7 loading (MCM2-7 encircling DNA).

Recombinant hMCM is capable of unwinding duplex DNA. Under the conditions shown here, 38% and 50% displacement of the labelled strand by 176 nM and 352 nM hMCM respectively was observed. This is broadly comparable to the reported 52% displacement by 110 nM *S. cerevisiae* MCM2-7 (Bochman and Schwacha, 2008).

Overall, these results indicate that the recombinant hMCM complex exhibits DNA helicase activity and that posttranslational modifications to hMCM or accessory proteins such as Cdc45 and GINS are not required for the unwinding of naked DNA. The requirement for Cdc45 and GINS may only be required when loading MCM2-7 onto DNA or unwinding DNA packaged into chromatin.

### 3.4.5 Structural analysis

The following work was carried out in collaboration with Prof. E. Orlova at Birkbeck, University of London. hMCM samples were previously produced by Dr Richard P. Parker-Manuel and analysed under standard buffer conditions. Negative stain electron microscopy images of hMCM samples were taken by Dr Yuriy Chaban. Electron microscopy images were processed as described in the methods. The reconstruction of hMCM alone was calculated from the best 100 classes containing ~11 images each. For hMCM plus DNA, the final reconstruction was calculated from the best 155 classes containing ~10 images

each (Fig. 3.13). The forked DNA substrate consisted of a 45 bp duplex region, a 35 nucleotide 5' tail and a 60 nucleotide 3' tail. Images of the samples were taken at 50,000 x magnification with pixel size of 2.5 Å/pix to produce a 23 Å resolution, 3D, asymmetric reconstruction (Fig. 3.14 and 3.15).

The reconstructions show hMCM forms a ring-shaped single hexamer with a diameter of 145 Å and a height of 120 Å, consistent with the organisation of oligomeric complexes reported for MCM complexes from other eukaryotes (Costa et al., 2011, Remus et al., 2009, Pape et al., 2003, Gomez-Llorente et al., 2005) (Fig. 3.14). The reconstructions have C1 symmetry, suggesting that the complexes present contain six different subunits (2-7) as opposed to a dimer of MCM4, 6, 7 trimers (which would produce C2 symmetry), or a trimer of MCM4, 7 dimers (C3 symmetry). In the presence of forked DNA (Fig. 3.14B, middle column) the hMCM structure undergoes a conformational change and clearly shows a different conformation, with a more defined two-tiered hexameric shape and a more obviously open central cavity. Interestingly, the conformation of hMCM bound to DNA is more similar to what has been reported for *S. cerevisiae* MCM2-7 in the absence of DNA (Samel et al., 2014). One possible reason for the differences observed between the *S. cerevisiae* and human proteins in the absence of DNA could be due to the differences in the primary sequences of the *S. cerevisiae* and human proteins (outlined in Table 1.1). The prominent projection that appears on the top surface of one of the hMCM subunits in the presence of DNA (red circle) could be either the bound double-stranded portion of the DNA substrate, or a section of protein displaced by the presence of the DNA, such as the N-terminal S-Trx-His tag on MCM7, which would also be consistent with the clearing of the apparently occluded central channel in the DNA-free reconstruction when DNA is added. Currently there is no literature that shows preferential DNA binding to a particular subunit.

The crystal structure of *Sso*MCM (Brewster et al., 2008) was fitted into the 3D map of hMCM and hMCM plus DNA complexes manually using Chimera (Goddard et al., 2007). Our reconstruction clearly fits the *Sso*MCM crystal structure (3F9V, Fig 3.15, 3.16). The 3F9V crystal structure is amino acids 7 – 601 of *Sso*MCM (Brewster et al., 2008). Full length *Sso*MCM is 686 amino acids in

length and this crystal structure is missing 70 amino acids from the C terminal. In comparison to hMCM subunits, the 3F9V crystal structure is between 17% and 34% smaller (see Table 3.2). Space in the hMCM alone reconstruction is limited however there is visibly more room available in the hMCM plus DNA reconstruction which would allow for the amino acid insertions (Fig. 3.15, bottom panel).

**Table 3.2. MCM amino acid insertion comparison of Human (*Hs*) and *Sulfolobus solfataricus* (*Sso*) MCM.** The number of amino acids present in *Sso*MCM or the amino acids crystalised to produce the 3F9C structure are compared to the human MCM2-7. Each MCM subunit in hMCM is larger than *Sso*MCM subunits.

| MCM | *Human* (aa*) | aa difference (*Hs - Sso*) | aa difference (*Hs* – 3F9V) |
|---|---|---|---|
| 2 | 904 | 218 (24%) | 309 (34%) |
| 3 | 808 | 122 (14%) | 213 (26%) |
| 4 | 863 | 177 (21%) | 268 (31%) |
| 5 | 734 | 48 (7%) | 139 (19%) |
| 6 | 821 | 135 (16%) | 226 (28%) |
| 7 | 719 | 33 (17%) | 124 (17%) |

* amino acids

Analysis of a population of *Drosophila* MCM2-7 complexes revealed that they exist in two different states: a planar, notched ring and an open spiral shape (Costa et al., 2011) and reconstructions of MCM2-7 from *E. cuniculi* suggest that MCM2-7 is naturally found in the open spiral shape (Lyubimov et al., 2012). The reconstruction of the human complex is clearly more similar to the notched ring, but this does not preclude the existence of spiral shaped complexes in the sample, although they are clearly not the predominant form under the conditions used to visualise the protein.

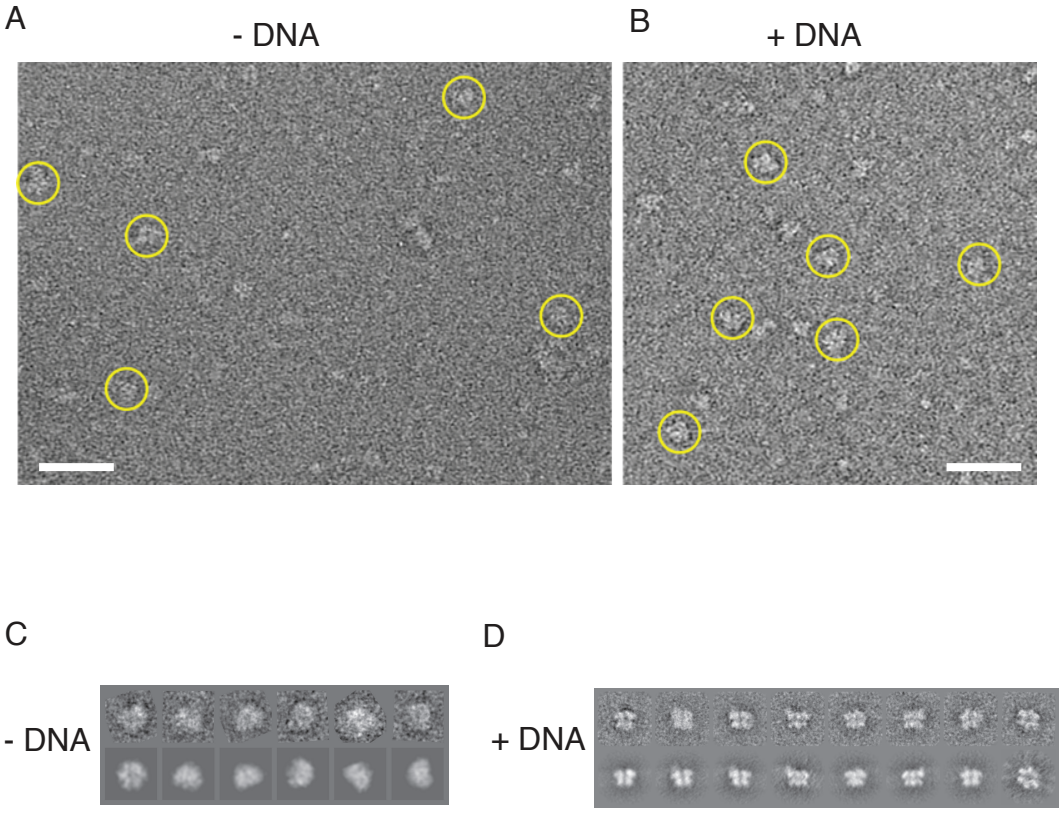


**Figure 3.13.** Negative stain electron microscopy of hMCM. An example of the raw micrograph hMCM (A) and hMCM plus DNA (B). Representative images of particles are outlined by circles in yellow. Scale bar is 50 nm. C. hMCM classes and reprojections used in final reconstruction for hMCM alone. D. As in A for hMCM plus DNA.

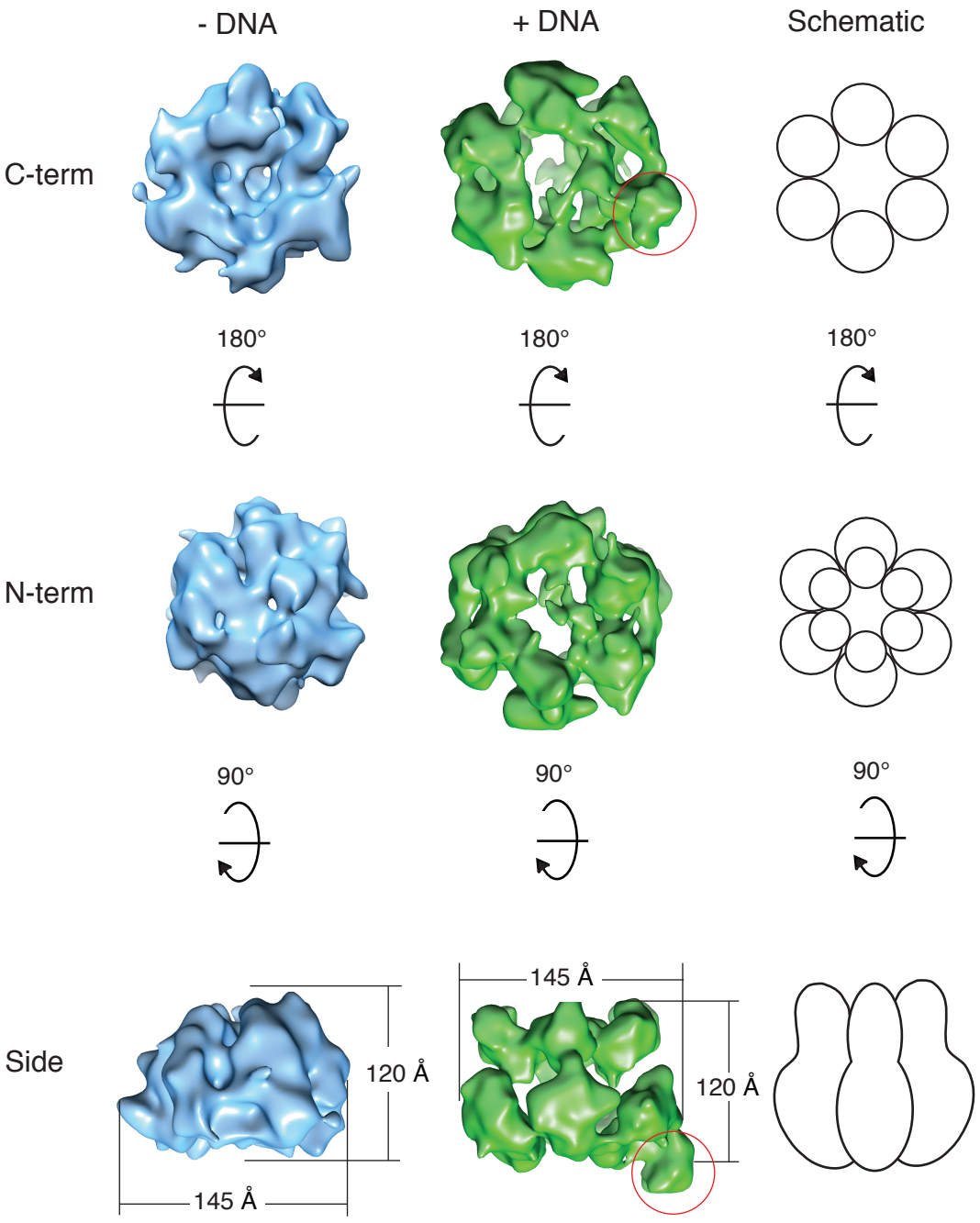


**Figure 3.14.** hMCM undergoes a conformational change when bound to forked DNA. Negative stain, single particle electron microscopy (EM) asymmetric reconstruction to 23Å resolution. Top row: C-terminal view hMCM alone (blue), hMCM bound to DNA (green) and schematic representation of hMCM subunit configuration. Middle: N-terminal view as above. Bottom: Side view as above. Red circle highlights protrusion thought to be DNA binding to hMCM. Size indicated in angstroms (Å).

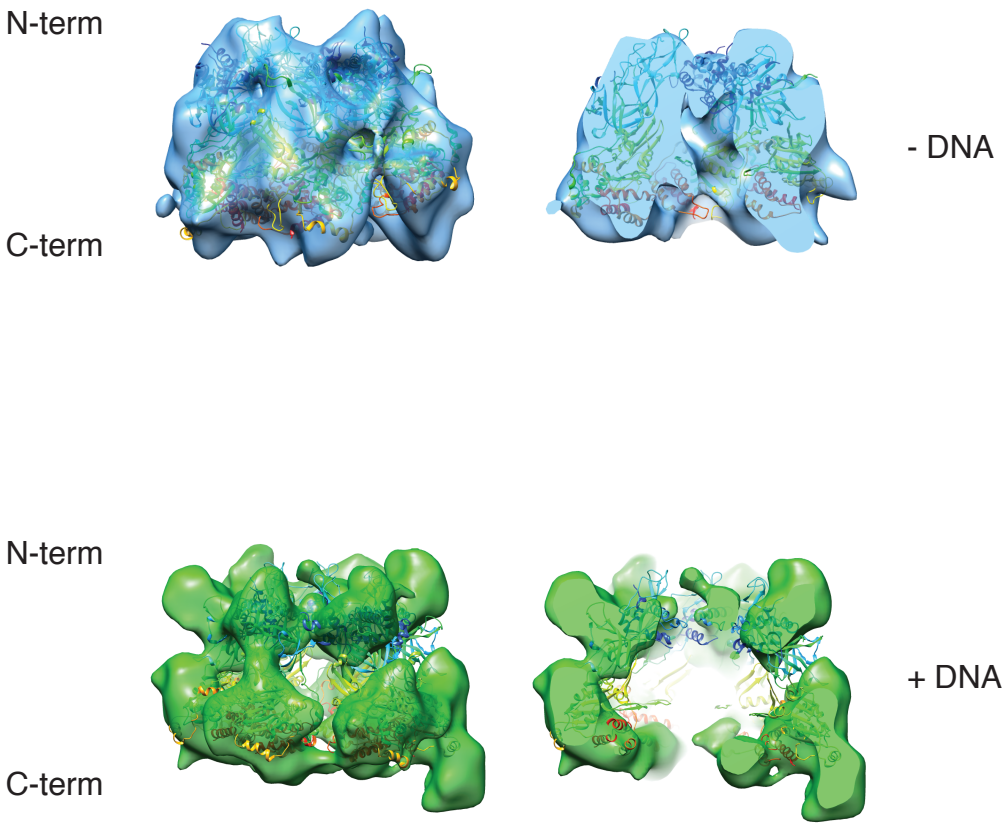


**Figure 3.15.** hMCM EM reconstructions fit crystal structures. hMCM alone (blue) and hMCM bound to forked DNA (green) fitted with 'nearly full length' *Sulfolobus solfataricus* (*Sso*) MCM crystal structure (3F9V, Brewster et al., 2008). The full hMCM structure (left) and slice through hMCM (right) shows clear central cavity in both reconstructions.

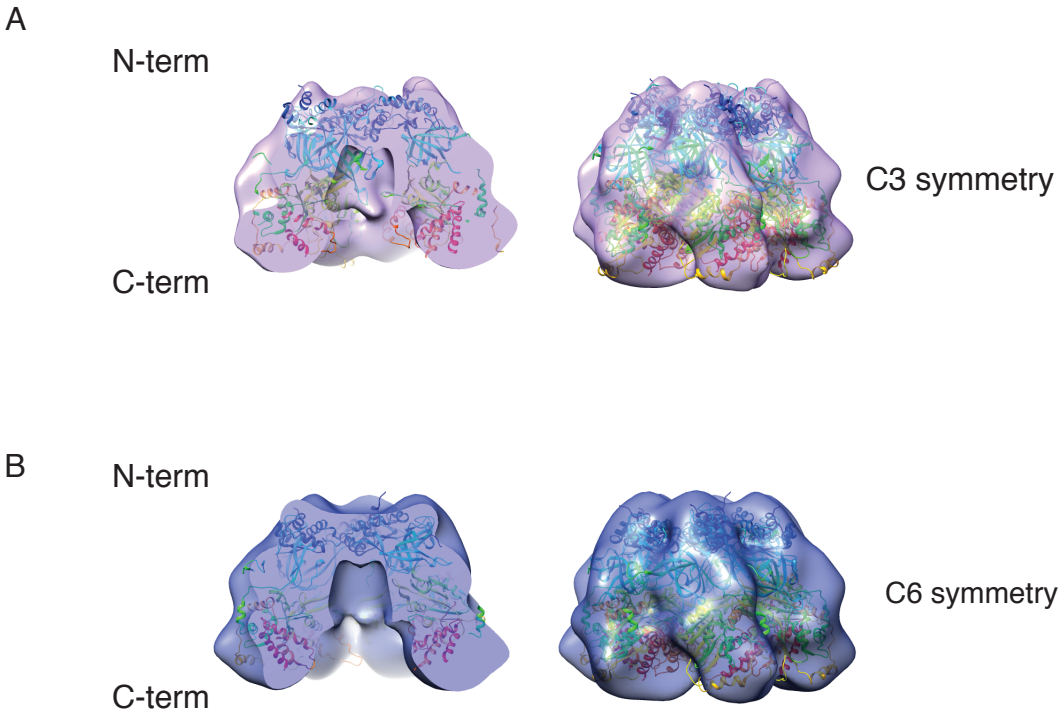


**Figure 3.16.** Additional views of hMCM reconstructions. A. hMCM alone with 3-fold symmetry (C3). *Sso*MCM crystal structure (3F9V, Brewster et al., 2008) fitted into reconstruction. The full hMCM (C3) structure (left) and slice through hMCM (C3) structure (right) show a central cavity. B. hMCM with 6 fold symmetry (C6). *Sso*MCM crystal structure (3F9V, Brewster et al., 2008) fitted into reconstruction. The full hMCM (C6) structure (left) and slice through hMCM (C6) structure (right) show a central cavity.

## 3.5 Conclusion

Recombinant hMCM provides an important tool for understanding the mechanisms governing human DNA replication through the reconstitution of replication licensing factor and DNA unwinding. The ability to produce significant quantities of hMCM for analysis is an important step forward. The biochemical findings show that the recombinant complex is active *in vitro* and the structural studies show that its conformation is altered when bound to DNA. Production of recombinant hMCM enables the targeted manipulation of individual proteins within the hMCM complex, providing the potential to address in detail the important differences between individual subunits in the hMCM heterohexamer. It could also be used in screens for clinically relevant hMCM inhibitors.

*Chapter 4*

# Expression and localisation of endogenous mammalian MCM proteins

# 4 Expression and localisation of endogenous mammalian MCM proteins

The following work has been accepted for publication and is shown in paper format in Appendix D.

## 4.1 Introduction

The nuclear matrix is a biochemically defined ribonuclear protein framework in higher eukaryotic cells, which withstands a range of extraction conditions (see Chapter 1 for more details). A number of studies have begun to look at the relationship of MCM proteins with the nuclear matrix in asynchronous populations of cells, with contradictory results. MCM3, MCM5 and MCM7 have been shown to be resistant to nuclease digestion and therefore nuclear matrix bound (Fujita et al., 2002, Burkhart et al., 1995). However, numerous studies show MCM2, MCM3, MCM5 and MCM7 to be solubilised by nuclease digestion and therefore not nuclear matrix bound (Fujita et al., 1997, Stoeber et al., 1998, Cook et al., 2004, Cook et al., 2002, Mendez and Stillman, 2000). The lack of consensus may be due to a transient interaction of MCM proteins with the nuclear matrix, which may be undetectable in the context of the bulk MCM protein content when studying asynchronous cells. Additionally, the investigations noted above were carried out in a variety of different cell types. Studies have shown tumours, transformed cells in culture, and stem-like cells appear to have a compromised or immature nuclear matrix (Munkley et al., 2011, Zink et al., 2004) making the choice of cell model important. Furthermore, these studies do not validate the extent of nuclease activity with controls to demonstrate full chromatin digestion.

This work focuses on the fine temporal resolution of the nuclear binding characteristics of MCM2 as cells pass through late G1 phase, in order to describe the types of interaction that occur during expression, assembly, initiation and elongation. Using mouse 3T3 cells that can be manipulated to undergo synchronised passage through G1 phase, without the use of chemical inhibitors,

three distinct binding states of MCM2 in the G1 phase following quiescence are demonstrated.

## 4.2 Aims

- To profile mammalian MCM protein expression in relation to the cell cycle following release from quiescence.
- To examine the sub-cellular localisation of mammalian MCM proteins during G1 – S phase of the cell cycle.
- To investigate MCM protein binding to the nuclear matrix in relation to the cell cycle.

## 4.3 Experimental design

Mouse 3T3 cells were used for all the experiments in this chapter. Cells were synchronised in quiescence and harvested at multiple time points following release (2.2.2). For immunofluorescence, cells were grown on coverslips and washed with a range of reagents to reveal detergent, salt or DNase-resistant sub-populations of MCM2. For western blot analysis, cells were grown in tissue culture dishes and extracted to produce the same fractions, plus the supernatant fractions that were released after each buffer. The antibody used to detect MCM2 is exceptionally good at recognising mouse MCM2 and so was used to give the majority of the data in this chapter. Other antibodies were tested but gave unreliable results.

## 4.4 Results

### 4.4.1 Cells released from quiescence enter G1 in a highly regulated manner

Mouse 3T3 cells were synchronised in quiescence by contact inhibition and serum depletion, then released into cycle as a synchronous wave of cells that pass through G1 landmarks at defined time points (Fig. 4.1). Under the conditions used here, serum-independent entry to S phase is triggered at 15 hours after release from quiescence (restriction point) and does not vary much between experiments (maximum one hour variance based on appearance of cyclins, Coverley et al., 2002). Entry to S phase is monitored by incorporation of

Edu, a nucleotide analogue that is incorporated into newly synthesised DNA and can be monitored by fluorescent microscopy. Cells begin to enter S phase at around 16 hours, approximately one hour after the restriction point (Fig. 4.1A). The majority of cells in the population enter S phase after 20 hours, reaching a maximum of 60 - 70% after 24 hours, which is typical for this protocol. Cells released from quiescence move through G1 phase in a wave, some quiescent cells may have died on release or entered senescence and so never re-enter the cell cycle. Cyclin A expression increases dramatically after 15 hours, consistent with its role in the activation of DNA replication machinery, and inhibition of pre-RC assembly (Coverley et al., 2002). These two outputs show reproducible cell synchrony kinetics, confirming that the system is properly calibrated and will support detailed analysis of the expression, assembly and function of MCM2-7 during G1 to S phase.

The results in figure 4.1A and previously published work (Coverley et al., 2002) are summarised in a model for events that occur following release from quiescence (Fig. 4.1B). Cells are released from quiescence at 0 hours and an extended G1 phase lasts until the initiation of DNA replication at around 19 hours. The cells are committed to the cell cycle once they pass the restriction point, which happens at roughly 15 hours. Between the restriction point (15 hours) and the initiation of DNA replication (19 hours) there is a 'window of opportunity' where conditions are permissive for pre-RC assembly.

### 4.4.2 MCM protein expression peaks at the initiation of DNA replication

Whole cell lysates were harvested in the absence of protease inhibitors at late G1 phase of the cell cycle until late S phase (17 – 24 hours after release from quiescence) to determine if the level of MCM proteins varied during the transition from G1 - S phase. The relative amounts of MCM2, MCM3 and MCM7 were determined by western blotting and expressed relative to actin. MCM proteins are first evident from the restriction point onwards with a noticeable peak at 19 hours after release from quiescence (Fig. 4.2A). MCM proteins appear to be degraded immediately before and after their peak of expression at 19 hours suggesting a transient protection from proteolysis (Fig. 4.2A). This temporal

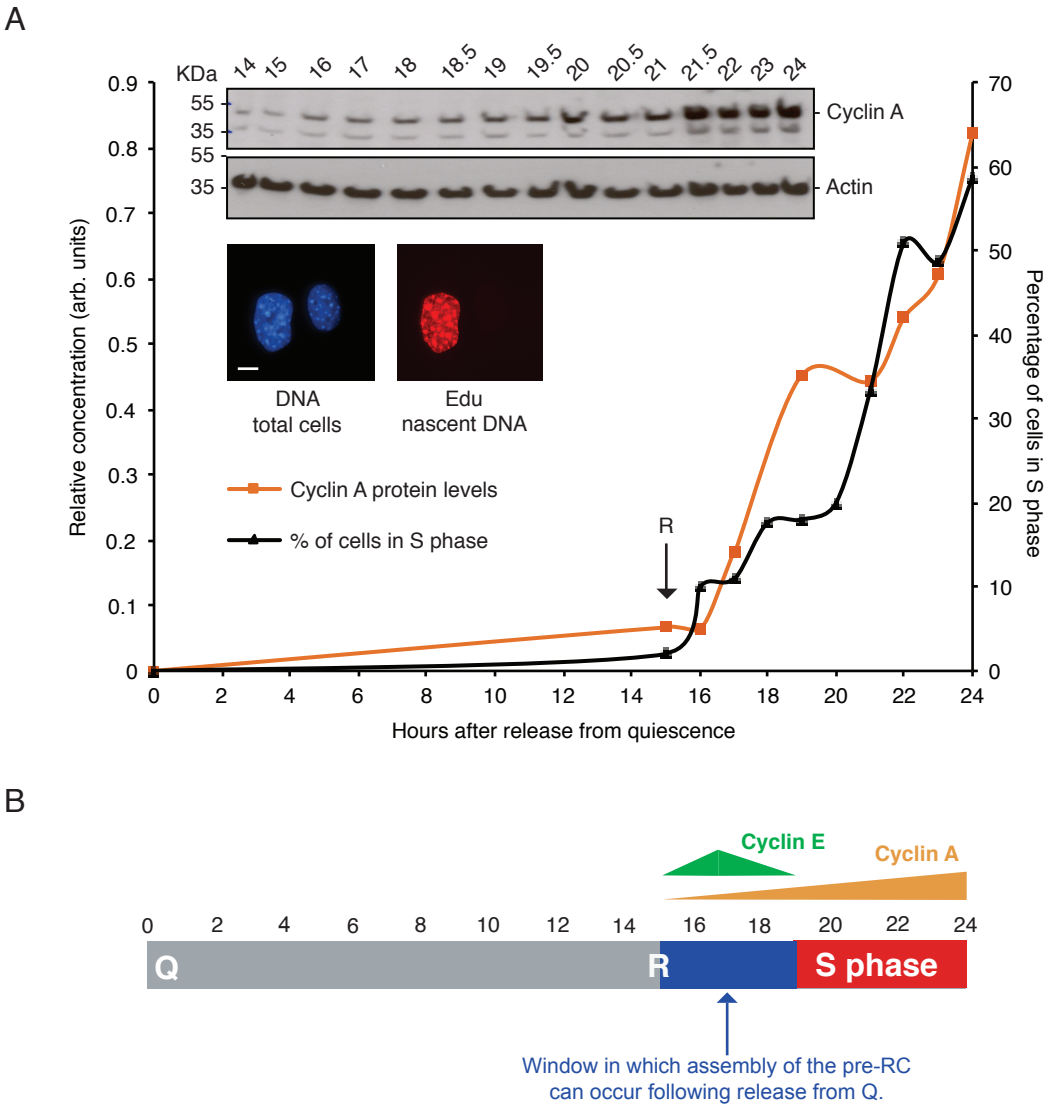


**Figure 4.1.** Cell cycle re-entry from quiescence. A. The percentage of cells engaged in DNA synthesis over 24 hours (black). The majority of the population first incorporate labelled nucleotides after 20 hours. The relative concentration of total cyclin A protein, estimated by densitometry (averaged from two biological replicates) and expressed after normalisation to actin (orange) demonstrates a similar profile. Insert (top) are representative western blots of cyclin A and actin, and (bottom) micrographs to illustrate incorporation of Edu into newly synthesised DNA in replicating cells (red). The total cell population is stained with Hoechst 33258 (blue). Marker is PageRuler Plus Prestained (Thermo Scientific). Scale bar is 10 µm. B. Mouse 3T3 cells re-enter the cell cycle from quiescence in a temporally well-defined manor, passing out of quiescence (Q) and through the restriction point (R) after approximately 15 hours. They enter S phase (S) as a wave of cells from 16 hours onwards. The 'window of opportunity' for assembling pre-replication complexes lies between the emergence of cyclin E (green), which opens it, and cyclin A (orange), which closes it and initiates DNA synthesis.

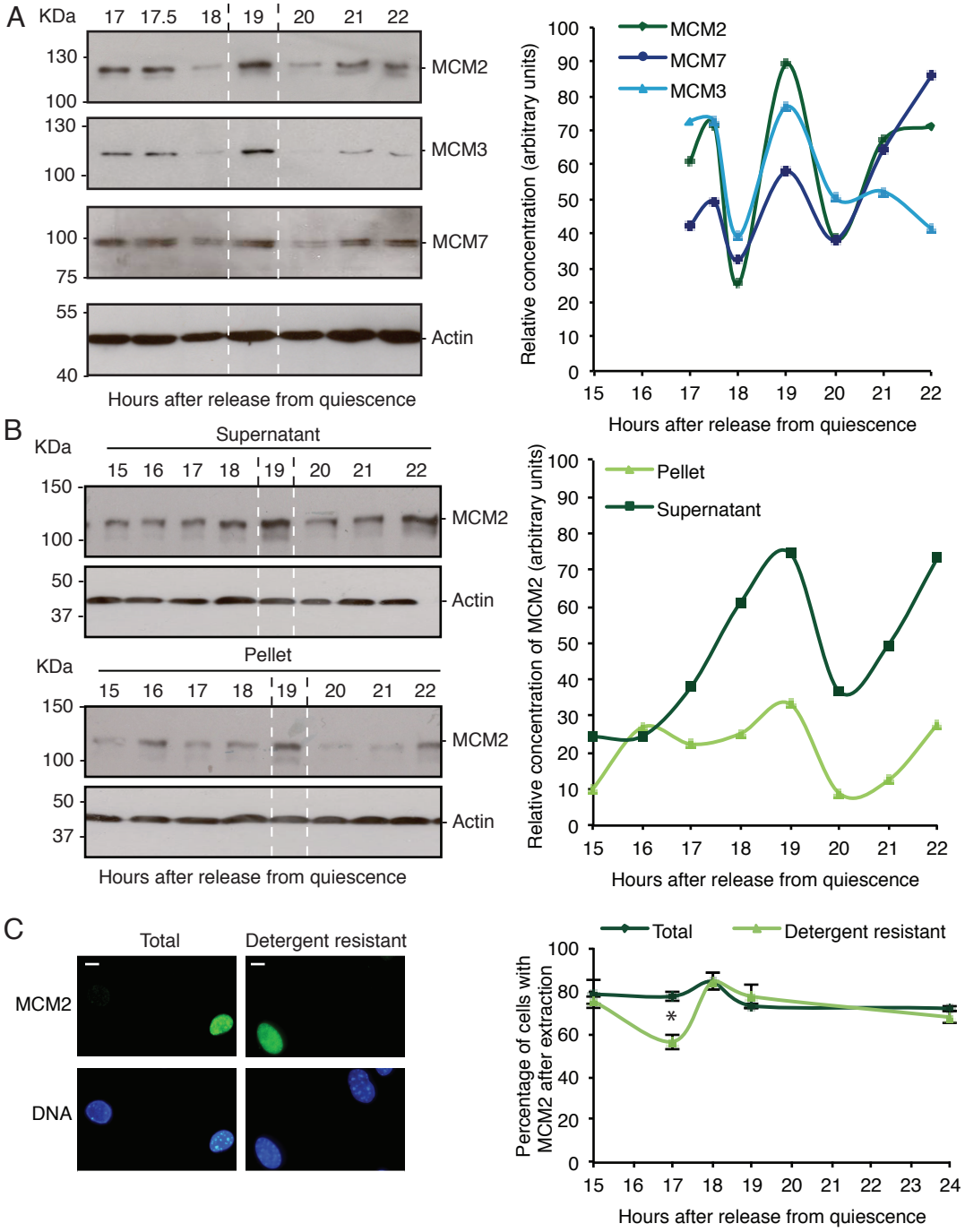


**Figure 4.2.** MCM protein levels peak at initiation. A. Western blots of MCM2, MCM3 and MCM7 protein levels in whole cell lysates recovered when harvested without protease inhibitors. Graph shows data quantified by densitometry and normalised to actin B. Western blots of MCM2 protein levels in soluble extract (detergent soluble supernatant) and nuclei fraction (detergent-resistant pellet), graph shows data quantified and normalised to actin. Marker is Precision Plus Protein standards (Bio-Rad). C. The percentage of cells with MCM2 in the nucleus in total and detergent resistant, detected by immunofluorescence. All labelled cells were scored regardless of intensity. Error bars show SEM of three technical replicates (n ≥ 100 for each). Representative images of total and detergent resistant MCM2 (green) and DNA (Hoechst 33258, blue) (left). Scale bar is 10 µm. * p=0.01.

profile is not apparent in whole cell lysates harvested in the presence of protease inhibitors (see Appendix D, Fig. 1B), it appears not to act *in vivo* on the bulk of the MCM proteins in the cell, having the greatest impact when cells are disrupted artificially. The peak at 19 hours after release from quiescence correlates with the requirement for MCM proteins at initiation of DNA replication.

### 4.4.3 Sub-cellular localisation of MCM2

To corroborate the striking peak of MCM subunit expression at 19 hours the sub-cellular location was analysed in an independent experiment. Soluble (supernatant) and insoluble (detergent resistant pellet) MCM2 fractions were quantified relative to actin in the adjacent graph (Fig. 4.2B). Intriguingly, a reproducible peak at 19 hours after release from quiescence was observed.

Using immunofluorescence to measure the proportion of cells with detectable MCM2 in the nucleus, the data show that populations are relatively uniform with a similar number of positive cells at 24 hours after release, as at 15 hours (Fig. 4.2C), in all cases exclusively nuclear. Thus, the quantity increase observed by western blot does not reflect expression in a greater number of cells. Looking specifically at the detergent-resistant fraction of MCM2, a significant fall in the number with detectable levels seen at 17 hours, consistent with pre-initiation proteolysis of this fraction.

### 4.4.4 MCM2 is transiently bound to the nuclear matrix

Analysis of the sub-nuclear location of MCM2 during the assembly window between the restriction point and S phase was carried out by a previous lab member (Dr John R. P. Knight, personal communication). By increasing NaCl concentration, specific proteins are sequentially eluted with different profiles. He found that MCM2 is transiently, and reproducibly, assembled into high salt-resistant immobilised complexes at 19 hours after release from quiescence but not at 18 or 20 hours (see Appendix D, Fig. 2B).

To investigate if this high salt-resistant complex reflects immobilisation on the nuclear matrix, the association of MCM2 was examined using a protocol where

histones and chromatin-associated proteins are eluted along with DNA fragments after digestion with DNase I. Under these conditions, MCM2 is apparently entirely eluted from asynchronous cells, with none evident in the nuclear matrix fraction (Fig. 4.3A). However, when this is applied specifically to a 19 hour population of cells (Fig. 4.3B), a small resistant fraction is evident, equivalent to approximately 4% of total MCM2 (addition of detergent P and SN) in the cell at that time (based on densitometry, Fig. 4.3). Successful nuclear matrix preparations are verified by digestion of chromatin by release of over 75% histone H3 from the nuclear matrix fraction (DNase P) and no histone H3 release in mock samples (Mock SN). Lamin B2 was used as a control for the presence of residual nucleus (DNase P). Similar analysis with an extensive set of antibodies raised against other MCM subunits failed to reveal nuclear matrix-associated populations. This could reflect underlying biology, however a strong conclusion cannot be drawn because none of these antibodies are as sensitive as that used to detect MCM2.

Nuclear matrix isolation was recapitulated over a time course (Fig. 4.4) with focus on the 0.5 M NaCl-resistant fraction of MCM2 (chromatin and/or nuclear matrix bound). This generated consistent results, which show a DNase I–resistant fraction at 19 hours partially persisting in this time-course, to 20 hours after release from quiescence (Fig. 4.4A). At 19 hours, 76% of this immobilised fraction of MCM2 is in fact nuclear matrix bound (resistant to DNase I extraction), compared to only 5% of histone H3 and 83% of Lamin B2 (based on densitometry, Fig. 4.4A). Quantification of the number of nuclei with MCM2 by immunofluorescence again identified a peak of resistance at 19 hours (Fig. 4.4B). This argues that the 0.5 M NaCl resistant fraction that exists at 19 hours reflects the behaviour of approximately 50% of cells. No decrease in fluorescence intensity was observed in the chromatin-depleted population compared to the mock treated population (Fig. 4.4C), showing that all of the MCM2 that resists 0.5 M NaCl is in fact attached to the nuclear matrix at this point.

Together the data argue that even though only a small fraction of MCM2 is resistant to DNase I (Fig. 4.3B), this is the case for around half of the cells at 19 hours after release from quiescence (Fig. 4.4B). Moreover, as resistance is a

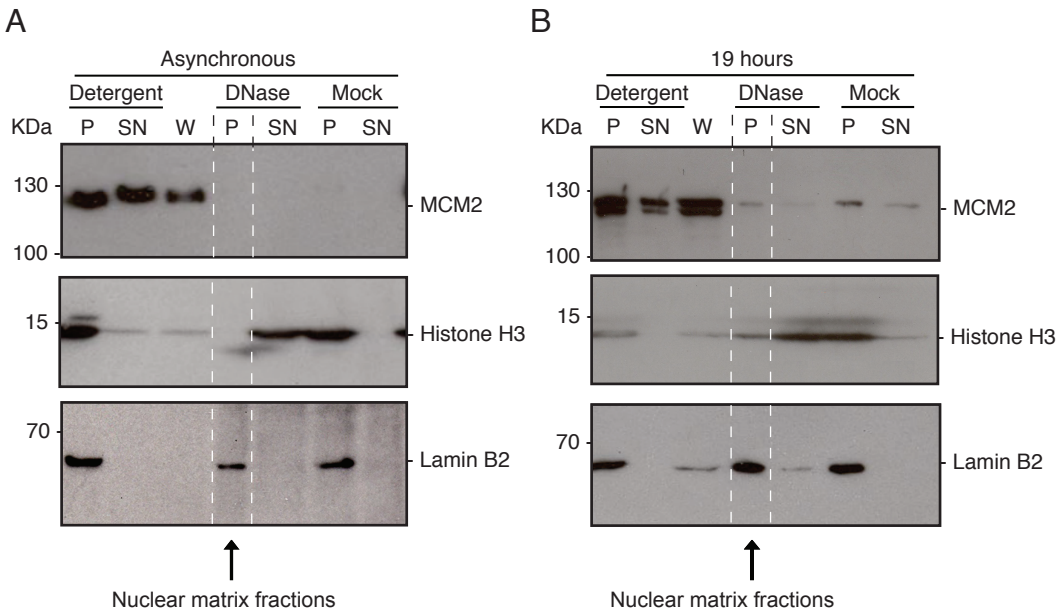


**Figure 4.3.** Nuclear matrix binding revealed by DNase I digestion. Protein fractions prepared from asynchronous 3T3 cells (A), and from late G1 phase cells harvested at 19 hours after release from quiescence (B), showing MCM2, histone H3 and lamin B2. Detergent-resistant pellet (P), detergent-soluble supernatant (SN), 0.5 M NaCl wash (W), DNase I resistant (nuclear matrix, DNase I P), DNase I soluble (chromatin, DNase SN), Mock treated (nuclear matrix and chromatin, Mock P) fractions. Histone H3 shows efficiency of digestion and lamin B2 the residual nuclear matrix fraction (indicated with an white dotted lines). A small fraction of the total MCM2 in the cell resists extraction at 19 hours, but is not detectable in the asynchronous population. Marker is PageRuler Plus Prestained (Thermo Scientific).

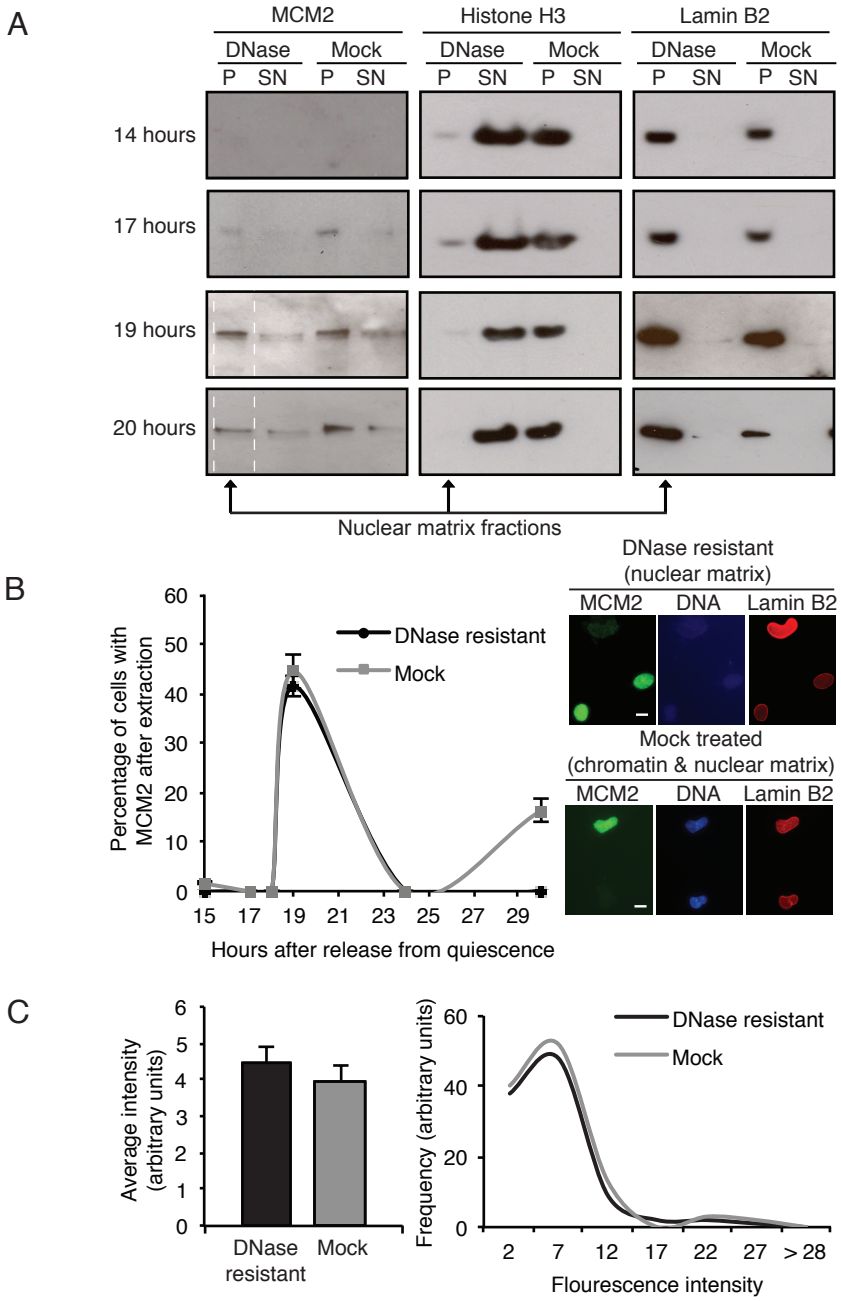


**Figure 4.4.** Nuclear matrix binding revealed by DNase I digestion in G1 phase and early S. A. Western blots of 0.5 M washed pellets after treatment with DNase I (indicated by white dotted line) or mock treatment, harvested at 14 hours (pre-R), 17 hours (pre-initiation), 19 hours (initiation) and 20 hours. B. Percentage of cells with detectable MCM2 after DNase I (nuclear matrix) or mock (nuclear matrix and chromatin) treatment, detected by immunofluorescence. The number of positive cells peaks dramatically at 19 hours, indicating that it becomes temporarily resistant to both 0.5 M NaCl and DNase I (n ≥ 100 for each). Representative images show MCM2 (green), DNA (blue) and lamin B2 (red) after the indicated extractions. Scale bar is 10 μm. C. Mean MCM2 fluorescence intensity in arbitrary units (left) of DNase (n=100) and Mock (n=110) nuclei corrected for background. Intensity distribution (right, showing upper bin value) in arbitrary units. Results show there is no difference between DNase and Mock samples indicating that all 0.5 M NaCl-resistant MCM2 is attached to the nuclear matrix.

transient state, which may in fact last less than an hour, it is likely that more than 50% of the population pass through this state at around this time in late G1 phase.

### 4.4.5 MCM2 is tightly associated with chromatin after initiation

In order to reveal further binding characteristics of MCM2, cells were treated (prior to serial extraction) with DTSP, a cell-permeable reducing cross-linker which specifically links proteins (Baumert and Fasold, 1989) and then analysed by immunofluorescence. Using DTSP allows identification of different MCM2 binding states (Fig. 4.5A). i. MCM2 is bound to chromatin only (released by DNase I with or without DTSP), ii. MCM2 is associated with the nuclear matrix (recovered in the nuclear matrix fraction with or without DTSP), and iii. MCM2 is functionally bound to chromatin and associated with proteins that are themselves resistant to extraction by 0.5 M NaCl (recovered in the pellet fraction only if cross-linked by DTSP).

Levels remained high across the time course (with some fluctuation, Fig. 4.5B) with total and detergent resistant levels of MCM2 similar in the presence or absence of DTSP (Fig. 4.2C), demonstrating crosslinking with DTSP had little affect on overall levels. However, distinct time-dependent shifts were demonstrated in the 0.5 M NaCl-resistant fraction (Mock, Fig. 4.5B). Again a peak is observed at 19 hours, consistent with transient association with the nuclear matrix in all positive nuclei. Example images show full digestion of chromatin in DNase I-resistant fraction (Fig. 4.5B). At 19 hour there was no reduction in fluorescence intensity after depletion of chromatin indicating that all immobilised MCM2 is actually attached to non-chromatin structures (nuclear matrix, Fig. 4.5C). However at 24 hours the response to digestion with DNase I distinguishes a fraction that is not bound to the nuclear matrix (released by DNase I), but is cross-linked to proteins that are themselves tightly associated to chromatin (mock, possibly stabilisation of the heterohexameric ring), and which resist 0.5 M NaCl in a fraction of nuclei.

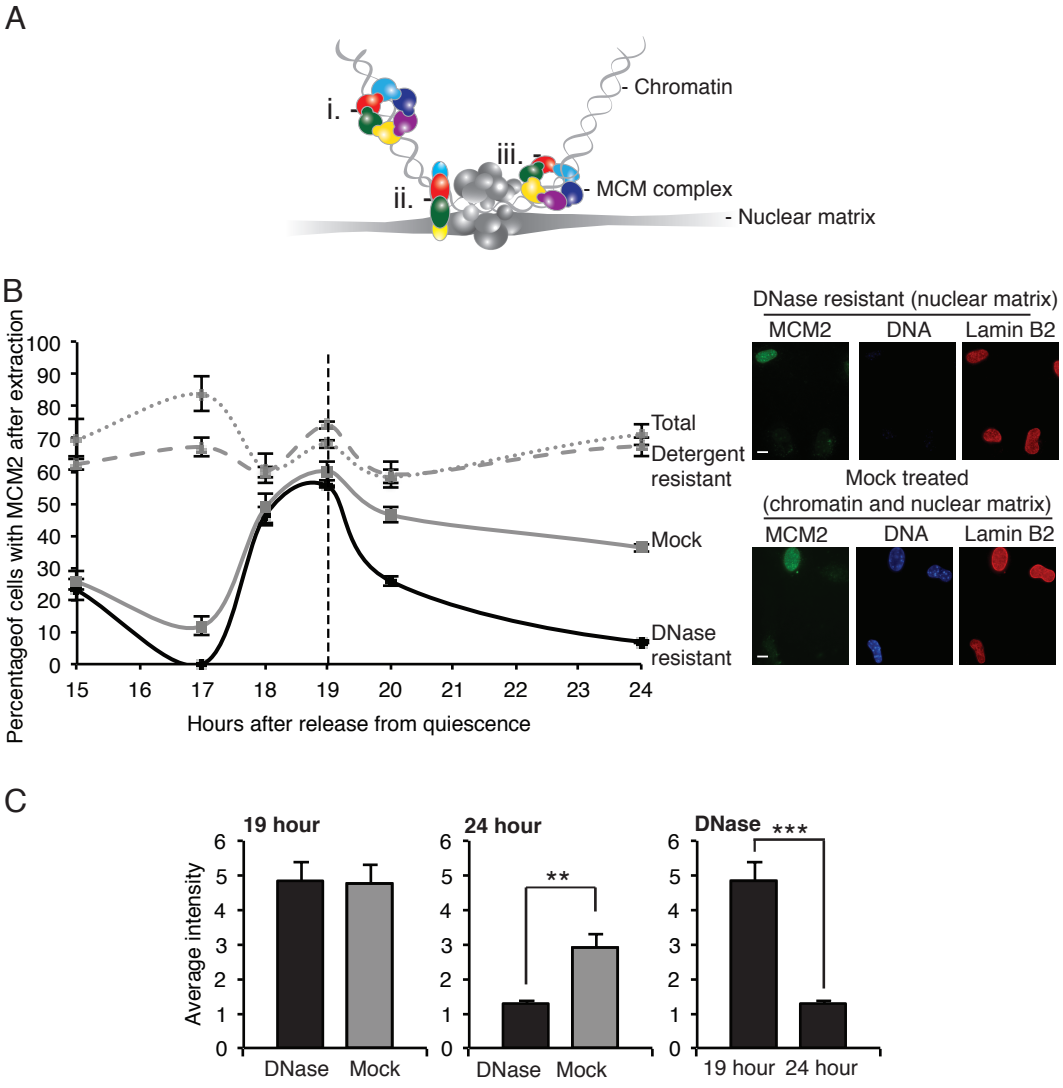


**Figure 4.5.** Using DTSP MCM2 is shown to be associated with chromatin after initiation. A. Schematic showing MCM complex proteins in three states, i. when bound to chromatin only (released by DNase I with or without DTSP), ii. when associated with the nuclear matrix (recovered in the nuclear matrix fraction with or without DTSP), and iii. when functionally bound to chromatin and associated with proteins that are themselves resistant to extraction by 0.5 M NaCl in the pellet fraction (only if cross-linked by DTSP). B. The percentage of nuclei with MCM2, detected by immunofluorescence, in synchronised, cross-linked populations showing total, detergent-resistant, DNase I-resistant, and 0.5 M NaCl-resistant protein (mock) ($n \geq 100$ for each). Mock-treated samples reveal a more gradual loss of immobilisation after 19 hours than that seen when chromatin is digested with DNase I. Dotted line indicates peak of nuclear matrix bound MCM2 at 19 hours. All labelled cells were scored regardless of intensity. Representative images show MCM2 (green), DNA (Hoechst 33258, blue) and lamin B2 (red) after the indicated extractions. Scale bar is 10 µm. C. Mean MCM2 fluorescence intensity after DNase I or mock extraction at 19 hours, ($n = 99$ and 105 respectively, left) and at 24 hours ($n = 107$ and 101 respectively, centre). A comparison of DNase I resistant MCM2 at 19 and 24 hour is also shown ($n = 99$ and 107 respectively, right). ** $p = 8.6 \times 10^{-5}$, *** $p = 2.4 \times 10^{-9}$.

## 4.5 Discussion

Previous work in *S. cerevisiae* (Donovan et al., 1997), *Xenopus* (Chong et al., 1995) and cultured human cells (Symeonidou et al., 2013, Krude et al., 1996, Ohta et al., 2003, Kuipers et al., 2011, Mendez and Stillman, 2000) all demonstrate stable immobilisation of MCM2 in the nucleus during G1 phase, but do not further define the binding properties over this crucial period by distinguishing nuclear matrix-bound MCM2 from chromatin-bound MCM2. MCM2 has been shown to interact with the nuclear matrix anchoring protein AKAP95 (Eide et al., 2003). Disruption of this interaction inhibits both initiation and elongation of DNA replication hypothesised to be due to the inability to recruit MCM2 to the nuclear matrix (Eide et al., 2003). By applying nuclease digestion my results demonstrate a transient relationship between MCM2 and the nuclear matrix, immediately before the majority of cells first produce nascent DNA. Extensive evidence argues that initiation of DNA replication occurs at the base of nuclear matrix-associated chromatin loops in immobilised DNA replication factories (Radichev et al., 2005, Pardoll et al., 1980, Vogelstein et al., 1980, Jackson and Cook, 1986, Nakayasu and Berezney, 1989, Gerdes et al., 1994). Transient rather than sustained recruitment to the nuclear matrix implies a transition that involves function-related helicase loading or activation at the nuclear matrix. Furthermore, the data suggest that activity during the elongation phase of DNA synthesis takes place separate from the nuclear matrix, and possibly outside of replication factories. This is consistent with failure of MCM proteins to co-localise with newly synthesised DNA (Krude et al., 1996, Dimitrova et al., 1999, Madine et al., 1995) except when analysed in relation to labelled DNA from the previous cell cycle (Aparicio et al., 2012). Therefore, MCM proteins are recruited to nuclear matrix-associated replication factories prior to initiation, but occupy somewhat remote sites during DNA synthesis. The diffuse nature of replication origins in higher eukaryotic cells (reviewed in Mechali, 2010) implies that structural determinants related to transcription specify their location on the template, while presence of an active helicase appears to define their status as a functional site. Thus, MCM2-7 complex loading may be specified by activities that are themselves located at the nuclear matrix, with origin selection governed by template recruitment to these sites.

The abundance of MCM proteins is far higher than other components of the pre-RC such as ORC and Cdc6 (Lei et al., 1996, Donovan et al., 1997) and greatly in excess of the number of activated origins of replication, suggesting that only a small fraction of the total MCM protein in the cell is assembled at sites of initiation. In addition, using degron-tagged MCM mutants, very small amounts of MCM proteins were required for DNA replication initiation in *S. pombe* spores but significantly more MCM was required for elongation (Liang et al., 1999). Some of the excess MCM is loaded at secondary sites, such as those that are activated following stress by replication fork inhibition (Ge et al., 2007, Ibarra et al., 2008, McIntosh and Blow, 2012) and in fact multiple copies appear to be present at each origin (reviewed in Laskey and Madine, 2003). It is also possible that a stoichiometric excess of MCM2-7 complex helps to ensure enough availability for parallel, synchronous and complete loading at all specified origins, with non-functionally loaded hexamers depleted by localised proteolysis as implied by the data presented here.

This study adds to the growing body of evidence that initiation of DNA replication is spatially constrained by immobilisation on the nuclear matrix in mammalian cells. It also identifies a specific point in time and location at the nuclear matrix offering a direct route to the identification of the factors that spatially constrain MCM2-7 complex loading and initiation in mammalian cells. Future work in the area will exploit this information to identify interaction partners of MCM2 at the nuclear matrix.

### 4.6 Conclusions

Taken together the data are consistent with tight temporal regulation of pre-RC assembly at G1/S and point to uniform presence in the nucleus, but three states of MCM2-7 complex binding in late G1 phase; i. resistance to detergent but extraction with DNase I identifies a chromatin–associated nuclear fraction before 19 hours, ii. resistance to extraction with DNase I identifies a transient attachment to (and protection by) the nuclear matrix, iii. cross-linking to DNase I-sensitive protein that is resistant to 0.5 M NaCl identifies tight association with chromatin at 24 hours. Based on their timing in relation to initiation of DNA

replication and cyclin A expression (Fig. 4.1A), I suggest this represents i. pre-initiation binding, ii. functional loading at initiation, iii. and post-initiation helicase presence on chromatin (Fig. 4.6).

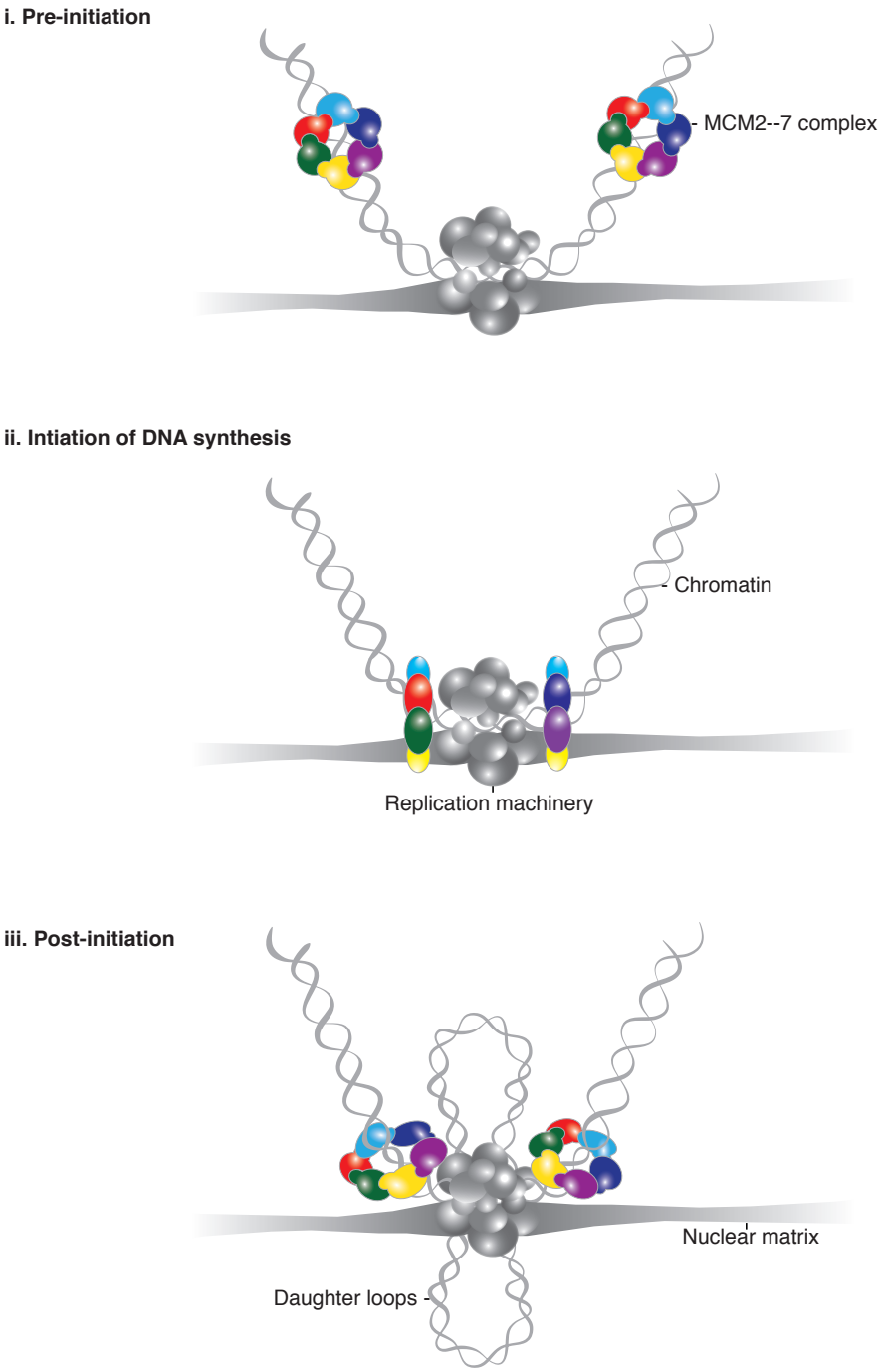


**Figure 4.6.** Schematic showing three states of MCM2-7 complex binding in late G1 phase, superimposed on the prevailing model of DNA replication, in which the replication machinery is fixed to the nuclear matrix at chromatin loop bases, with newly synthesised DNA extruded from fixed sites at two nascent daughter loops (Cook, 1991). Our data suggest that i. before initiation the MCM2-7 complex exists as a chromatin–associated nuclear protein, ii. functional loading immediately prior to initiation takes place coincidently with transient attachment to (and protection by) the nuclear matrix, iii. after initiation the MCM2-7 complex is functionally bound to chromatin but no longer associated with the nuclear matrix, and contributes to progression of the DNA replication fork. Images were prepared by graphics department to my design.

*Chapter 5*

# Functional assembly of recombinant hMCM

# 5 Functional assembly of recombinant hMCM

## 5.1 Introduction

The initiation of DNA replication has been reconstituted *in vitro* using *S. cerevisiae* cell free systems. Researchers use recombinant proteins and synchronised cell extracts to load MCM2-7 onto template DNA (Seki and Diffley, 2000 and others). Usually template DNA contains a known *S. cerevisiae* origin and is in the form of a plasmid or DNA physically attached to a bead. Using G1 extracts from *S. cerevisiae*, pre-RC assembly is dependent on the presence of origin sequences (Bowers et al., 2004, Seki and Diffley, 2000). However, using recombinant pre-RC proteins assembly is not origin dependent (Evrin et al., 2009, Remus et al., 2009), demonstrating promiscuity in origin selection on naked template. Recently, full replication of plasmid DNA was achieved, independent of origin sequences, using a *S. cerevisiae* cell free system over-expressing multiple initiation proteins (Gros et al., 2014, On et al., 2014). Thus, initiation has been effectively reconstituted. However, even in the presence of defined origins from *S. cerevisiae*, initiation is independent of origin sequence. This suggests that in the context of whole nuclei there are other constraints controlling MCM2-7 functional loading that cannot be identified using naked template. Thus it is necessary to analyse MCM2-7 loading onto DNA packaged into chromatin, ideally within nuclei themselves. This is particularly important when studying mammalian DNA replication where origins are not defined by sequence and chromosome structure is believed to play a part in origin selection (reviewed in Mechali, 2010).

This chapter demonstrates the regulated loading of recombinant hMCM in isolated nuclei from mammalian cells. In this system hMCM loading is functional and has the ability to promote the initiation of DNA replication *in vitro*. In addition, I describe the use of recombinant proteins to determine the exact requirements for inducing a conformational change in hMCM. This conformation of hMCM (monitored using a mobility shift in MCM2) is normally exclusively found in S phase cells.

## 5.2 Aims

Using purified recombinant hMCM hexamer my goals were to:

- Reconstitute mammalian MCM2-7 complex assembly in mammalian nuclei, and determine the requirement for its properly regulated function.
- Analyse the post-translational modifications to hMCM, and reconstitute conditions that induce a shift from 'G1' and 'S' phase conformation.

## 5.3 Experimental design

The production of purified recombinant hMCM in *E. coli*, to avoid post-translational modifications (Chapter 3), enables the analysis of G1/S phase kinases on naïve hMCM complexes. In conjunction with a cell free system, using synchronised cell extracts and nuclei from mouse 3T3 cells (section 2.2.2), this permits an ideal platform to analyse the functional assembly of MCM2-7 in mammalian DNA replication initiation. Due to the emerging differences reported between *S. cerevisiae*, *Xenopus* and mammalian systems (see Chapter 1 for details) analysis of human MCM2-7 is essential to understand details that may be of use in a clinical setting.

## 5.4 Results and discussion

### 5.4.1 Cell free characterisation

Cell free components are obtained by synchronising cells in quiescence (as described in 2.2.2 and Chapter 4) and harvesting the cells at specific time points following release, in order to generate extracts with stage specific composition (Fig. 5.1). At approximately 15 hours after release from quiescence, cells are in mid-G1 phase where levels of CDKs are low, at 17 hours after release from quiescence cells are in late-G1 phase and levels of CDKs are rising. Once in S phase the cell has everything required to replicate its DNA including nucleotides and DNA polymerase. The different levels of kinases within cells at these time points are believed to regulate the temporal separation of MCM2-7 loading and activation (reviewed in Sclafani and Holzen, 2007, Li and Araki, 2013). Protein

extract isolated at 15 hours, 17 hours and in S phase represent the average of a population of cells enriched for the required cell cycle phase.

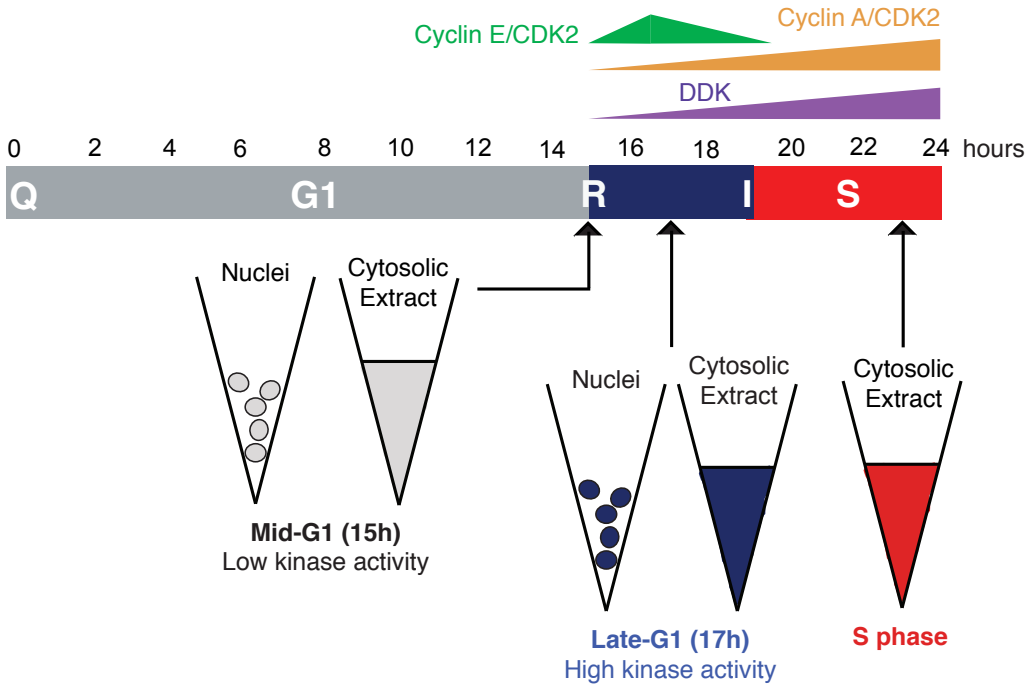


**Figure 5.1.** Schematic representation of cell free components prepared from cells synchronised by re-entry to the cell cycle from quiescence (Q). The time the cell passes through G1 phase (G1), the restriction point (R), initiation of DNA replication (I) and S phase (S) are shown. The relative concentration gradients of cyclin E/CDK2 (green), cyclin A/CDK2 (orange) and DDK (purple) are also indicated. Arrows show where cells are harvested for 15 hour (mid-G1), 17 hour (late-G1) and S phase extracts and nuclei preparations.

Using nuclei and cytoplasmic extracts, a working system that recapitulates nuclear events was developed as described previously (Krude et al., 1997, Coverley et al., 2002). Addition of an ATP regenerating system (phosphocreatine and creatine phosphokinase) and nucleotides to cell extracts enables *in vitro* initiation of DNA synthesis in isolated G1 phase nuclei. This is a powerful system, used here to dissect the functional loading of MCM2-7. Each batch of nuclei was tested for replication competency. When incubated in mid-G1 phase extract the number of nuclei able to replicate DNA from already initiated origins (i.e. run on synthesis) was compared to the number of nuclei undergoing DNA

replication when incubated in S phase extract (i.e. run on synthesis plus new initiation events). If more nuclei are able to replicate their DNA when incubated in S phase extract compared to mid-G1 phase extract a proportion of the nuclei have initiated DNA synthesis *in vitro* and this represents the 'replication competent' fraction within the population. Nuclei populations in which the replication competent fraction is large enough to be reproducibly and accurately scored were used for future analysis.

### 5.4.2 Regulated binding of hMCM in isolated nuclei

To determine whether recombinant hMCM can bind to chromatin within nuclei, a cell free assay was devised. A replication competent late-G1 phase nuclei population was incubated in both mid-G1 phase and late-G1 phase extracts to determine whether hMCM binding is more or less efficient in the two extracts (Fig. 5.2A). The data show that MCM2, MCM4 and MCM7 preferentially bound to late-G1 nuclei when incubated in mid-G1 phase (15 hour) extract compared to late-G1 phase (17 hour) extract (Fig 5.2B-E), demonstrating regulated assembly of hMCM *in vitro*.

Mid-G1 phase nuclei populations contain low numbers of replicating nuclei (less than 10%, Fig. 4.1A) and even fewer replication competent nuclei. Moreover, levels of endogenous MCM proteins are also low (Fig. 4.2B). Because MCM2-7 is believed to load onto chromatin in mid-G1 phase (Coverley et al., 2002), these nuclei represent a more functionally relevant content for analysis of MCM2-7 loading. When analysed in the same way as late-G1 phase nuclei (Fig. 5.3A), binding of hMCM was also most efficient in mid-G1 phase extract (Fig 5.3B and C). A negative control, where hMCM was incubated with extract in the absence of nuclei demonstrates that recovery of hMCM is dependent on nuclei (Fig. 5.3B) and therefore represents a detergent resistant association rather than unspecific recovery. These results led to the hypothesis that components in the late-G1 phase extract inhibit hMCM loading. As cellular kinases are responsible for cell cycle control following the restriction point (Aguda, 2001) and levels of kinases are higher in late-G1 phase extracts compared to mid-G1 phase extract (Fig. 5.1) it

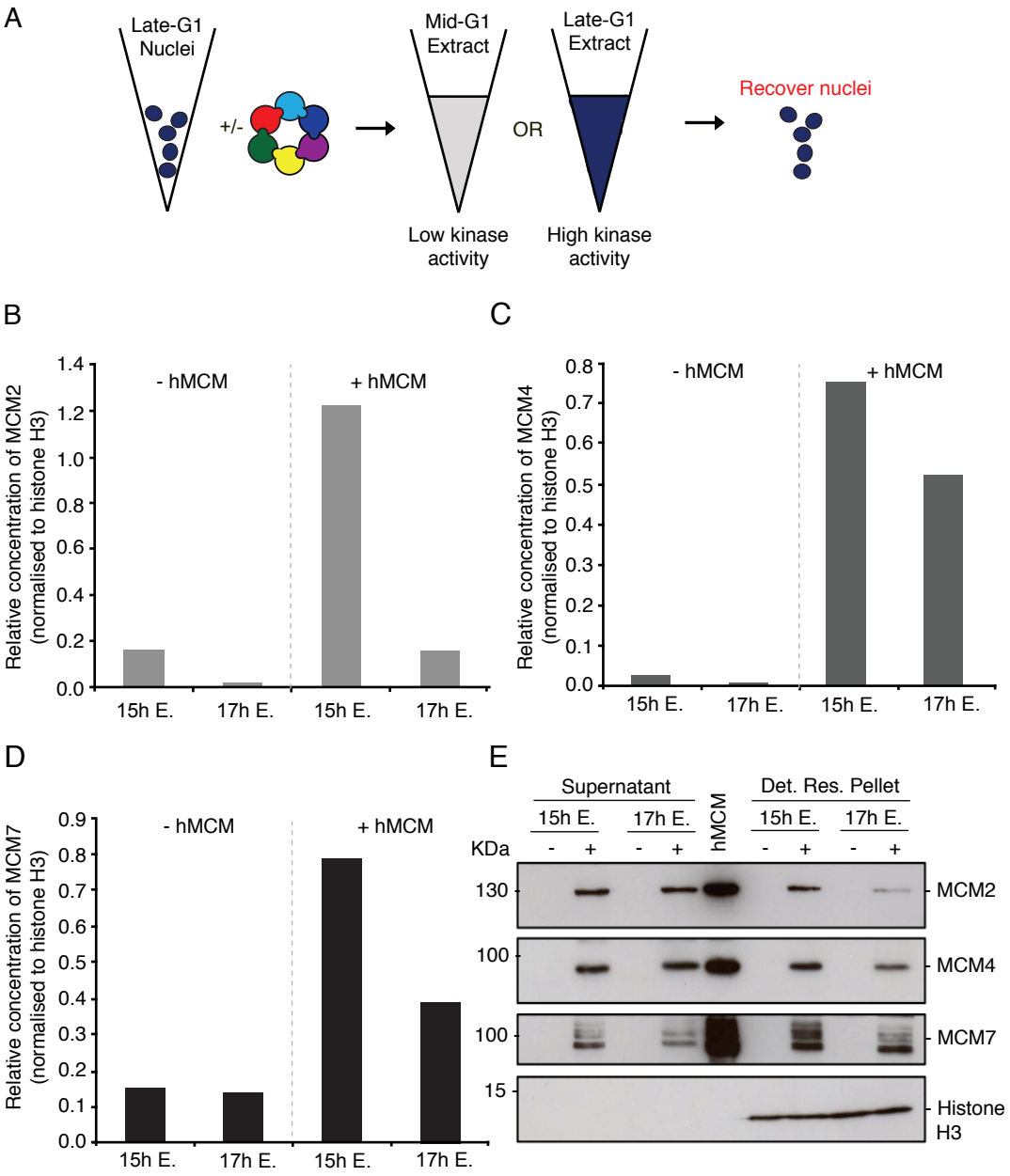


**Figure 5.2.** Regulated binding of hMCM within late-G1 phase nuclei *in vitro*. A. Schematic to represent cell free experiment. Late-G1 phase (17h) nuclei were incubated in either mid-G1 phase (15h) extract (E.) or late-G1 phase extract in the presence or absence of recombinant hMCM. Histograms show quantification of western blot (E) showing detergent resistant (Det. Res.) levels of MCM2 (B), MCM4 (C) and MCM7 (D) in recovered nuclei. Results are quantified by densitometry and expressed relative to histone H3 concentrations. Marker is PageRuler Prestained Plus (Thermo Scientific).

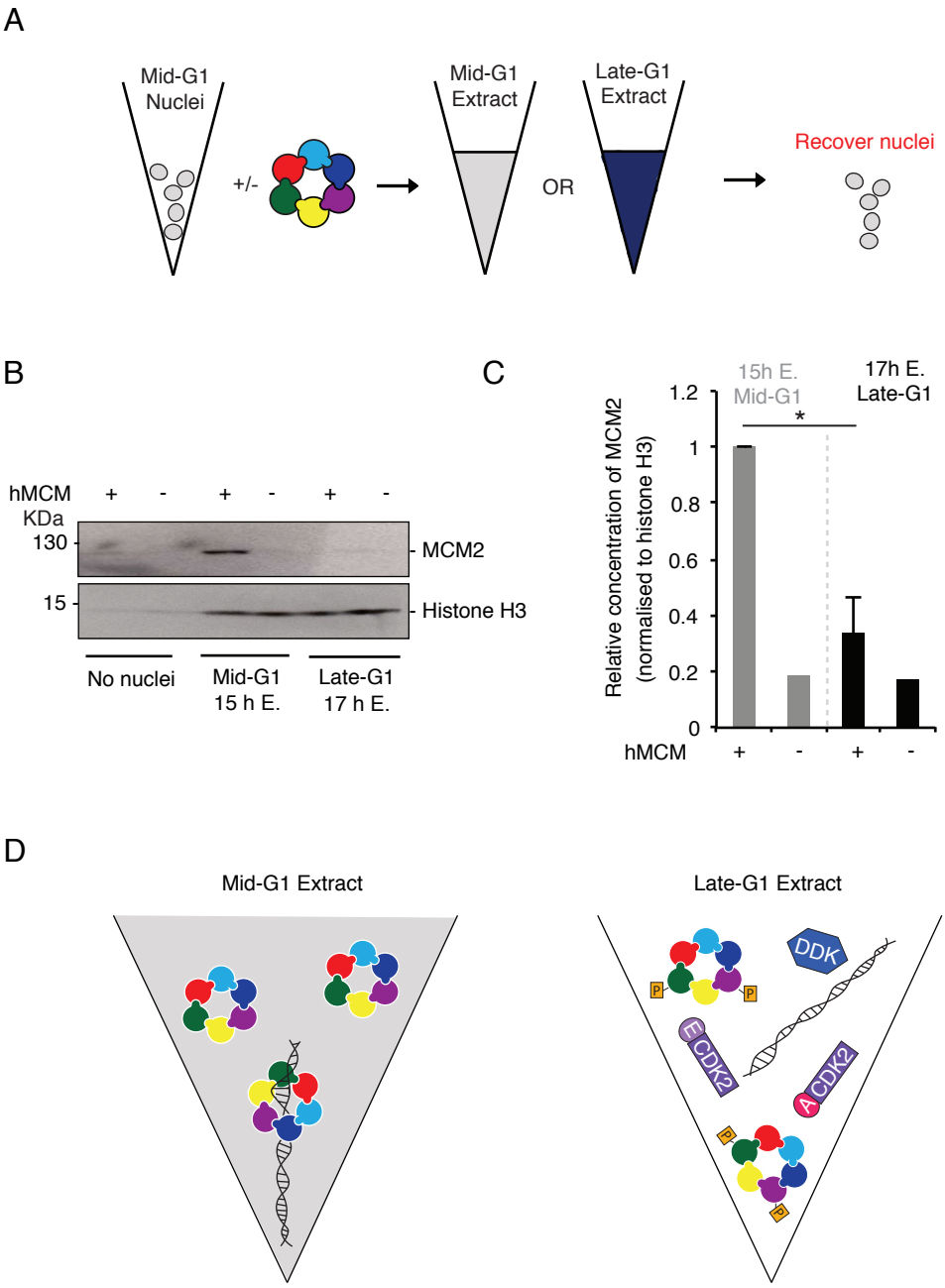


**Figure 5.3.** Regulated binding of hMCM within mid-G1 phase nuclei *in vitro*. A. Schematic to represent cell free experiment. Mid-G1 phase (15h) nuclei were incubated in either mid-G1 phase extract (E.) or late-G1 phase (17h) extract in the presence or absence of recombinant hMCM. B. Western blot analysis of detergent resistant MCM2 and histone H3. No nuclei is shown as a negative control. Marker is PageRuler Prestained Plus (Thermo Scientific). C. Quantification of western blot (B) to show detergent resistant levels of MCM2 relative to histone H3 concentrations. For + hMCM the average of three biological replicates is shown. Error bars show +SEM. *p = 0.01. D. Model for regulated hMCM binding. In mid-G1 extract hMCM loads onto chromatin. In late-G1 extract binding is supressed by comparison of the extracts, most likely due to elevated cellular kinases (such as cyclin A/CDK2, cyclin E/CDK2 and DDK). Regulated binding argues that hMCM binding is physiologically relevant and that hMCM is subjected to regulatory post-translational modifications.

is likely that the inhibitory factors in the 17 hour extract are regulatory kinases (Fig. 5.3D).

### 5.4.3 Recombinant cyclin A/CDK2 and cyclin E/CDK2 improve hMCM loading in isolated nuclei

In order to unpick the requirements for hMCM loading, cyclin E/CDK2 and cyclin A/CDK2 were added to hMCM cell free loading experiments (Fig. 5.4A). Cyclin E/CDK2 boosted hMCM loading over two-fold when used at 6.8 nM (Fig. 5.4B). In previous published work, endogenous MCM2 loading peaked at 2.72 nM cyclin E/CDK2 (Coverley et al., 2002), as recombinant hMCM is added at a concentration approximately 10-fold higher than endogenous MCM2-7, these concentrations are in the same range and suggests that recombinant hMCM loading is regulated in a similar way to endogenous MCM2-7. Furthermore, in cells where cyclin E is ablated, the association of MCM proteins with chromatin was decreased (Geng et al., 2003) and over production of cyclin E in cultured mammalian cells speeds up G1 phase (Ohtsubo and Roberts, 1993) possibly by increasing MCM loading.

Addition of recombinant cyclin A/CDK2 also increased the ability of hMCM to bind to chromatin (Fig. 5.4C). This is not expected as cyclin A/CDK2 has previously been shown to inhibit loading of pre-RC components (Coverley et al., 2002, Wheeler et al., 2008). However, these results could be due to sequence and structural similarity between cyclins E and A and under the conditions tested, cyclin A may substitute for cyclin E.

### 5.4.4 hMCM is functionally loaded onto chromatin *in vitro*

To understand if the recombinant hMCM that is loaded *in vitro* is functional within mammalian nuclei I analysed the ability of nuclei to replicate when supplied with an S phase environment. As cyclin E/CDK2 was most efficient at promoting the ability of hMCM to load, nuclei were pre-loaded in the presence or absence of hMCM and/or cyclin E/CDK2. Following the loading reaction nuclei were transferred to an S phase extract supplemented with labelled nucleotides (Fig. 5.5A), this provides the nuclei with everything required for

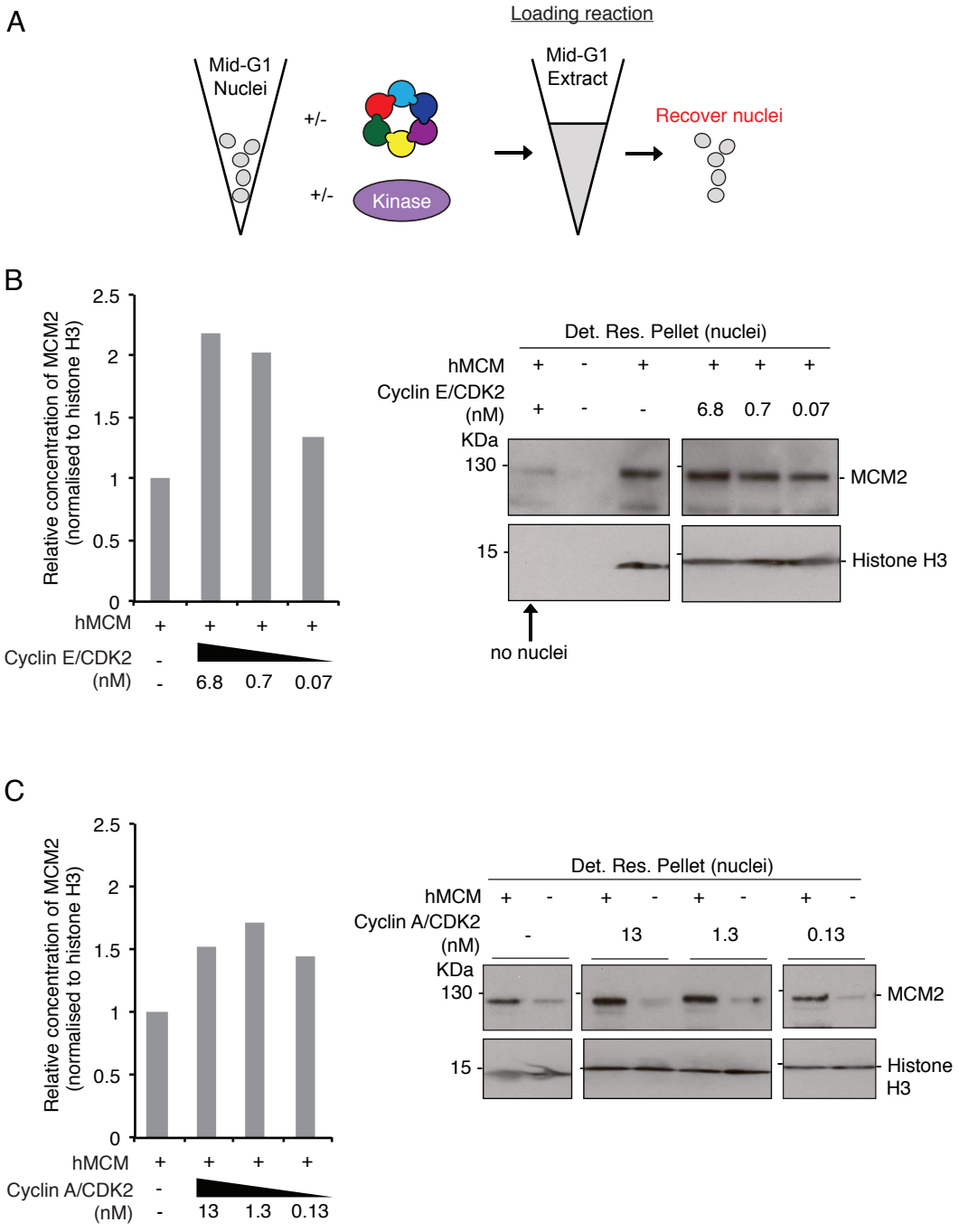


**Figure 5.4.** Effect of recombinant cyclin E/CDK2 and cyclin A/CDK2 on hMCM loading. A. Schematic to represent cell free experiment in which mid-G1 phase (15 hour) nuclei were incubated in mid-G1 phase extract in the presence or absence of recombinant hMCM and kinase. B. Concentration of detergent resistant MCM2 quantified from western blot (right) relative to histone H3 in the presence of decreasing concentrations of cyclin E/CDK2. C. As in (B) in the presence of decreasing cyclin A/CDK2. Marker is PageRuler Plus Prestained (Thermo Scientific).

DNA replication. In the absence of recombinant proteins approximately 7% of the nuclei were capable of DNA replication (Fig. 5.5B). When nuclei were pre-loaded with recombinant hMCM, the number of nuclei undergoing DNA replication was boosted over two-fold. The number of replicating nuclei was further increased to over three-fold in the presence of recombinant cyclin E/CDK2 and hMCM. This demonstrates that *in vitro* loaded recombinant hMCM is functional. Cyclin E/CDK2 alone is also capable of increasing the number of nuclei able to replicate DNA (Fig. 5.5B), possibly by promoting endogenous MCM2-7 loading as reported previously (Coverley et al., 2002).

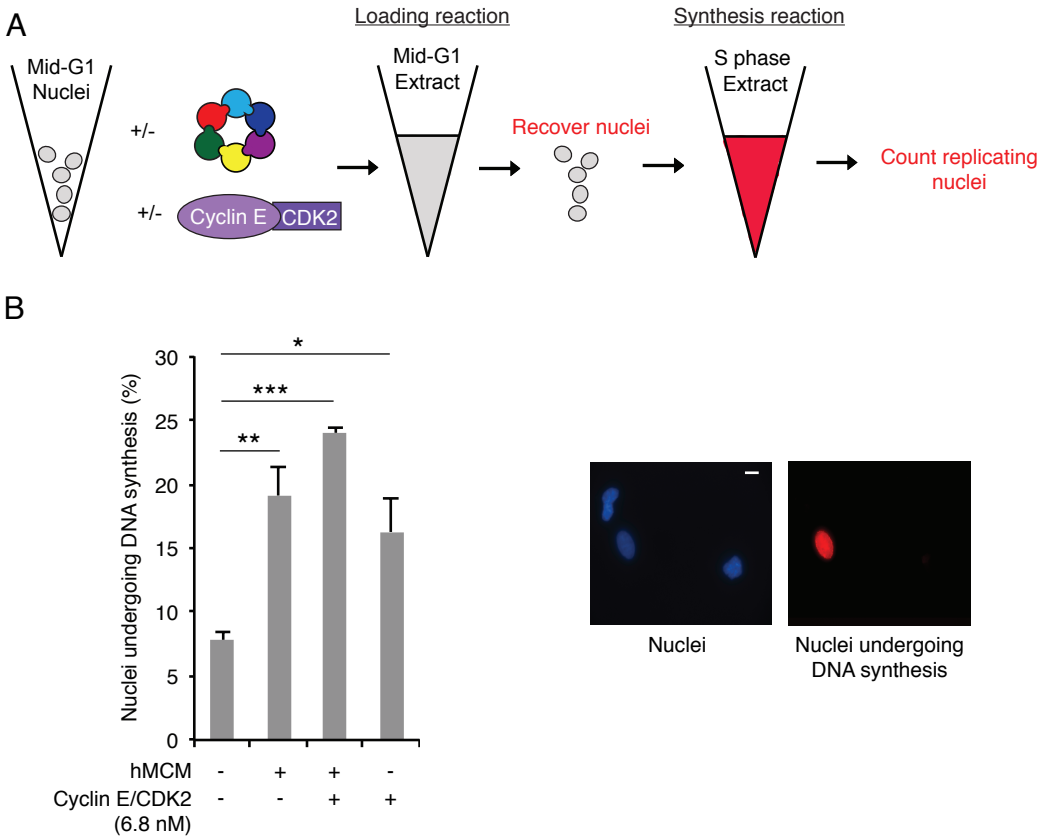


**Figure 5.5.** Effect of recombinant cyclin E/CDK2 on initiation of DNA replication. A. Schematic to represent cell free experiment in which mid-G1 phase (15 hour) nuclei were incubated in mid-G1 phase extract in the presence or absence of recombinant hMCM and/or cyclin E/CDK2. Nuclei were recovered and incubated in S phase extract supplemented with labelled nucleotides. B. Nuclei undergoing DNA synthesis after incubation in loading reaction. Error bars show +SEM for three technical replicates, *p = 0.03, **p = 0.07 and ***p = 0.0001. Right – micrograph showing nuclei stained with Hoechst 33258 (blue), and nuclei undergoing DNA synthesis in red. Scale bar is 10 μm.

### 5.4.5 Effect of DDK on hMCM loading

The kinase activity of DDK is associated with activating the MCM2-7 complex to unwind DNA (reviewed in Sclafani and Holzen, 2007, Li and Araki, 2013, Labib, 2010). However the role of DDK in loading MCM2-7 onto chromatin is not understood, so I analysed the effect of DDK in cell free loading experiments (Fig. 5.6A). DDK inhibited hMCM binding when present at low concentrations (1.8 nM, Fig. 5.6B). However high concentrations of DDK (711 nM), appeared to have little effect on the amount of hMCM that is able to load onto chromatin (Fig. 5.6B). Conversely, by analysis of human cells synchronised in quiescence and released into the cell cycle using a similar method to that employed here, DDK phosphorylation at MCM2-Ser5 has been shown to be required for endogenous MCM loading (Chuang et al., 2009). In the cell free system, the presence of endogenous DDK may be responsible for phosphorylating MCM2 at Ser5 allowing its association with chromatin in the supplemented reaction. Together these results suggest that chromatin association of MCM2-7 is tightly controlled, however the effect of DDK on MCM2-7 loading is unclear.

Interestingly, 711 nM DDK causes an increased mobility of MCM2 in SDS PAGE and 180 nM DDK caused the mobility shift in approximately half of the loaded MCM2, indicating two populations of MCM2 (Fig. 5.6B, right). MCM2 with increased mobility is recovered in both detergent resistant pellet fraction (nuclei) and supernatant fractions, indicating that under these conditions, both forms of MCM2 appear to bind to chromatin. Previously the mobility shift of MCM2 in SDS PAGE has been linked with phosphorylation (Masai et al., 2000, Fujita et al., 1998, Coverley et al., 2002), though because the shift is towards increased mobility it must represent an unusual state of the denatured polypeptide chain.

### 5.4.6 MCM2 mobility shift is dependent on both DDK and cyclin A/CDK2

To understand if DDK is exclusively responsible for the mobility shift of MCM2 on SDS PAGE, the effect on hMCM of recombinant kinases (analysed in the absence of cell extract) was investigated. This demonstrated that DDK, cyclin A/CDK2 and cyclin E/CDK2 seperately are not capable of causing the mobility shift under the concentrations tested (Fig. 5.7). However, the presence of both

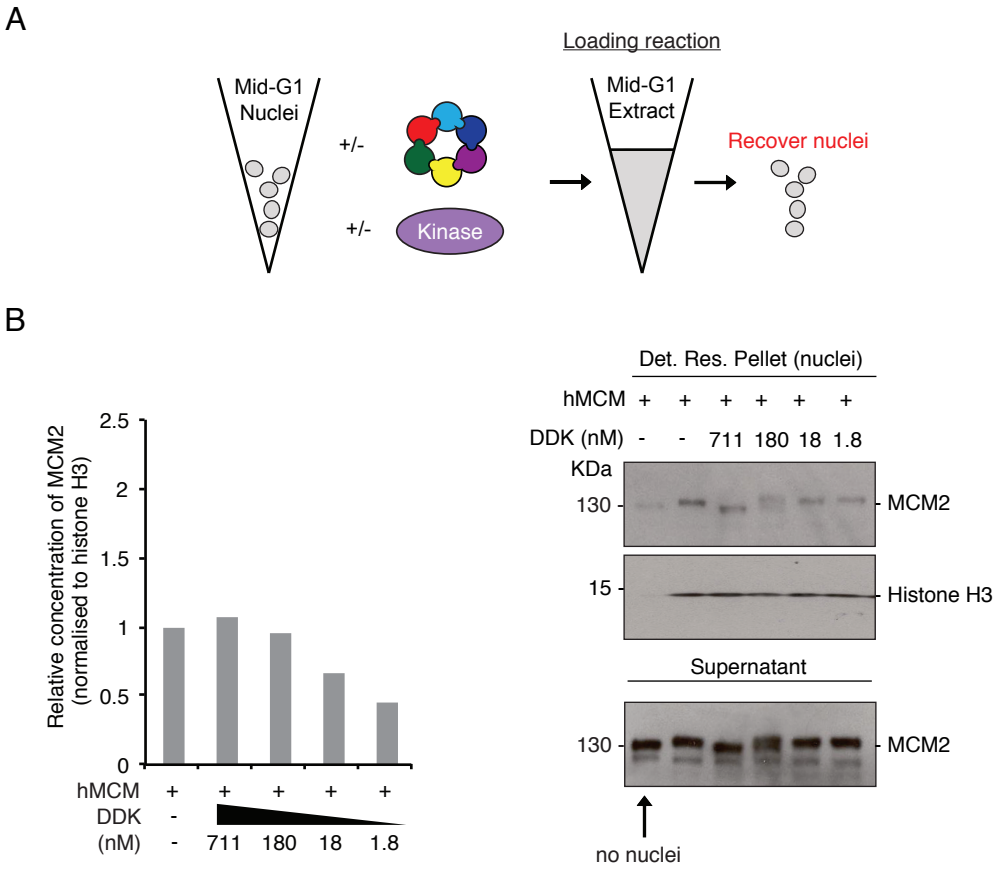


**Figure 5.6.** Effect of recombinant DDK on hMCM loading. A. Schematic to represent cell free experiment in which mid-G1 phase (15h) nuclei were incubated in mid-G1 phase extract in the presence or absence of recombinant hMCM and DDK. B. Concentration of detergent resistant MCM2 quantified from western blot (right) relative to histone H3 loading control in the presence of decreasing concentrations of DDK. Supernatant samples (i.e. recombinant hMCM which did not bind) are also shown. Marker is PageRuler Plus Prestained (Thermo Scientific).

DDK and cyclin A/CDK2 are capable of causing the shift (Fig. 5.7A, *). The increased mobility and likely conformational change in MCM2 may reflect an important regulatory event related to activating the MCM2-7 helicase.

The effect of recombinant kinases on the other MCM2-7 proteins was also investigated (Fig. 5.7A). The only other hMCM subunit with a notable mobility shift in SDS PAGE was MCM4. In the case of MCM4, addition of cyclin A/CDK2 alone was capable of causing a large decrease in mobility, suggesting an increased molecular weight, presumably due to hyperphosphorylation. Addition of both cyclin A/CDK2 and cyclin E/CDK2 also increased the molecular weight of MCM4, similarly to cyclin A/CDK2 alone. Interestingly addition of cyclin A/CDK2 and DDK increased the molecular weight of MCM4 even more than cyclin A/CDK2 alone (Fig 5.7A). These differential mobility shifts have also been noted in endogenous chromatin bound MCM2 and MCM4 in S phase cells (Masai et al., 2006, Fujita et al., 1998). There also appears to be a number of different bands present when MCM4 is treated with DDK and/or CDK2 demonstrating a number of different phosphorylation states. (Fig 5.7A). The recombinant kinases did not have a large effect on the mobility of the remaining hMCM subunits under the conditions tested (Fig. 5.7A). Studies indicate that in the context of the MCM2-7 hexamer, the main targets of DDK are MCM2, MCM4 and MCM6 (Francis et al., 2009). Here a shift in mobility is only seen for MCM2 and MCM4. This of course does not rule out phosphorylation of MCM6. It is possible that, if used at a higher concentration, cyclin E/CDK2 would be capable of shifting MCM4 (and MCM2 in the presence of DDK). However, the concentration used here (6.8 nM), was chosen based on its ability to stimulate endogenous MCM2 loading (Coverley et al., 2002), and so is in the physiologically relevant range.

To examine the effect of recombinant kinases on the overall hMCM structure, kinase treated hMCM was analysed by native PAGE (Fig. 5.7B). Analysis of MCM2 and MCM4 gave similar results, with the most intense band containing MCM proteins at around 480 KDa, which is broadly consistent with the molecular weight of recombinant hMCM (567 KDa). On the other hand, when probed for MCM6, the most intense band on native PAGE ran below 720 KDa

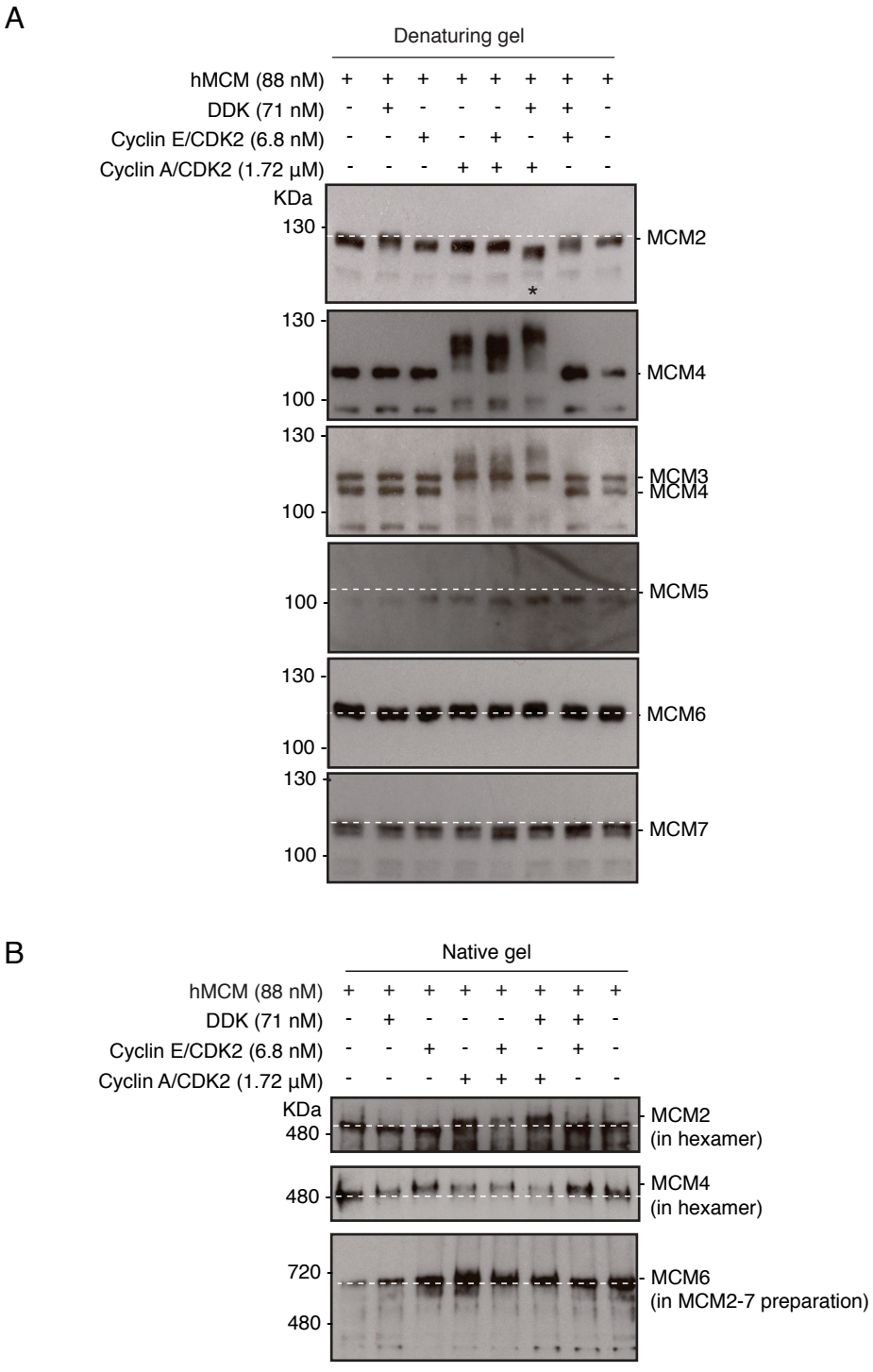


**Figure 5.7.** Both cyclin A/CDK2 and DDK are required to shift MCM2 but only cyclin A/CDK2 is required to shift MCM4. A. Recombinant hMCM was incubated with recombinant kinases as indicated, analysed by SDS PAGE and probed for MCM2 – MCM7. The highlighted lane (*) shows that both DDK and cyclin A/CDK2 are required to induce the shift in mobility of MCM2. Marker is PageRuler Plus Prestained (Thermo Scientific). B. Recombinant hMCM was incubated with recombinant kinases as indicated, analysed by native PAGE and probed for MCM2, MCM4 and MCM6. Marker is NativeMark Unstained (Life technologies).

(Fig. 5.7B). As this is at a different weight to the band detected by MCM2 and MCM4 it suggests that the hMCM preparation may not be an evenly stoichiometrically balanced heterohexamer. It is also possible that the complex may fall apart when run on native PAGE. In addition it is possible MCM6 has aggregated causing it to run at a larger molecular weight. Interestingly addition of cyclin A/CDK2 caused retarded mobility of the hexamer when probed with MCM2, MCM4 and MCM6, conversely, addition of cyclin E/CDK2 only retarded the mobility of the hexamer when probed with MCM4. More investigation is required to understand the effect of kinases on the mobility of the hMCM hexamer, as hMCM may not be stable under native PAGE conditions.

### 5.4.7 Mobility shift of MCM proteins is a reversible phosphorylation

Increased mobility of MCM2 is not as expected for a phosphorylated protein. Lambda phosphatase was used to investigate if the mobility shift noted for MCM2 and MCM4 is in fact caused by phosphorylation (Fig. 5.8). Samples were incubated with recombinant kinases as before, following which one half of the reaction was treated with Lambda phosphatase. These results clearly show the effect of cyclin A/CDK2 and DDK on MCM2 is due to phosphorylation and it is reversible. The same is also true for MCM4 (Fig. 5.8). Moreover when blotted for MCM4 there is an additional species, which runs at approximately 50 KDa. This could be degraded MCM4. The antibody used was raised against the N-terminal (amino acids 1 – 300), this suggests that the phosphorylation is in the N-terminal portion of MCM4 and the structural change produced, inferred from decreased mobility, occurs in this small 50 KDa truncated protein. This is consistent with studies in *S. cerevisiae* that have intensely analysed the phosphorylation sites in MCM4, demonstrating they are exclusively N-terminal (Masai et al., 2000, Devault et al., 2008, Sheu and Stillman, 2010, Sheu and Stillman, 2006, Masai et al., 2006).

### 5.4.8 Cyclin A/CDK2 is required before DDK to induce increased mobility of MCM2

There has been controversy over the order in which cellular kinases react with MCM2-7 (reviewed in Sclafani and Holzen, 2007). Within the cell, kinases are

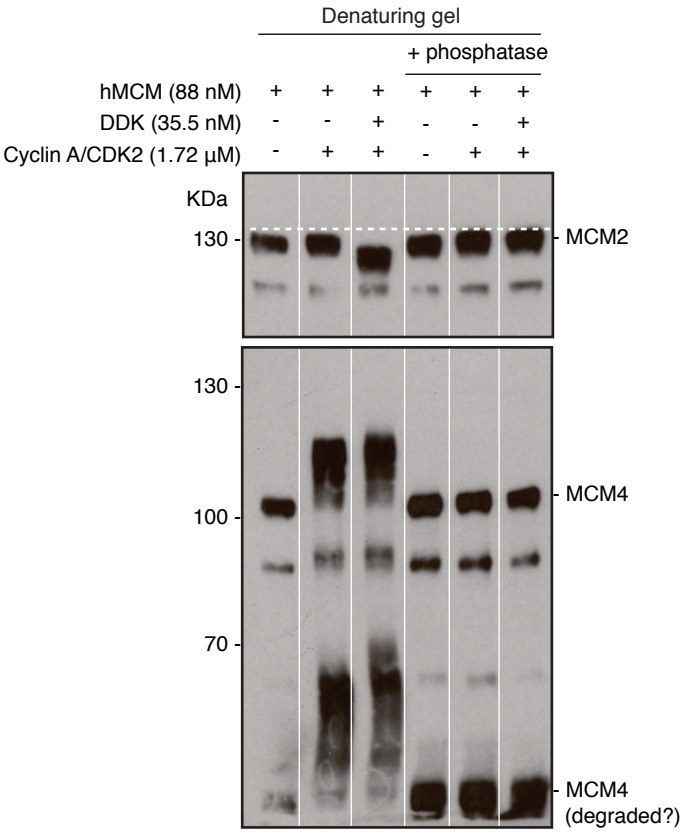


**Figure 5.8.** MCM2 and MCM4 mobility shift is reversed by dephosphorylation by Lambda phosphatase. Recombinant hMCM was incubated with recombinant kinases as indicated. Following incubation half the reaction was treated with Lambda phosphatase. Samples were analysed by SDS PAGE and western blotted for MCM2 and MCM4. Marker is PageRuler Plus Prestained (Thermo Scientific).

differentially expressed and activated to control DNA replication initiation and so MCM2-7 is usually exposed to kinases in a specific order and over a gradient of concentrations. In mammalian cells, hMCM would be exposed to cyclin E/CDK2 in G1 phase followed by cyclin A/CDK and DDK in S phase (Fig. 5.1). Therefore, I wanted to investigate if the order in which hMCM is exposed to cyclin A/CDK2 and DDK is important in inducing the increased mobility of MCM2. This analysis requires inhibitors that are specific to either CDK2 or DDK. Roscovitine is a CDK inhibitor that has been extensively used and is specific to CDKs (Meijer et al., 1997). Addition of 20 μM roscovitine to hMCM in the presence of cyclin A/CDK2 was sufficient to inhibit the phosphorylation of MCM4 (Fig. 5.9A, compare lanes 2 and 3). However, in the presence of DDK and cyclin A/CDK2, 20 μM roscovitine did not block the shift to increased mobility of MCM2 (Fig. 5.9A, compare lanes 4 and 5). This raises the possibility that the effect of cyclin A/CDK2 on MCM2 mobility may be kinase independent. To test this, the effect of cyclin A and DDK on hMCM was monitored and found not to induce the shift of MCM2 (Fig. 5.9B, lane 2). Another possibility is that only a small amount of CDK kinase activity is required to increase the mobility of MCM2 (less than that required to shift MCM4). Agreeing with this theory, 0.2 mM roscovitine (10-fold higher than used previously) was sufficient to inhibit the MCM2 shift (Fig. 5.9B, lane 1).

PHA-767491 is a newly identified Cdc7 inhibitor, which has been shown to inhibit both DDK activity and CDK2 activity (Montagnoli et al., 2008, Natoni et al., 2011). However, in cells, the concentration required to inhibit CDK is 20 fold more than DDK activity (Montagnoli et al., 2008). Using 20 μM PHA-767491, the MCM2 shift was not inhibited; however, the CDK dependent MCM4 shift was inhibited (Fig 5.10A, compare lanes 1 and 2). This implies that, at the concentrations used, PHA-767491 is not specific to DDK in this purified system. To optimise the use of PHA-767491, the minimum amount of DDK required to induce the MCM2 shift was determined (Fig. 5.10B). The data show that 35 nM DDK is capable of inducing the MCM2 shift and that this can be inhibited by 20 μM PHA-767491 (Fig. 5.10B, compare lanes 4 and 5). However, the CDK dependent shift of MCM4 is also inhibited, illustrating that CDK activity is also affected. Therefore, PHA-767491 was titrated down to identify the minimal

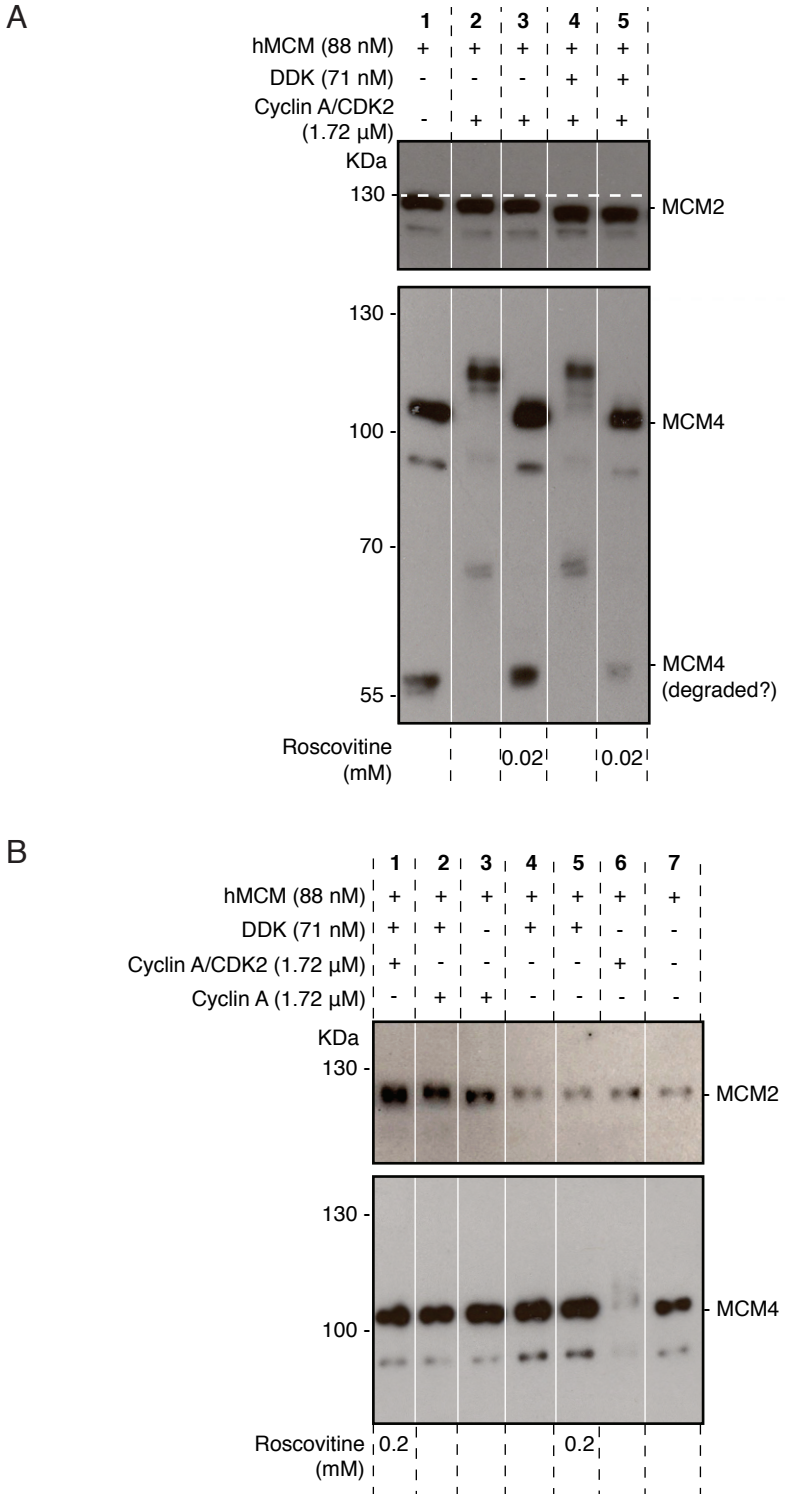


**Figure 5.9.** Effect of the CDK2 inhibitor roscovitine on MCM2 and MCM4 mobility shifts. A. Recombinant hMCM was exposed to 0.02 mM roscovitine before and during incubation with recombinant kinases as indicated. Samples were analysed by SDS PAGE and western blotted for MCM2 and MCM4. 0.02 mM roscovitine inhibits MCM4 shift (compare lanes 2 and 3) but is not sufficient to inhibit MCM2 shift (lanes 4 and 5). B. As in (A) using 0.2 mM roscovitine, which inhibits both MCM2 and MCM4 shift (Lane 1). Marker is PageRuler Plus Prestained (Thermo Scientific).

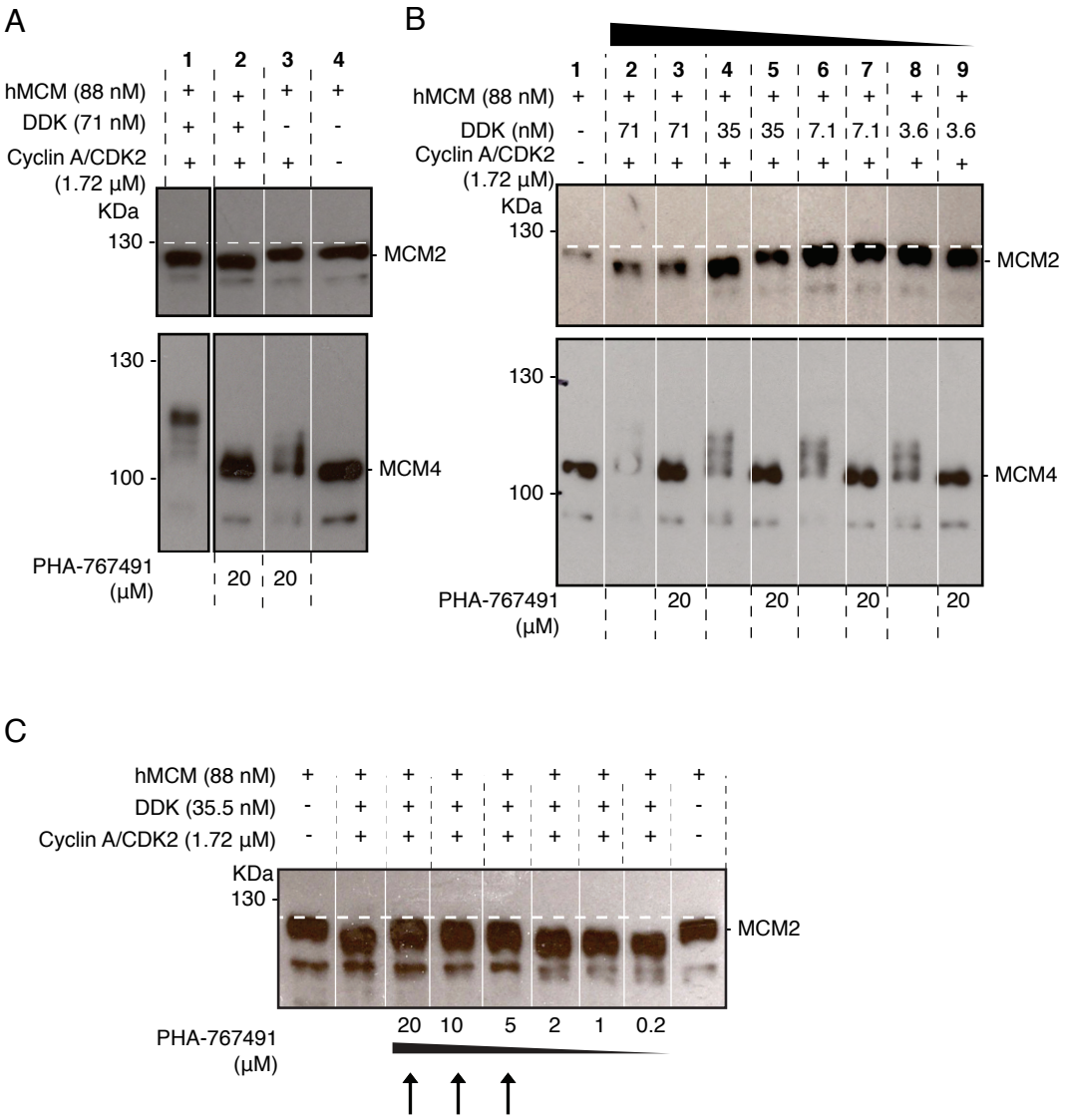


**Figure 5.10.** Effect of DDK inhibitor PHA-767491 on MCM2 mobility shift. A. Recombinant hMCM was exposed to PHA-767491 before and during incubation with recombinant kinases as indicated. Samples were analysed by SDS PAGE and western blotted for MCM2 and MCM4. 20 µM PHA-767491 inhibits MCM4 shift but not MCM2 shift (compare lanes 1 and 2). B. As in A. but using reduced concentrations of DDK as indicatited. 35 nM DDK is sufficient to induce MCM2 shift and is inhibited by 20 µM PHA-767491 (compare lanes 4 and 5). C. As in B. PHA-767491 inhibits the mobility shift of MCM2 at lanes highlighted with arrow. Marker is PageRuler Plus Prestained (Thermo Scientific).

concentration that is able to inhibit the MCM2 mobility shift (Fig. 5.10C). Three concentrations were identified (20 μM, 10 μM and 5 μM), 10 μM PHA-767491 (10-fold lower than used previously) was chosen for future experiments. In these experiments the use of an ATP regenerating system means that the ATP concentration cannot be determined. As both of these inhibitors are ATP competitive this is an important consideration when analysing kinase inhibition.

To analyse if the order in which hMCM is exposed to cyclin A/CDK2 or DDK affected the mobility shift, hMCM was incubated with either cyclin A/CDK2 or DDK, which was subsequently inhibited before addition of the second kinase (Fig. 5.11A). Using 10 μM PHA-767491 inhibition is specific to DDK as the decreased mobility of MCM4 is apparent in both the presence and absence of PHA-767491 (Fig. 5.11B, compare lanes 4 and 9). The mobility shift of MCM2 is observed when cyclin A/CDK2 is added before DDK (Fig. 5.11B, lane 5), but not when added in the reverse order (Fig. 5.11B, lane 6). However, there does appear to be a small increase in mobility when DDK is added before CDK, possibly due to a conformational change in the denatured MCM2. Also when DDK is added before cyclin A/CDK2, MCM4 appears to have a different mobility shift to when the kinases are added at the same time (Fig. 5.11B, compare lanes 6 and 7). This suggests DDK alters the ability of cyclin A/CDK2 kinase to access potential phosphorylation sites on MCM4.

Thus, the results suggest the following hypothesis; cyclin A/CDK2 activity causes a conformational change in the hMCM hexamer, which allows DDK to access phosphorylation sites on MCM2 previously concealed (Fig. 5.11C). This results in the forms of MCM2 and MCM4 usually seen only in S phase cells (Masai et al., 2006, Fujita et al., 1998). Studies analysing a bacterially expressed recombinant N-terminal fragment of MCM2, revealed the same DDK phosphorylation sites, independent of CDK2 pre-phosphorylation (Montagnoli et al., 2006). This suggests that pre-phosphorylation by CDK2 may only be required when MCM2 is within the MCM2-7 complex, and may therefore occur to subunits other than MCM2 and MCM4. In *S. cerevisiae* MCM6 has been shown to be a target for DDK and so is a possible candidate (Francis et al., 2009).

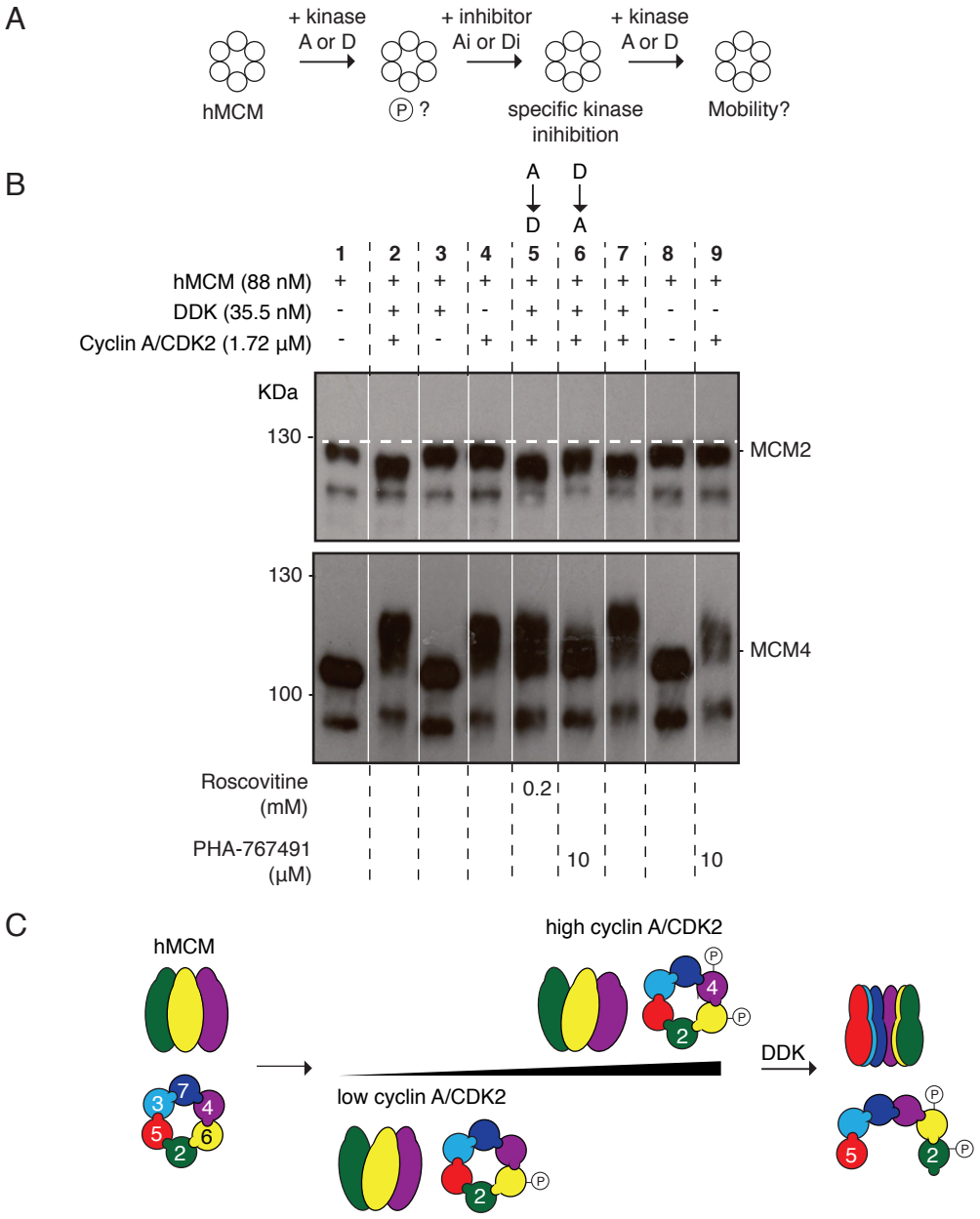


**Figure 5.11.** Order of addition experiment which shows that cyclin A/CDK2 must act before DDK in order to induce the MCM2 mobility shift. A. Schematic to show order in which cyclin A/CDK2 (A) or DDK (D) is incubated with hMCM. The kinase is then specifically inhibited using either roscovitine (CDK2 inhibitor - Ai) or PHA-767491 (DDK inhibitor – Di) before addition of the second kinase. The effect is monitored by the mobility of MCM2 and MCM4 in SDS PAGE. B. Western blot shows that 10 µM PHA-767491 does not inhibit MCM4 shift (compare lanes 4 and 9). MCM2 shift is only apparent if hMCM was incubated with cyclin A/CDK2 before addition of DDK (compare lane 5 and 6). Marker is PageRuler Plus Prestained (Thermo Scientific). C. Interpretation of results, low concentrations of cyclin A/CDK2 phosphorylate an unknown MCM subunit. Higher concentrations of cyclin A/CDK2 hyperphosphorylates MCM4. Pre incubation with cyclin A/CDK2 causes a conformational change in the hexameric complex allowing DDK to access additional phosphorylation sites, and cause a conformational change in MCM2.

In *S. cerevisiae* the only essential targets for CDK in S phase are Sld2 and Sld3 (Zegerman and Diffley, 2007, Tanaka et al., 2007). However in G1 phase CDK is required for processes other than activation of S phase (Zegerman and Diffley, 2007). The use of roscovitine (Fig. 5.9) demonstrates that only a low concentration of cyclin A/CDK2 is required to prime the MCM2-7 hexamer for DDK activity. Consistent with this, when recombinant hMCM is incubated with mid-G1 phase nuclei and extract, the mobility of MCM2 is increased with the addition of only recombinant DDK (Fig. 5.6B, right). This suggests that in mid-G1 phase, when cyclin A/CDK2 levels are low, hMCM is pre-phosphorylated leaving the complex susceptible to further phosphorylation by DDK in S phase.

## 5.5 Conclusions

Using a cell free system based on nuclei and extracts from defined points in G1 phase, recombinant hMCM can be loaded onto chromatin in a manner that is promoted by recombinant cyclin E/CDK2 within a narrow concentration range (Fig. 5.4B), and down-regulated in extracts from late G1 phase (Fig. 5.2 and 5.3). Regulated loading leads to an increase in the number of nuclei able to replicate their DNA *in vitro* (Fig. 5.5B), showing that *in vitro* loaded recombinant hMCM is functional. This system enables evaluation of the process requirements and the regulatory sites involved in hMCM loading and activation.

Using entirely recombinant proteins, I have demonstrated both cyclin A/CDK2 and DDK are required to shift recombinant MCM2 (in the context of hMCM hexamer). Moreover, MCM4 (but not MCM6) is affected under the same conditions implying a structural alteration. The phosphorylated forms of MCM2 and MCM4 are normally exclusively found in S phase. This is the first time phosphorylation of naïve MCM2-7 has been studied and the results clearly show that to induce the increased mobility form of MCM2, the hMCM hexamer must be exposed to cyclin A/CDK2 prior to DDK.

*Chapter 6*

# Discussion and future work

# 6 Discussion and future work

The mechanistic biology of the initiation of DNA replication is relevant to ageing (Flach et al., 2014, reviewed in Minton, 2014) and cancer (Blow and Gillespie, 2008). Abnormalities in licensing can lead to re-replication, replication stress and genomic instability, which are powerful drivers toward the acquisition of mutations. MCM proteins, as well as other components of the pre-RC, are elevated in a range of cancer types and have been shown to have diagnostic value (Gonzalez et al., 2005, Hook et al., 2007, Williams and Stoeber, 2007, Xouri et al., 2004, Lau et al., 2007, Dudderidge et al., 2010, Lau et al., 2010, Neskoromna-Jedrzejczak et al., 2010, Kelly et al., 2012, Williams and Stoeber, 2012, Coleman and Laskey, 2009). The mechanistic implications of elevated expression of MCM proteins and potential strategies to intervene, hinge on a detailed knowledge of the process as it occurs in mammalian cells. Understanding the regulation of MCM2-7 in mammals has potential to generate information that can be translated for the benefit of human health, and will yield insight into a fundamental biological process.

To expand on the current knowledge of MCM2-7 loading and activation in eukaryotes, mainly generated from studies in *S. cerevisiae*, my thesis analyses MCM2-7 in mammals. I have produced data regarding the production and characterisation of recombinant hMCM, the profile of endogenous MCM2-7 expression and localisation, evidence that probes the functional loading of hMCM in isolated nuclei and phosphorylation of naïve hMCM.

## 6.1 Recombinant hMCM is active

We have produced the first recombinant hMCM in *E. coli* (Chapter 3). To date, analysis of MCM2-7 activity has been determined for complexes purified from eukaryotic systems or recombinantly expressed in eukaryotic systems (Ilves et al., 2010, Moyer et al., 2006, Bochman and Schwacha, 2008). Thus, may not be naïve due to phosphorylation by cellular kinases present in the expression systems. Phosphorylation may inhibit or activate the MCM2-7 complex. Using ATP hydrolysis assays and helicase assays, I have demonstrated that

recombinant hMCM is active in the absence of any post-translational modifications, suggesting 'activating kinases' are not required for duplex unwinding. In the present work, the DNA template used is a naked forked DNA substrate (Appendix B, Fig. B1). The implications of kinases on unwinding DNA packaged into chromatin are not clear. Accessory proteins such as Cdc45 and GINS in addition to kinase activities may be required for unwinding packaged DNA in a nuclear environment.

### 6.1.1 hMCM stoichiometry

An initial human MCM complex purified from HeLa cells was found in a dimer of trimers conformation - two of each MCM4, 6 and 7 (Ishimi, 1997). Currently the stoichiometry of our recombinant hMCM is unknown. Homohexameric MCM complexes and sub-complexes containing MCM4, 6 and 7 have ATP hydrolysis activity that is stimulated by DNA (Ishimi et al., 1998, Lee and Hurwitz, 2000, Lee and Hurwitz, 2001, You et al., 2003, Liew and Bell, 2011, McGeoch et al., 2005, Kasiviswanathan et al., 2004). In contrast, the ATP hydrolysis activity of our recombinant hMCM and heterohexameric MCM2-7 from *S. cerevisiae,* is not stimulated by DNA (Fig. 3.10B, Schwacha and Bell, 2001, Davey et al., 2003, Bochman and Schwacha, 2008). As our hMCM behaves in a similar way to *S. cerevisiae* MCM2-7 this suggests our hMCM is heterohexameric. Furthermore, our EM reconstructions show asymmetric symmetry (Fig. 3.14). Investigation into the stoichiometry of hMCM would consolidate future analysis. Size Exclusion Chromatography - Multi-Angle Laser Light Scattering (SEC-MALLS) would allow identification of the exact molecular weight of hMCM (567 KDa if heterohexameric, 580 KDa if a dimer of MCM4, 6, 7). In addition, to investigate the homogeneity, SEC-MALLS could be used to compare hMCM alone with hMCM bound by an antibody that is specific to MCM2, 3 or 5 as these are not found in the MCM4, 6, 7 sub-complex. If the sample is pure heterohexameric hMCM, there will be a shift in the size of the total sample. If the sample is a mixture of dimer of trimers and heterohexameric hMCM, the output will be two peaks.

### 6.1.2 Essential residues in hMCM

Recombinant hMCM allows detailed analyses of essential residues. A number of conserved residues have been identified in lower organisms such as; the h2i mutation which inhibits helicase activity but not ATP hydrolysis (Jenkinson and Chong, 2006) and MCM2-G400D in *S. cerevisiae*, which bypasses a requirement for MCM10 in origin firing (Lee et al., 2010). The identification of essential residues in hMCM would allow researchers to extend our understanding from archaea and *S. cerevisiae* to mammalian systems. In addition, the production of phosphomimetic mutants and insertion of unphosphorylatable residues could be used to analyse the MCM2-7 control by kinases (see below for more details).

## 6.2 Recombinant hMCM undergoes a conformational change when bound to DNA

Production of asymmetric single particle hMCM reconstructions demonstrated that MCM2-7 undergoes a conformational change when bound to DNA (Fig. 3.14 – 3.16). In the presence of DNA, our structure appears similar to previous EM studies of *Mt*MCM and *S. cerevisiae* MCM2-7 (Yu et al., 2002, Pape et al., 2003, Samel et al., 2014). However, EM reconstructions of MCM2-7 purified from *Drosophila* and *E. cuniculi* demonstrate MCM2-7 is naturally found in a 'cracked ring' conformation (Fig. 1.3B, Costa et al., 2011, Lyubimov et al., 2012). Importantly these studies analyse *Drosophila* or *E. cuniculi* MCM2-7 produced in *Baculovirus* and so may not be naïve complexes due to possible phosphorylation by host cellular kinases. In addition, *E. cuniculi* MCM2-7 is a simplified MCM2-7 model, which lacks the N-terminal domain in each subunit (Lyubimov et al., 2012). *S. cerevisiae* and mammalian MCM2 and MCM4 are phosphorylated at residues in the N-terminal domain by cellular kinases (Sheu and Stillman, 2006, Masai et al., 2006, Masai et al., 2000, Devault et al., 2008, Sheu and Stillman, 2010, Montagnoli et al., 2006, Cho et al., 2006, Tsuji et al., 2006, Montagnoli et al., 2008). Furthermore, the N-terminal of MCM4 in *S. cerevisiae* is believed to inhibit DNA replication and this inhibition is alleviated by phosphorylation (Sheu and Stillman, 2010). Together these data suggest the N-terminal segments of MCM

proteins may be essential for opening the MCM2-7 ring and so may represent an important intermediate conformation in MCM2-7 loading.

### 6.2.1 Subunit arrangement and orientation

The crystal structure of archaeal *Sso*MCM has been fitted into our hMCM EM reconstructions (Fig. 3.15 and 3.16, Brewster et al., 2008). However the orientation of the complex is not explicit. The crystal structures were fitted into our EM maps using Chimera (Goddard et al., 2007). The X-ray crystallography fits contain the least amount of error, i.e. with the largest amount of the crystal structure fitted within our EM maps (Fig. 3.15 and 3.16). The orientation shown is preferential as it gives the lowest amount of error using Chimera (Goddard et al., 2007). To identify the correct orientation of our reconstructions, hMCM bound to a gold-labelled antibody could be analysed by EM. The gold-labelled antibody would be detected by EM and allow identification of the hMCM subunit to which it is bound. If the antibody is specific for either the N-terminal or C-terminal of an hMCM subunit it will allow identification of subunits orientation.

### 6.2.2 Which MCM2-7 subunit preferentially binds DNA?

The hMCM reconstruction in the presence of DNA has a projection on one subunit (Fig. 3.14, red circle). This projection could be either bound DNA or the purification tags on MCM7 (molecular weight is 15 KDa) that have been displaced by the addition of DNA. If the projection was DNA it would be interesting to investigate if a particular subunit of hMCM preferentially binds to the DNA. Currently there is no literature that shows preferential DNA binding to a particular subunit, this could be identified using gold-labelled antibodies as described above.

### 6.2.3 X-ray crystal structure of hMCM

I have sent 9 mg of recombinant hMCM to Xiaojiang Chen, a collaborator at the University of Southern California, for X-ray crystallography analysis. To date the only X-ray crystallography images of MCMs are from homohexameric archaeal complexes (Fletcher et al., 2003, Liu et al., 2008, Bae et al., 2009, Brewster et al., 2008, Miller et al., 2014, Froelich et al., 2014). An X-ray crystallography structure

of the hMCM will allow us to analyse how the subunits interact with each other and so will give further insight into the mechanism of functional heterohexameric hMCM. One gap in our current knowledge concerning the eukaryotic MCM complex relates to the heterohexameric nature of this complex. Data from *S. cerevisiae* show that the subunits are not functionally equivalent (Labib et al., 2000, Kang et al., 2014), but how this inequivalence relates to the mechanism of unwinding is unclear. Production of an X-ray crystallography structure of hMCM is likely to yield useful insights into how ATP hydrolysis, DNA translocation and duplex unwinding all occur in concert and the mechanisms of control that can be exerted over these processes.

## 6.3 MCM2 is transiently associated with the nuclear matrix at initiation

Chapter 4 adds to the growing body of evidence that initiation of DNA replication is spatially constrained by immobilisation of DNA replication machinery on the nuclear matrix in mammalian cells, and suggests that functional assembly of the MCM2-7 complex occurs during a transient presence in nuclear matrix-associated loading bays. However it does not explain why association is transient, or give clarity to the mechanism of loading or the regulation of ring opening. The data identify a specific point in time and location at the nuclear matrix, offering a direct route to the identification of the factors that spatially constrain the MCM2-7 complex and mediate its transition from one state to another at this critical point in the initiation process in mammalian cells.

### 6.3.1 Effect of kinase inhibitors on transient nuclear matrix binding of MCM2

The effect of the specific CDK2 and DDK inhibitors roscovitine (Meijer et al., 1997) and PHA-767491 (Montagnoli et al., 2008) on recruitment or displacement of MCM2 from the nuclear matrix could be monitored over the 15-20 hour window. Cells could be synchronised in quiescence and released into the cell cycle in the presence of either roscovitine or PHA-767491. This would allow us to distinguish if CDK2 and/or DDK activity supports MCM2 nuclear matrix binding or release of MCM2 from the nuclear matrix. At 19 hours following

release from quiescence, both phosphorylation species of MCM2 are detectable. However nuclear matrix bound MCM2 is exclusively the higher molecular weight MCM2, i.e. the naïve, unphosphorylated form (Fig. 4.3B). Consequently, I predict that CDK2 and/or DDK inhibition at 18 hours will not prevent MCM2 recruitment to the nuclear matrix at 19 hours, but will restrict its displacement from the nuclear matrix and possibly block initiation. Unfortunately due to time constraints and the need to complete other aspects of my project I was unable to do these experiments.

### 6.3.2 Additional proteins bound to nuclear matrix

The pre-LC assembles away from chromatin and does not appear to be highly conserved between *S. cerevisiae* and metazoans (see section 1.6.2). This suggests a different mechanism in metazoans for the formation of the CMG complex, compared with *S. cerevisiae*, which could involve the nuclear matrix. It would be interesting to examine if TopBP1, RecQ4, pol ε and GINS (members of the pre-LC) have a transient association with the nuclear matrix. In T98G glioblastoma cells, pol ε has been shown to be associated with the nuclear matrix from the G1/S border throughout S phase (Vaara et al., 2012), indicating the pre-LC may assemble at the nuclear matrix. However, in asynchronous HeLa and human fibroblast cells, RecQ4 has been shown to be not associated with the nuclear matrix (Petkovic et al., 2005, Sharma and Brosh, 2007). If the association of RecQ4 is transient, evidence of its nuclear matrix association in an asynchronous population of cells may be difficult (as with MCM2, Chapter 4). Furthermore the cell line chosen to analyse nuclear matrix associated proteins is essential as tumours, transformed cells in culture, and stem-like cells (Munkley et al., 2011, Zink et al., 2004) appear to have a compromised or immature nuclear matrix. To date there are no publications which analyse the relationship of TopBP1 or GINS with the nuclear matrix.

Identification of additional proteins bound to the nuclear matrix at the same time as MCM2 (such as components of the pre-LC or pre-IC) may allow us to understand more about the loading process. Nuclear matrix preparations from 19 hour nuclei could be evaluated for the presence of proteins involved in MCM2-7

complex loading and function. Analysis over a time course as shown in Fig. 4.4, will allow evaluation of whether association is similarly transient, or extends through late G1 and S phases. I expect pre-LC components to be detected in the nuclear matrix fraction before MCM2 association, possibly for a longer period of time. However, I would expect to find a short transient association of pre-IC components with the nuclear matrix in a similar way to MCM2.

### 6.3.3 Identification of novel proteins involved in DNA replication initiation

Novel mammalian proteins whose role is to spatially constrain loading by anchoring it to the nuclear matrix could be identified by DNase I extraction. To do this, standard synchrony experiments could be scaled up to generate DNase I nuclear matrix preparations from 19 hour nuclei, after protein-protein cross-linking with DTSP (Baumert and Fasold, 1989, as described for Fig. 4.5). Partner proteins would be isolated by immunopreticipitation (IP) and identified by tandem mass spectrometry (MS/MS). This would be a powerful and focused way to build a picture of the nuclear matrix-associated MCM 'loading bay' and could be controlled by comparison to pre or post 19 hour populations. Novel proteins identified as nuclear matrix bound at 19 hours could be tested for essentiality using short interfering (si) RNA. If proteins are essential, for DNA replication initiation, depletion of the newly identified proteins would stall cells prior to S phase.

## 6.4 Regulated hMCM loading

Recombinant hMCM can be functionally loaded in isolated mammalian nuclei (Chapter 5). Loading of hMCM has, reproducibly, been shown to be a regulated event, as a mid-G1 extract (low kinase activity) supports loading more efficiently than a late-G1 phase extract (high kinase activity, Fig. 5.2 and 5.3). This is consistent with cell free experiments in *S. cerevisiae* where pre-RC loading has been shown to assemble on template DNA only when CDK levels are low (reviewed in Sclafani and Holzen, 2007). Addition of low levels of recombinant cyclin E/CDK2 to cell free experiments boosts hMCM loading and the ability of nuclei to initiate DNA synthesis (Fig. 5.4A and 5.5). This is consistent with previous analysis in mammalian cells (Coverley et al., 2002, Geng et al., 2003,

Ohtsubo and Roberts, 1993), where cyclin E was shown to cooperate with Cdc6 to load endogenous MCM2. Monitoring histone H3 concentration in a 8% gel may not be an accurate method for measuring nuclei concentration and so although this method has been used widely in the literature (Coverley et al., 1998, Coverley et al., 2002, Coverley et al., 2005) a more accurate way of measuring nuclei content, such as immunofluorescence experiments (as described in 2.9.2.2) could be used in future experiments.

### 6.4.1 What component of late-G1 phase extract inhibits hMCM loading?

The component/s in late-G1 phase extract, which restrict hMCM binding, are not known. Analysis of the effect of DDK on hMCM loading, suggests low concentrations of DDK could be responsible (Fig. 5.6). To test this hypothesis specific inhibitors such as roscovitine (Meijer et al., 1997) or PHA-767491 (Montagnoli et al., 2008) to inhibit CDK2 and DDK respectively could be added to the extract to examine if hMCM binding is restored to that of mid-G1 phase extract.

### 6.4.2 Ability of ATPase deficient mutant hMCM to functionally load onto chromatin

In *Xenopus* egg extracts, mutation in the Walker A motif of MCM6 and MCM7 to inhibit ATP hydrolysis in these subunits, has been shown to have no effect on MCM2-7 loading but inhibits DNA replication initiation (Ying and Gautier, 2005). However, a recent study of *S. cerevisiae* MCM2-7 suggests ATPase activity of all subunit interfaces, other than MCM3/7, are required for loading (Kang et al., 2014, Coster et al., 2014). To test if ATP hydrolysis by recombinant hMCM is necessary for loading, our ATPase deficient mutant hMCM (Chapter 3) could be analysed using cell free loading reactions in the same way as WT hMCM (Chapter 5). This would identify if in mammals, the ATPase domains are required for loading and/or activation. Further more, individual MCM subunits could be mutated (Kang et al., 2014, Coster et al., 2014). Mutants could be tested in cell free loading and synthesis experiments (Chapter 5) in order to understand the different ATPase domains in mammalian MCM2-7.

### 6.4.3 Does hMCM bind to the nuclear matrix?

Functional loading of hMCM has been demonstrated, however the ability of hMCM to bind to the nuclear matrix has not been tested. Assembly of hMCM on chromatin compared to the nuclear matrix could be assessed using the cell free system. Nuclei could be loaded with recombinant hMCM (Chapter 5) and subsequently treated with DNase I to reveal proteins that are immobilised by attachment to the nuclear matrix (Chapter 4). Recombinant hMCM would be detected using specific antibodies (such as His-tag, Trx tag or S tag) to ensure the hMCM analysed by immunofluorescence was recombinant hMCM rather than endogenous MCM2-7.

### 6.4.4 Effect of DDK on *in vitro* DNA replication initiation

Low concentrations of DDK inhibited hMCM loading but higher concentrations of DDK had little effect on loading (Fig. 5.6). This is an unusual result, which should be repeated to confirm. In *S. cerevisiae*, DDK is believed to be the activating kinase involved in transitioning loaded double MCM2-7 hexamers to single hexamers that are capable of unwinding DNA (reviewed in Labib, 2010, Araki, 2010). However, recent work suggests in *S. cerevisiae* and *Xenopus*, DDK phosphorylation is not responsible for double MCM2-7 hexamer separation (Gambus et al., 2011, On et al., 2014). It would be interesting to assess the functionality of loaded hMCM in the presence of DDK by incubating nuclei pre loaded with hMCM and DDK (as in Fig. 5.6) followed by incubation in S phase extract (as in Fig. 5.5). The work described above would allow us to analyse if DDK is the 'activating kinase' in a mammalian system.

## 6.5 MCM2 undergoes a structural change by the sequential action of cyclin A/CDK2 followed by DDK

I have recapitulated *in vitro* the mobility shift of MCM2 and MCM4 associated with S phase of the cell cycle using entirely recombinant proteins (Fig. 5.7). There have been discrepancies in the data that reports on the order of addition in which eukaryotic cells require kinases to initiate DNA synthesis (reviewed in Sclafani and Holzen, 2007, Labib, 2010). In an *S. cerevisiae* cell free assay, DDK has been

shown to be required before CDK for initiation (Heller et al., 2011). Conversely another study also analysing *S. cerevisiae,* demonstrated CDK is required before DDK (Nougarede et al., 2000). In *Xenopus* egg extracts, DDK has been shown to act before CDK (Jares and Blow, 2000, Walter, 2000). It is suggested that these inconsistencies are due to the experimental approaches used (Heller et al., 2011). In addition, differences could also be species specific. What theses studies do not do is distinguish between the kinase concentrations at each stage. For example it is not unreasonable to think that CDK acts before and after DDK, possibly at a different concentration. The results presented here, clearly show that naïve hMCM must be exposed to CDK activity before DDK activity to induce the form of MCM2 associated with S phase.

### 6.5.1 Effect of phosphorylation on hMCM hexamer

When the hMCM hexamer is resolved on native PAGE (Fig. 5.7B), different results are obtained when blotted for different subunits. Both MCM2 and MCM4 run at approximately 480 KDa as expected for the heterohexamer (predicted molecular weight = 567 KDa). Whereas MCM6 runs at approximately 700 KDa. These results could suggest a mixed population of hMCM sub-complexes within the preparation or could simply be artifacts associated with running hMCM on native PAGE. To further analyse this, hMCM could be cross-linked with DTSP before running on the gel (Baumert and Fasold, 1989) to ensure the complex stays together and the complexes analysed are representative of the original preparation.

Another possibility is that the MCM6 band observed is aggregated MCM6 subunit. MCM6 has been shown to form a homohexamer in *Pisum sativum* (Tran et al., 2010). To investigate if this band is in fact aggregated MCM6 or if other MCM proteins are present, this band could be isolated, analysed by SDS PAGE and blotted for the remaining MCM subunits.

### 6.5.2 Role of phosphorylated MCM2 in DNA replication

The mobility shifts observed for MCM2 and MCM4 are associated with S phase (Masai et al., 2006, Fujita et al., 1998), however the function of these complexes is

not understood. Mutant *S. cerevisiae* MCM2 expressed at endogenous levels, with either one (Ser170) or two (Ser164 and Ser170) unphosphorylatable sites, grow normally (Stead et al., 2011). In contrast to this, introduction of one unphosphorylatable site in *S. cerevisiae* MCM2 (Ser170) has been shown to inhibit cell growth (Bruck and Kaplan, 2009). Differences between these results are thought to be due to expression levels of mutant proteins within the *S. cerevisiae* cell. Phosphomimetic mutant MCM2-7 (Ser164 and Ser170) reduced helicase activity by 50% compared to WT MCM2-7 due to increased DNA binding capability of the phosphomimetic mutant MCM2-7 (Stead et al., 2011). However these sites are not conserved in human MCM2-7. Analysis of human MCM2-7 in HeLa cells demonstrates DDK phosphorylation is critical for ATP hydrolysis activity (Tsuji et al., 2006). However our naïve recombinant hMCM clearly demonstrates ATP hydrolysis activity in the absence of DDK phosphorylation. It would be interesting to analyse if recombinant hMCM in relation to the current contrasting results regarding MCM2-7 phosphorylation by DDK. The activity of *in vitro* phosphorylated hMCM could be tested using ATP hydrolysis, DNA binding, duplex unwinding and processivity assays. In addition, analysis of *in vitro* phosphorylated hMCM in activity assays (as in Fig. 5.5) could be used to understand if this form of hMCM is able to initiate DNA synthesis *in vitro*. Ultimately this analysis will allow us to understand if mobility shifted hMCM is active or inactive.

### 6.5.3 Analysis of phosphorylation sites on hMCM

To investigate the MCM2 sites that are phosphorylated by sequential addition of cyclin A/CDK2 and DDK, *in vitro* phosphorylated hexamer preparations could be evaluated using phospho-site specific antibodies (Montagnoli et al., 2006). Strongly implicated sites could be mutated to produce phosphorylation-deficient or phosphomimetic hMCM2 and expressed as recombinant hexamer. Purified proteins could be subjected to functional analysis using biochemical assays to evaluate the effect of mutation on unwinding of naked forked templates, using strand displacement assays. Phosphomimetic mutant hMCM complexes could also be analysed in cell free activity assays (as in Fig. 5.5), to understand if mutants are able to initiate DNA synthesis *in vitro*.

### 6.5.4 Is the mobility shift of MCM2 due to a conformational change?

The impact of phosphorylation on the mobility of MCM2 and the possibility for a conformational change, has not been investigated. EM data suggest that the MCM2-7 hexamer can adopt different conformations and assembly states during the transition from loading to activation (Costa et al., 2014). The phosphorylated MCM2-7 complex with the increased mobility form of MCM2 could represent a crucial conformational change involved in MCM2-7 function. One possibility is that this MCM2-7 complex is open at the 2/5 gate (Fig. 1.2, Costa et al., 2011, Lyubimov et al., 2012). Another possibility could involve a conformational change resulting in splitting the MCM2-7 double hexamer. Reconstituted pre-RC complexes contain double hexamers (Gambus et al., 2011, Evrin et al., 2009, Remus et al., 2009), which when treated with DDK, undergoes a small conformational change, that can be observed using EM. However, the double hexamer does not split (On et al., 2014), suggesting that DDK is not sufficient to split the MCM2-7 double hexamer and initiation of DNA replication. In this study, researchers did not use both CDK and DDK for phosphorylation and the extent of MCM2-7 phosphorylation is not clear leaving the question open.

*In vitro* phosphorylated hexamer preparations could be subjected to cryo-EM structural analysis to visualise induced alterations in hexamer structure and then compared to naïve hMCM structures. It is becoming clear that conformational changes to hMCM are key to understanding how it is loaded and activated (Costa et al., 2014, Costa et al., 2011) and so it would be interesting to investigate if the MCM2-7 species induced by CDK2 and DDK phosphorylation *in vitro*, is active in *in vitro* biochemical assays and how it behaves in cell free loading and replication assays.

## 6.6 How does MCM2-7 unwind DNA?

The open centre of the MCM2-7 hexamer is large enough to accommodate either single stranded DNA or double stranded DNA (Evrin et al., 2009, Remus et al., 2009). Recent studies suggest that when incorporated into the CMG complex, MCM2-7 encircles single stranded DNA (Fu et al., 2011, Costa et al., 2014). If reconciled with the idea that MCM proteins are located outside of replication

factories during DNA synthesis (Kuipers et al., 2011, Dimitrova et al., 1999, Krude et al., 1996, Madine et al., 1995), this implies that template DNA is in single stranded form between the site of DNA synthesis and the site of helicase action. This is similar to the 'rotary pump' mechanism (reviewed in Laskey and Madine, 2003). However, this mechanism for unwinding DNA would require long lengths of single stranded DNA between the MCM2-7 helicase and the site of DNA replication that may be vulnerable to breakages.

## 6.7 Conclusions

In summary, this thesis shows a transient interaction of MCM2-7 with the nuclear matrix (Chapter 4) and that naïve hMCM undergoes a conformational change when treated with S phase kinases (Chapter 5) that is not associated with the nuclear matrix. Previous research on MCM2-7 and the data presented here, suggests the following order of events. Naïve MCM2-7 is functionally loaded onto chromatin at origins of replication. MCM2-7 is recruited to the nuclear matrix where it is activated by S phase kinases, causing dissociation from the nuclear matrix but continued association with chromatin. This suggests that activated MCM2-7 'pumps' single stranded DNA towards replication factories located at the nuclear matrix where DNA is replicated (Fig. 6.1).

The aims of this thesis were to combine two branches of research, biochemical and cell based biology. I have successfully developed both areas and brought the two elements together in the cell free assays, a system that allows analysis of the functional assembly of the mammalian MCM2-7 complex. Due to the discrepancies observed between *S. cerevisiae* and mammalian systems there is a need to move research into mammalian systems so that the details can be used to design novel, specific inhibitors that may find application as cancer therapies. Production of naïve, recombinant hMCM will allow analysis of the specific molecular function of the human DNA replication mechanism. Ultimately these insights could be important for our ability to manipulate cell proliferation and therefore design useful and specific cancer treatments.

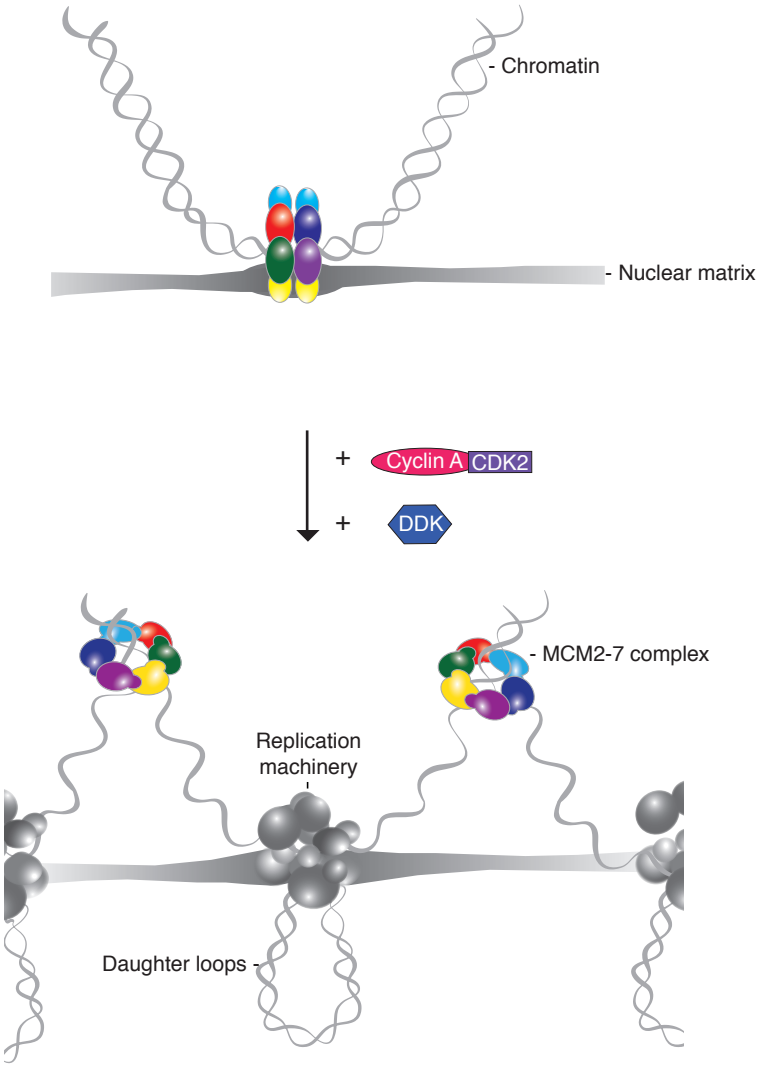


**Figure 6.1.** Model for MCM2-7 unwinding. Naïve MCM2-7 binds to chromatin as a double hexamer and is recruited to the nuclear matrix. Sequential phosphorylation of MCM2-7 by cyclin A/CDK2 followed by DDK causes a conformational change in MCM2-7. The double hexamer splits and dissociates from the nuclear matrix. The single MCM2-7 hexamer is now active and pumps single stranded DNA towards replication machinery. Additional proteins involved in MCM2-7 loading, such as the pre-IC and pre-LC are omitted for simplicity.

# Appendix A

The following work has been accepted for publication in Cold Spring Harbor Protocols. It provides an in detail introduction and protocol into the methods used in Chapter 4 to extract the nuclear matrix using DNase I.

Chapter

# The nuclear matrix: preparation for microscopy and biochemical analysis

Topic introduction

# The nuclear matrix: fractionation techniques and analysis

**Short title: Nuclear matrix fractionation**

Wilson, R. H. C.[1*] Hesketh, E.[1] and Coverley, D.[1]

[1] Department of Biology, University of York, Wentworth Way, York, YO10 5DD, UK

[*] Corresponding author: Wilson, R. H. C. rhcw500@york.ac.uk, 01904 328569

The first descriptions of an insoluble nuclear structure appeared more than 70 years ago, but it is only in recent years that a sophisticated picture of its significance has begun to emerge. In this article we explain multiple methods for the study of the nuclear matrix. These have led to the understanding that the nuclear matrix consists of core components that are consistently present, such as matrins, lamins, hnRNPs and other 'structural' proteins, and conditional proteins that are recruited into the nuclear matrix to facilitate specific processes (Mika and Rost 2005). These include components of the DNA replication machinery (reviewed in Wilson & Coverley 2013), transcription machinery (Jackson and Cook 1985), DNA repair (Qiao et al. 2001; Boisvert et al. 2005; Campalans et al. 2007), splicing (Zeitlin et al. 1987; Jagatheesan et al. 1999) and chromatin remodelling (Reyes et al. 1997) as well as a catalogue of proteins identified by proteomic analysis (Albrethsen et al. 2009). In most cases the functional significance of their immobilisation remains an area of study, nevertheless, a number of nuclear matrix proteins are already gaining credibility as clinically useful biomarkers (Keesee et al. 1999; Subong et al. 1999; Van Le et al. 2004; Higgins et al. 2012).

**A brief history**

Descriptions of a protein fraction that is resistant to extraction under high salt conditions were first made in 1942 (reviewed in Pederson 1998). However, the term 'nuclear matrix' was first used in 1974 to refer to those proteins resistant to extraction with 2.0 M NaCl (Berezney and Coffey 1974). 'Nuclear matrix' has become widely adopted as an overarching term for the proteins that resist aggressive methods of extraction, and we use it as such here. The 2.0 M NaCl method has been criticised because of its potential to cause aggregation of proteins. This led to the development of more refined extraction methods including lithium 3,5-diiodosalicylate (LIS), which was first used by Mirkovitch et al. (1984) to reveal a protein fraction termed the nuclear scaffold, and extraction after encapsulation in agarose under physiologically relevant salt concentrations (Jackson and Cook 1988) to reveal a substructure known as the nuclear skeleton (or nucleoskeleton). Further variations and refinement of these techniques have also been used (reviewed in Martelli et al. 2002). A modification of the original nuclear matrix method was developed by Capco et al (1982), which reduced the potential for aggregation by using more physiologically relevant buffers with lower salt (0.5 M NaCl) and used nucleases (DNase I or other enzymes) to digest chromatin into small diffusible fragments. This was termed the 'in situ nuclear matrix' as the cytoskeleton is also maintained under these conditions. Extraction with 2.0 M NaCl has subsequently been termed the 'core nuclear matrix'.

## A simple picture?

Despite the range of approaches used, some controversies have remained and reviews of the evidence for and against the nuclear matrix have come to conflicting conclusions (Pederson 1998; Hancock 2000; Nickerson 2001; Martelli et al. 2002). It has proved difficult to visualise the filamentous structure revealed by electron microscopy, using immunofluorescence-light microscopy, which typically reveal punctate foci for most of the 100s of nuclear matrix proteins that have been described. However it should be bourn in mind that the proteins which fractionate with the nuclear matrix and are identified by proteomic analysis may in fact make up highly dynamic 'local' matrices rather than one large static structure (Martelli et al. 2002).

One fundamental biological reason for the debate surrounding existence and nature of the nuclear matrix may in fact be that it exists in different forms in different cell types and may even be absent in some instances. We and others have shown that nuclear matrix composition varies dramatically with differentiation and disease status and that some proteins are actively recruited as part of normal cellular transitions (Getzenberg 1994; Zink et al. 2004; Munkley et al. 2011; Varma and Mishra 2011). Thus a lot of work previously undertaken on cancer cell lines, embryonic cells or Xenopus eggs must now be interpreted in this light to avoid clouding the picture in normal somatic cells (Munkley et al. 2011). There remains a need for a resurgence in nuclear matrix investigation that includes comparative analysis, the protocols that we use for this purpose accompany this topic introduction (The nuclear matrix: preparation protocol for parallel microscopy and biochemical analysis, Wilson et al. 2013).

## Approaches to functional analysis (for schematic see figure 1)

### *Electron microscopy*

The resolution of the electron microscope has allowed detailed visualisation of the fibrilar protein network within the nucleus of higher eukaryotic cells (Capco et al. 1982; Fey et al. 1986; Jackson and Cook 1988). It has been viewed after RNase digestion (Berezney and Coffey 1974), DNase digestion (Capco et al. 1982), removal of chromatin by electroelution (Jackson and Cook 1988) and in a range of buffer conditions designed to minimise artefacts (Mirkovitch et al. 1984; Jackson and Cook 1988; Nickerson et al. 1997; Engelhardt 1999; Wan et al. 1999). The nuclear matrix has also been viewed in paraformaldehyde fixed sections of unextracted nuclei, identifying protein rich inter chromosomal areas consistent with the description of a NM (Hendzel et al. 1999).

### *Proteomic analysis*

Studies to identify the component parts of the nuclear matrix were compiled in a database of Nuclear Matrix Proteins, NMPdb (Mika and Rost 2005). Since then, large-scale proteomic screens have been undertaken which compare nuclear matrix components enriched in tumour cells and at different developmental stages (Albrethsen et al. 2009; Albrethsen et al. 2010; Varma & Mishra 2011 and references therein for methods).

### *Analysis of attached DNA*

The proteinaceous structure isolated by nuclear matrix extraction protocols is associated with residual DNA as well as RNA. Attachment of DNA was first observed by electron microscopy in the 1970s (Paulson and Laemmli 1977). Various methods have since been used to study the attached DNA, including digestion of chromatin loops with restriction enzymes, DNase I or topoisomerase II to

reveal the attachment points (Mirkovitch et al. 1984; Djeliova et al. 2001; Linnemann et al. 2009; Rivera-Mulia et al. 2011), followed by isolation and sequencing, labelling by FISH, or by incorporation of nucleotide analogues. DNA that remains attached after extraction with high salt are termed MARs (matrix attached region), and those remaining following extraction for the scaffold or skeleton are known respectively, as SARs (scaffold attached region), or skeleton-attached sequences. The possible functional significance of these classes of attachment has been reviewed previously (Wilson & Coverley 2013).

Related protocols (Maximum Fluorescence Halo Radius) that extract histones and loosely attached proteins, but which leave chromatin undigested have been used to study the DNA loops that emanate from the attachment points on the nuclear matrix (Vogelstein et al. 1980; Gerdes et al. 1994; Lemaitre et al. 2005; Guillou et al. 2010). A method combining nuclear matrix extraction with chromosome conformation capture (3C) has also recently been developed, termed M3C (Gavrilov et al. 2010).

***Analysis by CSK protocol***

The following method describes the protocol that we prefer to use for the analysis of nuclear matrix related functions. This incorporates serial extraction with non-ionic detergent (Triton–X-100) to remove membranes and soluble proteins under physiologically relevant salt concentrations, followed by 0.5 M NaCl, then DNase I digestion and removal of fragmented DNA. Complimentary analysis by immunoblotting and immunofluorescence reveals information on isoforms and on spatial organisation. The protocol uses cytoskeletal (CSK) buffer to stabilise the cytoskeleton and nuclear matrix in relatively gentle conditions. CSK was first used by Lenk et al. (1977) and later by Capco et al. (1982) for electron microscopy. Others have used it for immuno-detection of individual nuclear matrix components (Nickerson et al. 1992; Grondin et al. 1996; Huang et al. 2004; Boisvert et al. 2005; Ainscough et al. 2007; Campalans et al. 2007), identification of protein domains required for nuclear matrix binding (Ainscough et al. 2007), analysis of temporally regulated recruitment (Fujita 1999; Fujita et al. 2002; Miccoli et al. 2003; Samaniego et al. 2006; Sree et al. 2012), and to compare recruitment between developmental or differentiation stages and between disease states (Munkley et al. 2011). The benefits of this method include the relatively gentle buffer conditions, potential to generate robust results by using imaging and biochemical analysis in parallel, and its flexibility to incorporate high salt to reveal the core nuclear matrix, or pre-treatment with a protein-protein crosslinker to reveal those proteins only weakly associated with the nuclear matrix. It can also be combined with other cellular manipulations for specific questions, such as cell synchrony protocols, depletion by RNAi and expression of ectopic proteins. Together, these offer the potential to uncover the functional relevance of recruitment to the nuclear matrix.

**Acknowledgements:**

Work in this laboratory is supported by the Biotechnology and Biological Sciences Research Council, UK and Yorkshire Cancer Research, UK.

**References:**

Ainscough JF, Rahman FA, Sercombe H, Sedo A, Gerlach B, Coverley D. 2007. C-terminal domains deliver the DNA replication factor Ciz1 to the nuclear matrix. *J Cell Sci* **120**: 115-124.

Albrethsen J, Knol JC, Jimenez CR. 2009. Unravelling the nuclear matrix proteome. *J Proteomics* **72**: 71-81.

Albrethsen J, Knol JC, Piersma SR, Pham TV, de Wit M, Mongera S, Carvalho B, Verheul HM, Fijneman RJ, Meijer GA et al. 2010. Subnuclear proteomics in colorectal cancer: identification of

proteins enriched in the nuclear matrix fraction and regulation in adenoma to carcinoma progression. *Mol Cell Proteomics* **9**: 988-1005.

Berezney R, Coffey DS. 1974. Identification of a nuclear protein matrix. *Biochem Biophys Res Commun* **60**: 1410-1417.

Boisvert FM, Hendzel MJ, Masson JY, Richard S. 2005. Methylation of MRE11 regulates its nuclear compartmentalization. *Cell Cycle* **4**: 981-989.

Campalans A, Amouroux R, Bravard A, Epe B, Radicella JP. 2007. UVA irradiation induces relocalisation of the DNA repair protein hOGG1 to nuclear speckles. *Journal of Cell Science* **120**: 23-32.

Capco DG, Wan KM, Penman S. 1982. The nuclear matrix: three-dimensional architecture and protein composition. *Cell* **29**: 847-858.

Djeliova V, Russev G, Anachkova B. 2001. Distribution of DNA replication origins between matrix-attached and loop DNA in mammalian cells. *J Cell Biochem* **80**: 353-359.

Engelhardt M. 1999. Demonstration of a DNase-sensitive network associated with the nuclear pore complexes in rat liver nuclei. *Chromosoma* **108**: 64-71.

Fey EG, Krochmalnic G, Penman S. 1986. The nonchromatin substructures of the nucleus: the ribonucleoprotein (RNP)-containing and RNP-depleted matrices analyzed by sequential fractionation and resinless section electron microscopy. *J Cell Biol* **102**: 1654-1665.

Fujita M. 1999. Cell cycle regulation of DNA replication initiation proteins in mammalian cells. *Front Biosci* **4**: D816-823.

Fujita M, Ishimi Y, Nakamura H, Kiyono T, Tsurumi T. 2002. Nuclear organization of DNA replication initiation proteins in mammalian cells. *J Biol Chem* **277**: 10354-10361.

Fujita M, Kiyono T, Hayashi Y, Ishibashi M. 1997. In vivo interaction of human MCM heterohexameric complexes with chromatin. Possible involvement of ATP. *J Biol Chem* **272**: 10928-10935.

Gavrilov AA, Zukher IS, Philonenko ES, Razin SV, Iarovaia OV. 2010. Mapping of the nuclear matrix-bound chromatin hubs by a new M3C experimental procedure. *Nucleic Acids Res* **38**: 8051-8060.

Gerdes MG, Carter KC, Moen PT, Jr., Lawrence JB. 1994. Dynamic changes in the higher-level chromatin organization of specific sequences revealed by in situ hybridization to nuclear halos. *J Cell Biol* **126**: 289-304.

Getzenberg RH. 1994. Nuclear matrix and the regulation of gene expression: tissue specificity. *J Cell Biochem* **55**: 22-31.

Grondin B, Bazinet M, Aubry M. 1996. The KRAB zinc finger gene ZNF74 encodes an RNA-binding protein tightly associated with the nuclear matrix. *Journal of Biological Chemistry* **271**: 15458-15467.

Guillou E, Ibarra A, Coulon V, Casado-Vela J, Rico D, Casal I, Schwob E, Losada A, Mendez J. 2010. Cohesin organizes chromatin loops at DNA replication factories. *Genes Dev* **24**: 2812-2822.

Hancock R. 2000. A new look at the nuclear matrix. *Chromosoma* **109**: 219-225.

Hendzel MJ, Boisvert F, Bazett-Jones DP. 1999. Direct visualization of a protein nuclear architecture. *Mol Biol Cell* **10**: 2051-2062.

Higgins G, Roper KM, Watson IJ, Blackhall FH, Rom WN, Pass HI, Ainscough JF, Coverley D. 2012. Variant Ciz1 is a circulating biomarker for early-stage lung cancer. *Proc Natl Acad Sci U S A*.

Huang JY, Shen BJ, Tsai WH, Lee SC. 2004. Functional interaction between nuclear matrix-associated HBXAP and NF-kappa B. *Experimental cell research* **298**: 133-143.

Jackson DA, Cook PR. 1985. Transcription occurs at a nucleoskeleton. *Embo J* **4**: 919-925.

-. 1988. Visualization of a filamentous nucleoskeleton with a 23 nm axial repeat. *Embo J* **7**: 3667-3677.

Jagatheesan G, Thanumalayan S, Muralikrishna B, Rangaraj N, Karande AA, Parnaik VK. 1999. Colocalization of intranuclear lamin foci with RNA splicing factors. *Journal of Cell Science* **112**: 4651-4661.

Keesee SK, Meyer JL, Hutchinson ML, Cibas ES, Sheets EE, Marchese J, Oreper A, Potz D, Wu YJ. 1999. Preclinical feasibility study of NMP179, a nuclear matrix protein marker for cervical dysplasia. *Acta Cytol* **43**: 1015-1022.

Lemaitre JM, Danis E, Pasero P, Vassetzky Y, Mechali M. 2005. Mitotic remodeling of the replicon and chromosome structure. *Cell* **123**: 787-801.

Lenk R, Ransom L, Kaufmann Y, Penman S. 1977. A cytoskeletal structure with associated polyribosomes obtained from HeLa cells. *Cell* **10**: 67-78.

Linnemann AK, Platts AE, Krawetz SA. 2009. Differential nuclear scaffold/matrix attachment marks expressed genes. *Hum Mol Genet* **18**: 645-654.

Martelli AM, Falcieri E, Zweyer M, Bortul R, Tabellini G, Cappellini A, Cocco L, Manzoli L. 2002. The controversial nuclear matrix: a balanced point of view. *Histol Histopathol* **17**: 1193-1205.

Miccoli L, Biard DSF, Frouin I, Harper F, Maga G, Angulo JF. 2003. Selective interactions of human kin17 and RPA proteins with chromatin and the nuclear matrix in a DNA damage- and cell cycle-regulated manner. *Nucleic Acids Research* **31**: 4162-4175.

Mika S, Rost B. 2005. NMPdb: Database of Nuclear Matrix Proteins. *Nucleic Acids Res* **33**: D160-163.

Mirkovitch J, Mirault ME, Laemmli UK. 1984. Organization of the higher-order chromatin loop: specific DNA attachment sites on nuclear scaffold. *Cell* **39**: 223-232.

Munkley J, Copeland NA, Moignard V, Knight JR, Greaves E, Ramsbottom SA, Pownall ME, Southgate J, Ainscough JF, Coverley D. 2011. Cyclin E is recruited to the nuclear matrix during differentiation, but is not recruited in cancer cells. *Nucleic Acids Res* **39**: 2671-2677.

Nickerson J. 2001. Experimental observations of a nuclear matrix. *J Cell Sci* **114**: 463-474.

Nickerson JA, Krockmalnic G, Wan KM, Penman S. 1997. The nuclear matrix revealed by eluting chromatin from a cross-linked nucleus. *Proceedings of the National Academy of Sciences of the United States of America* **94**: 4446-4450.

Nickerson JA, Krockmalnic G, Wan KM, Turner CD, Penman S. 1992. A normally masked nuclear matrix antigen that appears at mitosis on cytoskeleton filaments adjoining chromosomes, centrioles, and midbodies. *J Cell Biol* **116**: 977-987.

Paulson JR, Laemmli UK. 1977. The structure of histone-depleted metaphase chromosomes. *Cell* **12**: 817-828.

Pederson T. 1998. Thinking about a nuclear matrix. *J Mol Biol* **277**: 147-159.

Qiao F, Moss A, Kupfer GM. 2001. Fanconi anemia proteins localize to chromatin and the nuclear matrix in a DNA damage- and cell cycle-regulated manner. *J Biol Chem* **276**: 23391-23396.

Reyes JC, Muchardt C, Yaniv M. 1997. Components of the human SWI/SNF complex are enriched in active chromatin and are associated with the nuclear matrix. *J Cell Biol* **137**: 263-274.

Rivera-Mulia JC, Hernandez-Munoz R, Martinez F, Aranda-Anzaldo A. 2011. DNA moves sequentially towards the nuclear matrix during DNA replication in vivo. *BMC Cell Biol* **12**: 3.

Samaniego R, Jeong SY, de la Torre C, Meier I, de la Espina SMD. 2006. CK2 phosphorylation weakens 90 kDa MFP1 association to the nuclear matrix in Allium cepa. *Journal of Experimental Botany* **57**: 113-124.

Sree NK, Anesh R, Radha V. 2012. Dynamic changes in nuclear localization of a DNA-binding protein tyrosine phosphatase TCPTP in response to DNA damage and replication arrest. *Cell Biology and Toxicology* **28**: 409-419.

Subong EN, Shue MJ, Epstein JI, Briggman JV, Chan PK, Partin AW. 1999. Monoclonal antibody to prostate cancer nuclear matrix protein (PRO:4-216) recognizes nucleophosmin/B23. *Prostate* **39**: 298-304.

Van Le TS, Myers J, Konety BR, Barder T, Getzenberg RH. 2004. Functional characterization of the bladder cancer marker, BLCA-4. *Clin Cancer Res* **10**: 1384-1391.

Varma P, Mishra RK. 2011. Dynamics of nuclear matrix proteome during embryonic development in Drosophila melanogaster. *J Biosci* **36**: 439-459.

Vogelstein B, Pardoll DM, Coffey DS. 1980. Supercoiled loops and eucaryotic DNA replicaton. *Cell* **22**: 79-85.

Wan KM, Nickerson JA, Krockmalnic G, Penman S. 1999. The nuclear matrix prepared by amine modification. *Proc Natl Acad Sci U S A* **96**: 933-938.

Wilson RH, Coverley D. 2013. Relationship between DNA replication and the nuclear matrix. *Genes Cells* **18**: 17-31.

Zeitlin S, Parent A, Silverstein S, Efstratiadis A. 1987. Pre-mRNA splicing and the nuclear matrix. *Mol Cell Biol* **7**: 111-120.

Zink D, Fischer AH, Nickerson JA. 2004. Nuclear structure in cancer cells. *Nature reviews* **4**: 677-687.

**Figure legends:**

**Figure 1.** Schematic to show available methods for analysis of the nuclear matrix and its functional significance.

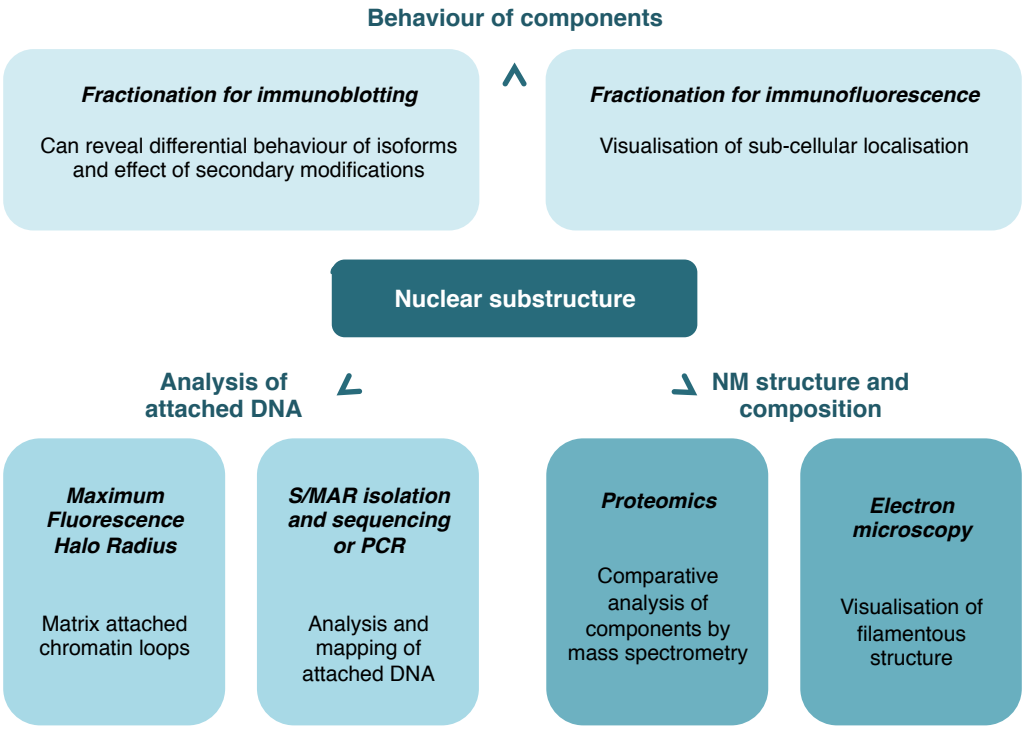
Behaviour of components
Fractionation for immunoblotting
Can reveal differential behaviour of isoforms and effect of secondary modifications
Fractionation for immunofluorescence
Visualisation of sub-cellular localisation
Nuclear substructure
Analysis of attached DNA
NM structure and composition
Maximum Fluorescence Halo Radius
Matrix attached chromatin loops
S/MAR isolation and sequencing or PCR
Analysis and mapping of attached DNA
Proteomics
Comparative analysis of components by mass spectrometry
Electron microscopy
Visualisation of filamentous structure

Protocol

# The nuclear matrix: preparation protocol for parallel microscopy and biochemical analysis

**Short title: Nuclear matrix protocol**

Wilson, R. H. C.[1*], Hesketh, E.[1] and Coverley, D.[1]

[1] Department of Biology, University of York, Wentworth Way, York, YO10 5DD, UK

[*] Corresponding author: Wilson, R. H. C. rhcw500@york.ac.uk, 01904 328569

**Abstract**

The immobilisation of nuclear proteins is usually investigated using extraction with detergent to reveal attachment to insoluble structures. This is often assumed to be chromatin and is described as such in many studies. However, the detergent resistant protein fraction consists of both chromatin-bound and nuclear matrix-bound proteins. To further separate these fractions DNA should be removed and the remaining proteins visualised in comparison to those in unextracted cells. We describe two related protocols that identify nuclear matrix proteins by immunofluorescence (IF) or immuoblotting (IB). IB has the advantage of resolving different forms of a protein of interest and includes analysis of soluble fractions excluded by the IF protocol. IF analysis has the advantage of allowing individual cells to be monitored rather than homogenised populations and can be performed on very low quantity samples. Analysis by IF will also reveal the spatial arrangement of proteins bound to residual nuclear structures. These methods have been used by many labs to study nuclear matrix proteins (Nickerson et al. 1992; Blencowe et al. 1994; Fujita et al. 1997) and by our laboratory to determine protein domains required for nuclear matrix binding (Ainscough et al. 2007), shifts in protein localisation during biological transitions (Munkley et al. 2011), and absence from the nuclear matrix fraction in diseased states (Munkley et al. 2011).

**Reagents**

Cells grown on coverslips or cytospun onto slides (IF), or one 15 cm plate of adherent cells at > 50% confluent density (IB)

*For transfected cells, first evaluate the transfection protocol for destabilizing effects on the nuclear matrix.*

Cytoskeletal buffer (CSK) and derivatives. Filter sterilise and store basic buffer in 50 ml aliquots at -20°C <R>

DNase I, and buffer recommended by supplier

*Determine optimal concentration, digestion time and temperature using release of DNA (IF) or chromatin bound proteins such as histone (IB) as indicator. This will vary with cell type, is unlikely to be 100% efficient and will not release MAR DNA. DNase must be RNase free (eg Roche, 04716728001). Test by incubation with prepared RNA and visualisation of products after electrophoresis.*

Hoechst or DAPI DNA counterstain (IF)

*Use at 0.1 µg/ml and keep constant to allow establishment of imaging conditions.*

Mounting medium (IF)

Paraformaldehyde (PFA) 4% <R> (IF)

Phosphate buffered saline (PBS)

PMSF – 200 mM stock in ethanol, stored at -20°C (IB)

Primary antibody to protein of interest and secondary antibody for detection.

*Concentration and conditions should be established using cells extracted with detergent. These represent a mid-point between unextracted and chromatin-depleted cells with which imaging parameters can be determined.*

SDS loading buffer (4x) – standard Laemmli recipe (IB)

Sodium chloride – 5 M stock

Triton X-100 – at 1%

**Equipment**

13 mm glass coverslips (IF)

15 cm culture plates (IB)

24 well culture plates (IF)

Cell scraper (IB)

Fine forceps and hooked needle for moving coverslips (IF)

Fluorescent microscope with 63 x oil immersion objective and image capture system (IF)

Gel electrophoresis and Western blotting equipment (IB)

Glass slides (IF)

Heat block at 95°C (IB)

Humidified chamber such as a plastic box with sealable lid (IF)

Incubator at 37°C

Parafilm (IF)

Refridgerated microcentrifuge (IB)

Vortex (IB)

**Method**

1. Thaw CSK, add supplements as required. See table 1 for volumes <R>. Keep all buffers on ice. DNase I should be kept at -20°C until required.

**A. Immunofluorescence**

2A. Transfer cells on coverslips to PBS in 24 well plates (3-4 per sample).

*Coverslips are processed throughout with cells uppermost. Coverslips can be moved between wells to change buffer, or buffers can be gently changed by pipette.*

*Coverslips are processed to reveal i) total protein (no extraction), ii) detergent-resistant proteins (immobilised by attachment to insoluble structures), iii) high-salt and DNase resistant proteins (bound to the nuclear matrix), iv) optional high-salt resistant proteins (tightly bound to chromatin or the nuclear matrix). For a summary of the method see figure 1A.*

3A. Transfer coverslip i into 4% PFA (10 minutes, RT). Move to PBS and store at 4°C.

4A. Move remaining coverslips to CSKb (1 minute, RT). Move ii to PBS and prepare for IF as 3A.

5A. Move remaining coverslips to CSKc (1 minute, RT).

6A. Wash coverslips twice in DNase buffer (1 minute, RT).

*Wash step reduces salt concentration in preparation for DNase treatment.*

7A. Place coverslips on parafilm in humidified chamber. For iii add DNase I in DNase buffer, or for iv buffer only (20 µl per coverslip). Seal and incubate using optimised time and temperature.

*Humidify chamber to prevent drying out by including a reservoir of sterile water (e.g. damp tissue).*

8A. Move coverslips to CSKc (1 minute, RT), then PBS and prepare for IF as 3A.

9A. Coverslips should be processed as soon as possible using standard immunofluorescence protocols, and imaged using high-resolution fluorescence microscopy and appropriate image capture system.

*Blocking agents such as BSA should be of ELISA grade and protease and RNase free (eg. Jackson 001-000-162). The contrast between treated and untreated samples should be verified by imaging, using the minimum effective concentration of DNA counterstain and constant image capture parameters (e.g. 10-20 ms). A dramatic reduction in DNA counterstain should be evident for DNase treated coverslips, though a small amount of DNA will remain. Immunostaining conditions and imaging should be kept constant across a sample set (e.g. 200-400 ms). DNase treated nuclei from which the protein of interest is also extracted can be hard to spot. In these cases use an RNA counterstain such as propidium iodide or co-stain for a nuclear structure protein, such as lamin B2. An example image is shown in figure 1B.*

**B. Immunoblotting**

2B. Rinse plate with PBS, then twice with CSKa. Remove and drain plates for 2 mins at 45° on ice. Remove excess buffer then scrape harvest cells (recover ~200 µl per 15 cm plate). Measure the volume, add 2 mM PMSF and TX100 to 0.1% final concentration. Divide equally between four 500 µl eppendorfs (i, ii, iii, iv) and record volume (1 x vol).

*Samples will be processed to reveal cell equivalents of 'T' total protein, 'det P' detergent-resistant pellet (proteins immobilised by attachment to insoluble structures), 'det SN' detergent-soluble supernatant, 'w' 0.5 M NaCl-soluble supernatant, 'DNase P' DNase-resistant pellet (bound to the*

*nuclear matrix), 'DNase SN' DNase-sensitive supernatant (bound to chromatin), 'mock P', high-salt resistant pellet (tightly bound to chromatin or the nuclear matrix) and 'mock SN' (released during control incubation). For a summary of the method see figure 1A.*

3B. To i (T), add 1/3 volume of 4 x SDS loading buffer. Vortex, heat to 95°C for 5 minutes and store at -20°C.

4B. After 2 minutes on ice, centrifuge ii, iii and iv at 6800g (2 minutes, 4 °C). Transfer supernatant from ii to a fresh tube (det SN) and resuspend pellet ii in 1 x vol CSKb (det P). Prepare both for SDS-PAGE as 3B.

5B. Discard supernatant from iii and iv. Resuspend pellets in 1 x vol CSKc (2 minutes on ice) and centrifuge at 6800g (3 minutes, 4 °C). Recover supernatant from iii to a fresh tube (w). Prepare for SDS-PAGE as 3B. Discard supernatant from iv.

6B. Resuspend pellets iii and iv in ~ 100 µl DNase buffer. Centrifuge 9500g, (3 minutes, 4 °C). Discard supernatants.

7B. Resuspend pellets iii and iv in 1 x vol DNase buffer, add DNase I to iii and incubate both tubes using optimised amount, time and temperature.

8B. Add 1/10 volume 5 M NaCl to both tubes and incubate for 5 minutes. Centrifuge 9500g (5 minutes, 4 °C), transfer supernatants from tubes iii and iv to fresh tubes (DNase SN and mock SN). Resuspend pellets in 1 x vol DNase buffer (DNase P and mock P). Prepare these samples for SDS-PAGE as 3B.

*Pellets iii and iv are very 'sticky' and can get stuck in the pipette tip. Resuspend by vortexing.*

9B. Samples can be processed using standard SDS-PAGE and western blotting protocols.

*In addition to the protein of interest, blots should be probed with a control antibody against a chromatin bound protein that is released when chromatin is digested (eg. histone H3). If studying a protein that is not normally nuclear matrix-bound a second control antibody should be used that detects an insoluble component of the nucleus (eg. lamin B2). A successful DNase extraction would be expected to release >75% of histone H3 into the DNase supernatant fraction, while retaining all histone H3 in the pellet fraction of the mock treated sample. Loss of histone from this fraction indicates contamination of buffers, or loss or degradation of residual nuclei. An example image is shown in figure 1C.*

**Troubleshooting**

**Problem:** DNA or protein is not released from DNase treated sample

**Solution:** Optimise DNase conditions and take care to remove high-salt buffer prior to digestion. For IB, mix digestion reaction periodically during incubation to ensure resuspension of pellet, and take care to mix after NaCl addition (step 8B).

**Problem:** Absence of expected antigen in DNase treated samples.

**Solution:** Buffers may be contaminated with proteases or RNases, both of which will degrade (part of) the nuclear matrix. Buffers should be remade, possibly with RNase inhibitors and equipment cleaned. Check for presence of a protein known to be nuclear matrix bound such as lamin B2.

**Related Information**

The nuclear matrix can also be revealed by the use of 2.0 M NaCl – the 'core' nuclear matrix. The protocol can be adapted to use high-salt treatments instead of DNase extraction. Keeping all the cell lysate in a single tube, follow Immunoblot protocol to step 2B, then proceed by resuspending pellet in CSKb supplemented with increasing NaCl. Repeat with 100mM stepwise increases in NaCl up to 1M, collecting each supernatant and the final pellet as separate samples (Ainscough et al. 2007).

Alternatively, the protocol can be adapted to reveal proteins associated with the nuclear matrix but less tightly bound. In this case a protein-protein cross-linker such as DTSP can be used before extraction to preserve protein complexes. For method see (Fujita et al. 1999).

For further information regarding alternative methods for extracting the nuclear matrix, see The nuclear matrix: fractionation techniques and analysis (Wilson et al. 2013).

**Recipes:**

| <R> | | Components | Recipe (per 50ml) | *Vol per 3 sets of 4 coverslips* (IF) | *Vol per 3 15cm plates* (IB) |
|---|---|---|---|---|---|
| Cyto-skeletal buffer (CSK) | a | 10mM PIPES/KOH pH 6.8<br>100mM NaCl<br>300mM Sucrose<br>1mM EGTA<br>1mM $MgCl_2$<br><br>Immediately before use add:-<br>1mM DTT<br>Protease inhibitor cocktail (eg Roche, 05 056 489 001) | 0.5ml of 1M<br>1ml of 5M<br>5.135g<br>0.2ml of 250mM<br>50µl of 1M<br><br><br><br>50ul of 1M<br>1 tablet | 50ml | 100ml |
| CSK 0.1% TX100 | b | Add<br>0.1% Triton X-100 | 0.5ml of 10% TX100 | 5ml | 1ml |
| CSK 0.1% TX100 high-salt | c | Add<br>0.1% Triton X-100<br>0.5M NaCl | 0.5ml of 10% TX100<br>4ml of 5M | 2ml | 1ml |
| PFA | | 4% paraformaldehyde<br>50mM HEPES/KOH 7.8 | 2g<br>2.5ml of 1M stock | 6ml | - |

**Acknowledgements**

Work in this laboratory is supported by the Biotechnology and Biological Sciences Research Council, UK and Yorkshire Cancer Research, UK.

**References:**

Ainscough JF, Rahman FA, Sercombe H, Sedo A, Gerlach B, Coverley D. 2007. C-terminal domains deliver the DNA replication factor Ciz1 to the nuclear matrix. *J Cell Sci* **120**: 115-124.

Albrethsen J, Knol JC, Jimenez CR. 2009. Unravelling the nuclear matrix proteome. *J Proteomics* **72**: 71-81.

Albrethsen J, Knol JC, Piersma SR, Pham TV, de Wit M, Mongera S, Carvalho B, Verheul HM, Fijneman RJ, Meijer GA et al. 2010. Subnuclear proteomics in colorectal cancer: identification of proteins enriched in the nuclear matrix fraction and regulation in adenoma to carcinoma progression. *Mol Cell Proteomics* **9**: 988-1005.

Berezney R, Coffey DS. 1974. Identification of a nuclear protein matrix. *Biochem Biophys Res Commun* **60**: 1410-1417.

Blencowe BJ, Nickerson JA, Issner R, Penman S, Sharp PA. 1994. Association of nuclear matrix antigens with exon-containing splicing complexes. *J Cell Biol* **127**: 593-607.

Boisvert FM, Hendzel MJ, Masson JY, Richard S. 2005. Methylation of MRE11 regulates its nuclear compartmentalization. *Cell Cycle* **4**: 981-989.

Campalans A, Amouroux R, Bravard A, Epe B, Radicella JP. 2007. UVA irradiation induces relocalisation of the DNA repair protein hOGG1 to nuclear speckles. *Journal of Cell Science* **120**: 23-32.

Capco DG, Wan KM, Penman S. 1982. The nuclear matrix: three-dimensional architecture and protein composition. *Cell* **29**: 847-858.

Coverley D, Marr J, Ainscough J. 2005. Ciz1 promotes mammalian DNA replication. *J Cell Sci* **118**: 101-112.

Djeliova V, Russev G, Anachkova B. 2001. Distribution of DNA replication origins between matrix-attached and loop DNA in mammalian cells. *J Cell Biochem* **80**: 353-359.

Engelhardt M. 1999. Demonstration of a DNase-sensitive network associated with the nuclear pore complexes in rat liver nuclei. *Chromosoma* **108**: 64-71.

Fey EG, Krochmalnic G, Penman S. 1986. The nonchromatin substructures of the nucleus: the ribonucleoprotein (RNP)-containing and RNP-depleted matrices analyzed by sequential fractionation and resinless section electron microscopy. *J Cell Biol* **102**: 1654-1665.

Fujita M. 1999. Cell cycle regulation of DNA replication initiation proteins in mammalian cells. *Front Biosci* **4**: D816-823.

Fujita M, Ishimi Y, Nakamura H, Kiyono T, Tsurumi T. 2002. Nuclear organization of DNA replication initiation proteins in mammalian cells. *J Biol Chem* **277**: 10354-10361.

Fujita M, Kiyono T, Hayashi Y, Ishibashi M. 1997. In vivo interaction of human MCM heterohexameric complexes with chromatin. Possible involvement of ATP. *J Biol Chem* **272**: 10928-10935.

Fujita M, Yamada C, Goto H, Yokoyama N, Kuzushima K, Inagaki M, Tsurumi T. 1999. Cell cycle regulation of human CDC6 protein. Intracellular localization, interaction with the human mcm complex, and CDC2 kinase-mediated hyperphosphorylation. *J Biol Chem* **274**: 25927-25932.

Gavrilov AA, Zukher IS, Philonenko ES, Razin SV, Iarovaia OV. 2010. Mapping of the nuclear matrix-bound chromatin hubs by a new M3C experimental procedure. *Nucleic Acids Res* **38**: 8051-8060.

Gerdes MG, Carter KC, Moen PT, Jr., Lawrence JB. 1994. Dynamic changes in the higher-level chromatin organization of specific sequences revealed by in situ hybridization to nuclear halos. *J Cell Biol* **126**: 289-304.

Getzenberg RH. 1994. Nuclear matrix and the regulation of gene expression: tissue specificity. *J Cell Biochem* **55**: 22-31.

Grondin B, Bazinet M, Aubry M. 1996. The KRAB zinc finger gene ZNF74 encodes an RNA-binding protein tightly associated with the nuclear matrix. *Journal of Biological Chemistry* **271**: 15458-15467.

Guillou E, Ibarra A, Coulon V, Casado-Vela J, Rico D, Casal I, Schwob E, Losada A, Mendez J. 2010. Cohesin organizes chromatin loops at DNA replication factories. *Genes Dev* **24**: 2812-2822.

Hancock R. 2000. A new look at the nuclear matrix. *Chromosoma* **109**: 219-225.

Hendzel MJ, Boisvert F, Bazett-Jones DP. 1999. Direct visualization of a protein nuclear architecture. *Mol Biol Cell* **10**: 2051-2062.

# Appendix B

Schematics of forked substrates used in Chapter 3.

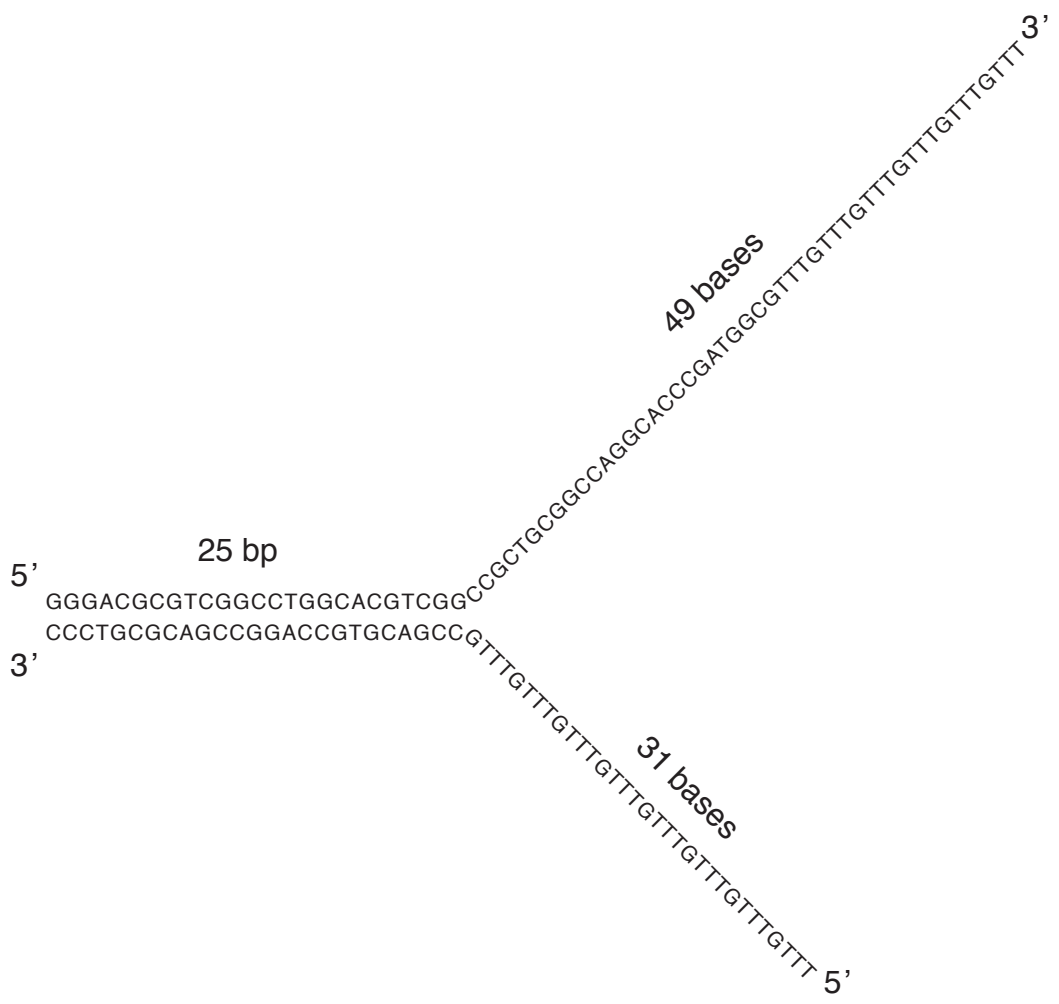


**Figure B1.** Forked DNA substrate used for ATP hydrolysis and helicase reactions (HS1 and HS2, Table 2.4).

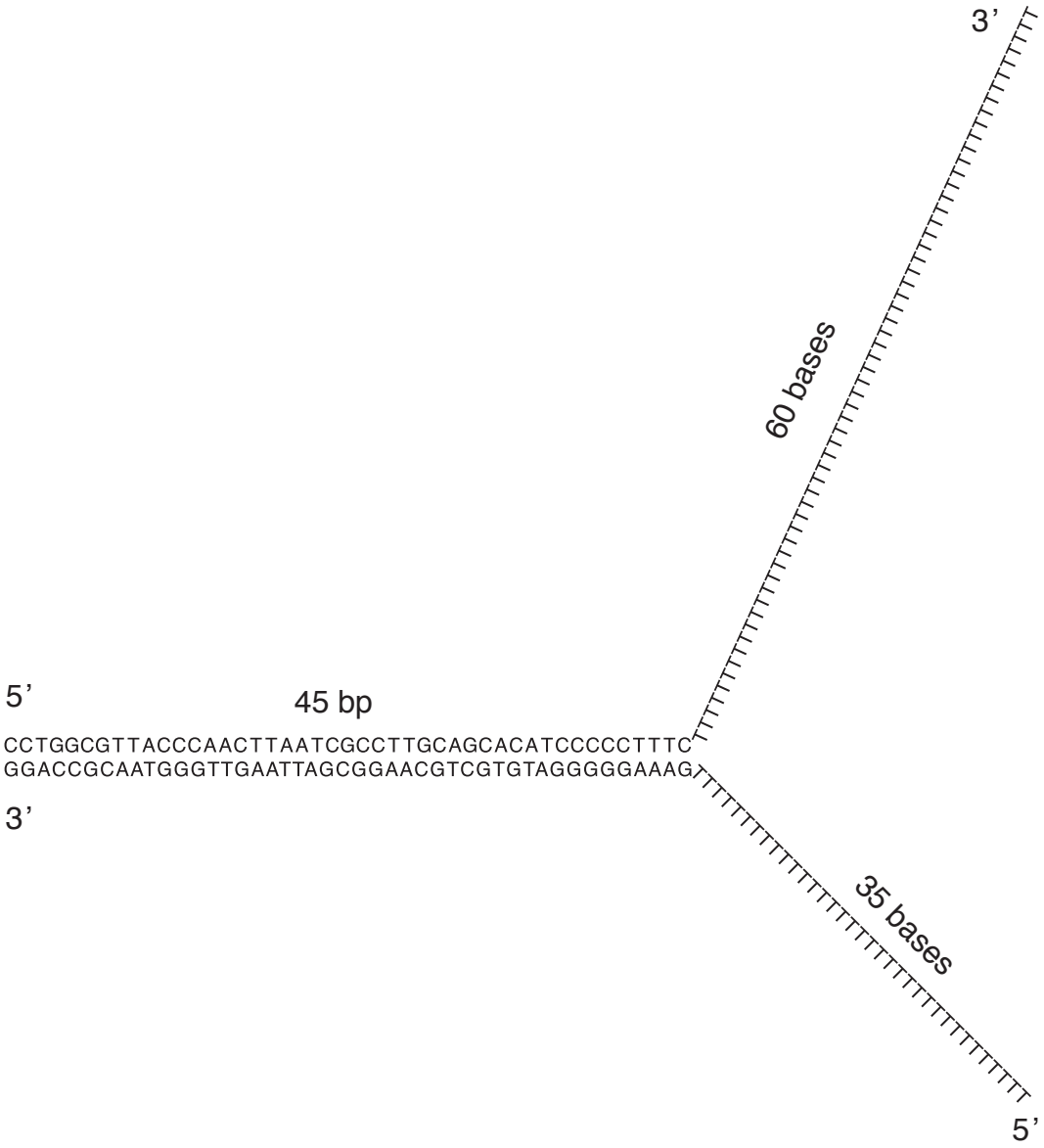


**Figure B2.** Forked DNA substrate bound to hMCM in EM reconstructions (HF150 and HR80, Table 2.4).

# Appendix C

The following work has been submitted for publication in The Journal of Biological Chemistry. It contains much of the work presented here in Chapter 3 and has additional information provided by other lab members.

# DNA induces conformational changes in a recombinant human minichromosome maintenance complex

Emma L. Hesketh[1]*, Richard P. Parker-Manuel[1, 2]*, Yuriy Chaban[3, 4], Rabab Satti[1, 5], Dawn Coverley[1], Elena V. Orlova[3], James P.J. Chong[1]

[1] Department of Biology, University of York, York YO10 5DD, UK
[2] Current address: Institute of Parasitology, Justus-Liebig-University Giessen, Schubertstrasse 81, Giessen, 35392, Germany
[3] Department of Crystallography, Birkbeck College London, London WC1E 7HX, UK
[4] Current address: The Institute of Cancer Research, 123 Brompton Road, London, SW7 3RP, UK
[5] Current address: Department of Biochemistry, Faculty of Biological Sciences, Quaid-i-Azam University, Islamabad, Pakistan
* These authors contributed equally to this work

Running title: Conformational change in recombinant hMCM

To whom correspondence should be addressed: James P.J. Chong, Department of Biology, University of York, York YO10 5DD, UK, Tel.: (44) 1904 328628; Fax: (44) 1904 328505; E-mail: james.chong@york.ac.uk

Keywords: ATP hydrolysis / DNA helicase / electron microscopy / minichromosome maintenance / MCM

**Background:** The human MCM complex (hMCM) is an important component of the DNA replication apparatus.
**Results:** hMCM, after being produced in *E. coli*, has ATPase and DNA helicase activity and undergoes a conformational change when bound to DNA.
**Conclusion:** Recombinant hMCM is functional *in vitro*.
**Significance:** hMCM provides an important tool for the biochemical reconstitution of the human replicative helicase.

**ATP-dependent DNA unwinding activity has been demonstrated for recombinant archaeal homohexameric minichromosome maintenance (MCM) complexes and their yeast heterohexameric counterparts, but in higher eukaryotes such as *Drosophila*, MCM-associated DNA helicase activity has only been observed in the context of a co-purified Cdc45-MCM-GINS (CMG) complex. Here we describe the production of recombinant human MCM complex (hMCM) in *E. coli*. This protein displays ATP hydrolysis activity and is capable of unwinding duplex DNA. Using single particle asymmetric electron microscopy reconstruction, we demonstrate recombinant hMCM forms a hexamer that undergoes a conformational change when bound to DNA. Recombinant hMCM produced without post-translational modifications is functional *in vitro* and provides an important tool for the biochemical reconstitution of the human replicative helicase.**

DNA replication is fundamental to the proliferation of all cells and as such has been the subject of intense scrutiny over many years. While this work has demonstrated many unifying similarities among all eukaryotes with regards to DNA replication, it has also become obvious that there are a number of differences in the details regarding these systems. Significantly, one of the main model organisms for eukaryotic DNA replication, the yeast *Saccharomyces cerevisiae* (*S. cerevisiae*), has a closed mitosis that requires replication proteins to cross the nuclear envelope in a manner not required by other eukaryotes (1). The minichromosome maintenance (MCM) proteins are a good example of such proteins and *S. cerevisiae* MCMs possess insertions to cater to this requirement (Table 1). The models used to study replication in *Xenopus* and *Drosophila* are egg-based and contain unusually high levels of

(likely pre-assembled) replication complexes not normally seen in post-embryonic systems (2). Data from human tissue culture studies are mainly based on transformed cells, which probably do not accurately reflect the cell cycle controls in primary explants (3). Thus, the use of recombinant components, which may more accurately reconstitute robust DNA helicase activity biochemically from recombinant components is of significant interest in understanding human DNA replication processes.

The MCM complex is essential for DNA replication in eukaryotes and archaea, where it is believed to act as the replicative DNA helicase (reviewed in (4)). Homohexameric archaeal MCM complexes have provided useful models for studying DNA helicase activity (5,6). The production of a number of crystallographic structures has facilitated mapping of key enzymatic residues and provided insight into the molecular mechanisms utilized in DNA unwinding and translocation (7,8). In addition to its essential role in DNA replication, the heterohexameric eukaryotic Mcm2-7 complex has been implicated in DNA damage responses, checkpoint signaling, transcription and chromatin remodeling (9-12).

Isolation of intact, functional MCM heterohexamers has proved challenging. Functional MCM complex purified from *Xenopus* egg extracts using a "replication licensing factor" (RLF) assay demonstrated an additional requirement for Cdt1 in MCM chromatin loading (13,14). A "CMG" (Cdc45-MCM-GINS) complex with DNA helicase activity has been isolated from *Drosophila* egg extracts (15). MCM function is post-translationally modulated *in vivo* by phosphorylation, although this is not essential for replication elongation (16). The presence of inhibitory phosphorylations might explain why some purified MCM complexes produced in eukaryotic expression systems do not demonstrate significant helicase activity. Current methods for Mcm2-7 complex analysis rely on purification from yeast or insect cells, potentially complicating the interpretation of results as the purified Mcm2-7 complexes may have been post-translationally modified prior to purification.

We report the development of a bacterial expression protocol that allows the production of a recombinant human Mcm2-7 (hMCM) complex in *E. coli*. Our hMCM complex exhibits DNA unwinding and ATP hydrolysis with a different salt sensitivity from that reported for the yeast complex (17). Structures of the protein obtained by electron microscopy (EM) methods show that hMCM forms an asymmetric hexameric complex that undergoes a conformational change in the presence of a forked DNA substrate that it is also capable of unwinding. The generation of recombinant hMCM represents the development of an important tool for understanding the mechanisms governing human DNA replication. This may ultimately improve our ability to manipulate cell proliferation and therefore design useful and specific cancer treatments.

## EXPERIMENTAL PROCEDURES

*Expression and purification of Mcm2-7 complex*- PCR amplified Mcm2-7 cDNAs (primers in Table 2) were cloned into Ek/LIC Duet vectors (Novagen). pET32-Mcm2&7, pRSF-Mcm3&5 and pCDF-Mcm4&6 were transformed into *E. coli* Rosetta 2 (DE3) (Novagen) and grown in a 75 litre fermenter. hMCM complex was bound to His-Select Cobalt Affinity gel (Sigma), passed over a Superdex 200 gel filtration and MonoQ columns. Fractions containing MCM2-7 were pooled, dialysed against 25 mM Hepes, pH 8.0, 200 mM sodium glutamate, 1 mM DTT, 0.5 mM PMSF, flash frozen in small aliquots and stored at -80°C. Site directed mutagenesis of pET32-Mcm2&7, pRSF-Mcm3&5 and pCDF-Mcm4&6 produced inactive point mutations in the Walker A motif for each hMCM subunit (Mcm2 – K529E, Mcm3 - K351E, Mcm4 - K516E, Mcm5 - K387E, Mcm6 - K402E and Mcm7 - K387E). ATPase deficient mutant protein was produced and purified as wild-type.

*Western blotting*- Individual Mcm subunits were confirmed by western blotting the purified protein using primary antibodies: Mcm2 (CS732) (18), Mcm3 (clone 3A2) Medical and Biological Laboratories, Mcm4 (G-7) Santa Cruz Biotechnology Inc., Mcm5 (clone 33) BD Biosciences., Mcm6 (clone 1/MCM6) BD Biosciences and Mcm7 (141.2) Santa Cruz Biotechnology Inc.

*ATPase assays*- Reactions were modified from (6) as follows: reactions contained (30 mM $K_2HPO_4/KH_2PO_4$ buffer, pH 8.5, 1 mM DTT, 100 µg/ml BSA, 2% (v/v) glycerol, 10 mM magnesium acetate (MgAc)) and 1.5 nmol cold ATP, 3.08 pmol of [$\alpha$-$^{32}$P] ATP (800 Ci/mmol, (ICN)), 3.5 nM double stranded circular DNA (pUC119 unless

stated otherwise) and 176 nM of protein were assembled on ice.

*DNA helicase substrate*- Oligonucleotide HS2 (Table 2) was radiolabelled and annealed to oligonucleotide HS1 (Table 2) as described in (6).

*Helicase assays*- Helicase reactions (4 nM $^{32}$P labelled forked substrate, Mcm2-7 as indicated, 30 mM $K_2HPO_4/KH_2PO_4$ buffer, pH 8.5, 300 mM potassium glutamate, 1 mM DTT, 100 µg/ml BSA, 2% (v/v) glycerol, 10 mM MgAc, 4 mM ATP) were incubated (1 hour, 37°C) and stopped using ¼ volume 80 mM EDTA, 0.8% (w/v) SDS, 40% (v/v) glycerol, 0.04% (w/v) xylene cyanol, 0.04% (w/v) bromphenol blue. Reaction products were separated on 11% (w/v) polyacrylamide TBE gels (2 hours, 80 V). Gels were dried, imaged and quantified using a Bio-Rad Molecular Imager FX and Quantity One software.

*Binding of duplex DNA to hMCM for electron microscopy*- hMCM was bound to duplex DNA. No salt annealing buffer (200 mM HEPES pH 8.0, 5 mM EDTA) was added to 1 µM (HF150, 150 bp) and 1 µM (HR80, 80 bp) oligo (Table 2). DNA was annealed as follows; 95°C for three minutes, cool at 0.02°C/s to 23°C. The temperature was kept at 23°C for one minute. 8 µg of hMCM was incubated with 60 nM duplex DNA in annealing buffer (50 mM HEPES pH7.5, 2 mM DTT, 50 µg/ml BSA, 10 mM magnesium acetate (MgAc) and 4 mM ATP) for 60 minutes at 37°C to bind the hMCM and duplex DNA. Samples were snap frozen in liquid nitrogen.

*Electron microscopy*- hMCM samples were applied to continuous carbon grids and stained with freshly made methylamine tungstate, pH 7. Data were collected on a FEI T12 microscope at magnification 67,000 and accelerating voltage 120 kV, recorded on Kodak SO-163 films and digitised using a Zeiss Photoscan densitometer (14µm scanning step, corresponding to 2.5 Å/pixel) before analysis.

*Image processing*- Particle picking was carried out automatically using 'Boxer' (EMAN suite (19)). Analysis of the CTF and correction was completed using 'CTFIT' (EMAN suite (19)). Image analysis was performed using IMAGIC-5 (20): Images were normalized to the same standard deviation and band-pass filtered; the low-resolution cut-off was ~100 Å to remove uneven background in particle images and the high-resolution cut-off was ~7 Å. Images were subjected to an alignment procedure followed by statistical analysis. Alignment and classification of images was performed as previously described (20) and yielded classes representing characteristic views of the molecule. Primary structural analysis for hMCM and hMCM plus DNA complexes was performed using an *ab initio* approach where the orientations of the best 10-15 image classes were determined by angular reconstitution using C1 start up. 3D maps were calculated using the exact-filter back projection algorithm (20). Structural analysis was performed using several starting models with several different sets of image classes for *ab initio* reconstructions. The first reconstructions were used for the following rounds of alignment and classification of images. The structures of the complexes were refined by an iterative procedure with the number of classes gradually increased. The final reconstruction for hMCM alone was calculated from the best 100 classes containing ~11 images each. For hMCM plus DNA, the final reconstruction was calculated from the best 155 classes containing ~10 images each. Resolution of the map was assessed using the 0.5 threshold of Fourier Shell Correlation (21), which corresponds to 23 Å. Domain fitting into the 3D map of hMCM and hMCM plus DNA complexes was performed manually with Chimera (22). Illustrations were generated using Chimera. Surface representations (unless stated otherwise) are displayed at a threshold level of 3σ (standard deviation of densities within EM maps) that corresponds to ~100% of the expected mass at the specific protein density of 0.84 kDa/Å$^3$.

## RESULTS

*Production of a soluble hMCM complex*

To avoid potential activity-inhibiting phosphorylation by kinases present in eukaryotic expression systems, we co-expressed the human Mcm2-7 proteins as a stable, soluble complex, in *E. coli* (Fig 1A). The complex was purified according to the scheme outlined in Fig 1B. The presence of all six hMCM subunits in the purified complex was demonstrated by western blotting using specific antibodies (Fig 1C). Consistent with our western blot results, visualisation of the complex using Coomassie stained SDS-PAGE revealed the presence of some putative degradation products in addition to all six full-length hMCM subunits (Fig 1D). Typically we produce 82.5 µg of hMCM per litre *E. coli* culture. A complex harbouring inactivating point

mutations in the Walker A motifs of each hMCM subunit (Mcm2 – K529E, Mcm3 - K351E, Mcm4 - K516E, Mcm5 - K387E, Mcm6 - K402E and Mcm7 - K387E) was produced in the same way.

*ATP hydrolysis activity of hMCM*

Purified wild type (WT) hMCM complex and ATPase deficient mutant complexes were tested for their ability to hydrolyse ATP in the presence and absence of a series of DNA substrates (at molar ratios of [hMCM hexamer]:[DNA] ranging from [110:1] to [3.8:1], Fig 2A). hMCM exhibited ATP hydrolysis that was not increased by the addition of DNA. High concentrations (46 nM) of double stranded closed circular DNA (dsDNA) inhibited ATP hydrolysis by ~50% compared to lower concentrations of dsDNA, possibly due to a substrate competition effect preventing the MCMs from forming a productive complex. A similar, but smaller, effect was observed for single stranded closed circular DNA (ssDNA). A forked DNA substrate had negligible effect on hydrolysis activity at the concentrations tested. Subsequent ATP hydrolysis assays were carried out in the presence of 3.5 nM dsDNA.

Based on previous reports of specific salt requirements for yeast MCM activity *in vitro* (17), we examined the ability of hMCM to hydrolyse ATP in the presence of sodium chloride, sodium glutamate, potassium chloride and potassium glutamate (Fig 2B). Increased sodium chloride concentrations resulted in a statistically significant decrease in ATP hydrolysis. A similar effect was observed for sodium glutamate. The addition of 50 mM potassium chloride resulted in a pronounced inhibition of ATPase activity. Strikingly the presence of 300 mM potassium glutamate, twice the physiological salt concentration, had no effect on ATPase activity (Fig 2B). As expected, increasing concentrations of hMCM resulted in increased ATP hydrolysis (Fig 2C). Addition of 20 mM EDTA significantly reduced ATP hydrolysis by hMCM, as did replacing the WT protein with the ATPase deficient mutant complex (Fig 2C) as expected from previous studies in *S. cerevisiae* (5,23). Using the optimal assay conditions identified (3.5 nM dsDNA, 300 mM potassium glutamate and 176 nM hMCM) we measured the rate of ATP hydrolysis for WT and mutant hMCM (Fig 2D). The maximum rate of ATP hydrolysis for WT hMCM was 16.7 pmol ADP released/min/pmol hMCM compared to 3.9 pmol ADP released/min/pmol mutant hMCM.

*ATP-dependent DNA unwinding by hMCM*

We tested our purified recombinant hMCM complexes for DNA helicase activity using a forked DNA substrate in the presence or absence of ATP. WT hMCM exhibited a protein concentration and ATP-dependent DNA unwinding activity (Fig 3). With WT hMCM we observed 38% and 50% displacement by 176 nM and 352 nM hMcm2-7 respectively (Fig 3), broadly comparable to the reported 52% displacement by 110 nM yeast Mcm2-7 (17). Under conditions where ATP could not be hydrolysed – that is, either WT hMCM in the absence of ATP, or mutant hMCM in the presence of ATP – helicase activity was substantially reduced (Fig 3B) consistent with ATP hydrolysis being required for helicase activity.

*EM structure of recombinant hMCM.*

The structures of purified hMCM, both complex alone and bound to forked DNA, were obtained using EM of negatively stained. Structures were obtained using single particle approach with C1 symmetry (Fig 4). Our results revealed that the complex formed ring-shaped hexamers with a diameter of 145 Å and a height of 120 Å (Fig 4A). Our asymmetric reconstructions (Fig 4) suggest that the complexes contain six different subunits (2-7) as opposed to a dimer of Mcm4/6/7 trimers (which would produce C2 symmetry), or a trimer of Mcm4/7 dimers (C3 symmetry). When observed in the presence of forked DNA (Fig 4A, bottom row), the hMCM structure has a different conformation, with a more defined two-tiered hexameric shape and a more obviously open central cavity. The atomic model of the hexamer of *Sulfolobus solfataricus (Sso)*MCM (3F9V) fits into our reconstruction (Fig 4B).

## DISCUSSION

ATP hydrolysis has been demonstrated for MCM complexes derived from archaea (5) and eukaryotes (23,24). We found that the addition of DNA did not stimulate ATP hydrolysis by purified hMCM. This is consistent with reports of *S. cerevisiae* Mcm2-7 where DNA did not stimulate ATP hydrolysis (23,25). It is worth noting that this is in contrast to the Mcm4/6/7 sub-complex, which is stimulated by DNA (26,27). In agreement with

observations from archaeal MCMs (5), high concentrations of dsDNA were in fact inhibitory. With respect to salt sensitivity, 50 mM potassium chloride strongly inhibited the ATPase activity of hMCM whereas potassium glutamate, even at a concentration of 300 mM, had no such effect. These findings are consistent with results reported for the DNA helicase activity of the *S. cerevisiae* MCM (17).

Binding and hydrolysis of ATP by MCM purified from *S. cerevisiae* has recently been shown to be required for CDT1 release and double hexamer formation (28), with the ATPase sites of different MCM subunits implicated in different stages of its loading and activation (29). The interface between subunits 2 and 5 of the *S. cerevisiae* Mcm2-7 complex is thought to function as an ATP-dependant "gate", the opening of which enables the toroidal complex to be loaded onto topologically closed DNA (17). The recombinant hMCM produced here is an important tool to analyse the loading and activation of the human complex in light of this finding.

Robust ATP-dependent DNA helicase activities were first demonstrated using archaeal homohexamers (5). Limited DNA helicase activity was originally demonstrated for a hexameric complex purified from HeLa cells that contained human Mcm subunits 4, 6 and 7, probably as a dimer of trimers (24). This activity was inhibited by the addition of mouse Mcm2 (30). Salt-sensitive DNA helicase activity of a heterohexameric Mcm2-7 complex was first demonstrated using *S. cerevisiae* proteins purified after *Baculovirus* expression (17), and DNA unwinding activity of higher eukaryotic MCM complexes has been observed with the CMG complex from *Drosophila* (15). Here we describe the first demonstration of helicase activity for the human Mcm2-7 complex.

Our results showed that ATP hydrolysis was a requirement for DNA helicase activity. The negligible unwinding and ATPase activities in the mutant hMCM assays suggests that the mutant and WT protein preparations were both free from contaminating *E. coli* helicases / ATPases. Under ATPase null conditions (either no ATP or mutant hMCM) a large proportion of the helicase substrate migrated more slowly by native PAGE. Similar mobility shift effects have been previously observed for the *Methanothermobacter thermautotrophicus* MCM when samples have been incubated on ice (6). This suggests that hMCM protein binds to the substrate in the absence of ATP (or ATP hydrolysis) but cannot unwind it. This is consistent with the idea that ATP hydrolysis is not required for DNA-protein interactions but is required for DNA unwinding (31).

Overall, these results indicate that the recombinant hMCM complex exhibits DNA helicase activity and that posttranslational modifications to hMCM or accessory proteins such as Cdc45 and GINS are not required for the unwinding of naked DNA. The requirement for Cdc45 and GINS may only be required for remodelling or unwinding DNA packaged into chromatin.

The size and shape of our hMCM complex is consistent with the organisation of oligomeric complexes reported for MCM from other eukaryotes (32,33). Analysis of a population of *Drosophila* Mcm2-7 complexes revealed that they exist in two different states: a planar, notched ring and an open spiral shape (32). Reconstructions of Mcm2-7 from *Encephalitozoon cuniculi* suggest that this Mcm2-7 is naturally found in the open spiral shape (34). Our reconstruction of the human complex is more similar to the notched ring, similar to *S. cerevisiae* (35), but this does not preclude the existence of a minority of spiral shaped complexes in our sample.

Interestingly, the conformation taken by hMCM in the presence DNA is somewhat similar to what has been reported for *S. cerevisiae* Mcm2-7 in the absence of DNA (36). One possible reason for the differences observed between the yeast and human proteins in the absence of DNA could be the differences in the primary sequences of the yeast and human proteins (outlined in Table 1). The prominent projection that appears on the top surface of one of the hMCM subunits in the presence of DNA (red circle) could be either the bound 45 base pair double-stranded portion of the DNA substrate, as ssDNA is too small to be visualised at this resolution, or a section of protein displaced by the presence of the DNA, such as the N-terminal S-Trx-His tag on Mcm7 (molecular weight is 15 KDa). Further work is required to determine which hMCM subunit binds DNA under these conditions.

Human MCM is an important factor in cell proliferation and therefore by extension cancer development. The ability to produce significant

quantities of hMCM for analysis is an important step forward. Our biochemical findings show that the recombinant complex is active *in vitro* and our structural studies show that its conformation is altered when bound to DNA. Our system enables the targeted manipulation of individual proteins within the hMCM complex, providing the potential to address in detail the important differences between individual subunits in the hMCM heterohexamer. It also provides the potential to develop screens for clinically relevant hMCM inhibitors.

## REFERENCES


1. Byers, B., and Goetsch, L. (1975) Behavior of spindles and spindle plaques in cell-cycle and conjugation of *Saccharomyces-cerevisiae*. *J. bact* **124**, 511-523
2. Kim, J. H., Na, C. Y., Choi, S. Y., Kim, H. W., Du Kim, Y., Kwon, J. B., Chung, M. Y., Hong, J. M., and Park, C. B. (2010) Integration of gene-expression profiles and pathway analysis in ascending thoracic aortic aneurysms. *Ann Vasc Surg* **24**, 538-549
3. Munkley, J., Copeland, N. A., Moignard, V., Knight, J. R., Greaves, E., Ramsbottom, S. A., Pownall, M. E., Southgate, J., Ainscough, J. F., and Coverley, D. (2011) Cyclin E is recruited to the nuclear matrix during differentiation, but is not recruited in cancer cells. *Nuc. Acid. Res.* **39**, 2671-2677
4. Tye, B. K. (1999) MCM proteins in DNA replication. *Ann. Rev. Biochem.* **68**, 649-686
5. Chong, J. P. J., Hayashi, M. K., Simon, M. N., Xu, R. M., and Stillman, B. (2000) A double-hexamer archaeal minichromosome maintenance protein is an ATP-dependent DNA helicase. *Proc. Nat. Academy of Sciences of the United States of America* **97**, 1530-1535
6. Jenkinson, E. R., and Chong, J. P. (2006) Minichromosome maintenance helicase activity is controlled by N- and C-terminal motifs and requires the ATPase domain helix-2 insert. *Proc Natl Acad Sci U S A* **103**, 7613-7618
7. Fletcher, R. J., Bishop, B. E., Leon, R. P., Sclafani, R. A., Ogata, C. M., and Chen, X. J. S. (2003) The structure and function of MCM from archaeal *M-thermoautotrophicum*. *Nature Structural Biology* **10**, 160-167
8. Brewster, A. S., Wang, G., Yu, X., Greenleaf, W. B., Maria Carazo, J., Tjajadia, M., Klein, M. G., and Chen, X. S. (2008) Crystal structure of a near-full-length archaeal MCM: Functional insights for an AAA plus hexameric helicase. *Proceedings of the National Academy of Sciences of the United States of America* **105**, 20191-20196
9. Stead, B. E., Brandl, C. J., and Davey, M. J. (2011) Phosphorylation of Mcm2 modulates Mcm2-7 activity and affects the cell's response to DNA damage. *Nucleic Acids Research* **39**, 6998-7008
10. Ibarra, A., Schwob, E., and Mendez, J. (2008) Excess MCM proteins protect human cells from replicative stress by licensing backup origins of replication. *Proceedings of the National Academy of Sciences of the United States of America* **105**, 8956-8961
11. Snyder, M., He, W., and Zhang, J. J. (2005) The DNA replication factor MCM5 is essential for Stat1-mediated transcriptional activation. *Proceedings of the National Academy of Sciences of the United States of America* **102**, 14539-14544
12. Groth, A., Corpet, A., Cook, A. J. L., Roche, D., Bartek, J., Lukas, J., and Almouzni, G. (2007) Regulation of replication fork progression through histone supply and demand. *Science* **318**, 1928-1931
13. Chong, J. P. J., Mahbubani, H. M., Khoo, C.-Y., and Blow, J. J. (1995) Purification of an MCM-containing complex as a component of the replication licensing system. *Nature* **375**, 418-421
14. Tada, S., Li, A., Maiorano, M., Mechali, M., and Blow, J. J. (2001) Repression of origin assembly in metaphase depends on onhibition of RLF-B/Cdt1 by geminin. *Nature Cell Biology* **3**, 107-113

15. Moyer, S. E., Lewis, P. W., and Botchan, M. R. (2006) Isolation of the Cdc45/Mcm2-7/GINS (CMG) complex, a candidate for the eukaryotic DNA replication fork helicase. *Proc. Nat. Acad. Sci. USA* **103**, 10236-10241
16. Poh, W. T., Chadha, G. S., Gillespie, P. J., Kaldis, P., and Blow, J. J. (2014) Xenopus Cdc7 executes its essential function early in S phase and is counteracted by checkpoint-regulated protein phosphatase 1. *Open Biol* **4**, 130138
17. Bochman, M. L., and Schwacha, A. (2008) The MCM2-7 complex has *in vitro* helicase activity. *Mol. Cell* **31**, 287-293
18. Ekholm-Reed, S., Mendez, J., Tedesco, D., Zetterberg, A., Stillman, B., and Reed, S. I. (2004) Deregulation of cyclin E in human cells interferes with prereplication complex assembly. *J. Cell. Biol.* **165**, 789-800
19. Tang, G., Peng, L., Baldwin, P. R., Mann, D. S., Jiang, W., Rees, I., and Ludtke, S. J. (2007) EMAN2: An extensible image processing suite for electron microscopy. *J. Struct. Biol.* **157**, 38-46
20. van Heel, M., Harauz, G., Orlova, E. V., Schmidt, R., and Schatz, M. (1996) A new generation of the IMAGIC image processing system. *J. Struct. Biol.* **116**, 17-24
21. van Heel, M., Gowen, B., Matadeen, R., Orlova, E. V., Finn, R., Pape, T., Cohen, D., Stark, H., Schmidt, R., Schatz, M., and Patwardhan, A. (2000) Single-particle electron cryo-microscopy: towards atomic resolution. *Quarterly Rev. Biophysics* **33**, 307-369
22. Goddard, T. D., Huang, C. C., and Ferrin, T. E. (2007) Visualizing density maps with UCSF Chimera. *J. Struct. Biol.* **157**, 281-287
23. Schwacha, A., and Bell, S. P. (2001) Interactions between two catalytically distinct MCM subgroups are essential for coordinated ATP hydrolysis and DNA replication. *Mol. Cell* **8**, 1093-1104
24. Ishimi, Y. (1997) A DNA helicase activity is associated with an MCM4, -6, and -7 protein complex. *J. Biol, Chem.* **272**, 24508-24513
25. Bochman, M. L., Bell, S. P., and Schwacha, A. (2008) Subunit organization of Mcm2-7 and the unequal role of active sites in ATP hydrolysis and viability. *Mol. Cell. Biol.* **28**, 5865-5873
26. Biswas-Fiss, E. E., Khopde, S. M., and Biswas, S. B. (2005) The Mcm467 complex of *Saccharomyces cerevisiae* is preferentially activated by autonomously replicating DNA sequences. *Biochemistry* **44**, 2916-2925
27. You, Z. Y., Ishimi, Y., Mizuno, T., Sugasawa, K., Hanaoka, F., and Masai, H. (2003) Thymine-rich single-stranded DNA activates Mcm4/6/7 helicase on Y-fork and bubble-like substrates. *EMBO J.* **22**, 6148-6160
28. Coster, G., Frigola, J., Beuron, F., Morris, Edward P., and Diffley, John F. X. Origin Licensing Requires ATP Binding and Hydrolysis by the MCM Replicative Helicase. *Mol. Cell*
29. Kang, S., Warner, Megan D., and Bell, Stephen P. (2014) Multiple functions for Mcm2–7 ATPase motifs during replication initiation. *Mol. Cell*
30. Ishimi, Y., Komamura, Y., You, Z., and Kimura, H. (1998) Biochemical function of mouse minichromosome maintenance 2 protein. *J. Biol. Chem.* **273**, 8369-8375
31. McGeoch, A. T., Trakselis, M. A., Laskey, R. A., and Bell, S. D. (2005) Organization of the archaeal MCM complex on DNA and implications for the helicase mechanism. *Nat. Struct. Mol. Biol.* **12**, 756-762
32. Costa, A., Ilves, I., Tamberg, N., Petojevic, T., Nogales, E., Botchan, M. R., and Berger, J. M. (2011) The structural basis for MCM2-7 helicase activation by GINS and Cdc45. *Nat. Struct. Mol. Biol* **18**, 471-U110
33. Remus, D., Beuron, F., Tolun, G., Griffith, J. D., Morris, E. P., and Diffley, J. F. X. (2009) Concerted loading of MCM2-7 double hexamers around DNA during DNA replication origin licensing. *Cell* **139**, 719-730
34. Lyubimov, A. Y., Costa, A., Bleichert, F., Botchan, M. R., and Berger, J. M. (2012) ATP-dependent conformational dynamics underlie the functional asymmetry of the replicative helicase from a minimalist eukaryote. *Proc. Nat. Acad. Sci. USA* **109**, 11999-12004

35. Samel, S. A., Fernandez-Cid, A., Sun, J., Riera, A., Tognetti, S., Herrera, M. C., Li, H., and Speck, C. (2014) A unique DNA entry gate serves for regulated loading of the eukaryotic replicative helicase MCM2-7 onto DNA. *Genes Dev.* **28**, 1653-1666
36. Evrin, C., Clarke, P., Zech, J., Lurz, R., Sun, J., Uhle, S., Li, H., Stillman, B., and Speck, C. (2009) A double-hexameric MCM2-7 complex is loaded onto origin DNA during licensing of eukaryotic DNA replication. *Proc. Nat. Acad. Sci. USA* **106**, 20240-20245

*Acknowledgements* - Thanks to Christoph Baumann and Peter McGlynn for comments on the manuscript. cDNA clones of hMCMs and CS732 polyclonal were gifts from J. Mendez (CNIO).

**FOOTNOTES**

This work was supported by Cancer Research UK (grant numbers A7771 and A10945), Wellcome VIP funds administered by the Department of Biology, University of York and Yorkshire Cancer Research (Y002PhD).

**FIGURE LEGENDS**

**Figure 1**. Purification of a bacterially-expressed human MCM complex. A. Schematic of recombinant hMCM complex. Predicted arrangement of MCM2-7 subunits indicating which subunits have N-terminal affinity tags to aid in protein purification. B. Purification scheme for the recombinant hMCM complex. C. Western blot using antibodies specific to individual MCM subunits, showing all six human Mcms in the purified complex. D. Purified hMCM complex separated by 10% (w/v) SDS-PAGE gel and visualised by Coomassie blue staining.

**Figure 2.** WT hMCM possesses ATPase activity. A. At 46 nM single stranded closed circular (sscc) DNA (a molar ratio of [hMCM hexamer]:[DNA] at [3.8:1]), reduced ATP hydrolysis by one third and double stranded closed circular (dscc) DNA reduced ATP hydrolysis by ~50%. Forked DNA had little overall effect. Statistics compare labelled bar to 0 nM DNA. *p=0.022 and **p=0.0019. B. Potassium Glutamate (KGlut) had no effect on ATPase activity in the presence of 3.5 nM dsDNA. Increasing the concentrations of Sodium Chloride (NaCl) and Sodium Glutamate (NaGlut) reduced ATP hydrolysis and addition of Potassium Chloride (KCl) greatly reduced ATP hydrolysis. Statistics compare labelled bar to 0 mM salt. *p=0.018, **p=0.013 and ***p=0.00027. C. ATPase activity increases with protein concentration in the presence of 3.5 nM dsDNA, and is inhibited by the addition of 20 mM EDTA to chelate the $Mg^{2+}$. The ATPase deficient mutant hMCM shows 6-fold lower ATP hydrolysis activity than WT hMCM. Statistics compare labelled bar to 352 nM hMCM . *p=0.0015 and **p=0.00014. D. The rate of ATP hydrolysis by WT hMCM and ATPase deficient mutant hMCM in molecules of ADP released per minute with optimized conditions (3.5 nM dsDNA, 300 mM potassium glutamate and 176 nM hMCM). The maximum rate of ATP hydrolysis for WT hMCM is 16.7 pmol ADP produced/min/pmol hMCM and 3.9 pmol ADP produced/min/pmol mutant hMCM in the presence of 3.5 nM dsDNA. (A), (B) and (C) are mean values of three replicates, the data in (D) are mean values of two assays; error bars show the standard deviation.

**Figure 3.** Recombinant hMCM displays DNA helicase activity. A. A forked DNA substrate was incubated with increasing concentrations of hMCM in the absence or presence of ATP. Heat denatured boiled substrate (★) and no protein lanes are included as controls. An arrow indicates the position of displaced substrate, an asterisk indicates substrate with unusual mobility, perhaps indicating hMCM that is bound to DNA. B. The amount of single stranded substrate in each reaction was quantified as a percentage of the boiled substrate control. The data shown are mean values for four independent assays, an example of which is shown in (A). Error bars indicate standard error of the mean. Statistics compare labelled lane to 352 nM hMCM plus ATP. ***p=0.00013 and **p=0.0014.

**Figure 4.** A. Negative stain, single particle EM 3D asymmetric reconstruction of hMCM to 23 Å resolution. Top row: hMCM alone (blue) from three different aspects. The complex undergoes a conformational change when the hMCM is bound to forked DNA (middle row, green). Red circle highlights protrusion thought to be DNA binding to hMCM. Size indicated in angstroms (Å). Bottom row: schematic representation of hMCM subunit configuration. B. The crystal structure of SsoMCM fitsinto out reconstructions. hMCM alone (blue) and hMCM bound to forked DNA (green) fitted with 'nearly full length' *Sulfolobus solfataricus (Sso)* MCM crystal structure (3F9V) (8). The full hMCM structure (left) and slice through hMCM (right) show a central cavity in both reconstructions.

**Table 1.** MCM amino acid insertions – comparison of *s. cerevisiae* and *H. Sapiens*.

| Mcm | *S. cerevisiae* (aa) | *H. sapiens* (aa) | aa difference (Sc-Hs) | insertion locations |
|---|---|---|---|---|
| 2 | 868 | 904 | -36 (-4%) | C |
| 3 | 971 | 808 | 163 (20%) | N, C |
| 4 | 933 | 863 | 70 (8%) | N |
| 5 | 775 | 734 | 41 (6%) | N |
| 6 | 1017 | 821 | 196 (24%) | N, (C) |
| 7 | 845 | 719 | 126 (18%) | N |

**Table 2.** List of oligonucleotide sequences used in the study.

| Oligo name: | Oligo sequence: |
|---|---|
| Mcm2 for | gcgggcccggcctccatggcggaatcatcggaatccttcacc |
| Mcm2 rev | gaggagaagcccggtcagaactgctgcaggatcattttcc |
| Mcm3 for | gcgggcccggccttcatggcgggtaccgtggtgctggac |
| Mcm3 rev | gaggagaagcccggtcagatgaggaagatgatgccctcag |
| Mcm4 for | gcgggcccggccttcatgtcgtccccggcgtcgacccc |
| Mcm4 rev | gaggagaagcccggtcagagcaagcgcacggtcttccc |
| Mcm5 for | gacgacgacaagatgtcgggattcgacgatcctggc |
| Mcm5 rev | cgcgggcggccgtcacttgaggcggtagagaaccttgc |
| Mcm6 for | gacgacgacaagatggacctcgcggcggcagcgg |
| Mcm6 rev | cgcgggcggccgtcaatcttcgagcaagtagttaggg |
| Mcm7 for | gacgacgacaagatggcactgaaggactacgcgctag |
| Mcm7 rev | cgcgggcggccgtcagacaaaagtgatccgtgtccggg |
| HF150 | cctggcgttacccaacttaatcgccttgcagcacatccccctttcttttttt

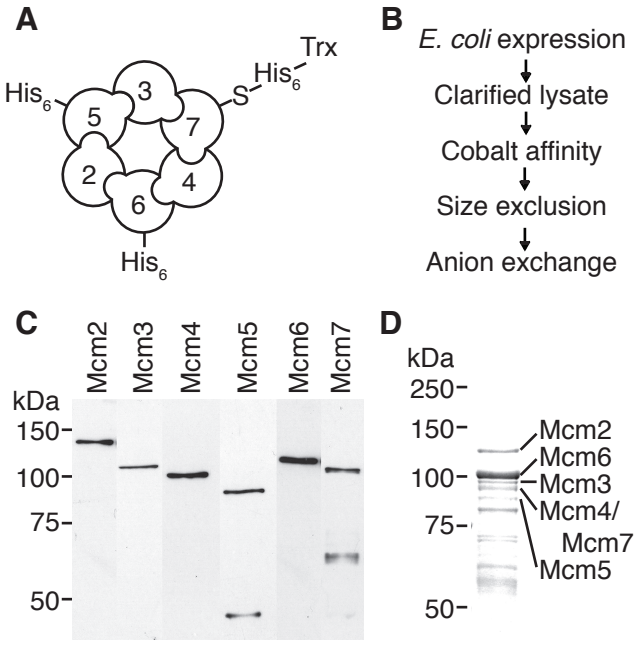


Figure 1. Hesketh et al 2014

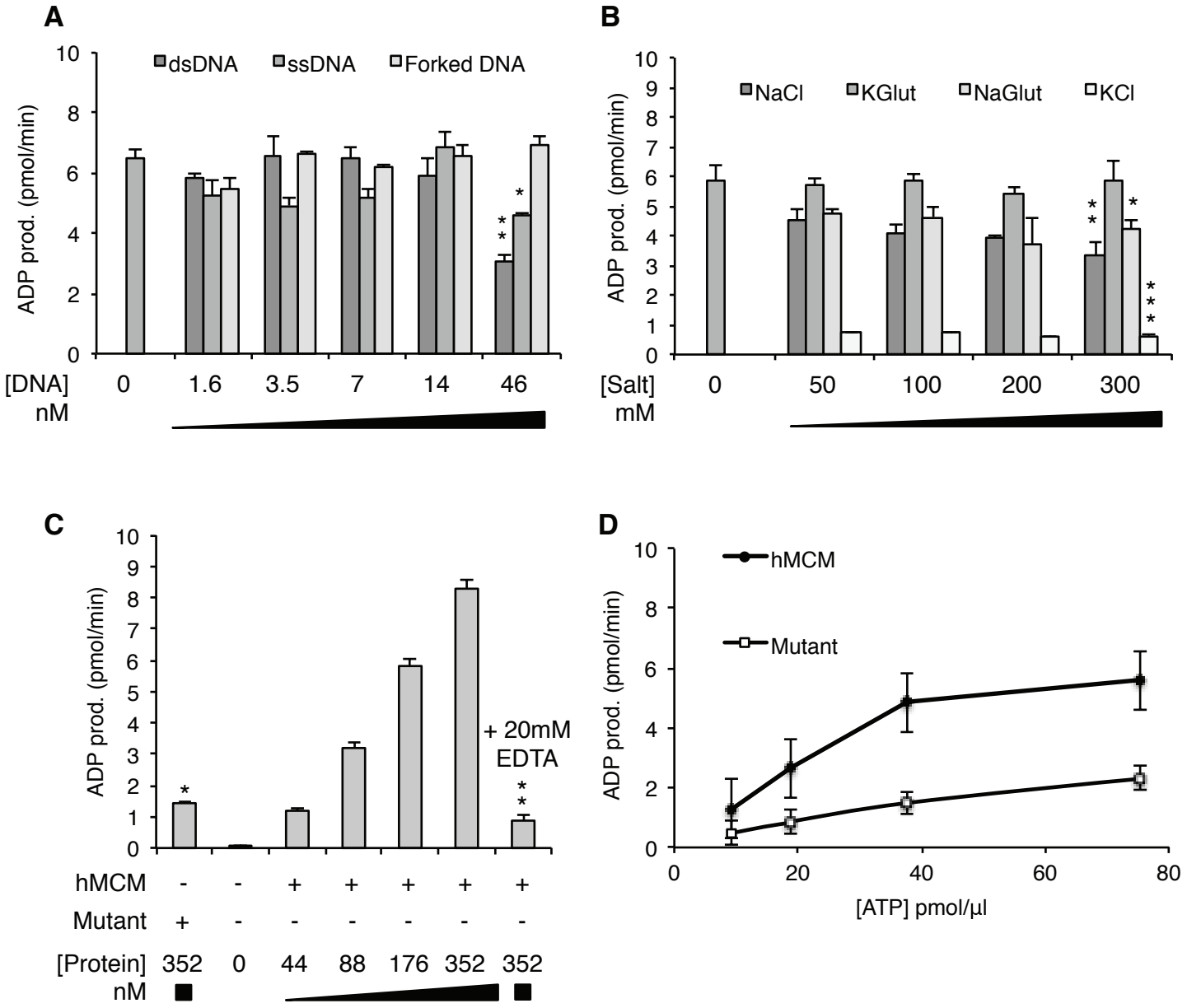


Figure 2. Hesketh et al 2014

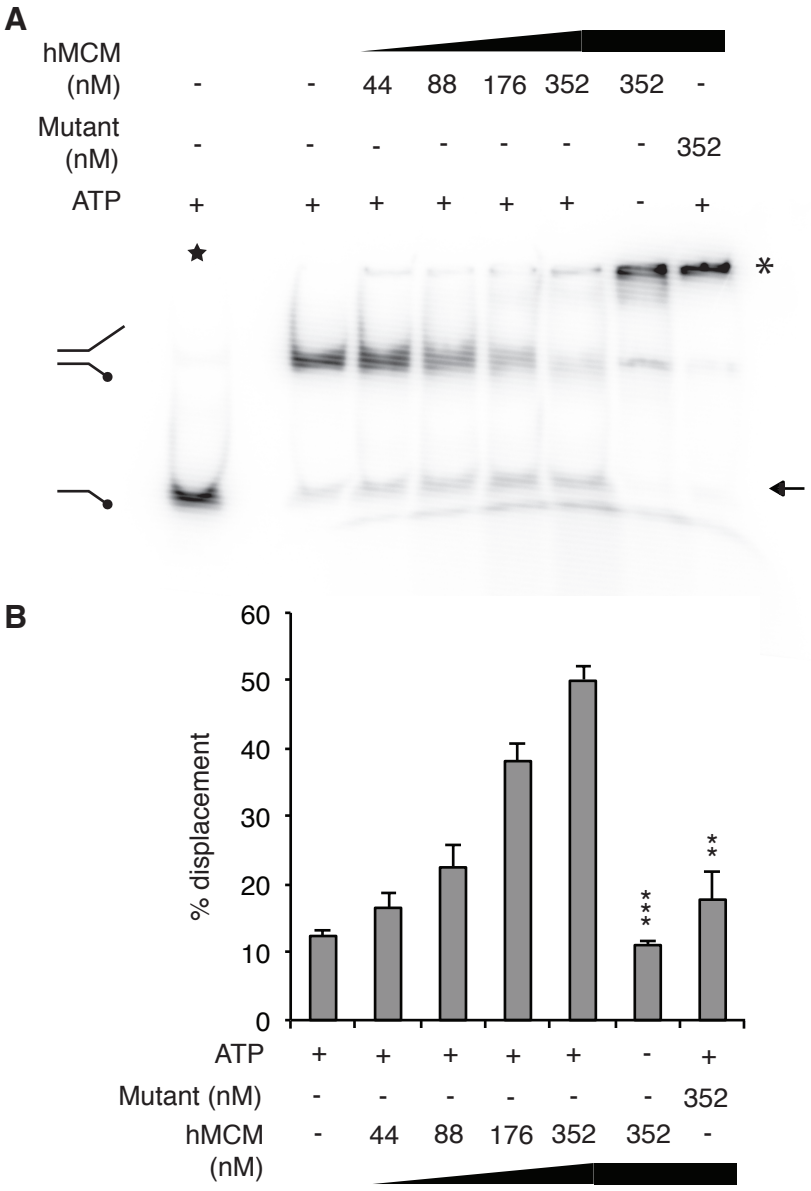


Figure 3. Hesketh et al 2014

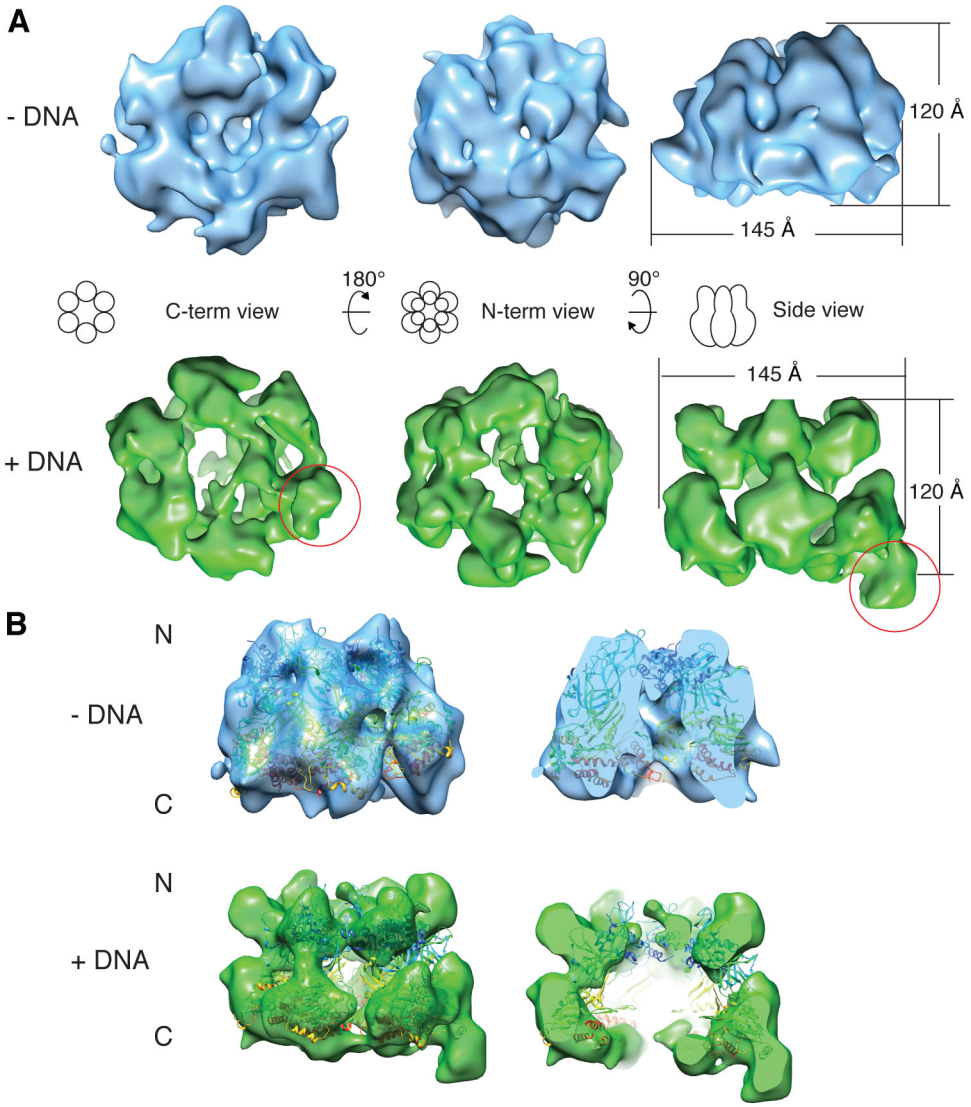


Figure 4. Hesketh et al 2014

# Appendix D

The following work has been accepted for publication in Cell Cycle. It contains much of the work presented here in Chapter 4 and has additional information provided by other lab members.

**Transient association of MCM complex proteins with the nuclear matrix during initiation of mammalian DNA replication**

Emma L. Hesketh[1]*, John R. P. Knight[1,2], Rosemary H. C. Wilson[1,3], James P. J. Chong[1], Dawn Coverley[1]

[1] Department of Biology, University of York, York YO10 5DD, UK

[2] Current address: MRC Toxicology Unit, University of Leicester, Leicester, LE1 9HN, UK

[3] Current address: Wellcome Trust Centre for Human Genetics, University of Oxford, Oxford, OX3 7BN, UK

*Author for correspondence elh537@york.ac.uk

Running title: Temporally regulated MCM loading

**Abstract**

The minichromosome maintenance complex (MCM2-7) is the putative DNA helicase in eukaryotes, and essential for DNA replication. By applying serial extractions to mammalian cells synchronized by release from quiescence, we reveal dynamic changes to the sub-nuclear compartmentalization of MCM2 as cells pass through late G1 and early S phase, identifying a brief window when MCM2 becomes transiently attached to the nuclear-matrix. The data distinguish three states that correspond to loose association with chromatin prior to DNA replication, transient highly stable binding to the nuclear-matrix coincident with initiation, and a post-initiation phase when MCM2 remains tightly associated with chromatin but not the nuclear-matrix. The data suggests that functional MCM complex loading takes place at the nuclear-matrix.

**Keywords:** cell cycle / minichromosome maintenance complex/ MCM2-7 / nuclear matrix / DNA replication / initiation

**Abbreviations:** Nuclear matrix (NM), Minichromosome maintenance (MCM),

## Introduction

The nuclear matrix (NM) is a biochemically defined ribonuclear protein framework in higher eukaryotic cells that persists when chromatin, soluble proteins and lipids are removed.[1] Chromatin is periodically attached to the NM specifying its characteristic loop organisation in interphase nuclei, with functional protein assemblies immobilized at loop bases. Extensive evidence places DNA replication in proximity to the NM within DNA replication factories; aggregates of replication proteins and multiple co-regulated origins. ([2] and reviewed in ref. 3)

In cycling cells the nucleus is 'licensed' for DNA replication in early G1 phase when the hetero-hexameric MCM2-7 complex associates with chromatin.[4] This is dependent on the origin recognition complex (ORC1-6), CDT1 and CDC6. Binding and hydrolysis of ATP by MCM2-7 has been shown to be required for CDT1 release and double hexamer formation.[5] CDC45 and GINS bind to chromatin and together with MCM2-7 form the CMG complex, an active DNA helicase.[6] MCM loading occurs as the cell passes through the G1/S phase transition, functionally defined by the commencement of DNA synthesis. In eukaryotes, MCM activity is regulated by cyclin-dependent kinases (CDKs) and Dbf4-dependent kinase (DDK) (reviewed in ref. 7).

Recently, full replication of plasmid DNA was achieved, independent of origin sequences, using a yeast cell-free system over-expressing multiple initiation proteins.[8, 9] Thus, initiation has been effectively reconstituted, but the system is not fully defined and the mechanism of site selection is not clear. Intrinsic to this is the functional loading of the MCM helicase complex, which is believed to involve ring opening between MCM subunits 2 and 5.[10, 11] Exactly how this is achieved on chromatin, and rendered functional by accurate interaction with both template and accessory factors, is not fully understood even in yeast.

In higher eukaryotes where spatial constraints play a role in specifying origins, additional considerations come into play, necessitating a description of the relationship between the MCM complex and the NM. A number of studies have begun to look at this in cell lines engaged in continuous culture, with contradictory results. MCM3 and MCM7 have been reported to be resistant to nuclease digestion and therefore characterized as NM

bound.[12, 13] However, other studies show MCM2, MCM3, MCM5 and MCM7 to be solubilized by nuclease digestion and therefore not NM bound.[14-18] None of these studies validate the effect of nuclease by demonstrating release of chromatin-associated control proteins, so must be interpreted accordingly. Furthermore, transient interaction may be masked in asynchronous cells by the bulk fraction of MCM protein, making synchronization essential. Here we show fine temporal resolution of the nuclear binding characteristics of MCM2 as cells pass through late G1 phase, in order to describe the types of interaction that occur during expression, assembly, initiation and beyond. Using murine 3T3 cells that can be manipulated to undergo synchronized passage through G1 phase, without the use of chemical inhibitors, we demonstrate three distinct binding states of MCM2 in G1 phase following quiescence. These are i. chromatin binding prior to initiation of DNA replication, ii. transient association with the NM approximately four hours later, which we postulate reflects functional loading, and iii. stabilized post-initiation presence on chromatin.

**Results**

Murine 3T3 cells can be synchronized in quiescence by contact inhibition and serum depletion, then released into cycle as a synchronous wave of cells that pass through G1 landmarks at defined points (Fig. 1A). Under these conditions serum-independent S phase entry is triggered at 15 hours after release from quiescence (restriction point, R) and does not vary much between experiments (maximum one hour variance based on appearance of cyclins).[19] Entry to S phase is first apparent around one hour later, though most cells in the population enter S phase after 20 hours, reaching a maximum of 60-70% after 24 hours. Cyclin A expression increases steadily over the same period and can be used as a surrogate marker of passage through post-restriction point G1.

***Expression of MCM2 in late G1 phase*** MCM complex proteins are first evident after R, and increase through late G1 (Fig. 1B), paralleling the expression of cyclin A. When cells are separated into detergent-soluble and insoluble (nuclei) fractions immediately after harvesting (Fig. 1B), a notable peak is detected at 19 hours after release from quiescence, and a short period of instability both before and after this time. This suggests a mechanism that functions to deplete unprotected MCM during this time. Because this temporal profile is not apparent in whole cell lysates, this appears not to act on the bulk of the MCM in the cell, having the greatest impact when cells are disrupted artificially. Chromatin-bound CDC6 does not appear to suffer the same depletion (Fig. 1C), though does peak at the same time as chromatin-bound MCM2 (at 18 hours after release from quiescence in this independent experiment). From this data we can say that chromatin binding of CDC6 occurs earlier in G1 than NM-binding of MCM2.

Using an immunofluorescence based measure of the proportion of cells with MCM2, the data show that populations are relatively uniform with a similar number of positive cells at 24 hours after release, as at 15 hours (Fig. 1D), in all cases exclusively nuclear. Thus, the quantity increase observed by western blot at 19 hours does not reflect expression in a greater number of cells. Looking specifically at the detergent-resistant fraction of MCM2, a

significant fall in numbers is seen at 17 hours, consistent with the suggestion that MCM2 may be unstable at this time.

***MCM2 is transiently bound to the NM*** Detergent-resistant proteins are immobilized by interaction with cellular components that are themselves not elutable under physiological buffer conditions; in the nucleus this means chromatin and/or the NM. By increasing NaCl concentration proteins are eluted with different profiles, exemplified here with cyclins A and E,[20] and histone H3 (Fig. 2A). MCM2 is released gradually from asynchronous cells between 0.1 and 1 M NaCl, describing a heterogeneous population, of which the bulk of MCM2 is unable to resist extraction. However, when applied to synchronized cells, a highly resistant sub-population of MCM2 is evident at 19 hours (Fig. 2B), suggesting that MCM2 becomes transiently associated with the NM at this time.

Similar results were obtained using a different NM isolation protocol, in which salt concentration does not exceed 0.5 M, but histones and chromatin-associated proteins are eluted along with DNA fragments after digestion with DNase1. Under these conditions, MCM2 is apparently entirely eluted from asynchronous cells, with none evident in the NM fraction (Fig. 3A). However, when this is applied specifically to a 19 hour population a resistant fraction is evident, estimated to be 4% of total MCM2 within the cell at this time (based on densitometry, Fig. 3A). Similar analysis with an extensive set of antibodies raised against other MCM subunits failed to reveal NM-associated populations. This could reflect underlying biology, however we cannot draw a strong conclusion because none of these antibodies are as sensitive as that used to detect MCM2.

NM isolation by DNase1 extraction was recapitulated over a time course (Fig. 3B), focusing on the 0.5 M NaCl-resistant fraction (chromatin and/or NM), generating consistent results, which show a resistant fraction of MCM2 at 19 hours, partially persisting in this time course to 20 hours. At 19 hours, 76% of this immobilized fraction of MCM2 is in fact NM bound (resistant to DNase1 extraction), compared to only 5% of histone H3 and 83% of Lamin B2 (based on densitometry, Fig 3B). Immunofluorescence analysis of the 0.5 M NaCl-resistant fraction of MCM2 with (NM) and without (NM and chromatin) digestion with

DNase1, again identified a resistant fraction at 19 hours (Fig. 3C). This shows the number of cells with MCM2 in the nucleus regardless of intensity. The data argue that the 0.5 M resistant fraction that exists at 19 hours reflects the behavior of the majority of cells. No decrease in fluorescence intensity was observed in the chromatin-depleted (NM) population compared to the mock treated (NM and chromatin) population (Fig. 3D), showing that all of the protein that resists 0.5 M NaCl is in fact attached to the NM. Together the data argue that even though only a small fraction of MCM2 is resistant to DNase1 (Fig. 3B), this is the case for around half of the cells at 19 hours after release from quiescence (Fig. 3C). Moreover, as resistance is a transient state, which may in fact last less than an hour, it is likely that more than 50% of the population pass through this state at around this time in late G1 phase.

***MCM2 is tightly associated with chromatin after initiation*** When cells were treated (prior to extraction) with dithiobis succinimidyl propionate (DTSP), a cell-permeable reducing cross-linker which binds proteins to proteins,[21] additional binding characteristics were inferred. While the number of nuclei with MCM2, and detergent-resistant MCM2 remained generally high across the time course, the 0.5 M NaCl-resistant fraction reports on distinct time-dependent shifts (Fig. 4A). Again a peak is observed at 19 hours, consistent with transient association with the NM, and there was no reduction in fluorescence intensity for MCM2 after depletion of chromatin at this point (Fig. 4B). However at 24 hours the response to digestion with DNase1 distinguishes a fraction of MCM2 that is not bound to the NM but is cross-linked to proteins that are themselves tightly-associated with chromatin (possibly stabilization of the heterohexameric ring), and which resists 0.5 M NaCl.

**Discussion**

Abnormalities in DNA replication are linked to disease (reviewed in ref. 22), and in particular to the licensing of DNA for replication (reviewed in ref. 23). Inappropriate licensing can lead to re-replication, replication stress and genomic instability,[23] which is a powerful driver toward acquisition of mutations. MCM proteins, as well as other components of the pre-RC, have been shown to be elevated in a range of cancer types,[24-33] and MCM complex proteins have been shown to have diagnostic value.[34] The mechanistic implications of elevated expression and potential strategies to intervene, hinge on a detailed knowledge of the process as it occurs in mammalian cells. Previous work in yeast,[35] *Xenopus*,[4] cancer cells,[36, 37] and CHO cells,[38] all demonstrate stable immobilisation of MCM2 in the nucleus during G1 phase, however these analyses do not further define the binding properties over this crucial period or distinguish NM-bound MCM from chromatin-bound MCM.

Using controlled extraction criteria we have shown a transient relationship between MCM2 and the NM, immediately before the majority of cells first produce nascent DNA. In the cell populations illustrated in Fig. 1A approximately 20% have begun to incorporate nascent DNA by 18/19 hours, with the majority delayed by a further 2-3 hours, indicating that NM-association is coincident with or precedes DNA synthesis.

In fact the data show three states of MCM binding (Fig. 4C); i. resistance to detergent but extraction with DNase1 or 2 M NaCl identifies a chromatin–associated nuclear fraction before 19 hours, ii. resistance to all extraction conditions identifies a transient attachment to the NM at 19 hours, iii. cross-linking to DNase1-sensitive protein that is resistant to 0.5 M NaCl identifies tight association with chromatin after 19 hours. Based on timing in relation to initiation of DNA replication and cyclin A expression (Fig. 1A), we suggest that this represents i. pre-initiation chromatin binding, ii. ‘functional loading’ , and, iii. post-initiation helicase presence on chromatin. We use the term ‘functional loading’ in order to distinguishing what happens at the NM from chromatin binding. It is clear that MCM2 is bound to chromatin both before and after its transient association with the NM, so NM-association is not likely to reflect loading as defined in most other studies (which do not

normally look at the effect of nuclease extraction and so largely report on chromatin binding). It is also clear that chromatin binding can be detected before DNA synthesis, so is not on its own sufficient to support initiation. Our hypothesis is that chromatin binding is converted to a 'functionally loaded' state at the NM. However, this may not yet be active helicase as the MCM complex appears to be located away from the NM (Fig. 4A) and outside of factories [37] at times when DNA synthesis is detected. Failure of MCM proteins to co-localize with newly synthesized DNA [39, 40] unless analyzed in relation to labeled DNA from the previous cell cycle [37] suggests that they are recruited to replication factories prior to initiation, but occupy remote sites during the synthesis phase. Thus, if helicase and polymerase function at the same time they appear not to do it in the same place. It therefore seems unlikely that MCM helicase is 'activated' during its brief association with the NM. For this reason we use the term 'functional loading' to distinguish this transient and highly extraction-resistant state from the more commonly used descriptions of 'loading' and 'activation'.

The abundance of MCM proteins is far higher than other components of the pre-RC,[41] and in excess of the number of activated origins of replication. Although multiple copies appear to be present at each origin, and some are loaded at secondary sites such as those that are activated by replication fork arrest,[42, 43] only a small fraction of MCM protein appears to be functionally assembled. In yeasts, use of degron mutants confirmed that very small amounts of MCM are required for initiation, but significantly more for elongation.[44] A stoichiometric excess of MCM complex may be significant, helping to ensure availability for parallel, synchronous and complete loading at all origins at a specific point in G1 phase. Our data is consistent with this picture, but could also reflect a very brief association with the NM for a far greater proportion of available protein than the 4% detected here (Fig. 3A). In fact after the 19 hour loading period MCM2 is in a different state to before 19 hours, and this applies to approximately half of the MCM protein in half of the nuclei quantified. Thus, the data are also consistent with a loading pipeline in which only ~4% of total MCM2 occupies the loading bay at any one time.

The diffuse nature of replication origins in higher eukaryotic cells (reviewed in ref.

45), argues that structural determinants related to transcription specify their location on the template, while association with an active helicase defines their status as a functional site. The data presented here suggest that functional loading of the MCM complex is specified by activities that are themselves located at the NM, implying that origin selection is governed by template recruitment to these sites. MCM2 has been linked with the NM anchoring protein AKAP95, and disruption of its interaction is shown to inhibit both initiation and elongation of DNA replication, consistent with the idea that NM-association is a requirement for MCM to function in the cellular context.[46]

In summary, this study adds to the growing evidence that initiation of DNA replication is spatially constrained by immobilization on the NM in mammalian cells, and suggests that functional assembly of the MCM complex occurs during transient presence in NM-associated loading bays. However it does not explain why association is transient, or shed light on the mechanism of loading or the regulation of ring opening. Although the open center of the MCM2-7 hexamer is large enough to accommodate either single stranded DNA or double stranded DNA,[47, 48] recent studies suggest that when incorporated into the CMG complex it encircles single stranded DNA.[49, 50] If reconciled with the idea that MCM proteins are located outside of replication factories during DNA synthesis, this implies that template DNA is in single stranded form between the site of DNA synthesis and the site of helicase action. Consistent with our observations, these data also argue that the MCM2-7 hexamer undergoes different conformations and assembly states during the transition from loading to activation.[50] Our data identify a specific point in time and location at the NM, offering a direct route to the identification of the factors that spatially constrain the MCM complex and mediate its transition from one state to another at this critical point in the initiation process in mammalian cells.

## Materials and methods

**Cell culture** Murine 3T3 cells were grown in Dulbecco's modified Eagle's medium (DMEM) with 10% foetal bovine serum and penicillin/streptomycin/glutamine (10 u/ml, 10 µg/ml, 2.92 mg/ml respectively) on culture dishes (Nunclon), or on glass coverslips, and synchronized in quiescence by contact inhibition and serum depletion as described previously.[19] Cells were released into cycle by splitting ¼ into fresh media. Click-iT Edu Cell Proliferation Assay kit (Life Technologies, Cat: C10337) was used as recommended, to analyse the percentage of cells in S phase after a 30 minute labeling period.

**Cellular fractionation** Total cell lysates were prepared from adherent cells after rinsing in cold PBS and scape harvesting into cold cytoskeletal buffer (CSK; 10 mM Pipes pH 6.8, 300 mM sucrose, 100 mM NaCl, 1 mM $MgCl_2$, 1 mM EGTA, 1 mM DTT), with protease inhibitor cocktail (cOmplete®, EDTA-free; Roche) and 2 mM PMSF, as indicated. For separation into detergent-soluble (SN) and detergent-resistant (pellet, P) fractions, lysates were supplemented with 0.1% triton X-100, incubated on ice for 2 minutes and separated by centrifugation. Serial salt extractions were performed as described previously,[51] in cold CSK supplemented with protease inhibitors and the indicated concentration of NaCl. Insoluble material was removed by centrifugation after 5 minute incubations on ice in each buffer, and resuspended in a volume of CSK equal to the starting lysate.

NM isolation was carried out as described previously.[52] Cell lysates were harvested and supplemented with 0.1% triton X-100, divided into three aliquots, and separated into pellet and supernatant by centrifugation. Pellets were washed by resuspension in CSK plus 0.1% triton X-100 and 0.5 M NaCl and salt wash supernatant (W) recovered by centrifugation. Pellets were rinsed in DNase1 buffer (400 mM Tris-HCl, 100 mM NaCl, 60 mM $MgCl_2$, 10 mM $CaCl_2$ pH 7.9), resuspended in the same buffer and incubated at 37°C with DNase1 (RNase free, Roche), or in buffer alone (Mock). After one-hour samples were supplemented with 0.5 M NaCl and separated into SN and P by centrifugation. Cell equivalents were analysed by western blot.

**Western blot analysis** All fractions were immediately boiled in SDS-PAGE sample buffer (240 mM Tris pH 6.8, 8% SDS, 40% glycerol, 0.1% bromophenol blue and 6.8% β mecaptoethanol). Samples were separated by 8% SDS-PAGE, transferred to nitrocellulose or PVDF, blocked with 1 x TBS, 10% dried milk, 0.1% Tween 20, and probed with anti-MCM2 at 1/1000 (BM28, BD Transduction Laboratories), anti-cyclin A at 1/1000 (C4710, Sigma), anti-lamin B2 at 1/1000 (ab138516, Abcam), anti-histone H3 at 1/10 000 (ab1791, Abcam) anti-actin at 1/1000 (AC40, Sigma), anti-cyclin E at 1/500 (ab7959-1, Abcam) or anti-Cdc6 at 1/250 (sc-9964, Santa Cruz Biotech). Secondary antibodies, anti-mouse HRP (ab6789, Abcam) and anti- rabbit HRP (ab6721, Abcam), were used at 1/10 000. Blots were developed using enhanced chemiluminescence (ECL) solution (Amersham). Blots were quantified using NIH ImageJ. Quantification is comparable within each dataset but not between different datasets as all values are relative.

**Immunofluorescence** Cells grown on coverslips were washed in PBS, and either fixed immediately in 4% paraformaldehyde (PFA), to visualise 'total' protein, or washed with 0.1% triton X-100 in CSK, then PBS before fixing in 4% PFA (detergent resistant samples). DNase1 and Mock samples were washed first in CSK plus 0.1% triton X-100, then CSK plus 0.1% triton X-100 and 0.5 M NaCl, and twice in DNase1 incubation buffer before incubation with DNase1, (RNase free, Roche) diluted in incubation buffer (DNase) or incubation buffer only (Mock), for one hour at 37°C. Cells were further washed in CSK plus 0.1% triton X-100 and 0.5 M NaCl, followed by PBS before fixing in 4% PFA.[52] Coverslips were rinsed in PBS, then blocked in 10% BSA, 0.02% SDS, 0.1% triton X-100 in PBS, before incubation with anti-MCM2 at 1/50 (BM28, BD Transduction Laboratories), or anti-Lamin B2 1/100 (ab138516, Abcam). DNA was counterstained with Hoechst 33258. Images were collected using a Zeiss Axiovert 200 M and Openlab image acquisition software, using constant image acquisition parameters. Three technical replicates were analysed for all samples ($n \geq 99$ for each).

**Cross-linking** Cells growing on 15 cm dishes were washed three times with PBS at room temperature, then incubated in 15 ml cross-link buffer (PBS, 1 mM $MgCl_2$, 0.01% triton X-

100) with DTSP (Sigma) at 200 μg/ml, on a rotary shaker for 10 minutes.[51] Reactions were quenched with 10 ml 10 mM Tris-HCl pH 7.6, 1 mM EDTA, before extraction as described.

**Statistics** Analyses were performed using students T-test, with significance indicated by stars; *** $p<0.001$, ** $p<0.01$, * $p<0.05$. Error bars are standard error of the mean (SEM) in all cases.

**Acknowledgements**

This work was funded by Yorkshire Cancer Research (Y002PhD). We thank Justin Ainscough for critical comments on the manuscript and Eve Ainscough for graphics.

**Author contributions**

ELH designed experiments, acquired and analysed data and wrote the manuscript. JK and RHCW acquired and analysed data. JC advised on design and helped write the manuscript. DC designed experiments, analysed data and wrote the manuscript.

**Conflict of interest**

The authors declare no competing commercial interests in this work.

**References**

1. Capco DG, Wan KM, Penman S. The nuclear matrix: three-dimensional architecture and protein composition. Cell 1982; 29:847-58.
2. Cook PR. The nucleoskeleton and the topology of replication. Cell 1991; 66:627-35.
3. Wilson RH, Coverley D. Relationship between DNA replication and the nuclear matrix. Genes Cells 2013; 18:17-31.
4. Chong JPJ, Mahbubani HM, Khoo C-Y, Blow JJ. Purification of an MCM-containing complex as a component of the replication licensing system. Nature 1995; 375:418-21.
5. Coster G, Frigola J, Beuron F, Morris Edward P, Diffley John FX. Origin Licensing Requires ATP Binding and Hydrolysis by the MCM Replicative Helicase. Molecular Cell.
6. Moyer SE, Lewis PW, Botchan MR. Isolation of the Cdc45/Mcm2-7/GINS (CMG) complex, a candidate for the eukaryotic DNA replication fork helicase. Proceedings of the National Academy of Sciences of the United States of America 2006; 103:10236-41.
7. Labib K. How do Cdc7 and cyclin-dependent kinases trigger the initiation of chromosome replication in eukaryotic cells? Genes & Development 2010; 24:1208-19.
8. Gros J, Devbhandari S, Remus D. Origin plasticity during budding yeast DNA replication *in vitro*. The EMBO journal 2014; 33:621-36.

9. On KF, Beuron F, Frith D, Snijders AP, Morris EP, Diffley JFX. Prereplicative complexes assembled *in vitro* support origin-dependent and independent DNA replication. The EMBO journal 2014; 33:605-21.
10. Lyubimov AY, Costa A, Bleichert F, Botchan MR, Berger JM. ATP-dependent conformational dynamics underlie the functional asymmetry of the replicative helicase from a minimalist eukaryote. Proceedings of the National Academy of Sciences of the United States of America 2012; 109:11999-2004.
11. Samel SA, Fernandez-Cid A, Sun J, Riera A, Tognetti S, Herrera MC, Li H, Speck C. A unique DNA entry gate serves for regulated loading of the eukaryotic replicative helicase MCM2-7 onto DNA. Genes & Development 2014; 28:1653-66.
12. Fujita M, Ishimi Y, Nakamura H, Kiyono T, Tsurumi T. Nuclear organization of DNA replication initiation proteins in mammalian cells. J Biol Chem 2002; 277:10354-61.
13. Burkhart R, Schulte D, Hu B, Musahl C, Gohring F, Knippers R. Interactions of human nuclear proteins P1Mcm3 and P1Cdc46. Eur J Biochem 1995; 228:431-8.
14. Fujita M, Kiyono T, Hayashi Y, Ishibashi M. *In vivo* interaction of human MCM heterohexameric complexes with chromatin. Possible involvement of ATP. J Biol Chem 1997; 272:10928-35.
15. Stoeber K, Mills AD, Kubota Y, Krude T, Romanowski P, Marheineke K, Laskey RA, Williams GH. Cdc6 protein causes premature entry into S phase in a mammalian cell-free system. Embo J 1998; 17:7219-29.
16. Cook JG, Chasse DA, Nevins JR. The regulated association of Cdt1 with minichromosome maintenance proteins and Cdc6 in mammalian cells. J Biol Chem 2004; 279:9625-33.
17. Mendez J, Stillman B. Chromatin association of human origin recognition complex, cdc6, and minichromosome maintenance proteins during the cell cycle: assembly of prereplication complexes in late mitosis. Mol Cell Biol 2000; 20:8602-12.
18. Cook JG, Park C-H, Burke T, Leone G, DeGregori J, Engel A, Nevins J. Analysis of Cdc6 function in the assembly of mammalian prereplication complexes. Proc Natl Acad Sci USA 2002; 99:1347-52.
19. Coverley D, Laman H, Laskey RA. Distinct roles for cyclins E and A during DNA replication complex assembly and activation. Nature Cell Biology 2002; 4:523-8.
20. Munkley J, Copeland NA, Moignard V, Knight JR, Greaves E, Ramsbottom SA, Pownall ME, Southgate J, Ainscough JF, Coverley D. Cyclin E is recruited to the nuclear matrix during differentiation, but is not recruited in cancer cells. Nucleic Acids Res 2011; 39:2671-7.
21. Baumert HG, Fasold H. Cross-linking techniques. Methods Enzymol 1989; 172:584-609.
22. Masai H, Matsumoto S, You Z, Yoshizawa-Sugata N, Oda M. Eukaryotic Chromosome DNA Replication: Where, When and How? In: Kornberg RD, Raetz CRH, Rothman JE, Thorner JW, eds. Annual Review of Biochemistry, Vol 79, 2010:89-130.
23. Blow JJ, Gillespie PJ. Replication licensing and cancer - a fatal entanglement? Nature Reviews Cancer 2008; 8:799-806.
24. Gonzalez MA, Tachibana KK, Laskey RA, Coleman N. Innovation - Control of DNA replication and its potential clinical exploitation. Nature Reviews Cancer 2005; 5:135-41.
25. Hook SS, Lin JJ, Dutta A. Mechanisms to control rereplication and implications for cancer. Current opinion in cell biology 2007; 19:663-71.
26. Williams GH, Stoeber K. Cell cycle markers in clinical oncology. Current opinion in cell biology 2007; 19:672-9.
27. Xouri G, Lygerou Z, Nishitani H, Pachnis V, Nurse P, Taraviras S. Cdt1 and geminin are down-regulated upon cell cycle exit and are over-expressed in cancer-derived cell lines. Eur J Biochem 2004; 271:3368-78.
28. Lau E, Tsuji T, Guo L, Lu S-H, Jiang W. The role of pre-replicative complex (pre-RC) components in oncogenesis. Faseb Journal 2007; 21:3786-94.
29. Dudderidge TJ, Kelly JD, Wollenschlaeger A, Okoturo O, Prevost T, Robson W, Leung HY, Williams GH, Stoeber K. Diagnosis of prostate cancer by detection of

minichromosome maintenance 5 protein in urine sediments. British journal of cancer 2010; 103:701-7.
30. Lau KM, Chan QKY, Pang JCS, Li KKW, Yeung WW, Chung NYF, Lui PC, Tam YS, Li HM, Zhou L, et al. Minichromosome maintenance proteins 2, 3 and 7 in medulloblastoma: overexpression and involvement in regulation of cell migration and invasion. Oncogene 2010; 29:5475-89.
31. Neskoromna-Jedrzejczak A, Tyndorf M, Arkuszewski P, Kobos J. Potential prognostic value of MCM2 expression evaluation in oral cavity squamous cell carcinoma. Wspolczesna Onkologia-Contemporary Oncology 2010; 14:196-9.
32. Kelly JD, Dudderidge TJ, Wollenschlaeger A, Okoturo O, Burling K, Tulloch F, Halsall I, Prevost T, Prevost AT, Vasconcelos JC, et al. Bladder Cancer Diagnosis and Identification of Clinically Significant Disease by Combined Urinary Detection of Mcm5 and Nuclear Matrix Protein 22. Plos One 2012; 7.
33. Williams GH, Stoeber K. The cell cycle and cancer. Journal of Pathology 2012; 226:352-64.
34. Coleman N, Laskey RA. Minichromosome maintenance proteins in cancer screening. European journal of cancer (Oxford, England : 1990) 2009; 45 Suppl 1:416-7.
35. Donovan S, Harwood J, Drury LS, Diffley JF. Cdc6-dependent loading of Mcm proteins onto pre-replicative chromatin in budding yeast. Proc Natl Acad Sci USA 1997; 94:5611-6.
36. Symeonidou I-E, Kotsantis P, Roukos V, Rapsomaniki M-A, Grecco HE, Bastiaens P, Taraviras S, Lygerou Z. Multi-step loading of human minichromosome maintenance proteins in live human cells. Journal of Biological Chemistry 2013; 288:35852-67.
37. Aparicio T, Megias D, Mendez J. Visualization of the MCM DNA helicase at replication factories before the onset of DNA synthesis. Chromosoma 2012; 121:499-507.
38. Kuipers MA, Stasevich TJ, Sasaki T, Wilson KA, Hazelwood KL, McNally JG, Davidson MW, Gilbert DM. Highly stable loading of Mcm proteins onto chromatin in living cells requires replication to unload. J Cell Biol 2011; 192:29-41.
39. Krude T, Musahl C, Laskey RA, Knippers R. Human replication proteins hCdc21, hCdc46 and P1Mcm3 bind chromatin uniformly before S-phase and are displaced locally during DNA replication. J Cell Sci 1996; 109:309-18.
40. Dimitrova DS, Todorov IT, Melendy T, Gilbert DM. Mcm2, but not RPA, is a component of the mammalian early G1-phase prereplication complex. Journal of Cell Biology 1999; 146:709-22.
41. Lei M, Kawasaki Y, Tye BK. Physical interactions among Mcm proteins and effects of Mcm dosage on DNA replication in *Saccharomyces cerevisiae*. Molecular and Cellular Biology 1996; 16:5081-90.
42. Ge XQ, Jackson DA, Blow JJ. Dormant origins licensed by excess Mcm2-7 are required for human cells to survive replicative stress. Genes & Development 2007; 21:3331-41.
43. Ibarra A, Schwob E, Mendez J. Excess MCM proteins protect human cells from replicative stress by licensing backup origins of replication. Proceedings of the National Academy of Sciences of the United States of America 2008; 105:8956-61.
44. Liang DT, Hodson JA, Forsburg SL. Reduced dosage of a single fission yeast MCM protein causes genetic instability and S phase delay. Journal of Cell Science 1999; 112:559-67.
45. Mechali M. Eukaryotic DNA replication origins: many choices for appropriate answers. Nat Rev Mol Cell Biol 2010; 11:728-38.
46. Eide T, Tasken KA, Carlson C, Williams G, Jahnsen T, Tasken K, Collas P. Protein kinase A-anchoring protein AKAP95 interacts with MCM2, a regulator of DNA replication. J Biol Chem 2003; 278:26750-6.
47. Evrin C, Clarke P, Zech J, Lurz R, Sun J, Uhle S, Li H, Stillman B, Speck C. A double-hexameric MCM2-7 complex is loaded onto origin DNA during licensing of eukaryotic DNA replication. Proceedings of the National Academy of Sciences of the United States of America 2009; 106:20240-5.

48. Remus D, Beuron F, Tolun G, Griffith JD, Morris EP, Diffley JFX. Concerted loading of Mcm2-7 double hexamers around DNA during DNA replication origin licensing. Cell 2009; 139:719-30.
49. Fu YV, Yardimci H, Long DT, The Vinh H, Guainazzi A, Bermudez VP, Hurwitz J, van Oijen A, Schaerer OD, Walter JC. Selective bypass of a lagging strand roadblock by the eukaryotic replicative DNA helicase. Cell 2011; 146:930-40.
50. Costa A, Renault L, Swuec P, Petojevic T, Pesavento JJ, Ilves I, MacLellan-Gibson K, Fleck RA, Botchan MR, Berger JM. DNA binding polarity, dimerization, and ATPase ring remodeling in the CMG helicase of the eukaryotic replisome. Elife 2014; 3.
51. Ainscough JF, Rahman FA, Sercombe H, Sedo A, Gerlach B, Coverley D. C-terminal domains deliver the DNA replication factor Ciz1 to the nuclear matrix. J Cell Sci 2007; 120:115-24.
52. Wilson RHC, Hesketh EL, Coverley D. Preparation of the nuclear matrix for parallel microscopy and biochemical analyses. Cold Spring Harb Protoc in press; 10.1101/pdb.prot083758.

**Legends**

**Fig. 1 Entry to S phase and expression of MCM2** A) Mouse 3T3 cells re-enter the cell cycle from quiescence in a temporally well-defined manner, passing out of quiescence (Q) and through the restriction point (R) after ~15 hours. They enter S phase (S) as a wave of cells from 16 hours onwards, with the majority of the population first incorporating labelled nucleotides after 20 hours. The percentage of cells engaged in DNA synthesis (black), and relative concentration of cyclin A protein, estimated by densitometry (averaged from three biological replicates) and expressed after normalisation to actin (orange), is shown. Inserts (top), show example western blots of cyclin A and actin, and (bottom) micrographs showing incorporation of Edu into newly synthesized DNA in replicating cells (red). DNA is blue. Scale bar is 10 μm. B) Western blots, and derived quantification, of MCM2 and actin in total cell lysates harvested into CSK buffer (upper), and after separation into detergent-soluble supernatant, and detergent-resistant pellet (nuclei, lower). C) MCM2, CDC6 and histone H3 in whole cell lysates and detergent resistant pellet (nuclei). CDC6 chromatin binding precedes MCM2 binding. D) The percentage of cells with MCM2 in the nucleus, detected by immunofluorescence (IF). All labelled cells were scored regardless of intensity, without prior extraction (total MCM2), and after extraction with 0.1% triton X-100 (detergent resistant). Error bars show SEM of three replicates ($n \geq 100$ for each). Representative images of MCM2 (green) and DNA (blue) are inset. Scale bar is 10 μm.

**Fig. 2 MCM2 is transiently resistant to high-salt extraction.** A) Protein fractions from asynchronous 3T3 cells derived by sequential NaCl washes showing MCM2, cyclins E, and A and histone H3 in the supernatants (SN). 2M pellet (P) represents the resistant fraction that includes the nuclear-matrix. B) Protein fractions prepared from synchronized cells in mid G1 to early S phase, using the indicated sequential NaCl concentrations, showing partitioning of MCM2 over time. Total cyclin A and actin are shown for reference. The 19 hour point contains a sub-population of MCM2 that is highly resistant to extraction (NM-associated), indicated by dotted white lines. Graph shows quantification of MCM2 levels from western

blots by densitometry (arbitrary units). Levels can be compared within each time course but not between different fractions. Results are shown relative to the lowest time point in all cases, except 2 M pellet fraction which is shown on a different scale to illustrate the peak at 19 hours.

**Fig. 3. MCM2 is transiently resistant to DNase1 extraction.** A) Protein fractions prepared from asynchronous 3T3 cells, and from G1 phase cells harvested at 19 hours, showing MCM2, histone H3 (to reveal efficiency of chromatin digestion) and lamin B2 (to reveal the residual nucleus). Detergent-resistant pellet (P), detergent-soluble supernatant (SN), 0.5 M NaCl wash (W), DNase1-resistant pellet (P, NM indicated with dotted lines), DNase-soluble supernatant (SN, chromatin), mock treatment-resistant pellet (P, NM and chromatin) and mock treatment-soluble supernatant (SN). A fraction of the total MCM2 in the cell resists extraction at 19 hours, but is not detectable in the asynchronous population. B) Western blots of 0.5 M washed pellets after treatment with DNase1 or mock treatment, from an independent experiment harvested at 14 hours (pre-R), 17 hours (few cells in S phase), 19 hours (most cells initiating) and 20 hours. C) Percentage of cells with MCM2 in the nucleus after DNase1 (NM) or mock treatment (NM and chromatin), detected by IF ($n \geq 100$ for each). Data shown for the 19 hour time point are the average of two biological replicates and three technical replicates. All other time points show the average of three technical replicates. All error bars show SEM. Representative images show MCM2 (green), DNA (blue) and lamin B2 (red). Scale bar is 10 μm. D) Mean MCM2 fluorescence intensity (left) of DNase1 ($n = 100$) and mock-extracted ($n = 110$) 19 hours nuclei, and intensity distribution (right, showing upper bin value).

**Fig. 4. Post-initiation association with chromatin, revealed by crosslinking with DTSP.** A) The percentage of nuclei with MCM2, detected by immunofluorescence, in synchronized, cross-linked populations showing total protein, detergent-resistant protein, DNase1-resistant, and 0.5 M NaCl-resistant protein (mock) ($n \geq 100$ for each). Representative images show

MCM2 (green), DNA (blue) and lamin B2 (red). Scale bar is 10 μm. B) Mean MCM2 fluorescence intensity after DNase1 or mock extraction at 19 hours, (n = 99 and 105 respectively, left) and at 24 hours (n = 107 and 101 respectively, centre). A comparison of DNase1 resistant MCM2 at 19 and 24 hour is also shown (n = 99 and 107 respectively, right). C) Schematic showing three states of MCM complex binding in late G1 phase, superimposed on the prevailing model of DNA replication in higher eukaryotic nuclei, in which the replication machinery is at chromatin loop bases on the nuclear matrix, with newly synthesized DNA extruded as nascent daughter loops.[2] Our data suggest that i. before initiation the MCM complex exists as a chromatin–associated nuclear protein, ii. functional loading immediately prior to initiation takes place coincidently with transient attachment to the NM, iii. after initiation the MCM complex is functionally bound to chromatin but no longer associated with the NM.

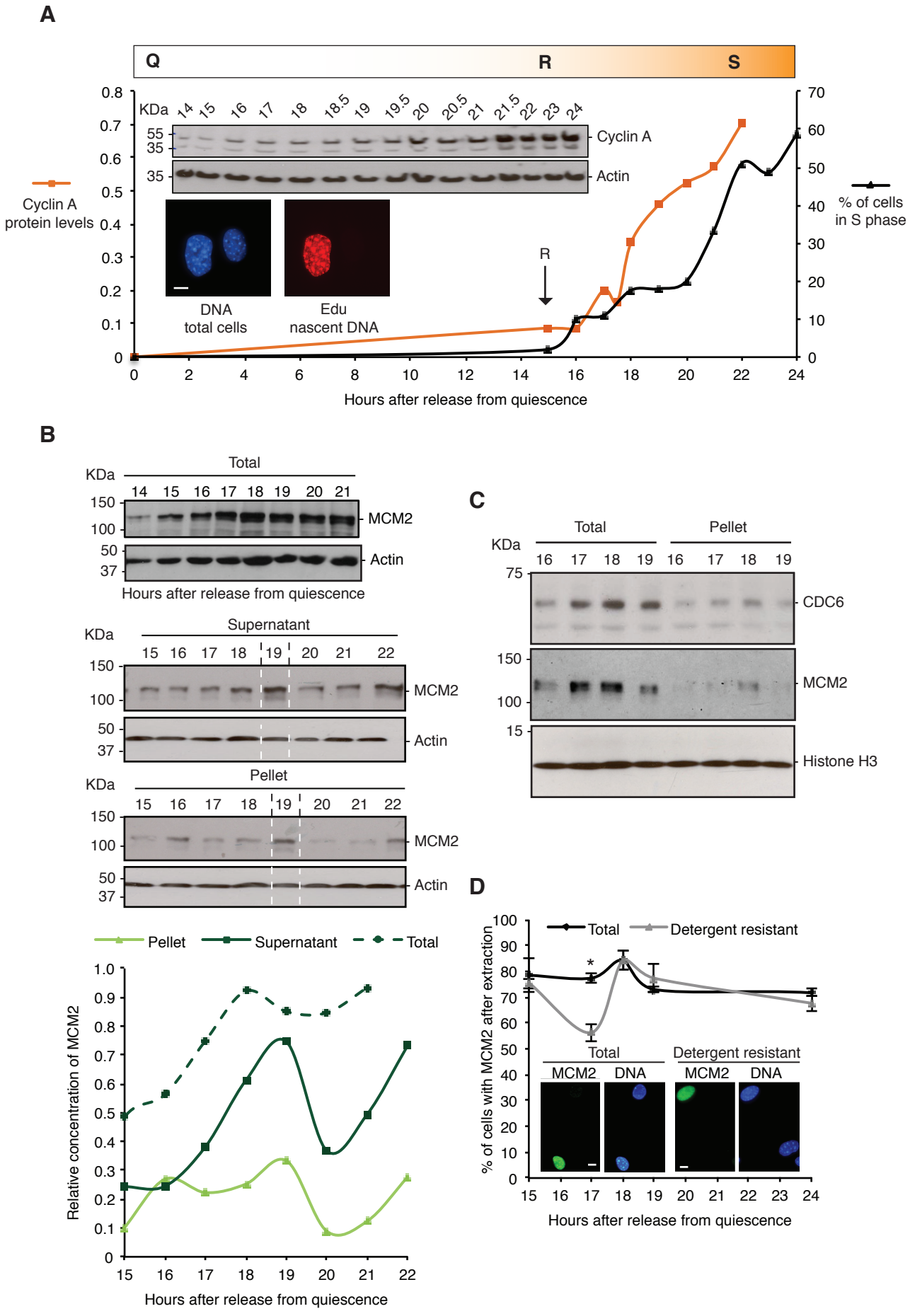


Figure 1. Hesketh et al 2014

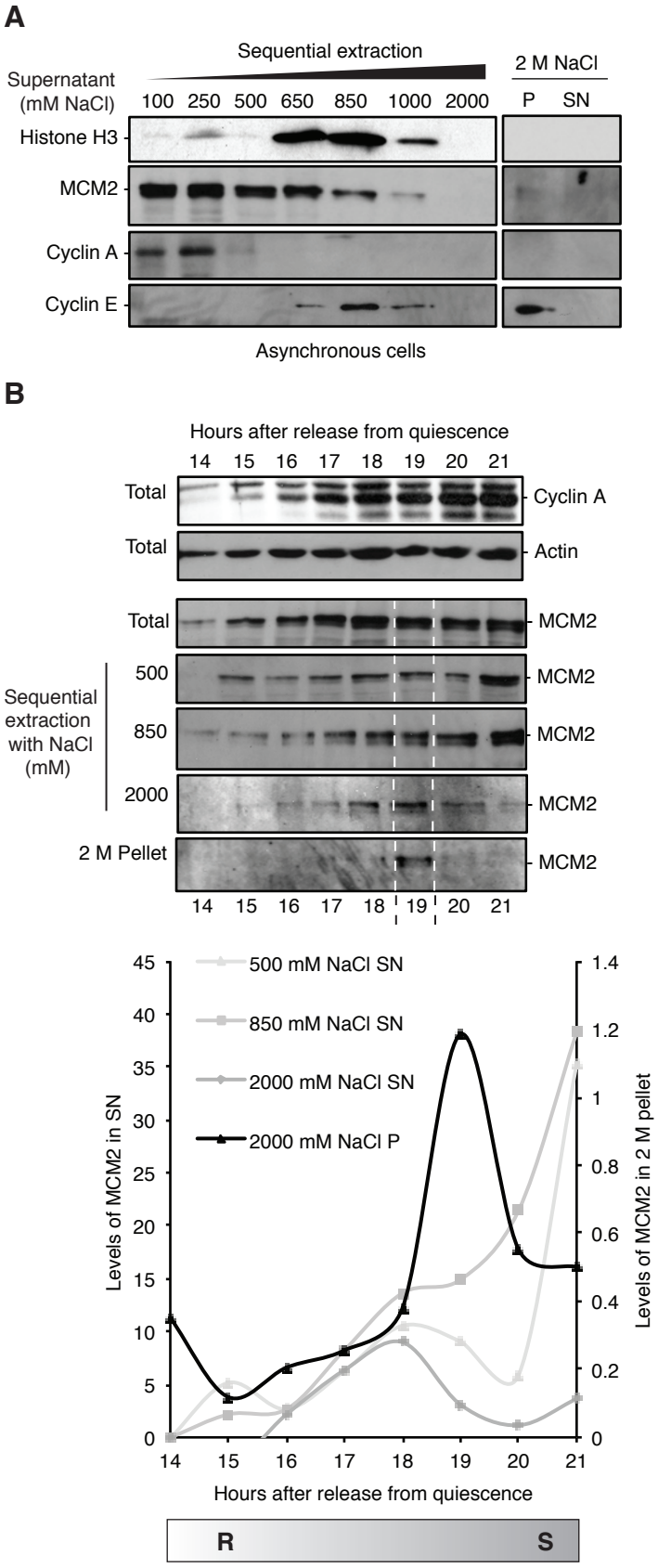


Figure 2. Hesketh et al 2014

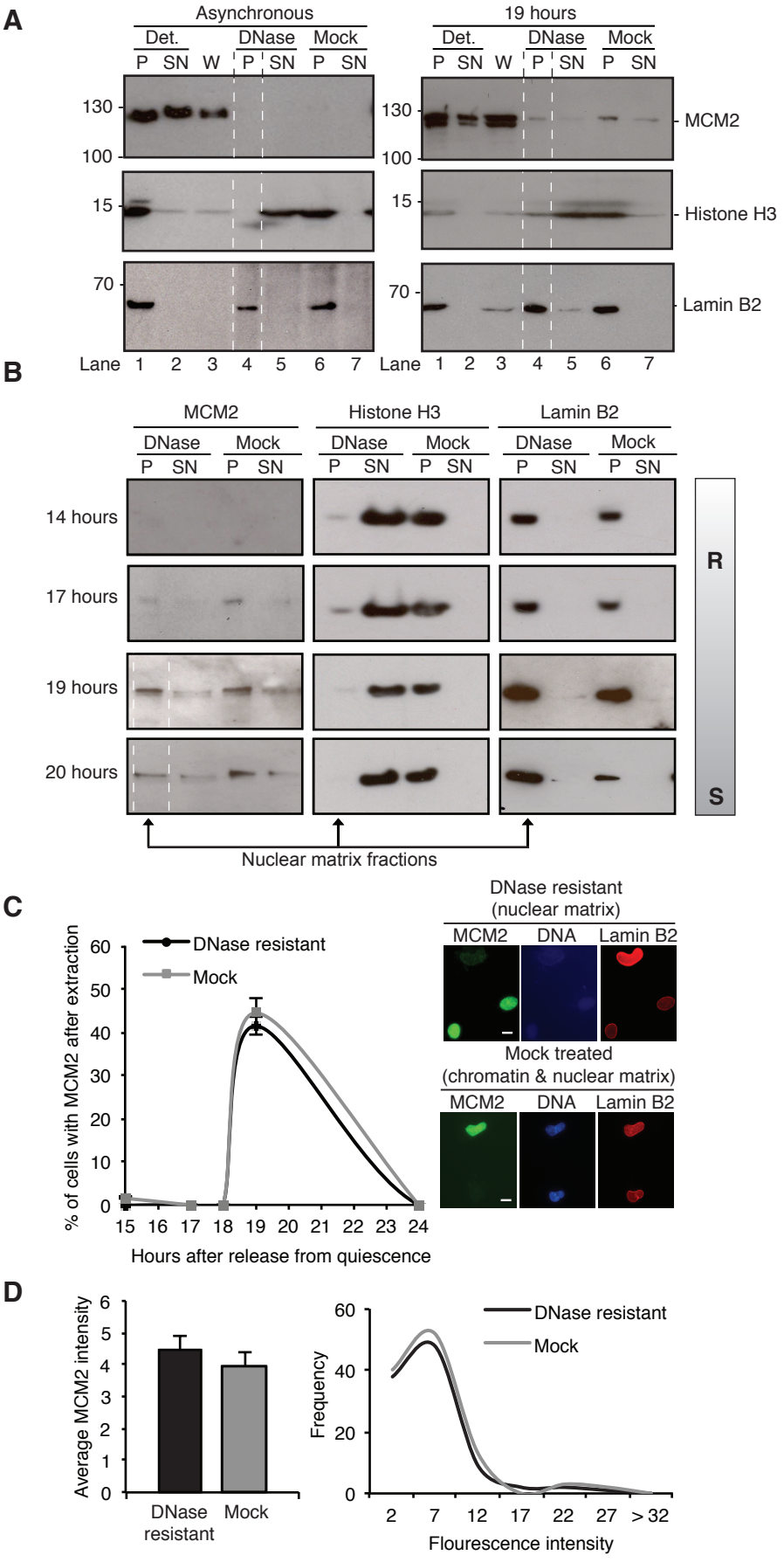


Figure 3. Hesketh et al. 2014

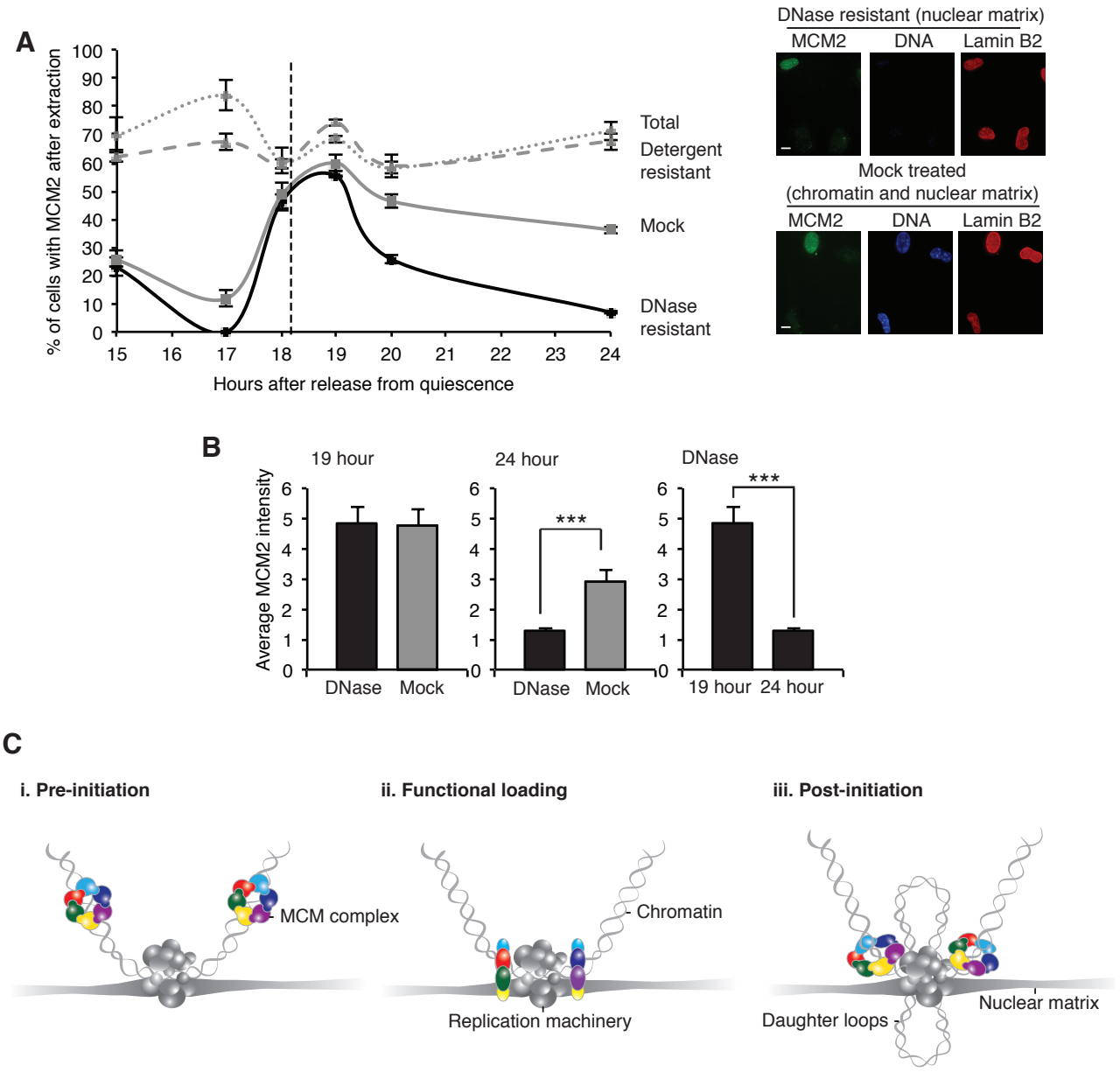


Figure 4. Hesketh et al 2014

# Abbreviations

| | |
|---|---|
| °C | degrees centigrade |
| 3D | three dimensional |
| A | alanine |
| aa | amino acids |
| ACS | ARS consensus sequence |
| AEBSF | 4-(2-Aminoethyl) benzenesulfonyl fluoride hydrochloride |
| APS | ammonium persulphate |
| ARS | autonomous replication sequence |
| ATP | adenosine 5'triphosphate |
| ATPase | ATP hydrolysis |
| bp | base pair |
| BSA | bovine serum albumin |
| Bq | becquerel |
| Cdc6 | cell division cycle 6 |
| Cdc7 | cell division cycle 7 |
| Cdc45 | cell division cycle 45 |
| CDK | cyclin dependent kinase |
| Cdt1 | chromosome licensing and DNA replication factor 1 |
| Ci | Curie |
| CMG | Cdc45-MCM2-7-GINS |
| CPK | creatine phosphate kinase |
| CSK | cytoskeletal buffer |
| CTP | cytidine triphosphate |
| CV | column volumes |
| D | aspartic acid |
| dATP | deoxyadenosine triphosphate |
| Dbf4 | Dumbbell-forming 4, |
| dCTP | deoxycytidine triphosphate |
| $ddH_20$ | double distilled $H_20$ |
| DDK | Dbf4-dependent kinase |

| | |
|---|---|
| dGTP | deoxygyanosine triphosphate |
| $dH_20$ | distilled $H_20$ |
| DMEM | Dulbecco's modified Eagle's medium |
| DNA | Deoxyribonucleic acid |
| Dpb11 | DNA polymerase B possible subunit 11 |
| dPBS | Dulbecco's phosphate buffered saline |
| Drf1 | Dbf4 related factor 1 |
| *Drosophila* | *Drosophila melanogaster* |
| ds | double stranded |
| DTSP | dithiobis succinimidyl propionate |
| DTT | dithiothreitol |
| dTTP | deoxythymidine triphosphate |
| DUE-B | DNA unwinding element binding protein |
| E | glutamic acid |
| EDTA | ethylenediaminetetraacetic acid |
| EdU | 5-ethynyl-2'-deoxyuridine |
| EGTA | ethylene glycol tetraacetic acid |
| EM | electron microscopy |
| *E. cuniculi* | *Encephalitozoon cuniculi* |
| G0 | quiescence |
| G1 | growth 1 phase |
| G2 | growth 2 phase |
| GEMC1 | geminin coiled coil containing protein |
| GINS | Go, Ichi, Nii and San |
| GTP | guanosine triphosphate |
| HBO1 | Histone acetylase binding to Orc1 |
| HEPES | 4-(2-Hydroxyethyl)piperazine-1-ethanesulfonic acid |
| His-tag | histidine tag |
| hMCM | human minichromosome maintenance complex |
| HOXD13 | homobox protein Hox-D13 |
| HRP | horseradish peroxide |
| *Hs* | human |
| h2i | helix 2 insert |
| IF | immunofluorescence |

| | |
|---|---|
| IPTG | isopropyl β-D-1-thiogalactopyranoside |
| K | lysine |
| Kbp | kilo base pairs |
| KDa | kilodalton |
| Kpsi | kilopound per square inch |
| LB | Luria Bertani broth |
| M | mitosis |
| mA | milliamps |
| MAR | matrix attachment region |
| MCM | minichromosome maintenance |
| min | minutes |
| ms | milliseconds |
| MSSB | MCM single-stranded binding motif |
| *Mt* | *Methanothermobacter thermautotrophicus* |
| NEB | New England Biolabs |
| NES | nuclear export signal |
| NLS | nuclear localisation signal |
| OD | optical density |
| Oligo | oligonucleotide |
| ON | overnight |
| ORC | origin recognition complex |
| Ori | origin of DNA replication |
| PAGE | poly acrylamide gel electrophoresis |
| PBS | phosphate buffered saline |
| PEI | polyethylenimine |
| *Pf* | *Pyrococcus furious* |
| PFA | paraformaldehyde |
| PI | protease inhibitor tablet |
| PMSF | phenylmethanesulfonylfluride |
| PNK | T4 polynucleotide kinase |
| pol | polymerase |
| Pre-IC | pre initiation complex |
| Pre-LC | pre loading complex |
| Pre-RC | pre replication complex |

| | |
|---|---|
| Psf | partner of Sld five |
| PSG | penicillin streptomycin glutamine |
| PVDF | polyvinylidene fluoride |
| Q | quiescence |
| R | restriction point |
| rpm | revolutions per minute |
| RT | room temperature |
| S | DNA synthesis phase |
| S | serine |
| SD | standard deviation |
| SDS | sodium dodecyl sulphate |
| SEM | standard error of the mean |
| Ser | serine |
| SF6 | superfamily 6 |
| SOB | super optimal broth |
| Sld | synthetically lethal with Dpb11 |
| *Sso* | *Sulfolobus solfataricus* |
| *S. cerevisiae* | *Saccharomyces cerevisiae* |
| *S. pombe* | *Schizosaccharomyces pombe* |
| T | threonine |
| TBE | tris borate EDTA |
| TBS | tris buffered saline |
| TEMED | N,N,N′,N′-tetramethylethylenediamine |
| TLC | thin layer chromatography |
| TRIS | tris(hydroxymethyl)aminomethane |
| Tx100 | Triton X-100 |
| UTP | uridine triphosphate |
| vol | volume |
| v/v | volume pre volume |
| w/v | weight per volume |
| WT | wild type |
| *Xenopus* | *Xenopus laevis* |

# References


ADACHI, Y., USUKURA, J. & YANAGIDA, M. 1997. A globular complex formation by Nda1 and the other five members of the MCM protein family in fission yeast. *Genes to Cells,* 2**,** 467-479.

AGUDA, B. D. 2001. Kick-starting the cell cycle: From growth-factor stimulation to initiation of DNA replication. *Chaos,* 11**,** 269-276.

AINSCOUGH, J. F., RAHMAN, F. A., SERCOMBE, H., SEDO, A., GERLACH, B. & COVERLEY, D. 2007. C-terminal domains deliver the DNA replication factor Ciz1 to the nuclear matrix. *Journal of Cell Science,* 120**,** 115-24.

APARICIO, O. M., STOUT, A. M. & BELL, S. P. 1999. Differential assembly of Cdc45p and DNA polymerases at early and late origins of DNA replication. *Proceedings of the National Academy of Sciences of the United States of America,* 96**,** 9130-9135.

APARICIO, O. M., WEINSTEIN, D. M. & BELL, S. P. 1997. Components and dynamics of DNA replication complexes in *S. cerevisiae*: Redistribution of MCM proteins and Cdc45p during S phase. *Cell,* 91**,** 59-69.

APARICIO, T., GUILLOU, E., COLOMA, J., MONTOYA, G. & MENDEZ, J. 2009. The human GINS complex associates with Cdc45 and MCM and is essential for DNA replication. *Nucleic Acids Research,* 37**,** 2087-2095.

APARICIO, T., MEGIAS, D. & MENDEZ, J. 2012. Visualization of the MCM DNA helicase at replication factories before the onset of DNA synthesis. *Chromosoma,* 121**,** 499-507.

ARAKI, H. 2010. Regulatory mechanism of the initiation step of DNA replication by CDK in budding yeast. *Biochimica Et Biophysica Acta-Proteins and Proteomics,* 1804**,** 520-523.

ARIAS, E. E. & WALTER, J. C. 2005. Replication-dependent destruction of Cdt1 limits DNA replication to a single round per cell cycle in *Xenopus* egg extracts. *Genes and Development,* 19**,** 114-126.

ARIAS, E. E. & WALTER, J. C. 2006. PCNA functions as a molecular platform to trigger Cdt1 destruction and prevent re-replication. *Nature Cell Biology,* 8**,** 84-U33.

BAE, B., CHEN, Y.-H., COSTA, A., ONESTI, S., BRUNZELLE, J. S., LIN, Y., CANN, I. K. O. & NAIR, S. K. 2009. Insights into the architecture of the replicative helicase from the structure of an archaeal MCM homolog. *Structure,* 17**,** 211-222.

BALESTRINI, A., COSENTINO, C., ERRICO, A., GARNER, E. & COSTANZO, V. 2010. GEMC1 is a TopBP1-interacting protein required for chromosomal DNA replication. *Nature Cell Biology,* 12**,** 484-U156.

BAUMERT, H. G. & FASOLD, H. 1989. Cross-linking techniques. *Methods Enzymology,* 172**,** 584-609.

BELL, S. P. & DUTTA, A. 2002. DNA replication in eukaryotic cells. *Annual Reviews Biochemistry,* 71**,** 333-74.

BELL, S. P. & STILLMAN, B. 1992. ATP-dependent recognition of eukaryotic origins of DNA replication by a multi-protein complex. *Nature,* 357**,** 128-134.

BEREZNEY, R. & COFFEY, D. S. 1974. Identification of a nuclear protein matrix. *Biochemical and Biophysical Research Communications,* 60**,** 1410-7.

BEREZNEY, R. & COFFEY, D. S. 1975. Nuclear protein matrix: association with newly synthesized DNA. *Science,* 189**,** 291-3.

BERTANI, G. 1951. Studies on lysogenesis. I. The mode of phage liberation by lysogenic *Escherichia coli*. *Journal of Bacteriology,* 62**,** 293-300.

BERTHET, C., ALEEM, E., COPPOLA, V., TESSAROLLO, L. & KALDIS, P. 2003. CDK2 knockout mice are viable. *Current Biology,* 13**,** 1775-85.

BISWAS-FISS, E. E., KHOPDE, S. M. & BISWAS, S. B. 2005. The Mcm467 complex of *Saccharomyces cerevisiae* is preferentially activated by autonomously replicating DNA sequences. *Biochemistry,* 44**,** 2916-2925.

BLAGOSKLONNY, M. V. & PARDEE, A. B. 2002. The restriction point of the cell cycle. *Cell Cycle,* 1**,** 103-10.

BLOW, J. J. & DUTTA, A. 2005. Preventing re-replication of chromosomal DNA. *Nature Review Molecular Cell Biology,* 6**,** 476-86.

BLOW, J. J. & GILLESPIE, P. J. 2008. Replication licensing and cancer - a fatal entanglement? *Nature Reviews Cancer,* 8**,** 799-806.

BOCHMAN, M. L., BELL, S. P. & SCHWACHA, A. 2008. Subunit organization of Mcm2-7 and the unequal role of active sites in ATP hydrolysis and viability. *Molecular and Cellular Biology,* 28**,** 5865-5873.

BOCHMAN, M. L. & SCHWACHA, A. 2007. Differences in the single-stranded DNA binding activities of Mcm2-7 and Mcm467 - Mcm2 and Mcm5 define a slow ATP-dependent step. *Journal of Biological Chemistry,* 282**,** 33795-33804.

BOCHMAN, M. L. & SCHWACHA, A. 2008. The MCM2-7 complex has *in vitro* helicase activity. *Molecular Cell,* 31**,** 287-293.

BOCHMAN, M. L. & SCHWACHA, A. 2010. The *Saccharomyces cerevisiae* Mcm6/2 and Mcm5/3 ATPase active sites contribute to the function of the putative Mcm2-7 'gate'. *Nucleic Acids Research,* 38**,** 6078-6088.

BOOS, D., FRIGOLA, J. & DIFFLEY, J. F. 2012. Activation of the replicative DNA helicase: breaking up is hard to do. *Current Opinion in Cell Biology,* 24**,** 423-30.

BOOS, D., SANCHEZ-PULIDO, L., RAPPAS, M., PEARL, L. H., OLIVER, A. W., PONTING, C. P. & DIFFLEY, J. F. X. 2011. Regulation of DNA replication through Sld3-Dpb11 interaction is conserved from yeast to humans. *Current Biology,* 21**,** 1152-1157.

BOOS, D., YEKEZARE, M. & DIFFLEY, J. F. X. 2013. Identification of a heteromeric complex that promotes DNA replication origin firing in human cells. *Science,* 340**,** 981-984.

BOUSSET, K. & DIFFLEY, J. F. 1998. The Cdc7 protein kinase is required for origin firing during S phase. *Genes and Development,* 12**,** 480-90.

BOWERS, J. L., RANDELL, J. C. W., CHEN, S. Y. & BELL, S. P. 2004. ATP hydrolysis by ORC catalyzes reiterative MCM2-7 assembly at a defined origin of replication. *Molecular Cell,* 16**,** 967-978.

BREWSTER, A. S., WANG, G., YU, X., GREENLEAF, W. B., MARIA CARAZO, J., TJAJADIA, M., KLEIN, M. G. & CHEN, X. S. 2008. Crystal structure of a near-full-length archaeal MCM: Functional insights for an AAA plus hexameric helicase. *Proceedings of the National Academy of Sciences of the United States of America,* 105**,** 20191-20196.

BROWN, G. W. & KELLY, T. J. 1998. Purification of Hsk1, a minichromosome maintenance protein kinase from fission yeast. *Journal of Biological Chemistry,* 273**,** 22083-22090.

BRUCK, I. & KAPLAN, D. 2009. Dbf4-Cdc7 phosphorylation of Mcm2 is required for cell growth. *Journal of Biological Chemistry,* 284**,** 28823-28831.

BRUCK, I. & KAPLAN, D. L. 2011. GINS and Sld3 complete with one another for MCM2-7 and Cdc45 binding. *Journal of Biological Chemistry,* 286**,** 14157-14167.

BUCKLER-WHITE, A. J., HUMPHREY, G. W. & PIGIET, V. 1980. Association of polyoma T antigen and DNA with the nuclear matrix from lytically infected 3T6 cells. *Cell,* 22**,** 37-46.

BUONGIORNO-NARDELLI, M., MICHELI, G., CARRI, M. T. & MARILLEY, M. 1982. A relationship between replicon size and supercoiled loop domains in the eukaryotic genome. *Nature,* 298**,** 100-2.

BURKE, T. W., COOK, J. G., ASANO, M. & NEVINS, J. R. 2001. Replication factors MCM2 and ORC1 interact with the histone acetyltransferase HBO1. *Journal of Biological Chemistry,* 276**,** 15397-15408.

BURKHART, R., SCHULTE, D., HU, B., MUSAHL, C., GOHRING, F. & KNIPPERS, R. 1995. Interactions of human nuclear proteins P1Mcm3 and P1Cdc46. *European Journal of Biochemistry,* 228**,** 431-438.

BYERS, B. & GOETSCH, L. 1975. Behavior of spindles and spindle plaques in cell-cycle and conjugation of *Saccharomyces-cerevisiae*. *Journal of Bacteriology,* 124**,** 511-523.

CAPCO, D. G., WAN, K. M. & PENMAN, S. 1982. The nuclear matrix: three-dimensional architecture and protein composition. *Cell,* 29**,** 847-58.

CARDOSO, M. C., LEONHARDT, H. & NADAL-GINARD, B. 1993. Reversal of terminal differentiation and control of DNA replication: Cyclin A and CDK2 specifically localise at subnuclear sites of DNA replication. *Cell,* 74**,** 1-20.

CARPENTER, P. B., MUELLER, P. R. & DUNPHY, W. G. 1996. Role for a *Xenopus* Orc2-related protein in controlling DNA replication. *Nature,* 379**,** 357-360.

CARPENTIERI, F., DE FELICE, M., DE FALCO, M., ROSSI, M. & PISANI, F. M. 2002. Physical and functional interaction between the mini-chromosome maintenance-like DNA helicase and the single-stranded DNA binding

protein from the crenarchaeon *Sulfolobus solfataricus*. *Journal of Biological Chemistry,* 277**,** 12118-12127.

CASPER, J. M., KEMP, M. G., GHOSH, M., RANDALL, G. M., VAILLANT, A. & LEFFAK, M. 2005. The c-myc DNA-unwinding element-binding protein modulates the assembly of DNA replication complexes *in vitro*. *Journal of Biological Chemistry,* 280**,** 13071-13083.

CHARYCH, D. H., COYNE, M., YABANNAVAR, A., NARBERES, J., CHOW, S., WALLROTH, M., SHAFER, C. & WALTER, A. O. 2008. Inhibition of Cdc7/Dbf4 kinase activity affects specific phosphorylation sites on MCM2 in cancer cells. *Journal of Cellular Biochemistry,* 104**,** 1075-1086.

CHEN, S. & BELL, S. P. 2011. CDK prevents MCM2-7 helicase loading by inhibiting Cdt1 interaction with Orc6. *Genes and Development,* 25**,** 363-372.

CHEN, S., DE VRIES, M. A. & BELL, S. P. 2007. Orc6 is required for dynamic recruitment of Cdt1 during repeated MCM2-7 loading. *Genes and Development,* 21**,** 2897-2907.

CHEN, Y. J., YU, X. O., KASIVISWANATHAN, R., SHIN, J. H., KELMAN, Z. & EGELMAN, E. H. 2005. Structural polymorphism of *Methanothermobacter thermautotrophicus* MCM. *Journal of Molecular Biology,* 346**,** 389-394.

CHO, W.-H., LEE, Y.-J., KONG, S.-I., HURWITZ, J. & LEE, J.-K. 2006. CDC7 kinase phosphorylates serine residues adjacent to acidic amino acids in the minichromosome maintenance 2 protein. *Proceedings of the National Academy of Sciences of the United States of America,* 103**,** 11521-11526.

CHONG, J. P. J., HAYASHI, M. K., SIMON, M. N., XU, R. M. & STILLMAN, B. 2000. A double-hexamer archaeal minichromosome maintenance protein is an ATP-dependent DNA helicase. *Proceedings of the National Academy of Sciences of the United States of America,* 97**,** 1530-1535.

CHONG, J. P. J., MAHBUBANI, H. M., KHOO, C.-Y. & BLOW, J. J. 1995. Purification of an MCM-containing complex as a component of the replication licensing system. *Nature,* 375**,** 418-421.

CHONG, J. P. J., THOMMES, P. & BLOW, J. J. 1996. The role of MCM/P1 proteins in the licensing of DNA replication. *Trends in Biochemical Sciences,* 21**,** 102-106.

CHOWDHURY, A., LIU, G., KEMP, M., CHEN, X., KATRANGI, N., MYERS, S., GHOSH, M., YAO, J., GAO, Y., BUBULYA, P. & LEFFAK, M. 2010. The DNA unwinding element binding protein DUE-B interacts with Cdc45 in preinitiation complex formation. *Molecular and Cellular Biology,* 30**,** 1495-1507.

CHUANG, L.-C., TEIXEIRA, L. K., WOHLSCHLEGEL, J. A., HENZE, M., YATES, J. R., MENDEZ, J. & REED, S. I. 2009. Phosphorylation of Mcm2 by Cdc7 promotes pre-replication complex assembly during cell-cycle re-entry. *Molecular Cell,* 35**,** 206-216.

CHUANG, R. Y. & KELLY, T. J. 1999. The fission yeast homologue of Orc4p binds to replication origin DNA via multiple AT-hooks. *Proceedings of the National Academy of Sciences of the United States of America,* 96**,** 2656-2661.

CLAREY, M. G., ERZBERGER, J. P., GROB, P., LESCHZINER, A. E., BERGER, J. M., NOGALES, E. & BOTCHAN, M. 2006. Nucleotide-dependent conformational changes in the DnaA-like core of the origin recognition complex. *Nature Structural & Molecular Biology,* 13**,** 684-690.

COCKER, J. H., PIATTI, S., SANTOCANALE, C., NASMYTH, K. & DIFFLEY, J. F. X. 1996. An essential role for the Cdc6 protein in forming the pre-replicative complexes of budding yeast. *Nature,* 379**,** 180-182.

COLEMAN, N. & LASKEY, R. A. 2009. Minichromosome maintenance proteins in cancer screening. *European journal of cancer (Oxford, England : 1990),* 45 Suppl 1**,** 416-7.

COLEMAN, T. R., CARPENTER, P. B. & DUNPHY, W. G. 1996. The *Xenopus* Cdc6 protein is essential for the initiation of a single round of DNA replication in cell-free extracts. *Cell,* 87**,** 53-63.

COLLER, H. A. 2007. What's taking so long? S-phase entry from quiescence versus proliferation. *Nature Review Molecular Cell Biology,* 8**,** 667-70.

COLLER, H. A., SANG, L. & ROBERTS, J. M. 2006. A new description of cellular quiescence. *PLOS Biology,* 4**,** e83.

COOK, J. G., CHASSE, D. A. & NEVINS, J. R. 2004. The regulated association of Cdt1 with minichromosome maintenance proteins and Cdc6 in mammalian cells. *Journal of Biological Chemistry,* 279**,** 9625-33.

COOK, J. G., PARK, C.-H., BURKE, T., LEONE, G., DEGREGORI, J., ENGEL, A. & NEVINS, J. 2002. Analysis of Cdc6 function in the assembly of mammalian prereplication complexes. *Proceedings of the National Academy of Sciences of the United States of America-Biological Sciences,* 99**,** 1347-1352.

COOK, P. R. 1991. The nucleoskeleton and the topology of replication. *Cell,* 66**,** 627-35.

COOK, P. R. 1999. The organization of replication and transcription. *Science,* 284**,** 1790-5.

COPELAND, N. A., SERCOMBE, H. E., AINSCOUGH, J. F. & COVERLEY, D. 2010. Ciz1 cooperates with cyclin-A-CDK2 to activate mammalian DNA replication *in vitro*. *Journal of Cell Science,* 123**,** 1108-15.

COPPOCK, D. L., KOPMAN, C., SCANDALIS, S. & GILLERAN, S. 1993. Preferential gene-expression in quiescent human lung fibroblasts. *Cell Growth & Differentiation,* 4**,** 483-493.

CORTEZ, D., GLICK, G. & ELLEDGE, S. J. 2004. Minichromosome maintenance proteins are direct targets of the ATM and ATR checkpoint kinases. *Proceedings of the National Academy of Sciences of the United States of America,* 101**,** 10078-10083.

COSTA, A., ILVES, I., TAMBERG, N., PETOJEVIC, T., NOGALES, E., BOTCHAN, M. R. & BERGER, J. M. 2011. The structural basis for MCM2-7 helicase activation by GINS and Cdc45. *Nature Structural & Molecular Biology,* 18**,** 471-U110.

COSTA, A., PAPE, T., VAN HEEL, M., BRICK, P., PATWARDHAN, A. & ONESTI, S. 2006. Structural basis of the *Methanothermobacter*

*thermautotrophicus* MCM helicase activity. *Nucleic Acids Research,* 34**,** 5829-5838.

COSTA, A., RENAULT, L., SWUEC, P., PETOJEVIC, T., PESAVENTO, J. J., ILVES, I., MACLELLAN-GIBSON, K., FLECK, R. A., BOTCHAN, M. R. & BERGER, J. M. 2014. DNA binding polarity, dimerization, and ATPase ring remodeling in the CMG helicase of the eukaryotic replisome. *eLife,* 3.

COSTA, A., VAN DUINEN, G., MEDAGLI, B., CHONG, J., SAKAKIBARA, N., KELMAN, Z., NAIR, S. K., PATWARDHAN, A. & ONESTI, S. 2008. Cryo-electron microscopy reveals a novel DNA-binding site on the MCM helicase. *The EMBO Journal,* 27**,** 2250-2258.

COSTER, G., FRIGOLA, J., BEURON, F., MORRIS, E. P. & DIFFLEY, J. F. 2014. Origin licensing requires ATP binding and hydrolysis by the MCM replicative helicase. *Molecular Cell,* 55**,** 666-77.

COVERLEY, D., LAMAN, H. & LASKEY, R. A. 2002. Distinct roles for cyclins E and A during DNA replication complex assembly and activation. *Nature Cell Biology,* 4**,** 523-528.

COVERLEY, D., MARR, J. & AINSCOUGH, J. 2005. Ciz1 promotes mammalian DNA replication. *Journal of Cell Science,* 118**,** 101-12.

COVERLEY, D., PELIZON, C., TREWICK, S. & LASKEY, R. A. 2000. Chromatin bound Cdc6 persists in S and G2 phases in human cells, while soluble Cdc6 is destroyed in a cyclin A-cdk2 dependent process. *Journal of Cell Science,* 113**,** 1929-1938.

COVERLEY, D., WILKINSON, H. R., MADINE, M. A., MILLS A. D., & LASKEY, R. A. 1998. Protein Kinase Inhibition in G2 Causes Mammalian Mcm Proteins to Reassociate with Chromatin and Restores Ability to Replicate. *Exp. Cell Research,* 238, 63-69

CREVEL, G., IVETIC, A., OHNO, K., YAMAGUCHI, M. & COTTERILL, S. 2001. Nearest neighbour analysis of MCM protein complexes in *Drosophila melanogaster*. *Nucleic Acids Research,* 29**,** 4834-4842.

DAHMANN, C., DIFFLEY, J. F. & NASMYTH, K. A. 1995. S-phase-promoting cyclin-dependent kinases prevent re-replication by inhibiting the transition of replication origins to a pre-replicative state. *Current Biology,* 5**,** 1257-69.

DALTON, S. & HOPWOOD, B. 1997. Characterization of Cdc47p-minichromosome maintenance complexes in *Saccharomyces cerevisiae*: Identification of Cdc45p as a subunit. *Molecular and Cellular Biology,* 17**,** 5867-5875.

DALTON, S. & WHITBREAD, L. 1995. Cell cycle-regulated nuclear import and export of Cdc47, a protein essential for the initiation of DNA replication in budding yeast. *Proceedings of the National Academy of Sciences of the United States of America-Biological Sciences,* 92**,** 2514-2518.

DAVEY, M. J., INDIANI, C. & O'DONNELL, M. 2003. Reconstitution of the MCM2-7p Heterohexamer, subunit arrangement, and ATP site architecture. *Journal of Biological Chemistry,* 278**,** 4491-4499.

DE MARCO, V., GILLESPIE, P. J., LI, A., KARANTZELIS, N., CHRISTODOULOU, E., KLOMPMAKER, R., VAN GERWEN, S., FISH, A., PETOUKHOV, M. V., ILIOU, M. S., LYGEROU, Z., MEDEMA, R. H., BLOW, J. J., SVERGUN, D. I., TARAVIRAS, S. & PERRAKIS, A. 2009. Quaternary structure of the human Cdt1-Geminin complex regulates DNA replication licensing. *Proceedings of the National Academy of Sciences of the United States of America,* 106**,** 19807-19812.

DELMOLINO, L. M., SAHA, P. & DUTTA, A. 2001. Multiple mechanisms regulate subcellular localization of human CDC6. *Journal of Biological Chemistry,* 276**,** 26947-26954.

DEPAMPHILIS, M. L. 2003. The 'ORC cycle': a novel pathway for regulating eukaryotic DNA replication. *Gene,* 310**,** 1-15.

DESHPANDE, A. M. & NEWLON, C. S. 1992. The ARS consensus sequence is required for chromosomal origin function in *Saccharomyces-cerevisiae*. *Molecular and Cellular Biology,* 12**,** 4305-4313.

DEVAULT, A., GUEYDON, E. & SCHWOB, E. 2008. Interplay between S-cyclin-dependent kinase and Dbf4-dependent kinase in controlling DNA replication through phosphorylation of yeast Mcm4 N-terminal domain. *Molecular Biology of the Cell,* 19**,** 2267-2277.

DIFFLEY, J. F., COCKER, J. H., DOWELL, S. J. & ROWLEY, A. 1994. Two steps in the assembly of complexes at yeast replication origins *in vivo*. *Cell,* 78**,** 303-16.

DIJKWEL, P. A., MULLENDERS, L. H. & WANKA, F. 1979. Analysis of the attachment of replicating DNA to a nuclear matrix in mammalian interphase nuclei. *Nucleic Acids Research,* 6**,** 219-30.

DIJKWEL, P. A., VAUGHN, J. P. & HAMLIN, J. L. 1991. Mapping of replication initiation sites in mammalian genomes by two-dimensional gel analysis: stabilization and enrichment of replication intermediates by isolation on the nuclear matrix. *Molecular and Cellular Biology,* 11**,** 3850-9.

DIMITROVA, D. S. & GILBERT, D. M. 1999. The spatial position and replication timing of chromosomal domains are both established in early G1 phase. *Molecular Cell,* 4**,** 983-993.

DIMITROVA, D. S., TODOROV, I. T., MELENDY, T. & GILBERT, D. M. 1999. Mcm2, but not RPA, is a component of the mammalian early G1-phase prereplication complex. *Journal of Cell Biology,* 146**,** 709-722.

DONALDSON, A. D., FANGMAN, W. L. & BREWER, B. J. 1998. Cdc7 is required throughout the yeast S phase to activate replication origins. *Genes and Development,* 12**,** 491-501.

DONOVAN, S., HARWOOD, J., DRURY, L. S. & DIFFLEY, J. F. 1997. Cdc6-dependent loading of Mcm proteins onto pre-replicative chromatin in budding yeast. *Proceedings of the National Academy of Sciences of the United States of America-Biological Sciences,* 94**,** 5611-5616.

DOWELL, S. J., ROMANOWSKI, P. & DIFFLEY, J. F. 1994. Interaction of Dbf4, the Cdc7 protein kinase regulatory subunit, with yeast replication origins *in vivo*. *Science,* 265**,** 1243-6.

DRURY, L. S., PERKINS, G. & DIFFLEY, J. F. X. 1997. The Cdc4/34/53 pathway targets Cdc6p for proteolysis in budding yeast. *The EMBO Journal,* 16**,** 5966-5976.

DUDDERIDGE, T. J., KELLY, J. D., WOLLENSCHLAEGER, A., OKOTURO, O., PREVOST, T., ROBSON, W., LEUNG, H. Y., WILLIAMS, G. H. & STOEBER, K. 2010. Diagnosis of prostate cancer by detection of minichromosome maintenance 5 protein in urine sediments. *British Journal of Cancer,* 103**,** 701-707.

DULIC, V., LEES, E. & REED, S. I. 1992. Association of human cyclin E with a periodic G1-S phase protein kinase. *Science,* 257**,** 1958-1961.

DUTTA, A. & BELL, S. P. 1997. Initiation of DNA replication in eukaryotic cells. *Annual Review of Cell and Developmental Biology,* 13**,** 293-332.

DYSON, N. 1998. The regulation of E2F by pRB-family proteins. *Genes and Development,* 12**,** 2245-2262.

EDENBERG, H. J. & HUBERMAN, J. A. 1975. Eukaryotic chromosome replication. *Annual Review of Genetics,* 9**,** 245-284.

EIDE, T., TASKEN, K. A., CARLSON, C., WILLIAMS, G., JAHNSEN, T., TASKEN, K. & COLLAS, P. 2003. Protein kinase A-anchoring protein AKAP95 interacts with MCM2, a regulator of DNA replication. *Journal of Biological Chemistry,* 278**,** 26750-6.

EISENBERG, S., KORZA, G., CARSON, J., LIACHKO, I. & TYE, B.-K. 2009. Novel DNA binding properties of the Mcm10 protein from *Saccharomyces cerevisiae*. *Journal of Biological Chemistry,* 284**,** 25412-25420.

EKHOLM, S. V., ZICKERT, P., REED, S. I. & ZETTERBERG, A. 2001. Accumulation of cyclin E is not a prerequisite for passage through the restriction point. *Molecular and Cellular Biology,* 21**,** 3256-65.

EKHOLM-REED, S., MENDEZ, J., TEDESCO, D., ZETTERBERG, A., STILLMAN, B. & REED, S. I. 2004. Deregulation of cyclin E in human cells interferes with prereplication complex assembly. *Journal of Cell Biology,* 165**,** 789-800.

ERLANDSSON, F., LINNMAN, C., EKHOLM, S., BENGTSSON, E. & ZETTERBERG, A. 2000. A detailed analysis of cyclin A accumulation at the G1/S border in normal and transformed cells. *Experimental Cell Research,* 259**,** 86-95.

ERZBERGER, J. P. & BERGER, J. M. 2006. Evolutionary relationships and structural mechanisms of AAA plus proteins. *Annual Review of Biophysics and Biomolecular Structure.*

EVRIN, C., CLARKE, P., ZECH, J., LURZ, R., SUN, J., UHLE, S., LI, H., STILLMAN, B. & SPECK, C. 2009. A double-hexameric MCM2-7 complex is loaded onto origin DNA during licensing of eukaryotic DNA replication. *Proceedings of the National Academy of Sciences of the United States of America,* 106**,** 20240-20245.

EVRIN, C., FERNANDEZ-CID, A., RIERA, A., ZECH, J., CLARKE, P., HERRERA, M. C., TOGNETTI, S., LURZ, R. & SPECK, C. 2014. The

ORC/Cdc6/MCM2-7 complex facilitates MCM2-7 dimerization during prereplicative complex formation. *Nucleic Acids Research,* 42**,** 2257-2269.

EVRIN, C., FERNANDEZ-CID, A., ZECH, J., HERRERA, M. C., RIERA, A., CLARKE, P., BRILL, S., LURZ, R. & SPECK, C. 2013. In the absence of ATPase activity, pre-RC formation is blocked prior to MCM2-7 hexamer dimerization. *Nucleic Acids Research,* 41**,** 3162-3172.

FERENBACH, A., LI, A., BRITO-MARTINS, M. & BLOW, J. J. 2005. Functional domains of the *Xenopus* replication licensing factor Cdt1. *Nucleic Acids Research,* 33**,** 316-324.

FERNANDEZ-CID, A., RIERA, A., TOGNETTI, S., HERRERA, M. C., SAMEL, S., EVRIN, C., WINKLER, C., GARDENAL, E., UHLE, S. & SPECK, C. 2013. An ORC/Cdc6/MCM2-7 complex is formed in a multistep reaction to serve as a platform for MCM double-hexamer assembly. *Molecular Cell,* 50**,** 577-588.

FITCH, M. J., DONATO, J. J. & TYE, B. K. 2003. Mcm7, a subunit of the presumptive MCM helicase, modulates its own expression in conjunction with Mcm1. *Journal of Biological Chemistry,* 278**,** 25408-25416.

FLACH, J., BAKKER, S. T., MOHRIN, M., CONROY, P. C., PIETRAS, E. M., REYNAUD, D., ALVAREZ, S., DIOLAITI, M. E., UGARTE, F., FORSBERG, E. C., LE BEAU, M. M., STOHR, B. A., MENDEZ, J., MORRISON, C. G. & PASSEGUE, E. 2014. Replication stress is a potent driver of functional decline in ageing haematopoietic stem cells. *Nature,* 512**,** 198-202.

FLETCHER, R. J., BISHOP, B. E., LEON, R. P., SCLAFANI, R. A., OGATA, C. M. & CHEN, X. J. S. 2003. The structure and function of MCM from archaeal *M-thermoautotrophicum*. *Nature Structural Biology,* 10**,** 160-167.

FORSBURG, S. L. 2004. Eukaryotic MCM Proteins: beyond replication initiation. *Microbiology and Molecular Biology Reviews,* 68**,** 109-131.

FOX, C. J., HAMMERMAN, P. S. & THOMPSON, C. B. 2005. Fuel feeds function: energy metabolism and the T-cell response. *Nature Reviews Immunology,* 5**,** 844-52.

FRANCIS, L. I., RANDELL, J. C. W., TAKARA, T. J., UCHIMA, L. & BELL, S. P. 2009. Incorporation into the prereplicative complex activates the Mcm2-7 helicase for Cdc7-Dbf4 phosphorylation. *Genes and Development,* 23**,** 643-654.

FRIGOLA, J., REMUS, D., MEHANNA, A. & DIFFLEY, J. F. X. 2013. ATPase-dependent quality control of DNA replication origin licensing. *Nature,* 495**,** 339-343.

FROELICH, C. A., KANG, S., EPLING, L. B., BELL, S. P. & ENEMARK, E. J. 2014. A conserved MCM single-stranded DNA binding element is essential for replication initiation. *eLife,* 3**,** e01993.

FROLOVA, N. S., SCHEK, N., TIKHMYANOVA, N. & COLEMAN, T. R. 2002. *Xenopus* Cdc6 performs separate functions in initiating DNA replication. *Molecular Biology of the Cell,* 13**,** 1298-1312.

FU, Y. V., YARDIMCI, H., LONG, D. T., THE VINH, H., GUAINAZZI, A., BERMUDEZ, V. P., HURWITZ, J., VAN OIJEN, A., SCHAERER, O. D. & WALTER, J. C. 2011. Selective bypass of a lagging strand roadblock by the eukaryotic replicative DNA helicase. *Cell,* 146**,** 930-940.

FUJITA, M., ISHIMI, Y., NAKAMURA, H., KIYONO, T. & TSURUMI, T. 2002. Nuclear organization of DNA replication initiation proteins in mammalian cells. *Journal of Biological Chemistry,* 277**,** 10354-61.

FUJITA, M., KIYONO, T., HAYASHI, Y. & ISHIBASHI, M. 1996. hCDC47, a human member of the MCM family - Dissociation of the nucleus-bound form during S phase. *Journal of Biological Chemistry,* 271**,** 4349-4354.

FUJITA, M., KIYONO, T., HAYASHI, Y. & ISHIBASHI, M. 1997. *In vivo* interaction of human MCM heterohexameric complexes with chromatin. Possible involvement of ATP. *Journal of Biological Chemistry,* 272**,** 10928-35.

FUJITA, M., YAMADA, C., TSURUMI, T., HANAOKA, F., MATSUZAWA, K. & INAGAKI, M. 1998. Cell cycle- and chromatin binding state-dependent phosphorylation of human MCM heterohexameric complexes - A role for cdc2 kinase. *Journal of Biological Chemistry,* 273**,** 17095-17101.

GAMBUS, A. & BLOW, J. J. 2013. Mcm8 and Mcm9 form a dimeric complex in *Xenopus* laevis egg extract that is not essential for DNA replication initiation. *Cell Cycle,* 12**,** 1225-1232.

GAMBUS, A., JONES, R. C., SANCHEZ-DIAZ, A., KANEMAKI, M., VAN DEURSEN, F., EDMONDSON, R. D. & LABIB, K. 2006. GINS maintains association of Cdc45 with MCM in replisome progression complexes at eukaryotic DNA replication forks. *Nature Cell Biology,* 8**,** 358-U41.

GAMBUS, A., KHOUDOLI, G. A., JONES, R. C. & BLOW, J. J. 2011. MCM2-7 form double hexamers at licensed origins in *Xenopus* egg extract. *Journal of Biological Chemistry,* 286**,** 11855-11864.

GAMBUS, A., VAN DEURSEN, F., POLYCHRONOPOULOS, D., FOLTMAN, M., JONES, R. C., EDMONDSON, R. D., CALZADA, A. & LABIB, K. 2009. A key role for Ctf4 in coupling the MCM2-7 helicase to DNA polymerase alpha within the eukaryotic replisome. *The EMBO Journal,* 28**,** 2992-3004.

GE, X. Q. & BLOW, J. J. 2009. *Conserved steps in eukaryotic DNA replication*.

GE, X. Q., JACKSON, D. A. & BLOW, J. J. 2007. Dormant origins licensed by excess Mcm2-7 are required for human cells to survive replicative stress. *Genes and Development,* 21**,** 3331-3341.

GENG, Y., YU, Q., SICINSKA, E., DAS, M., SCHNEIDER, J. E., BHATTACHARYA, S., RIDEOUT, W. M., BRONSON, R. T., GARDNER, H. & SICINSKI, P. 2003. Cyclin E ablation in the mouse. *Cell,* 114**,** 431-43.

GENG, Y., YU, Q., WHORISKEY, W., DICK, F., TSAI, K. Y., FORD, H. L., BISWAS, D. K., PARDEE, A. B., AMATI, B., JACKS, T., RICHARDSON, A., DYSON, N. & SICINSKI, P. 2001. Expression of cyclins E1 and E2 during mouse development and in neoplasia. *Proceedings of the National Academy of Sciences of the United States of America-Biological Sciences,* 98**,** 13138-43.

GERDES, M. G., CARTER, K. C., MOEN, P. T., JR. & LAWRENCE, J. B. 1994. Dynamic changes in the higher-level chromatin organization of specific sequences revealed by in situ hybridization to nuclear halos. *Journal of Cell Biology,* 126**,** 289-304.

GERNER, C., GOTZMANN, J., FROHWEIN, U., SCHAMBERGER, C., ELLINGER, A. & SAUERMANN, G. 2002. Proteome analysis of nuclear matrix proteins during apoptotic chromatin condensation. *Cell Death and Differentiation,* 9**,** 671-81.

GODDARD, T. D., HUANG, C. C. & FERRIN, T. E. 2007. Visualizing density maps with UCSF Chimera. *Journal of Structural Biology,* 157**,** 281-287.

GOMEZ, E. B., CATLETT, M. G. & FORSBURG, S. L. 2002. Different phenotypes *in vivo* are associated with ATPase motif mutations in *Schizosaccharomyces pombe* minichromosome maintenance proteins. *Genetics,* 160**,** 1305-1318.

GOMEZ-LLORENTE, Y., FLETCHER, R. J., CHEN, X. J. S., CARAZO, J. M. & MARTIN, C. S. 2005. Polymorphism and double hexamer structure in the archaeal minichromosome maintenance (MCM) helicase from Methanobacterium thermoautotrophicum. *Journal of Biological Chemistry,* 280**,** 40909-40915.

GONZALEZ, M. A., TACHIBANA, K. K., LASKEY, R. A. & COLEMAN, N. 2005. Innovation - Control of DNA replication and its potential clinical exploitation. *Nature Reviews Cancer,* 5**,** 135-141.

GROS, J., DEVBHANDARI, S. & REMUS, D. 2014. Origin plasticity during budding yeast DNA replication *in vitro*. *The EMBO journal,* 33**,** 621-36.

GROTH, A., CORPET, A., COOK, A. J. L., ROCHE, D., BARTEK, J., LUKAS, J. & ALMOUZNI, G. 2007. Regulation of replication fork progression through histone supply and demand. *Science,* 318**,** 1928-1931.

HARBOUR, J. W., LUO, R. X., SANTI, A. D., POSTIGO, A. A. & DEAN, D. C. 1999. Cdk phosphorylation triggers sequential intramolecular interactions that progressively block Rb functions as cells move through G1. *Cell,* 98**,** 859-869.

HARDY, C. F. J., DRYGA, O., SEEMATTER, S., PAHL, P. M. B. & SCLAFANI, R. A. 1997. mcm5/cdc46-bob1 bypasses the requirement for the S phase activator Cdc7p. *Proceedings of the National Academy of Sciences of the United States of America,* 94**,** 3151-3155.

HARTFORD, S. A., LUO, Y., SOUTHARD, T. L., MIN, I. M., LIS, J. T. & SCHIMENTI, J. C. 2011. Minichromosome maintenance helicase paralog MCM9 is dispensible for DNA replication but functions in germ-line stem cells and tumor suppression. *Proceedings of the National Academy of Sciences of the United States of America,* 108**,** 17702-17707.

HARTWELL, L. H., CULOTTI, J., PRINGLE, J. R. & REID, B. J. 1974. Genetic-control of cell-division cycle in yeast. *Science,* 183**,** 46-51.

HATEBOER, G., WOBST, A., PETERSEN, B. O., LE CAM, L., VIGO, E., SARDET, C. & HELIN, K. 1998. Cell cycle-regulated expression of mammalian Cdc6 is dependent on E2F. *Molecular and Cellular Biology,* 18**,** 6679-6697.

HELLER, R. C., KANG, S., LAM, W. M., CHEN, S., CHAN, C. S. & BELL, S. P. 2011. Eukaryotic origin-dependent DNA replication *in vitro* reveals sequential action of DDK and S-CDK kinases. *Cell,* 146**,** 80-91.

HESKETH, E. L., PARKER-MANUEL, R. P., CHABAN, Y., SATTI, R., ORLOVA, E. V., COVERLEY, D. & CHONG, J. P. under review. DNA induces conformational changes in a recombinant human minichromosome maintenance complex.

HESS, G. F., DRONG, R. F., WEILAND, K. L., SLIGHTOM, J. L., SCLAFANI, R. A. & HOLLINGSWORTH, R. E. 1998. A human homolog of the yeast CDC7 gene is overexpressed in some tumors and transformed cell lines. *Gene,* 211**,** 133-140.

HOANG, M. L., LEON, R. P., PESSOA-BRANDAO, L., HUNT, S., RAGHURAMAN, M. K., FANGMAN, W. L., BREWER, B. J. & SCLAFANI, R. A. 2007. Structural changes in Mcm5 protein bypass Cdc7-Dbf4 function and reduce replication origin efficiency in *Saccharomyces cerevisiae*. *Molecular and Cellular Biology,* 27**,** 7594-7602.

HONEYCUTT, K. A., CHEN, Z., KOSTER, M. I., MIERS, M., NUCHTERN, J., HICKS, J., ROOP, D. R. & SHOHET, J. M. 2006. Deregulated minichromosomal maintenance protein MCM7 contributes to oncogene driven tumorigenesis. *Oncogene,* 25**,** 4027-4032.

HOOK, S. S., LIN, J. J. & DUTTA, A. 2007. Mechanisms to control rereplication and implications for cancer. *Current Opinion in Cell Biology,* 19**,** 663-671.

IBARRA, A., SCHWOB, E. & MENDEZ, J. 2008. Excess MCM proteins protect human cells from replicative stress by licensing backup origins of replication. *Proceedings of the National Academy of Sciences of the United States of America,* 105**,** 8956-8961.

IIZUKA, M., SARMENTO, O. F., SEKIYA, T., SCRABLE, H., ALLIS, C. D. & SMITH, M. M. 2008. Hbo1 links p53-dependent stress signaling to DNA replication licensing. *Molecular and Cellular Biology,* 28**,** 140-153.

IIZUKA, M. & STILLMAN, B. 1999. Histone acetyltransferase HBO1 interacts with the ORC1 subunit of the human initiator protein. *Journal of Biological Chemistry,* 274**,** 23027-23034.

ILVES, I., PETOJEVIC, T., PESAVENTO, J. J. & BOTCHAN, M. R. 2010. Activation of the MCM2-7 helicase by association with Cdc45 and GINS proteins. *Molecular Cell,* 37**,** 247-258.

IM, J.-S., KI, S.-H., FARINA, A., JUNG, S., HURWITZ, J. & LEE, J.-K. 2009. Assembly of the Cdc45-Mcm2-7-GINS complex in human cells requires the Ctf4/And-1, RecQL4, and Mcm10 proteins. *Proceedings of the National Academy of Sciences of the United States of America,* 106**,** 15628-15632.

ISHIMI, Y. 1997. A DNA helicase activity is associated with an MCM4, -6, and -7 protein complex. *Journal of Biological Chemistry,* 272**,** 24508-24513.

ISHIMI, Y., KOMAMURA, Y., YOU, Z. Y. & KIMURA, H. 1998. Biochemical function of mouse minichromosome maintenance 2 protein. *Journal of Biological Chemistry,* 273**,** 8369-8375.

ISHIMI, Y. & KOMAMURA-KOHNO, Y. 2001. Phosphorylation of Mcm4 at specific sites by cyclin-dependent kinase leads to loss of Mcm4,6,7 helicase activity. *Journal of Biological Chemistry,* 276**,** 34428-34433.

ISHIMI, Y., KOMAMURA-KOHNO, Y., ARAI, K. & MASAI, H. 2001. Biochemical activities associated with mouse Mcm2 protein. *Journal of Biological Chemistry,* 276**,** 42744-52.

IYER, L. M., LEIPE, D. D., KOONIN, E. V. & ARAVIND, L. 2004. Evolutionary history and higher order classification of AAA plus ATPases. *Journal of Structural Biology,* 146**,** 11-31.

JACKSON, A. L., PAHL, P. M. B., HARRISON, K., ROSAMOND, J. & SCLAFANI, R. A. 1993. Cell-cycle regulation of the yeast cdc7 protein-kinase by association with the dbf4 protein. *Molecular and Cellular Biology,* 13**,** 2899-2908.

JACKSON, D. A. & COOK, P. R. 1986. Replication occurs at a nucleoskeleton. *The EMBO Journal* 5**,** 1403-10.

JARES, P. & BLOW, J. J. 2000. *Xenopus* Cdc7 function is dependent on licensing but not on XORC, XCdc6, or CDK activity and is required for XCdc45 loading. *Genes and Development,* 14**,** 1528-40.

JARES, P., DONALDSON, A. & BLOW, J. J. 2000. The Cdc7/Dbf4 protein kinase: target of the S phase checkpoint? *EMBO Reports,* 1**,** 319-322.

JENKINSON, E. R. & CHONG, J. P. 2006. Minichromosome maintenance helicase activity is controlled by N- and C-terminal motifs and requires the ATPase domain helix-2 insert. *Proceedings of the National Academy of Sciences of the United States of America-Biological Sciences,* 103**,** 7613-8.

JENKINSON, E. R., COSTA, A., LEECH, A. P., PATWARDHAN, A., ONESTI, S. & CHONG, J. P. J. 2009. Mutations in subdomain B of the minichromosome maintenance (MCM) helicase affect DNA binding and modulate conformational transitions. *Journal of Biological Chemistry,* 284**,** 5654-5661.

JEON, Y., KO, E., LEE, K. Y., KO, M. J., PARK, S. Y., KANG, J., JEON, C. H., LEE, H. & HWANG, D. S. 2011. TopBP1 deficiency causes an early embryonic lethality and induces cellular senescence in primary cells. *Journal of Biological Chemistry,* 286**,** 5414-5422.

JEON, Y., LEE, K. Y., KO, M. J., LEE, Y. S., KANG, S. & HWANG, D. S. 2007. Human TopBP1 participates in cyclin E/CDK2 activation and preinitiation complex assembly during G(1)/S transition. *Journal of Biological Chemistry,* 282**,** 14882-14890.

JIANG, W. & HUNTER, T. 1997. Identification and characterization of a human protein kinase related to budding yeast Cdc7p. *Proceedings of the National Academy of Sciences of the United States of America,* 94**,** 14320-14325.

JIANG, W., MCDONALD, D., HOPE, T. J. & HUNTER, T. 1999. Mammalian Cdc7-Dbf4 protein kinase complex is essential for initiation of DNA replication. *The EMBO Journal,* 18**,** 5703-13.

JOHANSSON, P., JEFFERY, J., AL-EJEH, F., SCHULZ, R. B., CALLEN, D. F., KUMAR, R. & KHANNA, K. K. 2014. SCF-FBXO31 E3 ligase targets DNA replication factor Cdt1 for proteolysis in the G(2) phase of cell cycle to prevent re-replication. *Journal of Biological Chemistry,* 289**,** 18514-18525.

JONES, D. R., PRASAD, A. A., CHAN, P. K. & DUNCKER, B. P. 2010. The Dbf4 motif C zinc finger promotes DNA replication and mediates resistance to genotoxic stress. *Cell Cycle,* 9**,** 2018-2026.

KALASZCZYNSKA, I., GENG, Y., IINO, T., MIZUNO, S., CHOI, Y., KONDRATIUK, I., SILVER, D. P., WOLGEMUTH, D. J., AKASHI, K. & SICINSKI, P. 2009. Cyclin A is redundant in fibroblasts but essential in hematopoietic and embryonic stem cells. *Cell,* 138**,** 352-65.

KAMADA, K., KUBOTA, Y., ARATA, T., SHINDO, Y. & HANAOKA, F. 2007. Structure of the human GINS complex and its assembly and functional interface in replication initiation. *Nature Structural & Molecular Biology,* 14**,** 388-396.

KAMIMURA, Y., TAK, Y. S., SUGINO, A. & ARAKI, H. 2001. Sld3, which interacts with Cdc45 (Sld4), functions for chromosomal DNA replication in *Saccharomyces cerevisiae*. *The EMBO Journal,* 20**,** 2097-2107.

KANEMAKI, M. & LABIB, K. 2006. Distinct roles for Sld3 and GINS during establishment and progression of eukaryotic DNA replication forks. *The EMBO Journal,* 25**,** 1753-1763.

KANEMAKI, M., SANCHEZ-DIAZ, A., GAMBUS, A. & LABIB, K. 2003. Functional proteomic identification of DNA replication proteins by induced proteolysis *in vivo*. *Nature,* 423**,** 720-4.

KANG, S., WARNER, MEGAN D. & BELL, STEPHEN P. 2014. Multiple functions for Mcm2–7 ATPase motifs during replication initiation. *Molecular Cell*.

KANG, Y.-H., GALAL, W. C., FARINA, A., TAPPIN, I. & HURWITZ, J. 2012. Properties of the human Cdc45/Mcm2-7/GINS helicase complex and its action with DNA polymerase e in rolling circle DNA synthesis. *Proceedings of the National Academy of Sciences of the United States of America,* 109**,** 6042-6047.

KANKE, M., KODAMA, Y., TAKAHASHI, T. S., NAKAGAWA, T. & MASUKATA, H. 2012. Mcm10 plays an essential role in origin DNA unwinding after loading of the CMG components. *The EMBO Journal,* 31**,** 2182-2194.

KANTER, D. M., BRUCK, I. & KAPLAN, D. L. 2008. Mcm subunits can assemble into two different active unwinding complexes. *Journal of Biological Chemistry,* 283**,** 31172-31182.

KASIVISWANATHAN, R., SHIN, J. H., MELAMUD, E. & KELMAN, Z. 2004. Biochemical characterization of the *Methanothermobacter thermautotrophicus* minichromosome maintenance (MCM) helicase N-terminal domains. *Journal of Biological Chemistry,* 279**,** 28358-28366.

KAWASAKI, Y., KIM, H. D., KOJIMA, A., SEKI, T. & SUGINO, A. 2006. Reconstitution of *Saccharomyces cerevisiae* prereplicative complex assembly *in vitro*. *Genes to Cells,* 11**,** 745-756.

KELLY, J. D., DUDDERIDGE, T. J., WOLLENSCHLAEGER, A., OKOTURO, O., BURLING, K., TULLOCH, F., HALSALL, I., PREVOST, T., PREVOST, A. T., VASCONCELOS, J. C., ROBSON, W., LEUNG, H. Y., VASDEV, N., PICKARD, R. S., WILLIAMS, G. H. & STOEBER, K. 2012. Bladder cancer diagnosis and identification of clinically significant disease by combined urinary detection of Mcm5 and nuclear matrix protein 22. *Plos One,* 7.

KELLY, T. J. & BROWN, G. W. 2000. Regulation of chromosome replication. *Annual Review of Biochemistry,* 69**,** 829-880.

KELLY, T. J., MARTIN, G. S., FORSBURG, S. L., STEPHEN, R. J., RUSSO, A. & NURSE, P. 1993. The fission yeast cdc18 gene product couples S phase to START and mitosis. *Cell,* 74**,** 371-382.

KELMAN, Z., LEE, J. K. & HURWITZ, J. 1999. The single minichromosome maintenance protein of *Methanobacterium thermoautotrophicum* Delta H contains DNA helicase activity. *Proceedings of the National Academy of Sciences of the United States of America,* 96**,** 14783-14788.

KIM, J. M., NAKAO, K., NAKAMURA, K., SAITO, I., KATSUKI, M., ARAI, K. & MASAI, H. 2002. Inactivation of Cdc7 kinase in mouse ES cells results in S-phase arrest and p53-dependent cell death. *The EMBO Journal,* 21**,** 2168-2179.

KIMURA, H., NOZAKI, N. & SUGIMOTO, K. 1994. DNA polymerase alpha associated protein P1, a murine homolog of yeast Mcm3, changes its intranuclear distribution during the DNA synthetic period. *The EMBO Journal,* 13**,** 4311-4320.

KINOSHITA, Y., JOHNSON, E. M., GORDON, R. E., NEGRI-BELL, H., EVANS, M. T., COOLBAUGH, J., ROSARIO-PERALTA, Y., SAMET, J., SLUSSER, E., BIRKENBACH, M. P. & DANIEL, D. C. 2008. Colocalization of MCM8 and MCM7 with proteins involved in distinct aspects of DNA replication. *Microscopy Research and Technique,* 71**,** 288-297.

KITAMURA, E., BLOW, J. J. & TANAKA, T. U. 2006. Live-cell imaging reveals replication of individual replicons in eukaryotic replication factories. *Cell,* 125**,** 1297-1308.

KLEMM, R. D. & BELL, S. P. 2001. ATP bound to the origin recognition complex is important for preRC formation. *Proceedings of the National Academy of Sciences of the United States of America,* 98**,** 8361-8367.

KOONIN, E. V. 1993. A common set of conserved motifs in a vast variety of putative nucleic acid-dependent ATPases including Mcm proteins involved in the initiation of eukaryotic DNA-replication. *Nucleic Acids Research,* 21**,** 2541-2547.

KRASTANOVA, I., SANNINO, V., AMENITSCH, H., GILEADI, O., PISANI, F. M. & ONESTI, S. 2012. Structural and functional insights into the DNA replication factor Cdc45 reveal an evolutionary relationship to the DHH family of phosphoesterases. *Journal of Biological Chemistry,* 287**,** 4121-4128.

KRUDE, T., JACKMAN, M., PINES, J. & LASKEY, R. A. 1997. Cyclin/Cdk-dependent initiation of DNA replication in a human cell-free system. *Cell,* 88**,** 109-19.

KRUDE, T., MUSAHL, C., LASKEY, R. A. & KNIPPERS, R. 1996. Human replication proteins hCdc21, hCdc46 and P1Mcm3 bind chromatin uniformly before S-phase and are displaced locally during DNA replication. *Journal of Cell Science,* 109**,** 309-318.

KUBOTA, Y., TAKASE, Y., KOMORI, Y., HASHIMOTO, Y., ARATA, T., KAMIMURA, Y., ARAKI, H. & TAKISAWA, H. 2003. A novel ring-like complex of *Xenopus* proteins essential for the initiation of DNA replication. *Genes and Development,* 17**,** 1141-1152.

KUIPERS, M. A., STASEVICH, T. J., SASAKI, T., WILSON, K. A., HAZELWOOD, K. L., MCNALLY, J. G., DAVIDSON, M. W. & GILBERT, D. M. 2011. Highly stable loading of Mcm proteins onto chromatin in living cells requires replication to unload. *Journal of Cell Biology,* 192**,** 29-41.

KUMAGAI, A., SHEVCHENKO, A., SHEVCHENKO, A. & DUNPHY, W. G. 2010. Treslin collaborates with TopBP1 in triggering the initiation of DNA replication. *Cell,* 140**,** 349-U59.

KUMAGAI, A., SHEVCHENKO, A., SHEVCHENKO, A. & DUNPHY, W. G. 2011. Direct regulation of Treslin by cyclin-dependent kinase is essential for the onset of DNA replication. *Journal of Cell Biology,* 193**,** 995-1007.

KUMAGAI, H., SATO, N., YAMADA, M., MAHONY, D., SEGHEZZI, W., LEES, E., ARAI, K. I. & MASAI, H. 1999. A novel growth- and cell cycle-regulated protein, ASK, activates human Cdc7-related kinase and is essential for G(1)/S transition in mammalian cells. *Molecular and Cellular Biology,* 19**,** 5083-5095.

LABIB, K. 2010. How do Cdc7 and cyclin-dependent kinases trigger the initiation of chromosome replication in eukaryotic cells? *Genes and Development,* 24**,** 1208-1219.

LABIB, K. & GAMBUS, A. 2007. A key role for the GINS complex at DNA replication forks. *Trends in Cell Biology,* 17**,** 271-278.

LABIB, K., TERCERO, J. A. & DIFFLEY, J. F. X. 2000. Uninterrupted MCM2-7 function required for DNA replication fork progression. *Science,* 288**,** 1643-1647.

LAGARKOVA, M. A., SVETLOVA, E., GIACCA, M., FALASCHI, A. & RAZIN, S. V. 1998. DNA loop anchorage region colocalizes with the replication origin located downstream to the human gene encoding lamin B2. *Journal of Cellular Biochemistry,* 69**,** 13-8.

LASKEY, R. A. & MADINE, M. A. 2003. A rotary pumping model for helicase function of MCM proteins at a distance from replication forks. *EMBO Reports,* 4**,** 26-30.

LAU, E., TSUJI, T., GUO, L., LU, S.-H. & JIANG, W. 2007. The role of pre-replicative complex (pre-RC) components in oncogenesis. *Faseb Journal,* 21**,** 3786-3794.

LAU, E., ZHU, C. J., ABRAHAM, R. T. & JIANG, W. 2006. The functional role of Cdc6 in S-G2/M in mammalian cells. *EMBO Reports,* 7**,** 425-430.

LAU, K. M., CHAN, Q. K. Y., PANG, J. C. S., LI, K. K. W., YEUNG, W. W., CHUNG, N. Y. F., LUI, P. C., TAM, Y. S., LI, H. M., ZHOU, L., WANG, Y., MAO, Y. & NG, H. K. 2010. Minichromosome maintenance proteins 2, 3 and 7 in medulloblastoma: overexpression and involvement in regulation of cell migration and invasion. *Oncogene,* 29**,** 5475-5489.

LEE, C., HONG, B., CHOI, J. M., KIM, Y., WATANABE, S., ISHIMI, Y., ENOMOTO, T., TADA, S., KIM, Y. C. & CHO, Y. J. 2004. Structural basis for inhibition of the replication licensing factor Cdt1 by geminin. *Nature,* 430**,** 913-917.

LEE, C., LIACHKO, I., BOUTEN, R., KELMAN, Z. & TYE, B. K. 2010. Alternative mechanisms for coordinating polymerase alpha and MCM helicase. *Molecular and Cellular Biology,* 30**,** 423-435.

LEE, D. G. & BELL, S. P. 1997. Architecture of the yeast origin recognition complex bound to origins of DNA replication. *Molecular and Cellular Biology,* 17**,** 7159-7168.

LEE, D. G. & BELL, S. P. 2000. ATPase switches controlling DNA replication initiation. *Current Opinion in Cell Biology,* 12**,** 280-285.

LEE, J. K. & HURWITZ, J. 2000. Isolation and characterization of various complexes of the minichromosome maintenance proteins of *Schizosaccharomyces pombe*. *Journal of Biological Chemistry,* 275**,** 18871-18878.

LEE, J. K. & HURWITZ, J. 2001. Processive DNA helicase activity of the minichromosome maintenance proteins 4, 6, and 7 complex requires forked DNA structures. *Proceedings of the National Academy of Sciences of the United States of America,* 98**,** 54-59.

LEE, J. K., MOON, K. Y., JIANG, Y. & HURWITZ, J. 2001. The *Schizosaccharomyces pombe* origin recognition complex interacts with multiple AT-rich regions of the replication origin DNA by means of the AT-hook domains of the spOrc4 protein. *Proceedings of the National Academy of Sciences of the United States of America,* 98**,** 13589-13594.

LEE, J. K., SEO, Y. S. & HURWITZ, J. 2003. The Cdc23 (Mcm10) protein is required for the phosphorylation of minichromosome maintenance complex by the Dfp1-Hsk1 kinase. *Proceedings of the National Academy of Sciences of the United States of America,* 100**,** 2334-2339.

LEI, M., CHENG, I. H., ROBERTS, L. A., MCALEAR, M. A. & TYE, B. K. 2002. Two mcm3 mutations affect different steps in the initiation of DNA replication. *Journal of Biological Chemistry,* 277**,** 30824-30831.

LEI, M., KAWASAKI, Y. & TYE, B. K. 1996. Physical interactions among Mcm proteins and effects of Mcm dosage on DNA replication in *Saccharomyces cerevisiae*. *Molecular and Cellular Biology,* 16**,** 5081-5090.

LEI, M., KAWASAKI, Y., YOUNG, M. R., KIHARA, M., SUGINO, A. & TYE, B. K. 1997. Mcm2 is a target of regulation by Cdc7-Dbf4 during the initiation of DNA synthesis. *Genes and Development,* 11**,** 3365-3374.

LEI, M. & TYE, B. K. 2001. Initiating DNA synthesis: from recruiting to activating the MCM complex. *Journal of Cell Science,* 114**,** 1447-1454.

LEMAITRE, J. M., DANIS, E., PASERO, P., VASSETZKY, Y. & MECHALI, M. 2005. Mitotic remodeling of the replicon and chromosome structure. *Cell,* 123**,** 787-801.

LI, A. & BLOW, J. J. 2005. Cdt1 downregulation by proteolysis and geminin inhibition prevents DNA re-replication in *Xenopus*. *The EMBO Journal,* 24**,** 395-404.

LI, Y. & ARAKI, H. 2013. Loading and activation of DNA replicative helicases: the key step of initiation of DNA replication. *Genes to Cells,* 18**,** 266-277.

LIANG, D. T., HODSON, J. A. & FORSBURG, S. L. 1999. Reduced dosage of a single fission yeast MCM protein causes genetic instability and S phase delay. *Journal of Cell Science,* 112**,** 559-567.

LIEW, L. P. & BELL, S. D. 2011. The interplay of DNA binding, ATP hydrolysis and helicase activities of the archaeal MCM helicase. *Biochemical Journal,* 436**,** 409-414.

LIGASOVA, A., RASKA, I. & KOBERNA, K. 2009. Organization of human replicon: Singles or zipping couples? *Journal of Structural Biology,* 165**,** 204-213.

LIKU, M. E., NGUYEN, V. Q., ROSALES, A. W., IRIE, K. & LI, J. J. 2005. CDK phosphorylation of a novel NLS-NES module distributed between two subunits of the Mcm2-7 complex prevents chromosomal rereplication. *Molecular Biology of the Cell,* 16**,** 5026-5039.

LIU, P. J., SLATER, D. M., LENBURG, M., NEVIS, K., COOK, J. G. & VAZIRI, C. 2009. Replication licensing promotes cyclin D1 expression and G(1) progression in untransformed human cells. *Cell Cycle,* 8**,** 125-136.

LIU, W., PUCCI, B., ROSSI, M., PISANI, F. M. & LADENSTEIN, R. 2008. Structural analysis of the *Sulfolobus solfataricus* MCM protein N-terminal domain. *Nucleic Acids Research,* 36**,** 3235-3243.

LUTZMANN, M., MAIORANO, D. & MECHALI, M. 2006. A Cdt1-geminin complex licenses chromatin for DNA replication and prevents rereplication during S phase in *Xenopus*. *The EMBO Journal,* 25**,** 5764-5774.

LUTZMANN, M. & MECHALI, M. 2008. MCM9 binds Cdt1 and is required for the assembly of prereplication complexes. *Molecular Cell,* 31**,** 190-200.

LYUBIMOV, A. Y., COSTA, A., BLEICHERT, F., BOTCHAN, M. R. & BERGER, J. M. 2012. ATP-dependent conformational dynamics underlie the functional asymmetry of the replicative helicase from a minimalist eukaryote. *Proceedings of the National Academy of Sciences of the United States of America,* 109**,** 11999-12004.

LYUBIMOV, A. Y., STRYCHARSKA, M. & BERGER, J. M. 2011. The nuts and bolts of ring-translocase structure and mechanism. *Current Opinion in Structural Biology,* 21**,** 240-248.

MADINE, M., KHOO, C.-Y., MILLS, A. D., MUSAHL, C. & LASKEY, R. A. 1995. The nuclear envelope prevents reinitiation of replication by regulating the binding of MCM3 to chromatin in *Xenopus* egg extracts. *Current Biology,* 5**,** 1270.

MAILAND, N. & DIFFLEY, J. F. 2005. CDKs promote DNA replication origin licensing in human cells by protecting Cdc6 from APC/C-dependent proteolysis. *Cell,* 122**,** 915-26.

MAINE, G. T., SINHA, P. & TYE, B. K. 1984. Mutants of *s-cerevisiae* defective in the maintenance of minichromosomes. *Genetics,* 106**,** 365-385.

MAIORANO, D., KRASINSKA, L., LUTZMANN, M. & MECHALI, M. 2005. Recombinant Cdt1 induces rereplication of G2 nuclei in *Xenopus* egg extracts. *Current Biology,* 15**,** 146-153.

MAIORANO, D., LUTZMANN, M. & MÉCHALI, M. 2006. MCM proteins and DNA replication. *Current Opinion in Cell Biology,* 18**,** 130-136.

MALUMBRES, M. & BARBACID, M. 2005. Mammalian cyclin-dependent kinases. *Trends in Biochemical Sciences,* 30**,** 630-641.

MARHEINEKE, K., HYRIEN, O. & KRUDE, T. 2005. Visulaisation of bidirectional initiation of chromosomal DNA replication in a human cell free system. *Nucleic Acids Research*, 21, 6931-41.

MARTIN, R. G. & STEIN, S. 1976. Resting state in normal and simian virus-40 transformed chinese-hamster lung-cells. *Proceedings of the National Academy of Sciences of the United States of America,* 73**,** 1655-1659.

MASAI, H. & ARAI, K. I. 2002. Cdc7 kinase complex: A key regulator in the initiation of DNA replication. *Journal of Cellular Physiology,* 190**,** 287-296.

MASAI, H., MATSUI, E., YOU, Z. Y., ISHIMI, Y., TAMAI, K. & ARAI, K. 2000. Human Cdc7-related kinase complex - *in vitro* phosphorylation of MCM by concerted actions of Cdks and Cdc7 and that of a critical threonine residue of Cdc7 by Cdks. *Journal of Biological Chemistry,* 275**,** 29042-29052.

MASAI, H., TANIYAMA, C., OGINO, K., MATSUI, E., KAKUSHO, N., MATSUMOTO, S., KIM, J.-M., ISHII, A., TANAKA, T., KOBAYASHI, T., TAMAI, K., OHTANI, K. & ARAI, K.-I. 2006. Phosphorylation of MCM4 by Cdc7 kinase facilitates its interaction with Cdc45 on the chromatin. *Journal of Biological Chemistry,* 281**,** 39249-39261.

MASUDA, T., MIMURA, S. & TAKISAWA, H. 2003. CDK- and Cdc45-dependent priming of the MCM complex on chromatin during S-phase in *Xenopus* egg extracts: possible activation of MCM helicase by association with Cdc45. *Genes to Cells,* 8**,** 145-61.

MATSUNO, K., KUMANO, M., KUBOTA, Y., HASHIMOTO, Y. & TAKISAWA, H. 2006. The N-terminal noncatalytic region of *Xenopus* RecQ4 is required for chromatin binding of DNA polymerase alpha in the initiation of DNA replication. *Molecular and Cellular Biology,* 26**,** 4843-4852.

MCGEOCH, A. T., TRAKSELIS, M. A., LASKEY, R. A. & BELL, S. D. 2005. Organization of the archaeal MCM complex on DNA and implications for the helicase mechanism. *Nature Structural & Molecular Biology,* 12**,** 756-762.

MCINTOSH, D. & BLOW, J. J. 2012. Dormant origins, the licensing checkpoint, and the response to replicative stresses. *Cold Spring Harbor perspectives in biology,* 4.

MECHALI, M. 2010. Eukaryotic DNA replication origins: many choices for appropriate answers. *Nature Reviews Molecular Cell Biology,* 11**,** 728-738.

MEIJER, L., BORGNE, A., MULNER, O., CHONG, J. P. J., BLOW, J. J., INAGAKI, N., INAGAKI, M., DELCROS, J. G. & MOULINOUX, J. P. 1997. Biochemical and cellular effects of roscovitine, a potent and selective inhibitor of the cyclin-dependent kinases Cdc2, CDK2 and CDK5. *European Journal of Biochemistry,* 243**,** 527-536.

MENDEZ, J. & STILLMAN, B. 2000. Chromatin association of human origin recognition complex, Cdc6, and minichromosome maintenance proteins during the cell cycle: Assembly of prereplication complexes in late mitosis. *Molecular and Cellular Biology,* 20**,** 8602-8612.

MESELSON, M. & STAHL, F. W. 1958. The replication of DNA in *Escherichia-coli*. *Proceedings of the National Academy of Sciences of the United States of America,* 44**,** 671-682.

MILLER, J. M., ARACHEA, B. T., EPLING, L. B. & ENEMARK, E. J. 2014. Analysis of the crystal structure of an active MCM hexamer. *eLife,* 3.

MINTON, K. 2014. Stem cells: Replication stress makes HSCs feel old. *Nature Reviews Molecular Cell Biology,* 15**,** 560-561.

MIOTTO, B. & STRUHL, K. 2008. HBO1 histone acetylase is a coactivator of the replication licensing factor Cdt1. *Genes and Development,* 22**,** 2633-2638.

MITULOVIC, G., STINGL, C., SMOLUCH, M., SWART, R., CHERVET, J. P., STEINMACHER, I., GERNER, C. & MECHTLER, K. 2004. Automated, on-line two-dimensional nano liquid chromatography tandem mass spectrometry for rapid analysis of complex protein digests. *Proteomics,* 4**,** 2545-57.

MIZUSHIMA, T., TAKAHASHI, N. & STILLMAN, B. 2000. Cdc6p modulates the structure and DNA binding activity of the origin recognition complex *in vitro*. *Genes and Development,* 14**,** 1631-1641.

MONTAGNOLI, A., BOSOTTI, R., VILLA, F., RIALLAND, M., BROTHERTON, D., MERCURIO, C., BERTHELSEN, J. & SANTOCANALE, C. 2002. Drf1, a novel regulatory subunit for human Cdc7 kinase. *The EMBO Journal,* 21**,** 3171-3181.

MONTAGNOLI, A., VALSASINA, B., BROTHERTON, D., TROIANI, S., RAINOLDI, S., TENCA, P., MOLINARI, A. & SANTOCANALE, C. 2006. Identification of Mcm2 phosphorylation sites by S-phase-regulating kinases. *Journal of Biological Chemistry,* 281**,** 10281-10290.

MONTAGNOLI, A., VALSASINA, B., CROCI, V., MENICHINCHERI, M., RAINOLDI, S., MARCHESI, V., TIBOLLA, M., TENCA, P., BROTHERTON, D., ALBANESE, C., PATTON, V., ALZANI, R., CIAVOLELLA, A., SOLA, F., MOLINARI, A., VOLPI, D., AVANZI, N., FIORENTINI, F., CATTONI, M., HEALY, S., BALLINARI, D., PESENTI, E., ISACCHI, A., MOLL, J., BENSIMON, A., VANOTTI, E. & SANTOCANALE, C. 2008. A Cdc7 kinase inhibitor restricts initiation of DNA replication and has antitumor activity. *Nature Chemical Biology,* 4**,** 357-365.

MORGAN, D. O. 1997. Cyclin-dependent kinases: Engines, clocks, and microprocessors. *Annual Review of Cell and Developmental Biology,* 13**,** 261-291.

MOYER, S. E., LEWIS, P. W. & BOTCHAN, M. R. 2006. Isolation of the Cdc45/Mcm2-7/GINS (CMG) complex, a candidate for the eukaryotic DNA replication fork helicase. *Proceedings of the National Academy of Sciences of the United States of America,* 103**,** 10236-10241.

MUNKLEY, J., COPELAND, N. A., MOIGNARD, V., KNIGHT, J. R., GREAVES, E., RAMSBOTTOM, S. A., POWNALL, M. E., SOUTHGATE, J., AINSCOUGH, J. F. & COVERLEY, D. 2011. Cyclin E is recruited to the nuclear matrix during differentiation, but is not recruited in cancer cells. *Nucleic Acids Research,* 39**,** 2671-7.

MURAMATSU, S., HIRAI, K., TAK, Y.-S., KAMIMURA, Y. & ARAKI, H. 2010. CDK-dependent complex formation between replication proteins Dpb11, Sld2, Pol epsilon, and GINS in budding yeast. *Genes and Development,* 24**,** 602-612.

MURRAY, A. W. 2004. Recycling the cell cycle: cyclins revisited. *Cell,* 116**,** 221-34.

NAKAJIMA, R. & MASUKATA, H. 2002. SpS1d3 is required for loading and maintenance of SpCdc45 on chromatin in DNA replication in fission yeast. *Molecular Biology of the Cell,* 13**,** 1462-1472.

NAKAYASU, H. & BEREZNEY, R. 1989. Mapping replicational sites in the eucaryotic cell nucleus. *Journal of Cell Biology,* 108**,** 1-11.

NATONI, A., MURILLO, L. S., KLISZCZAK, A. E., CATHERWOOD, M. A., MONTAGNOLI, A., SAMALI, A., O'DWYER, M. & SANTOCANALE, C. 2011. Mechanisms of action of a dual Cdc7/Cdk9 kinase inhibitor against quiescent and proliferating CLL cells. *Molecular Cancer Therapeutics,* 10**,** 1624-1634.

NESKOROMNA-JEDRZEJCZAK, A., TYNDORF, M., ARKUSZEWSKI, P. & KOBOS, J. 2010. Potential prognostic value of MCM2 expression evaluation in oral cavity squamous cell carcinoma. *Wspolczesna Onkologia-Contemporary Oncology,* 14**,** 196-199.

NEUWALD, A. F., ARAVIND, L., SPOUGE, J. L. & KOONIN, E. V. 1999. AAA(+): A class of chaperone-like ATPases associated with the assembly, operation, and disassembly of protein complexes. *Genome Research,* 9**,** 27-43.

NEVINS, J. R. 1998. Toward an understanding of the functional complexity of the E2F and retinoblastoma families. *Cell Growth & Differentiation,* 9**,** 585-593.

NGUYEN, V. Q., CO, C. & LI, J. J. 2001. Cyclin-dependent kinases prevent DNA re-replication through multiple mechanisms. *Nature,* 411**,** 1068-73.

NIEDUSZYNSKI, C. A., MURRAY, J. & CARRINGTON, M. 2002. Whole-genome analysis of animal A- and B-type cyclins. *Genome Biology,* 3.

NISHITANI, H., LYGEROU, T., NISHIMOTO, T. & NURSE, P. 2000. The Cdt1 protein is required to licence DNNA for replication in fission yeast. *Nature,* 404**,** 625-628.

NISHITANI, H., SUGIMOTO, N., ROUKOS, V., NAKANISHI, Y., SAIJO, M., OBUSE, C., TSURIMOTO, T., NAKAYAMA, K. I., NAKAYAMA, K., FUJITA, M., LYGEROU, Z. & NISHIMOTO, T. 2006. Two E3 ubiquitin ligases, SCF-Skp2 and DDB1-Cul4, target human Cdt1 for proteolysis. *The EMBO Journal,* 25**,** 1126-36.

NISHITANI, H., TARAVIRAS, S., LYGEROU, Z. & NISHIMOTO, T. 2001. The human licensing factor for DNA replication Cdt1 accumulates in G(1) and is destabilized after initiation of S-phase. *Journal of Biological Chemistry,* 276**,** 44905-44911.

NORBURY, C. & NURSE, P. 1992. Animal-cell cycles and their control. *Annual Review of Biochemistry,* 61**,** 441-470.

NOUGAREDE, R., DELLA SETA, F., ZARZOV, P. & SCHWOB, E. 2000. Hierarchy of S-phase-promoting factors: Yeast Dbf4-Cdc7 kinase requires prior S-phase cyclin-dependent kinase activation. *Molecular and Cellular Biology,* 20**,** 3795-3806.

OHTA, S., TATSUMI, Y., FUJITA, M., TSURIMOTO, T. & OBUSE, C. 2003. The ORC1 cycle in human cells: II. Dynamic changes in the human ORC complex during the cell cycle. *Journal of Biological Chemistry,* 278**,** 41535-40.

OHTSUBO, M. & ROBERTS, J. M. 1993. Cyclin-dependent regulation of G1 in mammalian fibroblasts. *Science,* 259**,** 1908-12.

ON, K. F., BEURON, F., FRITH, D., SNIJDERS, A. P., MORRIS, E. P. & DIFFLEY, J. F. X. 2014. Prereplicative complexes assembled *in vitro* support origin-dependent and independent DNA replication. *The EMBO journal,* 33**,** 605-21.

ORTEGA, S., PRIETO, I., ODAJIMA, J., MARTIN, A., DUBUS, P., SOTILLO, R., BARBERO, J. L., MALUMBRES, M. & BARBACID, M. 2003. Cyclin-dependent kinase 2 is essential for meiosis but not for mitotic cell division in mice. *Nature Genetics,* 35**,** 25-31.

OWENS, J. C., DETWEILER, C. S. & LI, J. J. 1997. CDC45 is required in conjunction with CDC7/DBF4 to trigger the initiation of DNA replication. *Proceedings of the National Academy of Sciences of the United States of America,* 94**,** 12521-12526.

PACEK, M., TUTTER, A. V., KUBOTA, Y., TAKISAWA, H. & WALTER, J. C. 2006. Localization of MCM2-7, Cdc45, and GINS to the site of DNA unwinding during eukaryotic DNA replication. *Molecular Cell,* 21**,** 581-587.

PACEK, M. & WALTER, J. C. 2004. A requirement for MCM7 and Cdc45 in chromosome unwinding during eukaryotic DNA replication. *The EMBO Journal,* 23**,** 3667-3676.

PAPE, T., MEKA, H., CHEN, S. X., VICENTINI, G., VAN HEEL, M. & ONESTI, S. 2003. Hexameric ring structure of the full-length archaeal MCM protein complex. *EMBO Reports,* 4**,** 1079-1083.

PARDEE, A. B. 1974. A restriction point for control of normal animal cell proliferation. *Proceedings of the National Academy of Sciences of the United States of America-Biological Sciences,* 71**,** 1286-90.

PARDOLL, D. M., VOGELSTEIN, B. & COFFEY, D. S. 1980. A fixed site of DNA replication in eucaryotic cells. *Cell,* 19**,** 527-36.

PASION, S. G. & FORSBURG, S. L. 1999. Nuclear localization of *Schizosaccharomyces pombe* Mcm2/Cdc19p requires MCM complex assembly. *Molecular Biology of the Cell,* 10**,** 4043-4057.

PATEL, P. K., KOMMAJOSYULA, N., ROSEBROCK, A., BENSIMON, A., LEATHERWOOD, J., BECHHOEFER, J. & RHIND, N. 2008. The Hsk1(Cdc7) replication kinase regulates origin efficiency. *Molecular Biology of the Cell,* 19**,** 5550-5558.

PELIZON, C., MADINE, M. A., ROMANOWSKI, P. & LASKEY, R. A. 2000. Unphosphorylatable mutants of Cdc6 disrupt its nuclear export but still support DNA replication once per cell cycle. *Genes and Development,* 14**,** 2526-33.

PEREVERZEVA, I., WHITMIRE, E., KHAN, B. & COUE, M. 2000. Distinct phosphoisoforms of the *Xenopus* Mcm4 protein regulate the function of the Mcm complex. *Molecular and Cellular Biology,* 20**,** 3667-3676.

PETKOVIC, M., DIETSCHY, T., FREIRE, R., JIAO, R. J. & STAGLJAR, I. 2005. The human Rothmund-Thomson syndrome gene product, RECQL4, localizes to distinct nuclear foci that coincide with proteins involved in the maintenance of genome stability. *Journal of Cell Science,* 118**,** 4261-4269.

PIERGIOVANNI, G. & COSTANZO, V. 2010. GEMC1 is a novel TopBP1-interacting protein involved in chromosomal DNA replication. *Cell Cycle,* 9**,** 3662-3666.

PINES, J. & HUNTER, T. 1990. Human cyclin A is adenovirus E1A-associated protein p60 and behaves differently from cyclin B. *Nature,* 346**,** 760-3.

POH, W. T., CHADHA, G. S., GILLESPIE, P. J., KALDIS, P. & BLOW, J. J. 2014. *Xenopus* Cdc7 executes its essential function early in S phase and is counteracted by checkpoint-regulated protein phosphatase 1. *Open Biology,* 4**,** 130138.

POLLOK, S., BAUERSCHMIDT, C., SÄNGER, J., NASHEUER, H. P. & GROSSE, F. 2007. Human Cdc45 is a proliferation-associated antigen. *FEBS Journal,* 274**,** 3669-3684.

POLLOK, S. & GIOSSE, F. 2007. Cdc45 degradation during differentiation and apoptosis. *Biochemical and Biophysical Research Communications,* 362**,** 910-915.

POLYAK, K., KATO, J. Y., SOLOMON, M. J., SHERR, C. J., MASSAGUE, J., ROBERTS, J. M. & KOFF, A. 1994. P27(kip1), a cyclin-cdk inhibitor, links transforming growth-factor-beta and contact inhibition to cell-cycle arrest. *Genes and Development,* 8**,** 9-22.

POPLAWSKI, A., GRABOWSKI, B., LONG, S. F. & KELMAN, Z. 2001. The zinc finger domain of the archaeal minichromosome maintenance protein is required for helicase activity. *Journal of Biological Chemistry,* 276**,** 49371-49377.

PROKHOROVA, T. A. & BLOW, J. J. 2000. Sequential MCM/P1 subcomplex assembly is required to form a heterohexamer with replication licensing activity. *Journal of Biological Chemistry,* 275**,** 2491-2498.

QIAO, F., MOSS, A. & KUPFER, G. M. 2001. Fanconi anemia proteins localize to chromatin and the nuclear matrix in a DNA damage- and cell cycle-regulated manner. *Journal of Biological Chemistry,* 276**,** 23391-6.

RADICHEV, I., PARASHKEVOVA, A. & ANACHKOVA, B. 2005. Initiation of DNA replication at a nuclear matrix-attached chromatin fraction. *Journal of Cellular Physiology,* 203**,** 71-7.

RAMER, M. D., SUMAN, E. S., RICHTER, H., STANGER, K., SPRANGER, M., BIEBERSTEIN, N. & DUNCKER, B. P. 2013. Dbf4 and Cdc7 proteins promote DNA replication through interactions with distinct Mcm2-7 protein subunits. *Journal of Biological Chemistry,* 288**,** 14926-14935.

RANDELL, J. C. W., BOWERS, J. L., RODRIGUEZ, H. K. & BELL, S. P. 2006. Sequential ATP hydrolysis by Cdc6 and ORC directs loading of the Mcm2-7 helicase. *Molecular Cell,* 21**,** 29-39.

RANDELL, J. C. W., FAN, A., CHAN, C., FRANCIS, L. I., HELLER, R. C., GALANI, K. & BELL, S. P. 2010. Mec1 is one of multiple kinases that prime the Mcm2-7 helicase for phosphorylation by Cdc7. *Molecular Cell,* 40**,** 353-363.

RANJAN, A. & GOSSEN, M. 2006. A structural role for ATP in the formation and stability of the human origin recognition complex. *Proceedings of the National Academy of Sciences of the United States of America,* 103**,** 4864-4869.

RAVNIK, S. E. & WOLGEMUTH, D. J. 1999. Regulation of meiosis during mammalian spermatogenesis: The A-type cyclins and their associated cyclin-dependent kinases are differentially expressed in the germ-cell lineage. *Developmental Biology,* 207**,** 408-418.

RAZIN, S. V., KEKELIDZE, M. G., LUKANIDIN, E. M., SCHERRER, K. & GEORGIEV, G. P. 1986. Replication origins are attached to the nuclear skeleton. *Nucleic Acids Research,* 14**,** 8189-207.

REMUS, D., BEURON, F., TOLUN, G., GRIFFITH, J. D., MORRIS, E. P. & DIFFLEY, J. F. X. 2009. Concerted loading of MCM2-7 double hexamers around DNA during DNA replication origin licensing. *Cell,* 139**,** 719-730.

REYES, J. C., MUCHARDT, C. & YANIV, M. 1997. Components of the human SWI/SNF complex are enriched in active chromatin and are associated with the nuclear matrix. *Journal of Cell Biology,* 137**,** 263-74.

RIALLAND, M., SOLA, F. & SANTOCANALE, C. 2002. Essential role of human CDT1 in DNA replication and chromatin licensing. *Journal of Cell Science,* 115**,** 1435-1440.

RICKE, R. M. & BIELINSKY, A. K. 2004. Mcm10 regulates the stability and chromatin association of DNA polymerase-alpha. *Molecular Cell,* 16**,** 173-185.

RIERA, A., TOGNETTI, S. & SPECK, C. 2014. Helicase loading: How to build a MCM2-7 double-hexamer. *Seminars in Cell & Developmental Biology,* 30**,** 104-109.

ROWLES, A., CHONG, J. P. J., HOWELL, M., EVAN, G. I. & BLOW, J. J. 1996. Interactions between the origin recognition complex and the replication licensing system in *Xenopus*. *Cell,* 87**,** 287-296.

ROWLEY, A., COCKER, J. H., HARWOOD, J. & DIFFLEY, J. F. 1995. Initiation complex assembly at budding yeast replication origins begins with the recognition of a bipartite sequence by limiting amounts of the initiator, ORC. *The EMBO Journal,* 14**,** 2631-41.

SALSI, V., FERRARI, S., FERRARESI, R., COSSARIZZA, A., GRANDE, A. & ZAPPAVIGNA, V. 2009. HOXD13 binds DNA replication origins to promote origin licensing and is inhibited by Geminin. *Molecular and Cellular Biology,* 29**,** 5775-5788.

SAMEL, S. A., FERNANDEZ-CID, A., SUN, J., RIERA, A., TOGNETTI, S., HERRERA, M. C., LI, H. & SPECK, C. 2014. A unique DNA entry gate serves for regulated loading of the eukaryotic replicative helicase MCM2-7 onto DNA. *Genes and Development,* 28**,** 1653-1666.

SANCHEZ-PULIDO, L., DIFFLEY, J. F. X. & PONTING, C. P. 2010. Homology explains the functional similarities of Treslin/Ticrr and Sld3. *Current Biology,* 20**,** R509-R510.

SANCHEZ-PULIDO, L. & PONTING, C. P. 2011. Cdc45: the missing RecJ ortholog in eukaryotes? *Bioinformatics,* 27**,** 1885-1888.

SANGRITHI, M. N., BERNAL, J. A., MADINE, M., PHILPOTT, A., LEE, J., DUNPHY, W. G. & VENKITARAMAN, A. R. 2005. Initiation of DNA replication requires the RECQL4 protein mutated in Rothmund-Thomson syndrome. *Cell,* 121**,** 887-98.

SANTOCANALE, C. & DIFFLEY, J. F. X. 1996. ORC- and Cdc6-dependent complexes at active and inactive chromosomal replication origins in *Saccharomyces cerevisiae*. *The EMBO Journal,* 15**,** 6671-6679.

SATO, N., ARAI, K. & MASAI, H. 1997. Human and *Xenopus* cDNA encoding budding yeast Cdc7-related kinases: *in vitro* phosphorylation of MCM subunits by a putative human homologue of Cdc7. *The EMBO Journal,* 16**,** 4340-4351.

SCHWACHA, A. & BELL, S. P. 2001. Interactions between two catalytically distinct MCM subgroups are essential for coordinated ATP hydrolysis and DNA replication. *Molecular Cell,* 8**,** 1093-1104.

SCLAFANI, R. A. & HOLZEN, T. M. 2007. Cell cycle regulation of DNA replication. *Annual Review Genetics,* 41**,** 237-80.

SEKI, T. & DIFFLEY, J. F. X. 2000. Stepwise assembly of initiation proteins at budding yeast replication origins *in vitro*. *Proceedings of the National Academy of Sciences of the United States of America,* 97**,** 14115-14120.

SEMPLE, J. W. & DUNCKER, B. P. 2004. ORC-associated replication factors as biomarkers for cancer. *Biotechnology Advances,* 22**,** 621-631.

SENGA, T., SIVAPRASAD, U., ZHU, W., PARK, J. H., ARIAS, E. E., WALTER, J. C. & DUTTA, A. 2006. PCNA is a cofactor for Cdt1 degradation by CUL4/DDB1-mediated N-terminal ubiquitination. *Journal of Biological Chemistry,* 281**,** 6246-52.

SEWING, A., BURGER, C., BRUSSELBACH, S., SCHALK, C., LUCIBELLO, F. C. & MULLER, R. 1993. Human cyclin d1 encodes a labile nuclear-protein whose synthesis is directly induced by growth-factors and suppressed by cyclic-amp. *Journal of Cell Science,* 104**,** 545-554.

SHARMA, S. & BROSH, R. M., JR. 2007. Human RECQ1 is a DNA damage responsive protein required for genotoxic stress resistance and suppression of sister chromatid exchanges. *Plos One,* 2.

SHECHTER, D. F., YING, C. Y. & GAUTIER, J. 2000. The intrinsic DNA helicase activity of *Methanobacterium thermoautotrophicum* Delta H minichromosome maintenance protein. *Journal of Biological Chemistry,* 275**,** 15049-15059.

SHEN, Z. & PRASANTH, S. G. 2012. Emerging players in the initiation of eukaryotic DNA replication. *Cell Division,* 7.

SHERR, C. J. 1994. G1 phase progression: cycling on cue. *Cell,* 79**,** 551-5.

SHERR, C. J. 1996. Cancer cell cycles. *Science,* 274**,** 1672-7.

SHERR, C. J. & ROBERTS, J. M. 1999. CDK inhibitors: positive and negative regulators of G1-phase progression. *Genes and Development,* 13**,** 1501-12.

SHERR, C. J. & ROBERTS, J. M. 2004. Living with or without cyclins and cyclin-dependent kinases. *Genes and Development,* 18**,** 2699-711.

SHEU, Y.-J. & STILLMAN, B. 2006. Cdc7-Dbf4 phosphorylates MCM proteins via a docking site-mediated mechanism to promote S phase progression. *Molecular Cell,* 24**,** 101-113.

SHEU, Y. J. & STILLMAN, B. 2010. The Dbf4-Cdc7 kinase promotes S phase by alleviating an inhibitory activity in Mcm4. *Nature,* 463**,** 113-7.

SHIMA, N., ALCARAZ, A., LIACHKO, I., BUSKE, T. R., ANDREWS, C. A., MUNROE, R. J., HARTFORD, S. A., TYE, B. K. & SCHIMENTI, J. C. 2007. A viable allele of Mcm4 causes chromosome instability and mammary adenocarcinomas in mice. *Nature Genetics,* 39**,** 93-98.

SIMON, A. C., ZHOU, J. C., PERERA, R. L., VAN DEURSEN, F., EVRIN, C., IVANOVA, M. E., KILKENNY, M. L., RENAULT, L., KJAER, S., MATAK-VINKOVIC, D., LABIB, K., COSTA, A. & PELLEGRINI, L. 2014. A Ctf4 trimer couples the CMG helicase to DNA polymerase alpha in the eukaryotic replisome. *Nature,* 510**,** 293-+.

SINGLETON, M. R., DILLINGHAM, M. S. & WIGLEY, D. B. 2007. Structure and mechanism of helicases and nucleic acid translocases. *Annual Review of Biochemistry.*

SMITH, J. A. & MARTIN, L. 1973. Do cells cycle. *Proceedings of the National Academy of Sciences of the United States of America,* 70**,** 1263-1267.

SNYDER, M., HE, W. & ZHANG, J. J. 2005. The DNA replication factor MCM5 is essential for Stat1-mediated transcriptional activation. *Proceedings of the National Academy of Sciences of the United States of America,* 102**,** 14539-14544.

SPECK, C., CHEN, Z. Q., LI, H. L. & STILLMAN, B. 2005. ATPase-dependent cooperative binding of ORC and Cdc6 to origin DNA. *Nature Structural & Molecular Biology,* 12**,** 965-971.

SPECK, C. & STILLMAN, B. 2007. Cdc6 ATPase activity regulates ORC center dot Cdc6 stability and the selection of specific DNA sequences as origins of DNA replication. *Journal of Biological Chemistry,* 282**,** 11705-11714.

SPENCER, S. L., CAPPELL, S. D., TSAI, F. C., OVERTON, K. W., WANG, C. L. & MEYER, T. 2013. The proliferation-quiescence decision is controlled by a bifurcation in CDK2 activity at mitotic exit. *Cell,* 155**,** 369-83.

STEAD, B. E., BRANDL, C. J. & DAVEY, M. J. 2011. Phosphorylation of Mcm2 modulates Mcm2-7 activity and affects the cell's response to DNA damage. *Nucleic Acids Research,* 39**,** 6998-7008.

STEAD, B. E., BRANDL, C. J., SANDRE, M. K. & DAVEY, M. J. 2012. Mcm2 phosphorylation and the response to replicative stress. *Bmc Genetics,* 13.

STINCHCOMB, D. T., STRUHL, K. & DAVIS, R. W. 1979. Isolation and characterization of a yeast chromosomal replicator. *Nature,* 282**,** 39-43.

STOEBER, K., MILLS, A. D., KUBOTA, Y., KRUDE, T., ROMANOWSKI, P., MARHEINEKE, K., LASKEY, R. A. & WILLIAMS, G. H. 1998. Cdc6 protein causes premature entry into S phase in a mammalian cell-free system. *The EMBO Journal,* 17**,** 7219-29.

SUN, J., EVRIN, C., SAMEL, S. A., FERNANDEZ-CID, A., RIERA, A., KAWAKAMI, H., STILLMAN, B., SPECK, C. & LI, H. 2013. Cryo-EM structure of a helicase loading intermediate containing ORC-Cdc6-Cdt1-MCM2-7 bound to DNA. *Nature Structural & Molecular Biology,* 20**,** 944-+.

SWORDS, R., MAHALINGAM, D., O'DWYER, M., SANTOCANALE, C., KELLY, K., CAREW, J. & GILES, F. 2010. Cdc7 kinase - A new target for drug development. *European Journal of Cancer,* 46**,** 33-40.

SYMEONIDOU, I.-E., KOTSANTIS, P., ROUKOS, V., RAPSOMANIKI, M.-A., GRECCO, H. E., BASTIAENS, P., TARAVIRAS, S. & LYGEROU, Z. 2013. Multi-step loading of human minichromosome maintenance proteins in live human cells. *Journal of Biological Chemistry,* 288**,** 35852-35867.

SZAMBOWSKA, A., TESSMER, I., KURSULA, P., USSKILAT, C., PRUS, P., POSPIECH, H. & GROSSE, F. 2014. DNA binding properties of human Cdc45 suggest a function as molecular wedge for DNA unwinding. *Nucleic Acids Research,* 42**,** 2308-2319.

TADA, S., CHONG, J. P. J., MAHBUBANI, H. M. & BLOW, J. J. 1999. The RLF-B component of the replication licensing system is distinct from Cdc6 and functions after Cdc6 binds to chromatin. *Current Biology,* 9**,** 211-214.

TADA, S., LI, A., MAIORANO, M., MECHALI, M. & BLOW, J. J. 2001. Repression of origin assembly in metaphase depends on inhibition of RLF-B/Cdt1 by geminin. *Nature Cell Biology,* 3**,** 107-113.

TAKAHASHI, T. S. & WALTER, J. C. 2005. Cdc7-Drf1 is a developmentally regulated protein kinase required for the initiation of vertebrate DNA replication. *Genes and Development,* 19**,** 2295-2300.

TAKARA, T. J. & BELL, S. P. 2011. Multiple Cdt1 molecules act at each origin to load replication-competent Mcm2-7 helicases. *The EMBO Journal,* 30**,** 4885-4896.

TAKAYAMA, Y., KAMIMURA, Y., OKAWA, M., MURAMATSU, S., SUGINO, A. & ARAKI, H. 2003. GINS, a novel multiprotein complex required for chromosomal DNA replication in budding yeast. *Genes and Development,* 17**,** 1153-65.

TAKEDA, T., OGINO, K., MATSUI, E., CHO, M. K., KUMAGAI, H., MIYAKE, T., ARAI, K. & MASAI, H. 1999. A fission yeast gene, him1(+)/dfp1(+), encoding a regulatory subunit for Hsk1 kinase, plays essential roles in S-phase initiation as well as in S-phase checkpoint control and recovery from DNA damage. *Molecular and Cellular Biology,* 19**,** 5535-5547.

TAKEI, Y. & TSUJIMOTO, G. 1998. Identification of a novel MCM3-associated protein that facilitates MCM3 nuclear localization. *Journal of Biological Chemistry,* 273**,** 22177-22180.

TAN, B. C. M., CHIEN, C. T., HIROSE, S. & LEE, S. C. 2006. Functional cooperation between FACT and MCM helicase facilitates initiation of chromatin DNA replication. *The EMBO Journal,* 25**,** 3975-3985.

TANAKA, H., KATOU, Y., YAGURA, M., SAITOH, K., ITOH, T., ARAKI, H., BANDO, M. & SHIRAHIGE, K. 2009. Ctf4 coordinates the progression of helicase and DNA polymerase alpha. *Genes to Cells,* 14**,** 807-820.

TANAKA, S. & ARAKI, H. 2010. Regulation of the initiation step of DNA replication by cyclin-dependent kinases. *Chromosoma,* 119**,** 565-574.

TANAKA, S. & ARAKI, H. 2011. Multiple regulatory mechanisms to inhibit untimely initiation of DNA replication are important for stable genome maintenance. *PLOS Genetics,* 7.

TANAKA, S. & DIFFLEY, J. F. 2002. Interdependent nuclear accumulation of budding yeast Cdt1 and Mcm2-7 during G1 phase. *Nature Cell Biology,* 4**,** 198-207.

TANAKA, S., UMEMORI, T., HIRAI, K., MURAMATSU, S., KAMIMURA, Y. & ARAKI, H. 2007. CDK-dependent phosphorylation of Sld2 and Sld3 initiates DNA replication in budding yeast. *Nature,* 445**,** 328-32.

TANAKA, T., KNAPP, D. & NASMYTH, K. 1997. Loading of an Mcm protein onto DNA replication origins is regulated by Cdc6p and CDKs. *Cell,* 90**,** 649-660.

TANAKA, T., UMEMORI, T., ENDO, S., MURAMATSU, S., KANEMAKI, M., KAMIMURA, Y., OBUSE, C. & ARAKI, H. 2011. Sld7, an Sld3-associated

protein required for efficient chromosomal DNA replication in budding yeast. *The EMBO Journal,* 30**,** 2019-2030.

TANG, G., PENG, L., BALDWIN, P. R., MANN, D. S., JIANG, W., REES, I. & LUDTKE, S. J. 2007. EMAN2: An extensible image processing suite for electron microscopy. *Journal of Structural Biology,* 157**,** 38-46.

TEER, J. K. & DUTTA, A. 2008. Human Cdt1 lacking the evolutionarily conserved region that interacts with MCM2-7 is capable of inducing re-replication. *Journal of Biological Chemistry,* 283**,** 6817-6825.

TENCA, P., BROTHERTON, D., MONTAGNOLI, A., RAINOLDI, S., ALBANESE, C. & SANTOCANALE, C. 2007. Cdc7 is an active kinase in human cancer cells undergoing replication stress. *Journal of Biological Chemistry,* 282**,** 208-215.

TERCERO, J. A., LABIB, K. & DIFFLEY, J. F. X. 2000. DNA synthesis at individual replication forks requires the essential initiation factor Cdc45p. *The EMBO Journal,* 19**,** 2082-2093.

THOMAE, A. W., PICH, D., BROCHER, J., SPINDLER, M.-P., BERENS, C., HOCK, R., HAMMERSCHMIDT, W. & SCHEPERS, A. 2008. Interaction between HMGA1a and the origin recognition complex creates site-specific replication origins. *Proceedings of the National Academy of Sciences of the United States of America-Biological Sciences,* 105**,** 1692-1697.

THÖMMES, P., FETT, R., SCHRAY, B., BURKHART, R., BARNES, M., KENNEDY, C., BROWN, N. C. & KNIPPERS, R. 1992. Properties of the nuclear P1 protein, a mammalian homologue of the yeast Mcm3 replication protein. *Nucleic Acids Research,* 20**,** 1069-1074.

THÖMMES, P., KUBOTA, Y., TAKISAWA, H. & BLOW, J. J. 1997. The RLF-M component of the replication licensing system forms complexes containing all six MCM/P1 polypeptides. *The EMBO Journal,* 16**,** 3312-3319.

THOMSON, A. M., GILLESPIE, P. J. & BLOW, J. J. 2010. Replication factory activation can be decoupled from the replication timing program by modulating Cdk levels. *Journal of Cell Biology,* 188**,** 209-221.

TODOROV, I. T., ATTARAN, A. & KEARSEY, S. E. 1995. BM28, a human member of the MCM2-3-5 family, is displaced from chromatin during DNA replication. *Journal of Cell Biology,* 129**,** 1433-45.

TRAN, N. Q., DANG, H. Q., TUTEJA, R. & TUTEJA, N. 2010. A single subunit MCM6 from pea forms homohexamer and functions as DNA helicase. *Plant Molecular Biology,* 74**,** 327-336.

TSAKRAKLIDES, V. & BELL, S. P. 2010. Dynamics of pre-replicative complex assembly. *Journal of Biological Chemistry,* 285**,** 9437-9443.

TSUJI, T., FICARRO, S. B. & JIANG, W. 2006. Essential role of phosphorylation of MCM2 by Cdc7/Dbf4 in the initiation of DNA replication in mammalian cells. *Molecular Biology of the Cell,* 17**,** 4459-72.

TYE, B.-K. 1999. MCM proteins in DNA replication. *Annual Review of Biochemistry,* 68**,** 649-686.

VAARA, M., ITKONEN, H., HILLUKKALA, T., LIU, Z., NASHEUER, H. P., SCHAARSCHMIDT, D., POSPIECH, H. & SYVAOJA, J. E. 2012. Segregation of replicative DNA polymerases during S phase: DNA polymerase epsilon, but not DNA polymerases alpha/delta, are associated with lamins throughout S phase in human cells. *Journal of Biological Chemistry,* 287**,** 33327-38.

VAN DER VELDEN, H. M., VAN WILLIGEN, G., WETZELS, R. H. & WANKA, F. 1984. Attachment of origins of replication to the nuclear matrix and the chromosomal scaffold. *FEBS Letters,* 171**,** 13-6.

VAN DEURSEN, F., SENGUPTA, S., DE PICCOLI, G., SANCHEZ-DIAZ, A. & LABIB, K. 2012. Mcm10 associates with the loaded DNA helicase at replication origins and defines a novel step in its activation. *The EMBO Journal,* 31**,** 2195-2206.

VAN HEEL, M., GOWEN, B., MATADEEN, R., ORLOVA, E. V., FINN, R., PAPE, T., COHEN, D., STARK, H., SCHMIDT, R., SCHATZ, M. & PATWARDHAN, A. 2000. Single-particle electron cryo-microscopy: towards atomic resolution. *Quarterly Reviews of Biophysics,* 33**,** 307-369.

VAN HEEL, M., HARAUZ, G., ORLOVA, E. V., SCHMIDT, R. & SCHATZ, M. 1996. A new generation of the IMAGIC image processing system. *Journal of Structural Biology,* 116**,** 17-24.

VARMA, P. & MISHRA, R. K. 2011. Dynamics of nuclear matrix proteome during embryonic development in *Drosophila melanogaster*. *Journal of Bioscience,* 36**,** 439-59.

VARRIN, A. E., PRASAD, A. A., SCHOLZ, R. P., RAMER, M. D. & DUNCKER, B. P. 2005. A mutation in Dbf4 motif M impairs interactions with DNA replication factors and confers increased resistance to genotoxic agents. *Molecular and Cellular Biology,* 25**,** 7494-7504.

VASHEE, S., SIMANCEK, P., CHALLBERG, M. D. & KELLY, T. J. 2001. Assembly of the human origin recognition complex. *Journal of Biological Chemistry,* 276**,** 26666-26673.

VOGELSTEIN, B., PARDOLL, D. M. & COFFEY, D. S. 1980. Supercoiled loops and eucaryotic DNA replicaton. *Cell,* 22**,** 79-85.

VOLKENING, M. & HOFFMANN, I. 2005. Involvement of human MCM8 in prereplication complex assembly by recruiting hCdc6 to chromatin. *Molecular and Cellular Biology,* 25**,** 1560-1568.

WALKER, J. E., SARASTE, M., RUNSWICK, M. J. & GAY, N. J. 1982. Distantly related sequences in the alpha-subunits and beta-subunits of ATP synthase, myosin, kinases and other ATP-requiring enzymes and a common nucleotide binding fold. *The EMBO Journal,* 1**,** 945-951.

WALTER, J. & NEWPORT, J. 2000. Initiation of eukaryotic DNA replication: Origin unwinding and sequential chromatin association of Cdc45, RPA, and DNA polymerase alpha. *Molecular Cell,* 5**,** 617-627.

WALTER, J. C. 2000. Evidence for sequential action of Cdc7 and CDK2 protein kinases during initiation of DNA replication in *Xenopus* egg extracts. *Journal of Biological Chemistry,* 275**,** 39773-39778.

WAN, K. M., NICKERSON, J. A., KROCKMALNIC, G. & PENMAN, S. 1999. The nuclear matrix prepared by amine modification. *Proceedings of the National Academy of Sciences of the United States of America-Biological Sciences,* 96**,** 933-8.

WASSERFALLEN, A., NOLLING, J., PFISTER, P., REEVE, J. & DE MACARIO, E. C. 2000. Phylogenetic analysis of 18 thermophilic *Methanobacterium* isolates supports the proposals to create a new genus. *International Journal of Systematic and Evolutionary Microbiology,* 50**,** 43-53.

WATASE, G., TAKISAWA, H. & KANEMAKI, M. T. 2012. Mcm10 plays a role in functioning of the eukaryotic replicative DNA helicase, Cdc45-MCM-GINS. *Current Biology,* 22**,** 343-349.

WEINREICH, M., LIANG, C., CHEN, H. H. & STILLMAN, B. 2001. Binding of cyclin-dependent kinases to ORC and Cdc6p regulates the chromosome replication cycle. *Proceedings of the National Academy of Sciences of the United States of America,* 98**,** 11211-11217.

WEINREICH, M. & STILLMAN, B. 1999. Cdc7p-Dbf4p kinase binds to chromatin during S phase and is regulated by both the APC and the RAD53 checkpoint pathway. *The EMBO Journal,* 18**,** 5334-5346.

WHEELER, L. W., LENTS, N. H. & BALDASSARE, J. J. 2008. Cyclin A-CDK activity during G(1) phase impairs MCM chromatin loading and inhibits DNA synthesis in mammalian cells. *Cell Cycle,* 7**,** 2179-2188.

WHITTAKER, A. J., ROYZMAN, I. & ORR-WEAVER, T. L. 2000. Drosophila Double parked: a conserved, essential replication protein that colocalises with the origin recognition complex and links DNA replication with mitosis and the down-regulation of S phase transcripts. *Genes and Development,* 14**,** 1765-1776.

WILLIAMS, G. H. & STOEBER, K. 2007. Cell cycle markers in clinical oncology. *Current Opinion in Cell Biology,* 19**,** 672-679.

WILLIAMS, G. H. & STOEBER, K. 2012. The cell cycle and cancer. *Journal of Pathology,* 226**,** 352-364.

WILMES, G. M., ARCHAMBAULT, V., AUSTIN, R. J., JACOBSON, M. D., BELL, S. P. & CROSS, F. R. 2004. Interaction of the S-phase cyclin Clb5 with an "RXL" docking sequence in the initiator protein Orc6 provides an origin-localized replication control switch. *Genes and Development,* 18**,** 981-91.

WILSON, R. H. & COVERLEY, D. 2013. Relationship between DNA replication and the nuclear matrix. *Genes to Cells,* 18**,** 17-31.

WILSON, R. H. C., HESKETH, E. L. & COVERLEY, D. 2014. Preparation of the nuclear matrix for parallel microscopy and biochemical analyses. *Cold Spring Harb Protoc,* 10.1101/pdb.prot083758.

WOHLSCHLEGEL, J. A., DWYER, B. T., DHAR, S. K., CVETIC, C., WALTER, J. C. & DUTTA, A. 2000. Inhibition of eukaryotic DNA replication by geminin binding to Cdt1. *Science,* 290**,** 2309-+.

WONG, P. G., WINTER, S. L., ZAIKA, E., CAO, T. V., OGUZ, U., KOOMEN, J. M., HAMLIN, J. L. & ALEXANDROW, M. G. 2011. Cdc45 limits replicon usage from a low density of preRCs in mammalian cells. *PLOS One,* 6.

WOODWARD, A. M., GOHLER, T., LUCIANI, M. G., OEHLMANN, M., GE, X. Q., GARTNER, A., JACKSON, D. A. & BLOW, J. J. 2006. Excess MCM2-7 license dormant origins of replication that can be used under conditions of replicative stress. *Journal of Cell Biology,* 173**,** 673-683.

WU, J., CAPP, C., FENG, L. & HSIEH, T.-S. 2008. *Drosophila* homologue of the Rothmund-Thomson syndrome gene: Essential function in DNA replication during development. *Developmental Biology,* 323**,** 130-142.

WU, Z.-Q. & LIU, X. 2008. Role for Plk1 phosphorylation of Hbo1 in regulation of replication licensing. *Proceedings of the National Academy of Sciences of the United States of America,* 105**,** 1919-1924.

XOURI, G., LYGEROU, Z., NISHITANI, H., PACHNIS, V., NURSE, P. & TARAVIRAS, S. 2004. Cdt1 and geminin are down-regulated upon cell cycle exit and are over-expressed in cancer-derived cell lines. *European Journal of Biochemistry,* 271**,** 3368-78.

XU, X., ROCHETTE, P. J., FEYISSA, E. A., SU, T. V. & LIU, Y. 2009. MCM10 mediates RECQ4 association with MCM2-7 helicase complex during DNA replication. *The EMBO Journal,* 28**,** 3005-3014.

YANAGI, K., MIZUNO, T., YOU, Z. Y. & HANAOKA, F. 2002. Mouse geminin inhibits not only Cdt1-MCM6 interactions but also a novel intrinsic Cdt1 DNA binding activity. *Journal of Biological Chemistry,* 277**,** 40871-40880.

YARDIMCI, H., LOVELAND, A. B., HABUCHI, S., VAN OIJEN, A. M. & WALTER, J. C. 2010. Uncoupling of sister replisomes during eukaryotic DNA replication. *Molecular Cell,* 40**,** 834-840.

YARDIMCI, H. & WALTER, J. C. 2014. Prereplication-complex formation: a molecular double take? *Nature Structural & Molecular Biology,* 21**,** 20-25.

YING, C. Y. & GAUTIER, J. 2005. The ATPase activity of MCM2-7 is dispensable for pre-RC assembly but is required for DNA unwinding. *The EMBO Journal,* 24**,** 4334-44.

YOSHIDA, K., KUO, F., GEORGE, E. L., SHARPE, A. H. & DUTTA, A. 2001. Requirement of CDC45 for postimplantation mouse development. *Molecular and Cellular Biology,* 21**,** 4598-603.

YOSHIDA, K., TAKISAWA, H. & KUBOTA, Y. 2005. Intrinsic nuclear import activity of geminin is essential to prevent re-initiation of DNA replication in *Xenopus* eggs. *Genes to Cells,* 10**,** 63-74.

YOU, Z. Y., ISHIMI, Y., MIZUNO, T., SUGASAWA, K., HANAOKA, F. & MASAI, H. 2003. Thymine-rich single-stranded DNA activates Mcm4/6/7 helicase on Y-fork and bubble-like substrates. *The EMBO Journal,* 22**,** 6148-6160.

YOU, Z. Y., KOMAMURA, Y. & ISHIMI, Y. 1999. Biochemical analysis of the intrinsic Mcm4-Mcm6-Mcm7 DNA helicase activity. *Molecular and Cellular Biology,* 19**,** 8003-8015.

YOUNG, M. R., SUZUKI, K., YAN, H., GIBSON, S. & TYE, B. K. 1997. Nuclear accumulation of *Saccharomyces cerevisiae* Mcm3 is dependent on its nuclear localization sequence. *Genes to Cells,* 2**,** 631-643.

YOUNG, M. R. & TYE, B. K. 1997. Mcm2 and Mcm3 are constitutive nuclear proteins that exhibit distinct isoforms and bind chromatin during specific cell cycle stages of *Saccharomyces cerevisiae*. *Molecular Biology of the Cell,* 8**,** 1587-1601.

YU, X., VANLOOCK, M. S., POPLAWSKI, A., KELMAN, Z., XIANG, T., TYE, B. K. & EGELMAN, E. H. 2002. The *Methanobacterium thermoautotrophicum* MCM protein can form heptameric rings. *EMBO Reports,* 3**,** 792-797.

ZEGERMAN, P. & DIFFLEY, J. F. X. 2007. Phosphorylation of Sld2 and Sld3 by cyclin-dependent kinases promotes DNA replication in budding yeast. *Nature,* 445**,** 281-285.

ZEITLIN, S., PARENT, A., SILVERSTEIN, S. & EFSTRATIADIS, A. 1987. Pre-mRNA splicing and the nuclear matrix. *Molecular and Cellular Biology,* 7**,** 111-20.

ZETTERBERG, A. & LARSSON, O. 1985. Kinetic-analysis of regulatory events in G1 leading to proliferation or quiescence of Swiss 3T3 cells. *Proceedings of the National Academy of Sciences of the United States of America,* 82**,** 5365-5369.

ZHANG, J., YU, L., WU, X., ZOU, L., SOU, K. K. L., WEI, Z., CHENG, X., ZHU, G. & LIANG, C. 2010. The interacting domains of hCdt1 and hMcm6 involved in the chromatin loading of the MCM complex in human cells. *Cell Cycle,* 9**,** 4848-4857.

ZINK, D., FISCHER, A. H. & NICKERSON, J. A. 2004. Nuclear structure in cancer cells. *Nature Reviews Cancer,* 4**,** 677-87.

ZOU, L. & STILLMAN, B. 1998. Formation of a preinitiation complex by S-phase cyclin CDK-dependent loading of Cdc45p onto chromatin. *Science,* 280**,** 593-596.

ZOU, L. & STILLMAN, B. 2000. Assembly of a complex containing Cdc45p, replication protein A, and Mcm2p at replication origins controlled by S-phase cyclin-dependent kinases and Cdc7p-Dbf4p kinase. *Molecular and Cellular Biology,* 20**,** 3086-3096.